

# High-Energy Astro-physics

[teresa.montaruli@unige.ch](mailto:teresa.montaruli@unige.ch)



CHIPP Winter School of Particle Physics 2017

13-14 Feb. 2017



# Contents

- Cosmic Rays and their unknowns: spectrum, composition, acceleration processes, propagation, and candidate sources.
- the cosmic ray - gamma - neutrino connection
- Recent results on multi-messenger astrophysics:  
**Looking for messengers from the Early Universe, the violent Universe and the invisible Universe !**
  - Strong relation with all other lectures (DM - M. Schumann; Neutrinos - A. Blondel, Detectors - F. Harmann; Collider Physics - M. Kado...)

# Something on methodology...

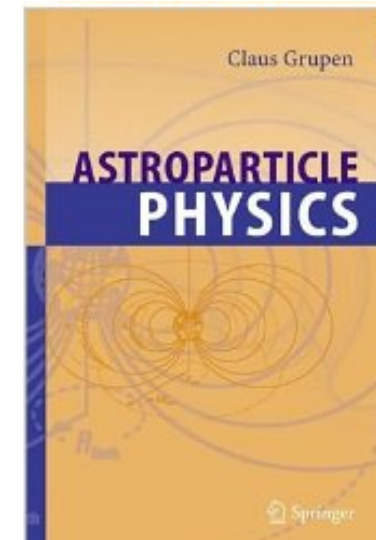
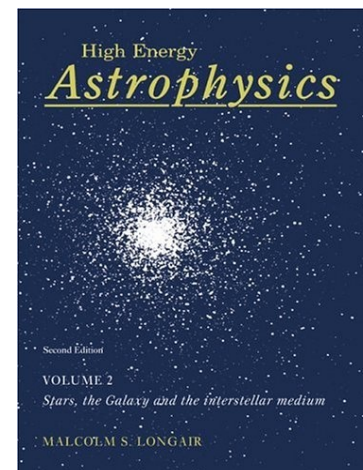
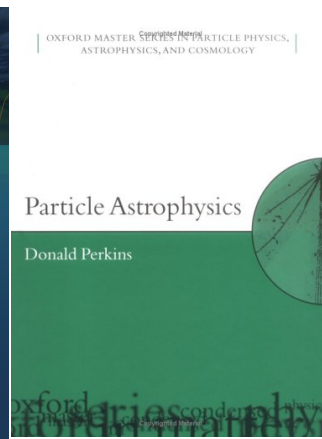
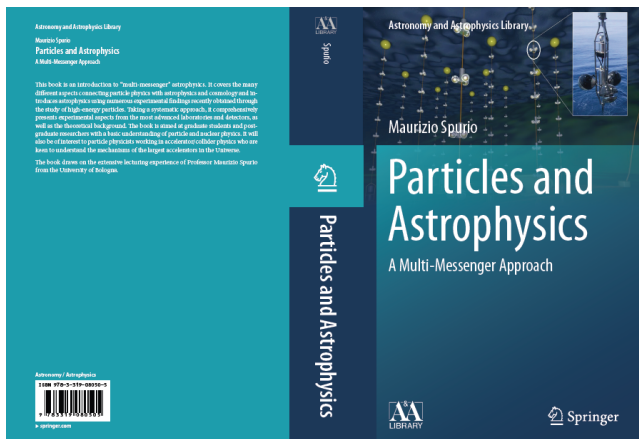
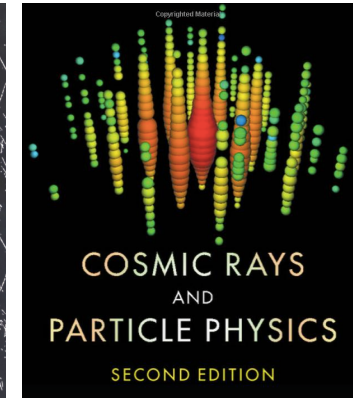
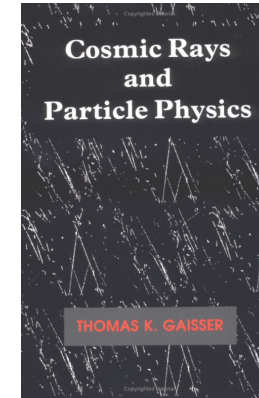


The real voyage of discovery consists not in seeking new landscapes, but in having new eyes. (*Marcel Proust*)



# My favorite textbooks in Astroparticle

- T.K. Gaisser Cosmic Rays and Particle Physics (new edition 2016 available!)
- D. Perkins, Particle Astrophysics (2nd ed. 2009)
- T. Stanev, High Energy Cosmic Rays, Springer, 2004
- M. S. Longair, High Energy Astrophysics, Cambridge U. Press, 2010
- S. Rosswog & M.Bruggen High-Energy Astrophysics
- C. Grupen, Astroparticle Physics, Springer, 2005
- M. Spurio Particles and Astrophysics, Springer
- L. Bergstrom and A. Goobar, Cosmology and Particle Astrophysics, Springer (2nd edition,2003)



# Data Particle Book

<http://pdg.lbl.gov/>

The physicist's book of truth

> 200 particles listed in PDB  
But only 27 have  $c\tau > 1\mu\text{m}$   
and only 13 have  $c\tau > 500\mu\text{m}$


The screenshot shows the PDG website homepage. At the top is the PDG logo (particle data group) with a navigation menu: About PDG, PDG Authors, PDG Citation, Contact Us. The main heading is "The Review of Particle Physics (2016)" by C. Patrignani et al. (Particle Data Group), Chin. Phys. C, 40, 100001 (2016). Below this is a navigation menu with buttons for: pdgLive - Interactive Listings, Summary Tables, Reviews, Tables, Plots, Particle Listings, and a Search box. Further down are sections for "Order: Book & Booklet", "Download or Print: Book, Booklet, Website, Figures & more", a table of "Previous Editions (& Errata) 1957-2016" with links to Physical Constants, Astrophysical Constants, Atomic & Nuclear Properties, and Astrophysics & Cosmology. There is also a "Most Popular" section with buttons for Reviews and Data Listings, a "PDG Outreach" section with links to Particle Adventure & Apps, CPEP Charts, and History book, and a "Non-PDG Resources" section with dropdown menus for HEP Papers, Databases & Info, and Institutions & People. At the bottom is a "Funded by:" section listing US DOE, CERN, MEXT (Japan), IHEP-CAS (China), INFN (Italy), MINECO (Spain), and IHEP (Russia).

**PDG**  
particle data group

About PDG | PDG Authors | PDG Citation | Contact Us

## The Review of Particle Physics (2016)

C. Patrignani et al. (Particle Data Group), Chin. Phys. C, **40**, 100001 (2016).



**pdgLive - Interactive Listings**

**Summary Tables**

**Reviews, Tables, Plots**

**Particle Listings**

**Search**

**Order:** Book & Booklet

**Download or Print:** Book, Booklet, Website, Figures & more

Previous Editions (& Errata) 1957-2016	Physical Constants
Errata in current edition	Astrophysical Constants
Figures in reviews	Atomic & Nuclear Properties
Mirror Sites	Astrophysics & Cosmology

**Most Popular**

**Reviews** | **Data Listings**

**PDG Outreach**

Particle Adventure & Apps | CPEP Charts | History book

**Non-PDG Resources**

▼ HEP Papers | ▼ Databases & Info | ▼ Institutions & People

**Funded by:**

US DOE, CERN, MEXT (Japan), IHEP-CAS (China), INFN (Italy), MINECO (Spain), IHEP (Russia)

# Online material

## On cosmic Rays:

- M. Settimo, Review on extragalactic cosmic rays detection, <https://arxiv.org/pdf/1612.08108.pdf>
- Gaisser, Stanev, Tilav, Cosmic Ray Energy Spectrum from Measurements of Air Showers, <https://arxiv.org/pdf/1303.3565v1.pdf>
- Kotera and Olinto, The Astrophysics of Ultrahigh Energy Cosmic Rays, <https://arxiv.org/abs/1101.4256>
- Blümer, Eger and Hörandel, Cosmic Rays from the Knee to the Highest Energies, <https://arxiv.org/pdf/0904.0725v1.pdf>

Anything on **neutrinos** : <http://www.nu.to.infn.it>;

Reviews on Astrophysics Neutrinos: <http://web.mit.edu/redingtn/www/netadv/Xnuastroph.html>

Book: <https://www.cambridge.org/core/books/cosmic-rays-and-particle-physics/C81BA71195ADFC89EFCC2C565B617702>

Recent results: <https://arxiv.org/pdf/1511.03820.pdf>

Atmospheric Neutrinos: <https://arxiv.org/abs/1605.03073>

Reviews on **gamma-ray astronomy**: <http://web.mit.edu/redingtn/www/netadv/Xgamma.html>



LIGO @LIGO

Follow

# Ripples in spacetime: @sciencemagazine

## ... detection of #GravitationalWaves as breakthrough of the Year

PRL 116, 061102 (2016)

Selected for a Viewpoint in Physics  
PHYSICAL REVIEW LETTERS

week ending  
12 FEBRUARY 2016

### Observation of Gravitational Waves from a Binary Black Hole Merger

B. P. Abbott *et al.*\*

(LIGO Scientific Collaboration and Virgo Collaboration)  
(Received 21 January 2016; published 11 February 2016)

On September 14, 2015 at 09:50:45 UTC the two detectors of the Laser Interferometer Gravitational-Wave Observatory simultaneously observed a transient gravitational-wave signal. The signal sweeps upwards in frequency from 35 to 250 Hz with a peak gravitational-wave strain of  $1.0 \times 10^{-21}$ . It matches the waveform predicted by general relativity for the inspiral and merger of a pair of black holes and the ringdown of the resulting single black hole. The signal was observed with a matched-filter signal-to-noise ratio of 24 and a false alarm rate estimated to be less than 1 event per 203 000 years, equivalent to a significance greater than  $5.1\sigma$ . The source lies at a luminosity distance of  $410^{+180}_{-180}$  Mpc corresponding to a redshift  $z = 0.09^{+0.03}_{-0.04}$ . In the source frame, the initial black hole masses are  $36^{+5}_{-4} M_{\odot}$  and  $29^{+4}_{-4} M_{\odot}$ , and the final black hole mass is  $62^{+4}_{-4} M_{\odot}$ , with  $3.0^{+0.3}_{-0.3} M_{\odot} c^2$  radiated in gravitational waves. All uncertainties define 90% credible intervals. These observations demonstrate the existence of binary stellar-mass black hole systems. This is the first direct detection of gravitational waves and the first observation of a binary black hole merger.

DOI: 10.1103/PhysRevLett.116.061102

#### I. INTRODUCTION

In 1916, the year after the final formulation of the field equations of general relativity, Albert Einstein predicted the existence of gravitational waves. He found that the linearized weak-field equations had wave solutions: transverse waves of spatial strain that travel at the speed of light, generated by time variations of the mass quadrupole moment of the source [1,2]. Einstein understood that gravitational-wave amplitudes would be remarkably small; moreover, until the Chapel Hill conference in 1957 there was significant debate about the physical reality of gravitational waves [3].

Also in 1916, Schwarzschild published a solution for the field equations [4] that was later understood to describe a black hole [5,6], and in 1963 Kerr generalized the solution to rotating black holes [7]. Starting in the 1970s theoretical work led to the understanding of black hole quasinormal modes [8–10], and in the 1990s higher-order post-Newtonian calculations [11] preceded extensive analytical studies of relativistic two-body dynamics [12,13]. These advances, together with numerical relativity breakthroughs in the past decade [14–16], have enabled modeling of binary black hole mergers and accurate predictions of their gravitational waveforms. While numerous black hole candidates have now been identified through electromagnetic observations [17–19], black hole mergers have not previously been observed.

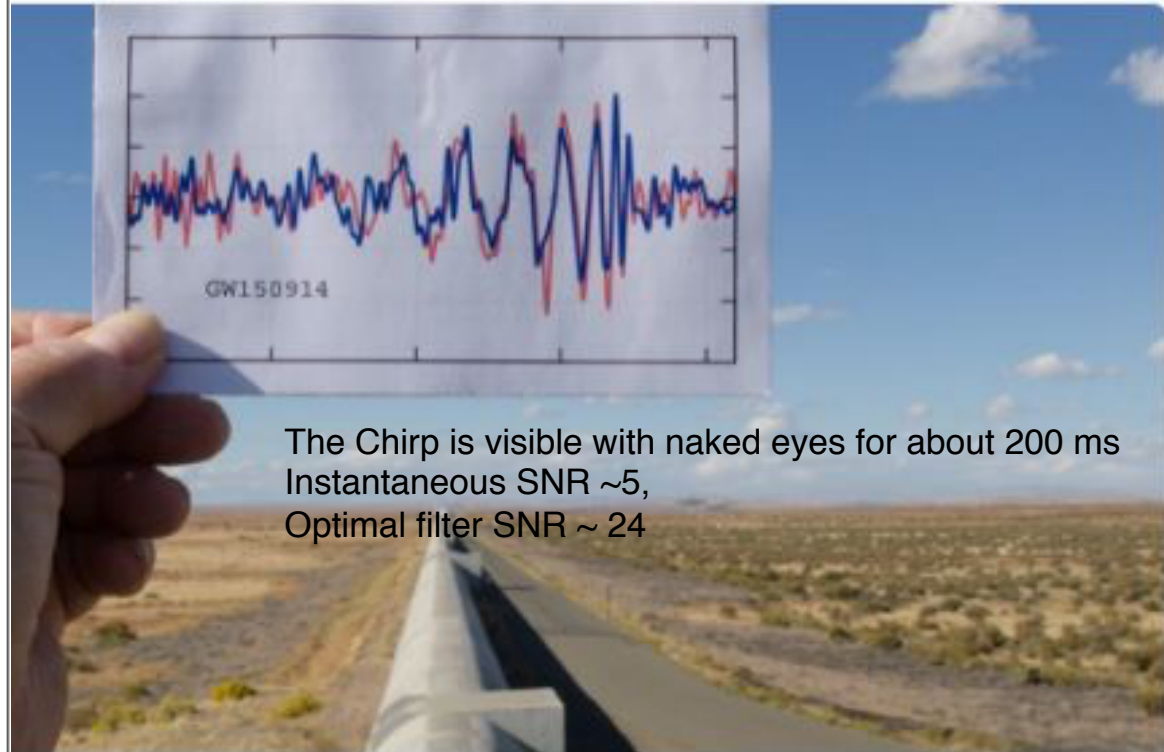
\*Full author list given at the end of the article.

Published by the American Physical Society under the terms of the Creative Commons Attribution 3.0 License. Further distribution of this work must maintain attribution to the author(s) and the published article's title, journal citation, and DOI.

0031-9007/16/116(6)/061102(16)

061102-1

Published by the American Physical Society



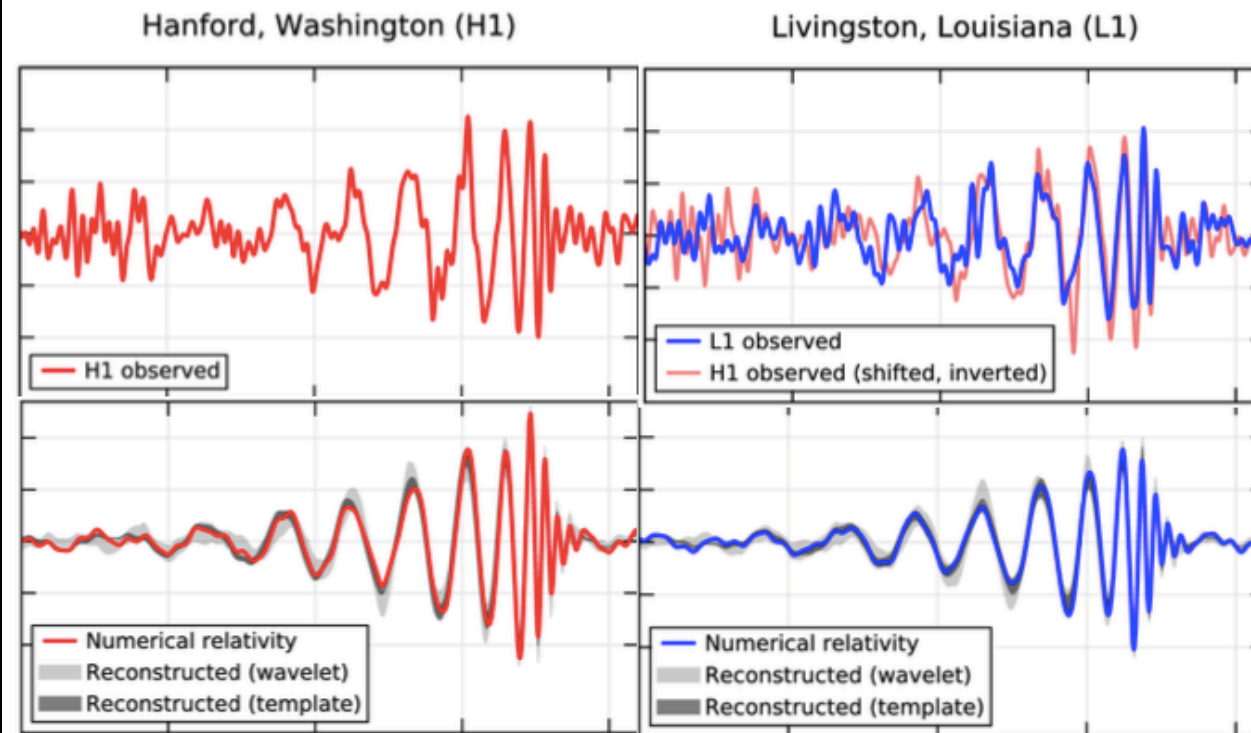
The Chirp is visible with naked eyes for about 200 ms  
Instantaneous SNR ~5,  
Optimal filter SNR ~ 24

time: Science's 2016 Breakthrough of the Year

Gravitational waves ended a 40-year quest--and began a new field

of study  
sciencemag.org

# The signals in the two LIGO interferometers



$$m_1 = (36 \pm 4)M_{\odot}$$

$$m_2 = (29 \pm 4)M_{\odot}$$

$$m_{\text{fin}} = (62 \pm 4)M_{\odot}$$

$$\Delta m = (3 \pm 0.5)M_{\odot}$$

$$D = (410 \pm 170) \text{ Mpc}$$

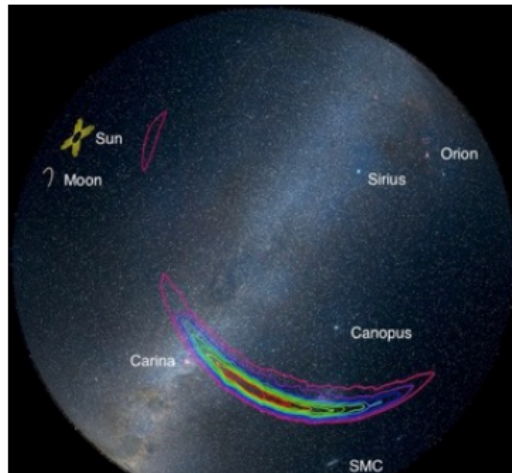




# Parameters from fitting (in source frame)

Primary black hole mass	$36^{+5}_{-4} M_{\odot}$
Secondary black hole mass	$29^{+4}_{-4} M_{\odot}$
Final black hole mass	$62^{+4}_{-4} M_{\odot}$
Final black hole spin	$0.67^{+0.05}_{-0.07}$
Luminosity distance	$410^{+160}_{-180} \text{ Mpc}$
Source redshift, $z$	$0.09^{+0.03}_{-0.04}$

- Radiated energy:  $3M_{\odot}$  ( $\pm 0.5$ )
- Peak luminosity:  $3.6 \times 10^{56} \text{ erg/s}$  ( $\pm 15\%$ ): 200 solar masses per second! (About  $1 \mu\text{W}/\text{cm}^2$  at detector,  $\sim 10^{12}$  millicrab!)



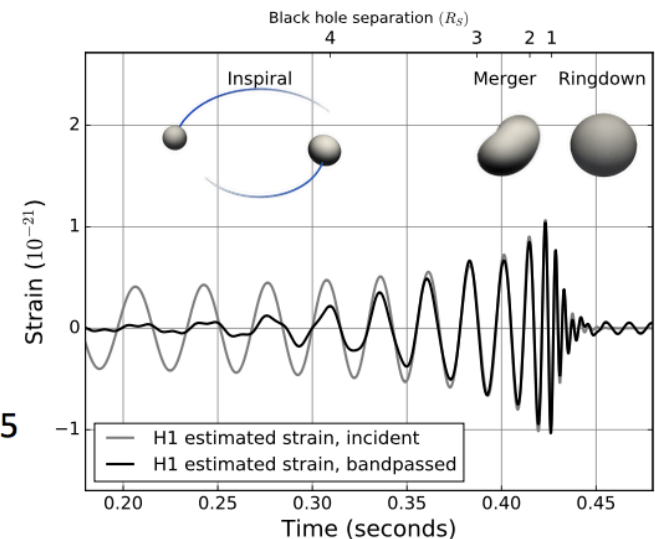
Bruce Allen, TeVPA 2016  
[https://indico.cern.ch/event/469963/contributions/2277620/attachments/1339053/2113990/TeVPA\\_2016\\_09\\_13.pdf](https://indico.cern.ch/event/469963/contributions/2277620/attachments/1339053/2113990/TeVPA_2016_09_13.pdf)



## Can only be two black holes!

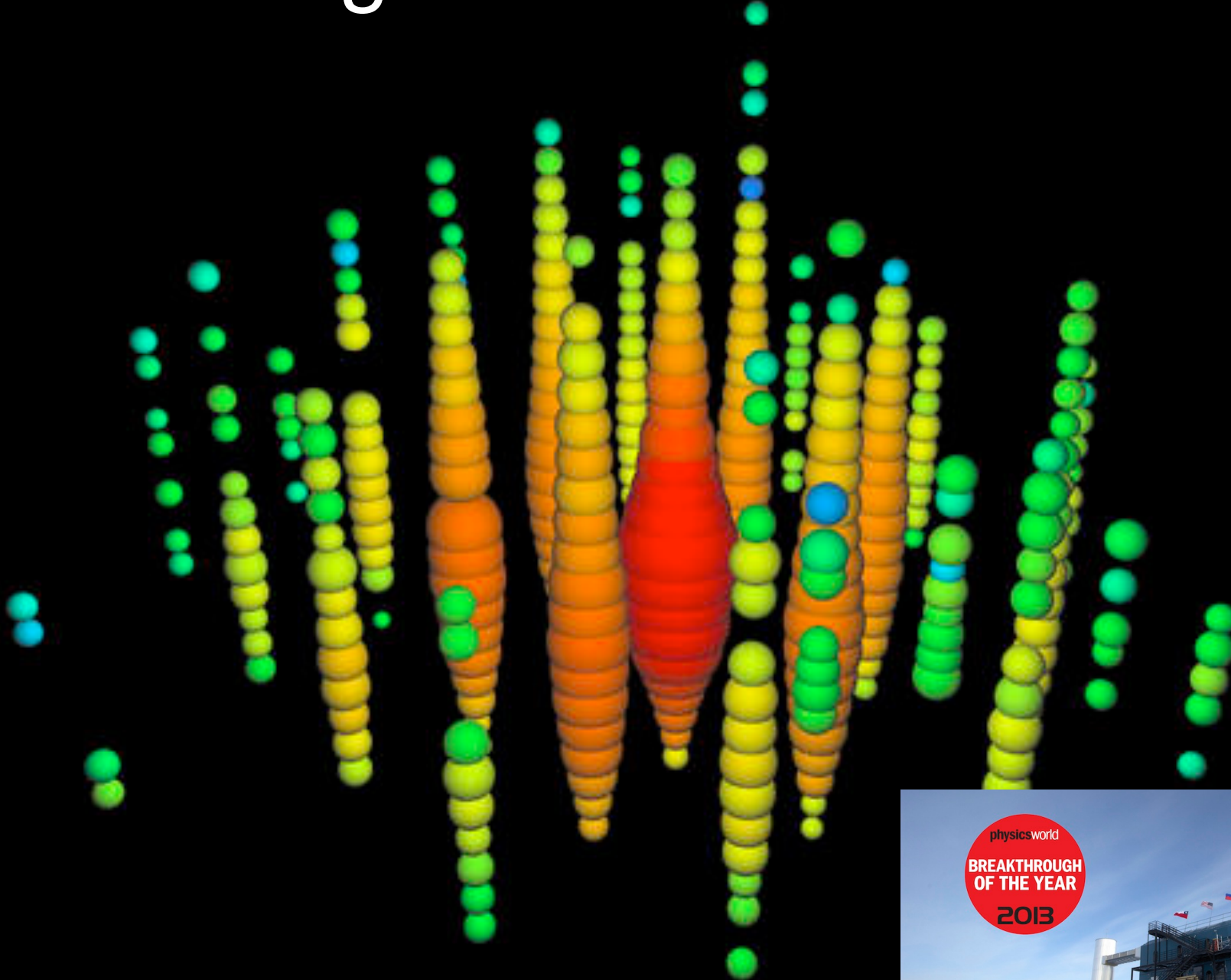
- One orbit => two gravitational wave cycles
- Newtonian approximation =>
 
$$\mathcal{M} = \frac{(m_1 m_2)^{3/5}}{(m_1 + m_2)^{1/5}} = \frac{c^3}{G} \left[ \frac{5}{96} \pi^{-8/3} f^{-11/3} \dot{f} \right]^{3/5}$$
- Chirp mass  $\mathcal{M} \sim 30 M_{\odot}$
- If equal:  $m_1 = m_2 \sim 35 M_{\odot}$   
=> Sum of Schwarzschild radii  $\geq 206 \text{ km}$
- At peak  $f_{\text{GW}} = 150 \text{ Hz}$ , orbital frequency = 75 Hz separation of Newtonian point masses 346km

- **Ordinary stars** are  $10^6 \text{ km}$  in size (merge at mHz). **White dwarfs** are  $10^4 \text{ km}$  (merge at 1 Hz). They are too big to explain this!
- **Neutron stars** are also not possible:  
 $m_1 = 4 M_{\odot} \Rightarrow m_2 = 600 M_{\odot}$   
 => Schwarzschild radius 1800km => too big!



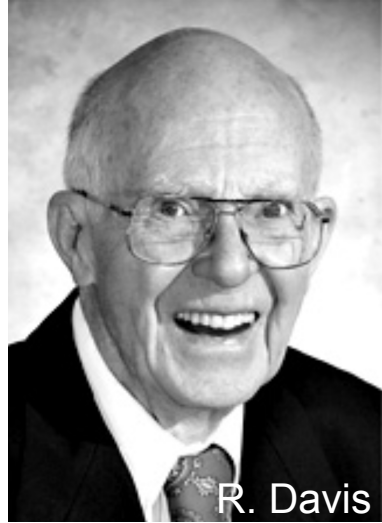
**Only black holes  
 are sufficiently  
 massive *and* compact!**

# New signals from the Heavens

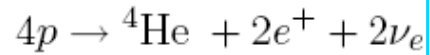


# Neutrinos winners!

Nobel prize 2002



Oscillations with neutrinos from thermonuclear reactions in the Sun



$$\sim 6 \times 10^{10} \nu \text{ cm}^{-2} \text{ s}^{-1}$$

$$E_\nu \sim 0.1 - 20 \text{ MeV}$$



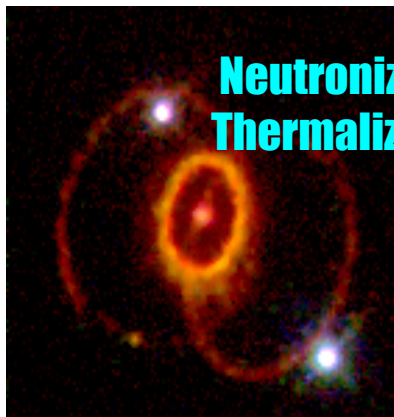
$\sim 100,000$  billion solar neutrinos pass through your body/s

$\sim 1$  neutrino stops in a lifetime!

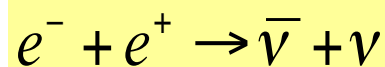
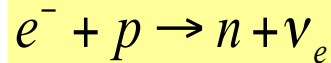
M. Koshiba



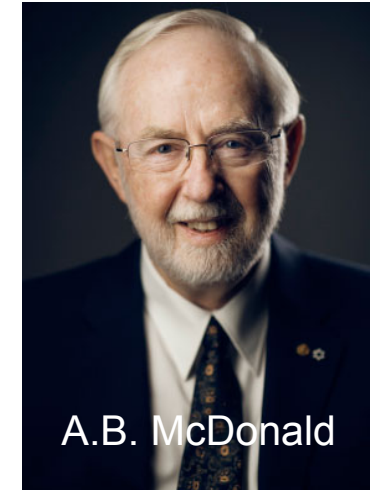
$\sim 10$  s bursts of 10 MeV vs from stellar collapse (I. Tamborra's lectures)



Neutronization  
Thermalization:



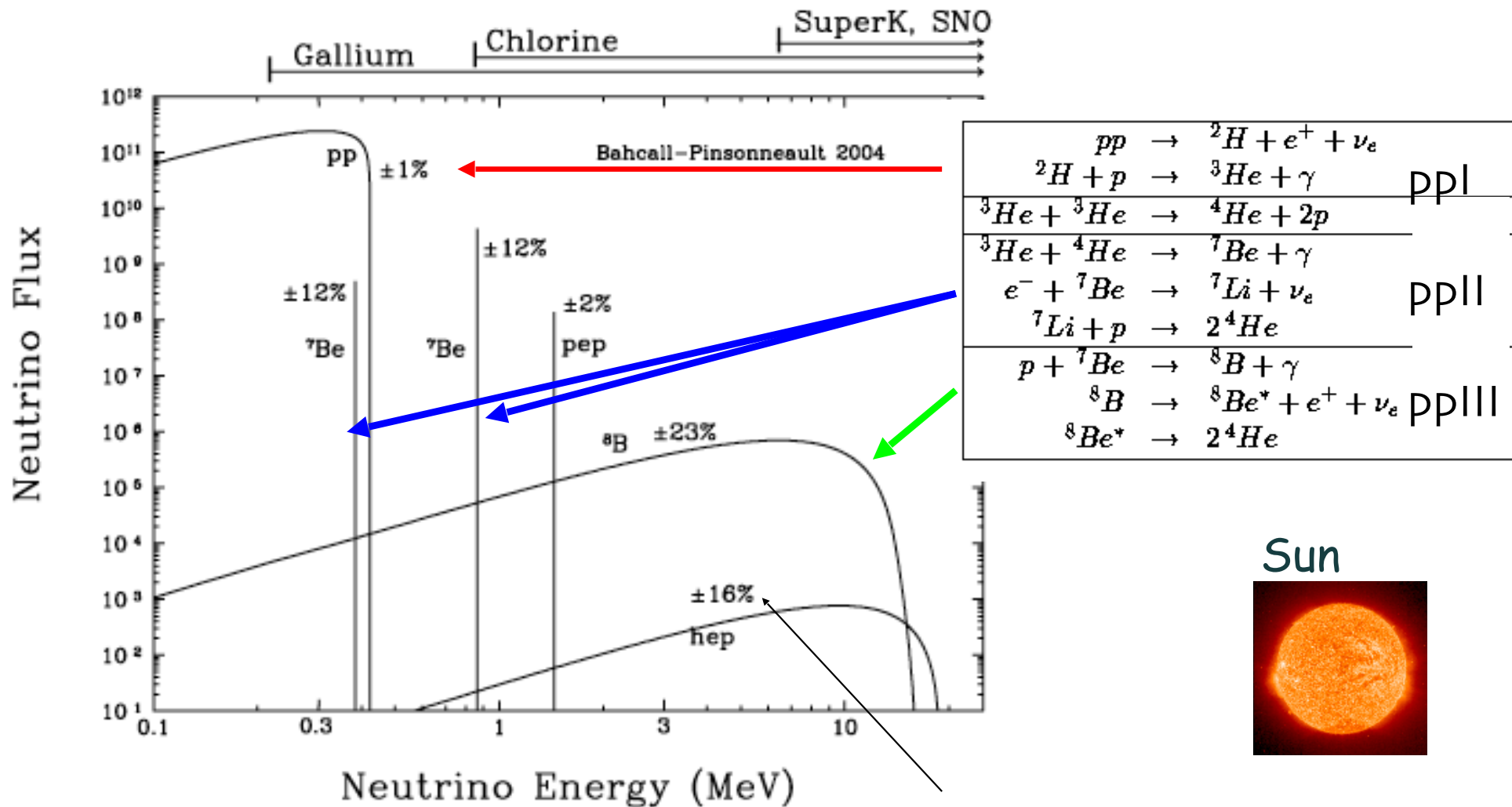
Nobel prize 2015



Nobel prize 2016  
Oscillations with atmospheric neutrinos



# Detected Extra-terrestrial neutrinos from sources: Solar neutrinos



Theoretical uncertainties

# Detected Extra-terrestrial neutrinos from sources: SN1987A



D = 55 kpc

Let's pick up 2 of these events (similar emission time )

$$t_1 = 0 \quad E_1 = 20 \text{ MeV}$$

$$t_2 = 12.5 \text{ s} \quad E_2 = 10 \text{ MeV}$$

$\Delta t_e = 0$  and  $\Delta t_d = |t_2 - t_1| = 12.5 \text{ s}$  and we find solving for the mass:

$$mc^2 = \sqrt{\frac{2cE_1E_2|\Delta t_d|}{d \times |E_2^2 - E_1^2|}} = 24 \text{ eV}$$

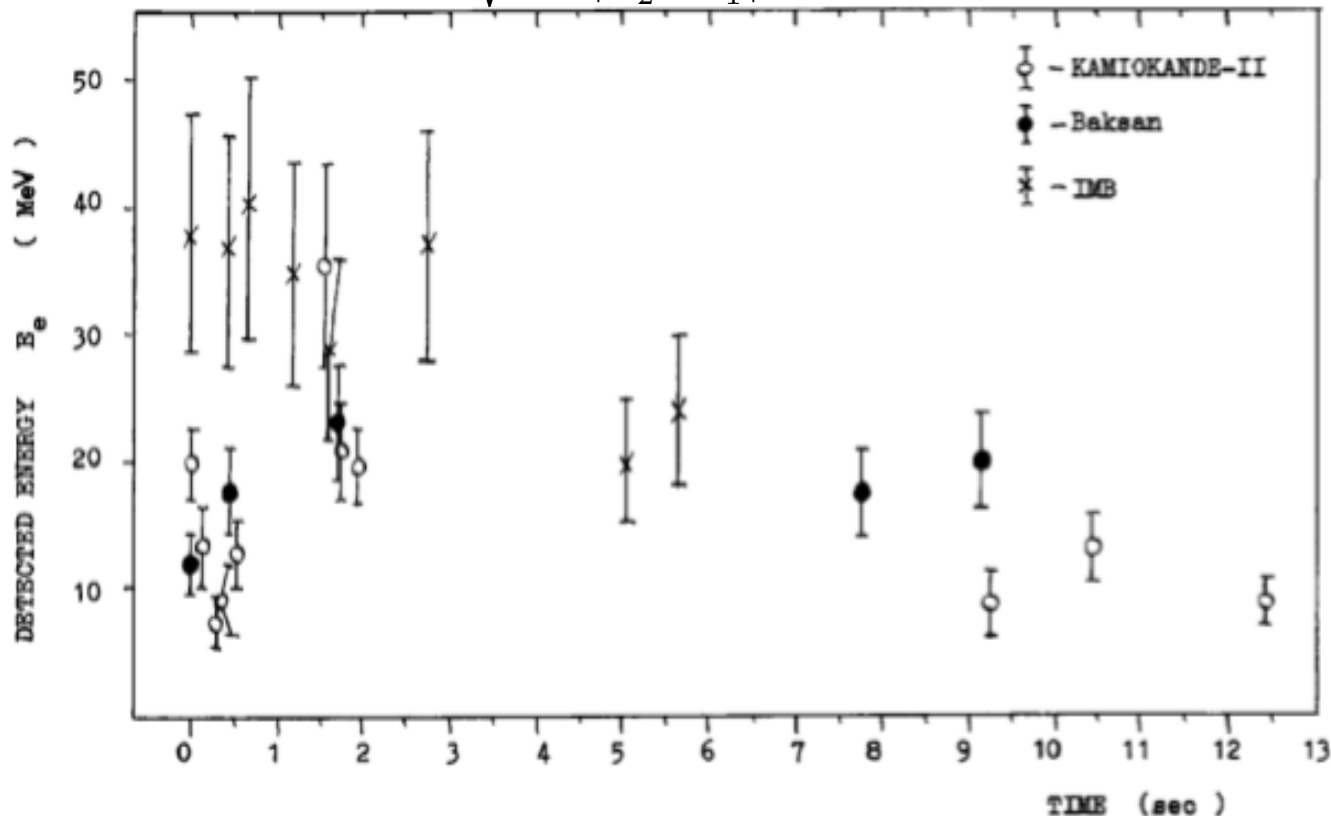
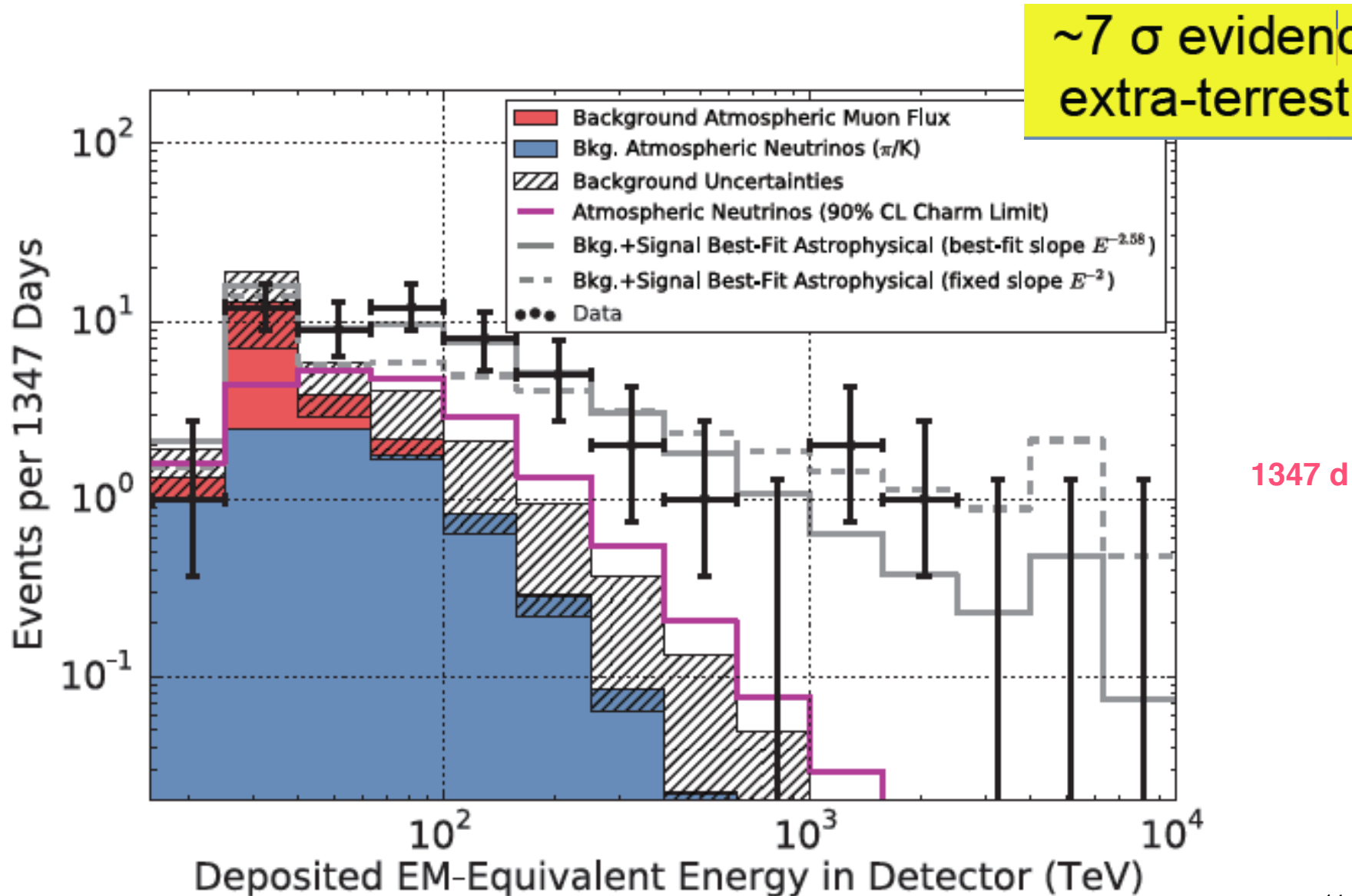


Fig. 3. Energies of all events detected at 7:35 UT on February 23, 1987 versus time.  $t=0.0$  is set as to be the time of the first event of each signal observed.

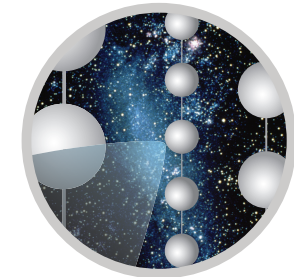
# Detected Extra-terrestrial diffuse neutrinos in IceCube

SN1987A

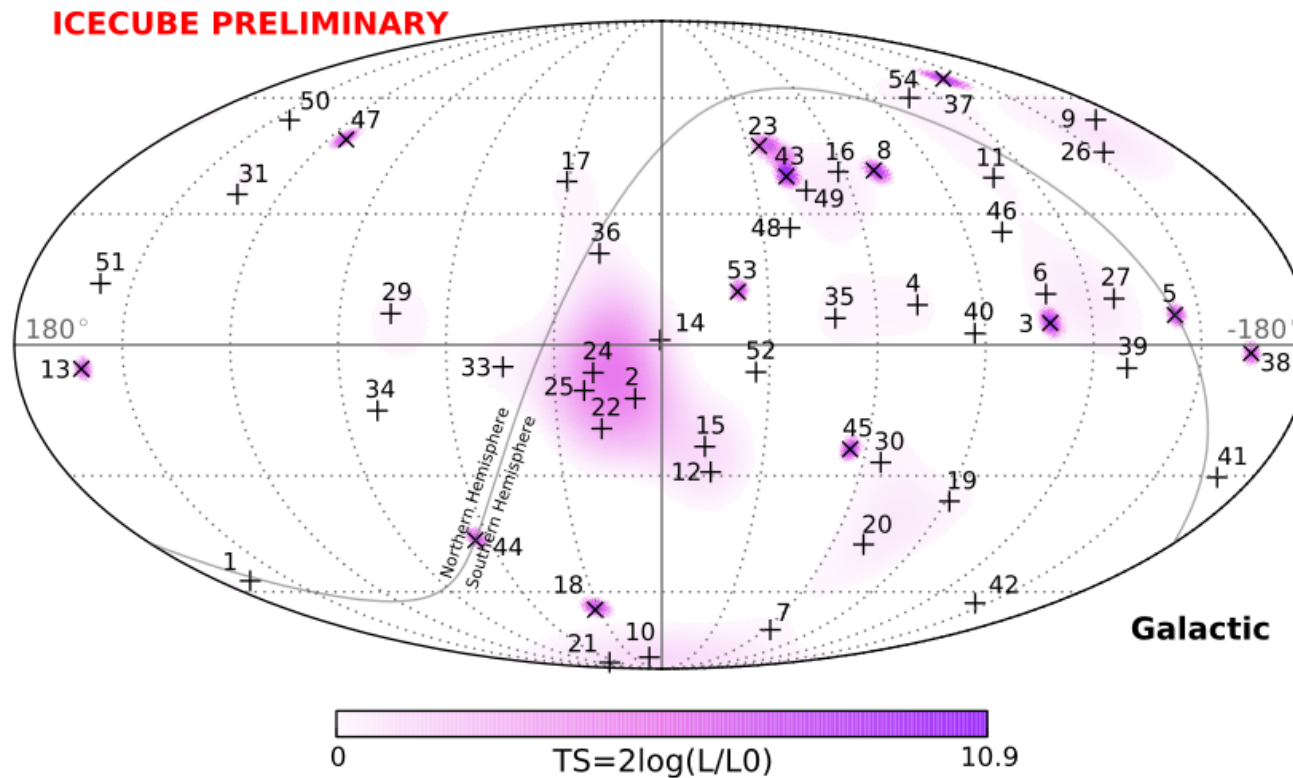


# Cosmic neutrinos yet of unknown origin

IceCube PeV energy astrophysical component



ICECUBE



# The long-standing puzzle on cosmic rays

More than 100 years of observations yet did not bring to a solution.  
 1912: VF Hess, after 7 balloon flights reaching an altitude of 5350m, found out:

- A radiation of high penetration power hits the atmosphere from above, which cannot be caused by radioactive emanations.
- This radiation contributes to the total amount of observed ionisation at lower altitudes as well.
- The sun is not the source of the extraterrestrial radiation. There is no difference between ionisation measured during the day and at night.

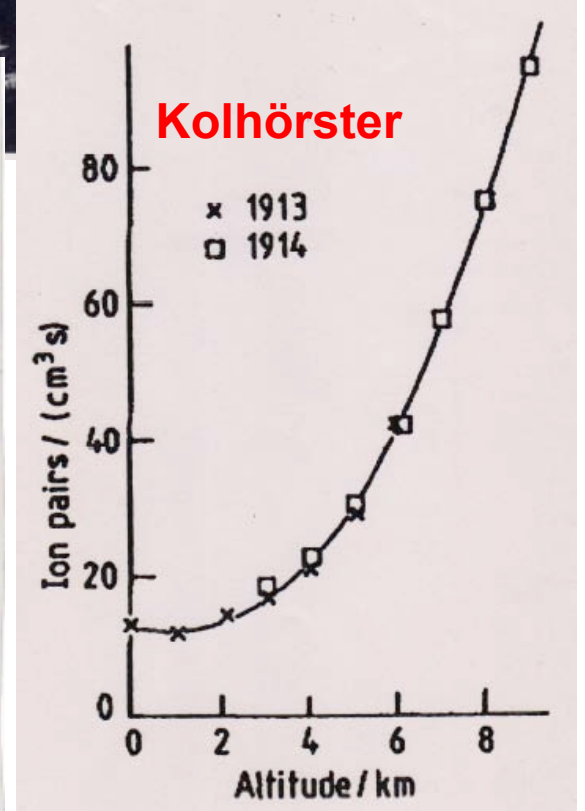


<http://www.desy.de/2012vhess>

7. Fahrt (7. August 1912).

Ballon: „Böhmen“ (1680 cbm Wasserstoff). Führer: Hauptmann W. Hoffory.  
 Meteorolog. Beobachter: E. Wolf. Luftelekt. Beobachter: V. F. Hess.

Nr.	Zeit	Mittlere Höhe		Beobachtete Strahlung				Temp.	Relat. Feucht. Proz.
		absolut m	relativ m	Apparat 1		Apparat 3			
				$\varphi_1$	$\varphi_2$	$\varphi_3$	reduz. $\varphi_3$		
1	15h 15—16h 15	156	0	17,3	12,9	—	—	1 1/2 Tag vor dem Aufstiege (in Wien)	
2	16h 15—17h 15	156	0	15,9	11,0	18,4	18,4		
3	17h 15—18h 15	156	0	15,8	11,2	17,5	17,5		
4	6h 45—7h 45	1700	1400	15,8	11,4	21,1	25,3	+6,4° 60	
5	7h 45—8h 45	2750	2500	17,3	12,3	22,5	31,2	+1,4° 41	
6	8h 45—9h 45	3850	3600	19,8	16,5	21,3	35,2	-6,3° 64	
7	9h 45—10h 45	4800	4700	40,7	31,8	—	—	-9,3° 40	
		(4400—5350)		—	—	—	—		
8	10h 45—11h 15	4400	4200	28,1	22,7	—	—	—	
9	11h 15—11h 45	1300	1200	(9,7)	11,5	—	—	—	
10	11h 45—12h 10	250	150	11,9	10,7	—	—	+16,0° 68	
11	12h 25—13h 12	140	0	15,0	11,6	—	—	(nach der Landung in Pieskow, Brandenburg)	





# Millikan's conclusions

*Nature (suppl) 121, 19, (1928)*

*Lecture at Leeds University*

These facts, combined with the further observation made both before and at this time, that within the limits of our observational error the rays came in equally from all directions of the sky, and supplemented finally by the facts that the observed absorption coefficient and total cosmic ray ionisation at the altitude of Muir Lake predict satisfactorily the results obtained in the 15.5 km. balloon flight, *all this constitutes pretty unambiguous evidence that the high altitude rays do not originate in our atmosphere, very certainly not in the lower nine-tenths of it, and justifies the designation 'cosmic rays,'* the most descriptive and the most appropriate name yet suggested for that portion of the penetrating rays which come in from above. We shall discuss just how unambiguous the evidence is at this moment after having presented our new results.

These represent two groups of experiments, one carried out in Boliviã in the High Andes at altitudes up to 15,400 ft. (4620 m.) in the fall of 1926, and the other in Arrowhead Lake and Gem Lake, California, in the summer of 1927.

# A bit of history...

Per Carlson (Physics Today, Feb 2012)

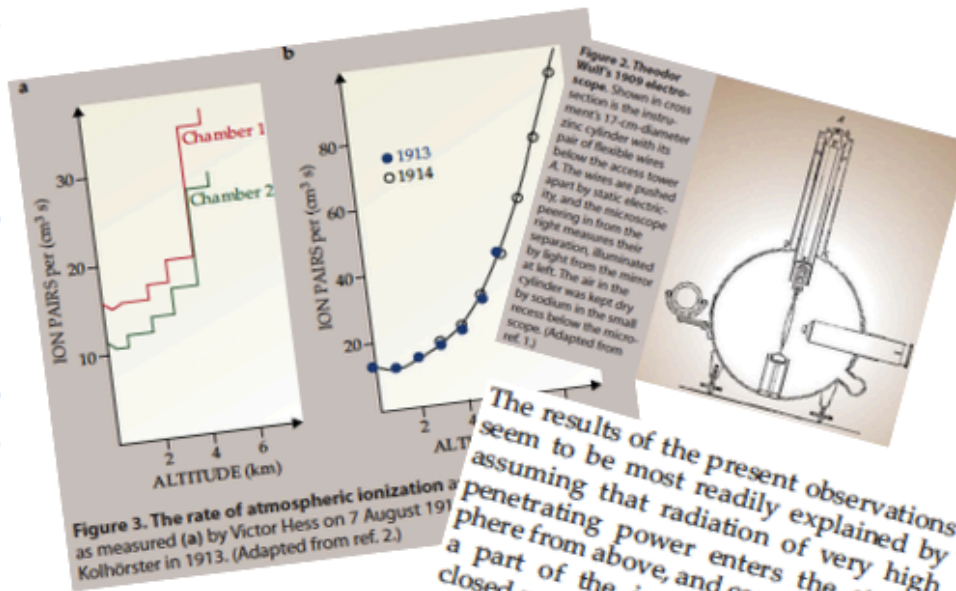


Figure 3. The rate of atmospheric ionization as measured (a) by Victor Hess on 7 August 1911 and (b) by Robert Millikan and Kohlhörster in 1913. (Adapted from ref. 2.)

The results of the present observations seem to be most readily explained by assuming that radiation of very high penetrating power enters the atmosphere from above, and can still produce a part of the ionization observed in closed vessels at the lowest altitudes.<sup>4</sup>

1912: Victor Hess discovers **cosmic rays** (named so in 1927 by Millikan) – **Nobel Prize 1936**

[1928: Paul Dirac predicts the existence of anti-particles – **Nobel Prize 1933**]

1932: Carl Anderson discovers the **positron** in **cosmic rays** - **Nobel Prize 1936** (*cloud chamber invented by C T R Wilson - Nobel Prize 1927*)

[1935: Hideki Yukawa predicts the existence of mesons – **Nobel Prize 1949**]

## A century of cosmic rays

1937: Seth Neddermeyer & Carl Anderson discover the **muon** in **cosmic rays**

1947: Cecil Powell discovers the **pion** in **cosmic rays** – **Nobel Prize 1950**

1947: George Rochester & Clifford Butler discover the **kaon**

(Patrick Blackett awarded **Nobel Prize 1948** “for development of the Wilson cloud chamber method”)

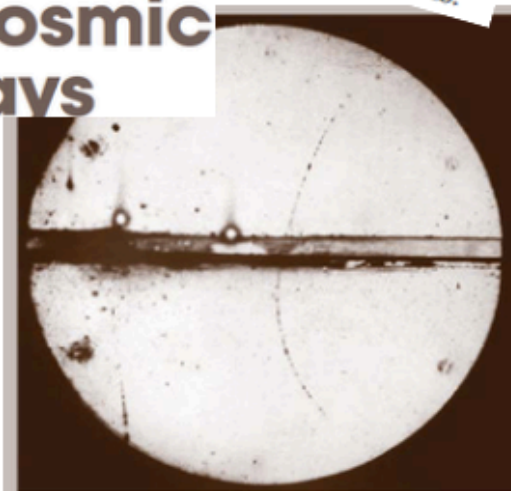
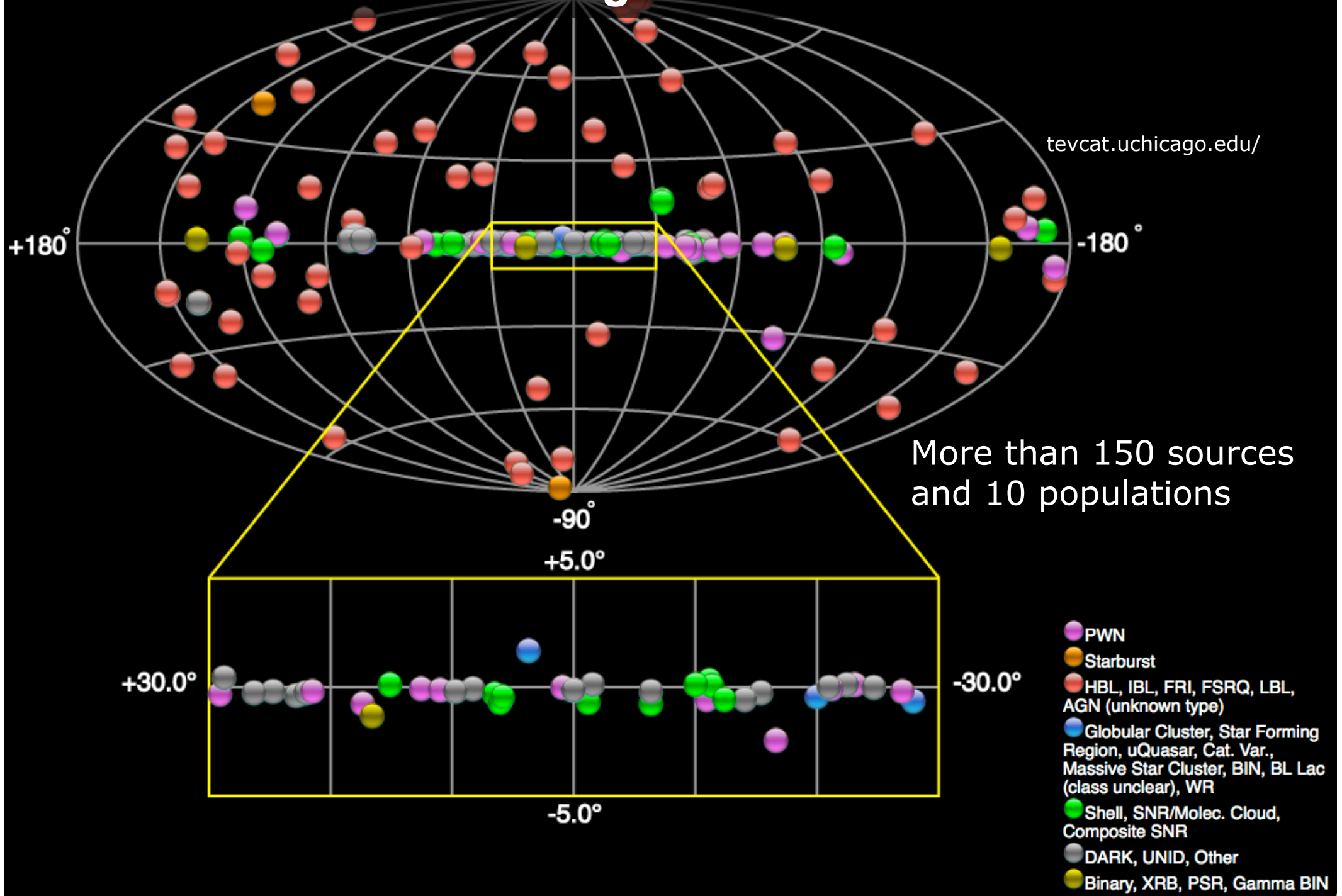


Figure 4. A historic cloud-chamber photograph taken by Carl Anderson in 1932 shows a positive particle, presumably from a cosmic-ray shower, entering from the top, curving in the chamber's transverse magnetic field, and losing energy in the lead plate. After traversing the plate, the track is much too long for a proton of that curvature. Also, the weak ionization density along the track indicated a particle much lighter than the proton. This was the first sighting of the positron proposed by Paul Dirac in 1928. (Adapted from ref. 10.)

# Approach to solve the puzzle:

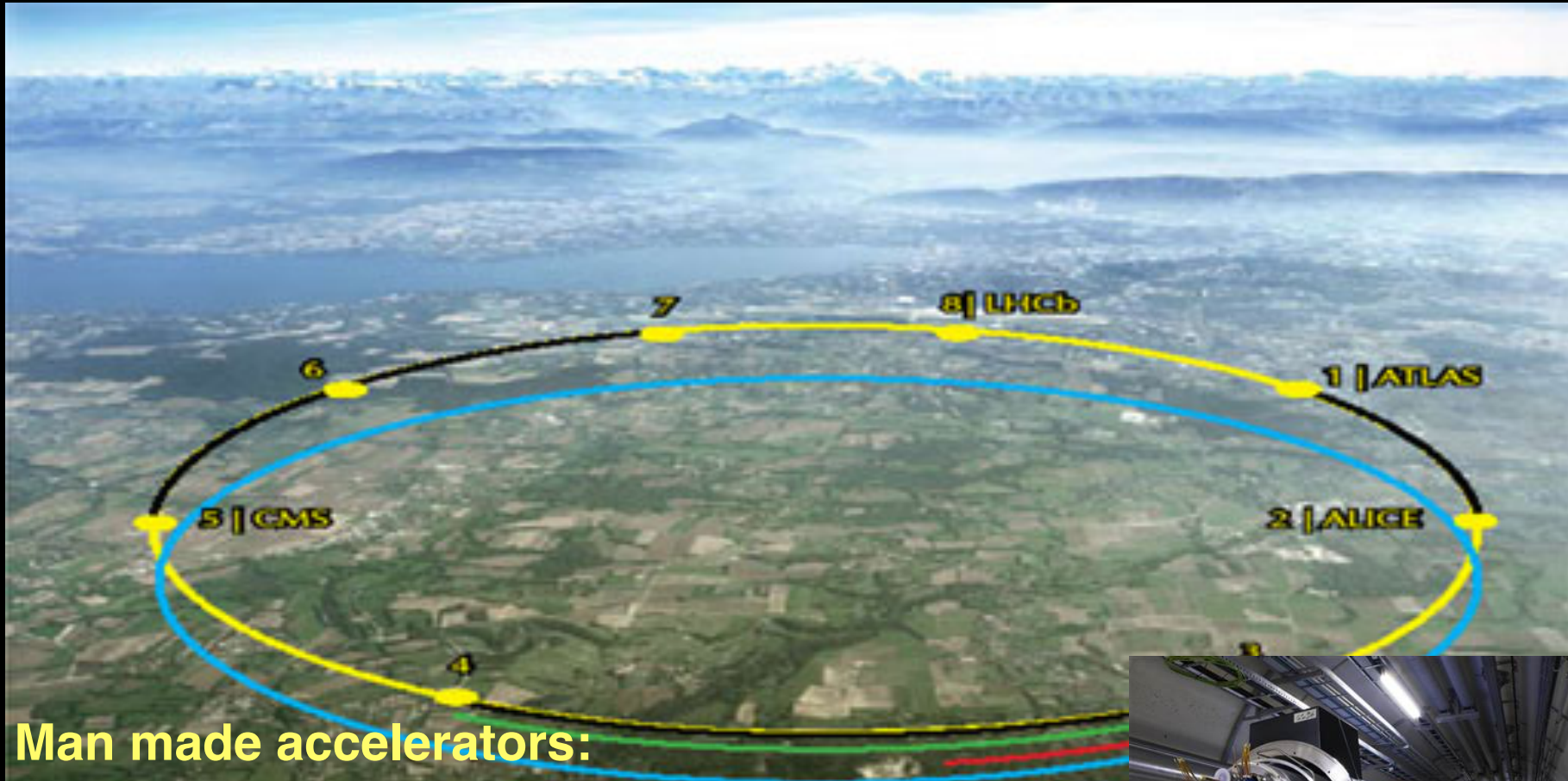
- A **multi-messenger** approach can help in untangling all unknowns but needs to cope with messenger properties (charged and neutral cosmic rays).
- Measure the **messenger's properties** (energy spectra, composition and direction);
- Identify candidate **sources** through understanding of acceleration mechanisms in extreme B-fields that can produce measured spectra and composition; **use information from photons.**
- Understand messenger **propagation in intergalactic and galactic media and in the atmosphere;**
- This requires good knowledge of nuclear cross sections and hadronic interactions in the fragmentation region and up to higher energies than colliders.
- Understanding propagation requires also understanding cosmological parameters (such as galaxy distributions, extragalactic background)
- Find direct evidence of cosmic sources on top of atmospheric backgrounds (mostly muons); gamma-rays have potential to classify such sources.
- Find the neutrinos from GZK interactions and interactions on ISM (they must be there!!)

# The most probable suspects would show up in databases of GeV-TeV gamma-sources



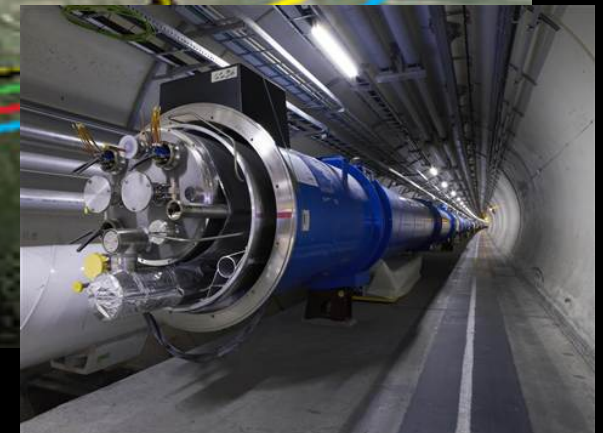
# Large Hadron Collider:

$$E_{\max} = c \cdot e \cdot B \cdot R = 7 \times 10^{12} \text{ eV}$$



## Man made accelerators:

- dynamical (collisions between particles)
- Electromagnetic: f.e.m are produced according to  $\nabla \times E = -\delta B / \delta t$



# Particle accelerator around the Earth : $10^3 \times$ LHC



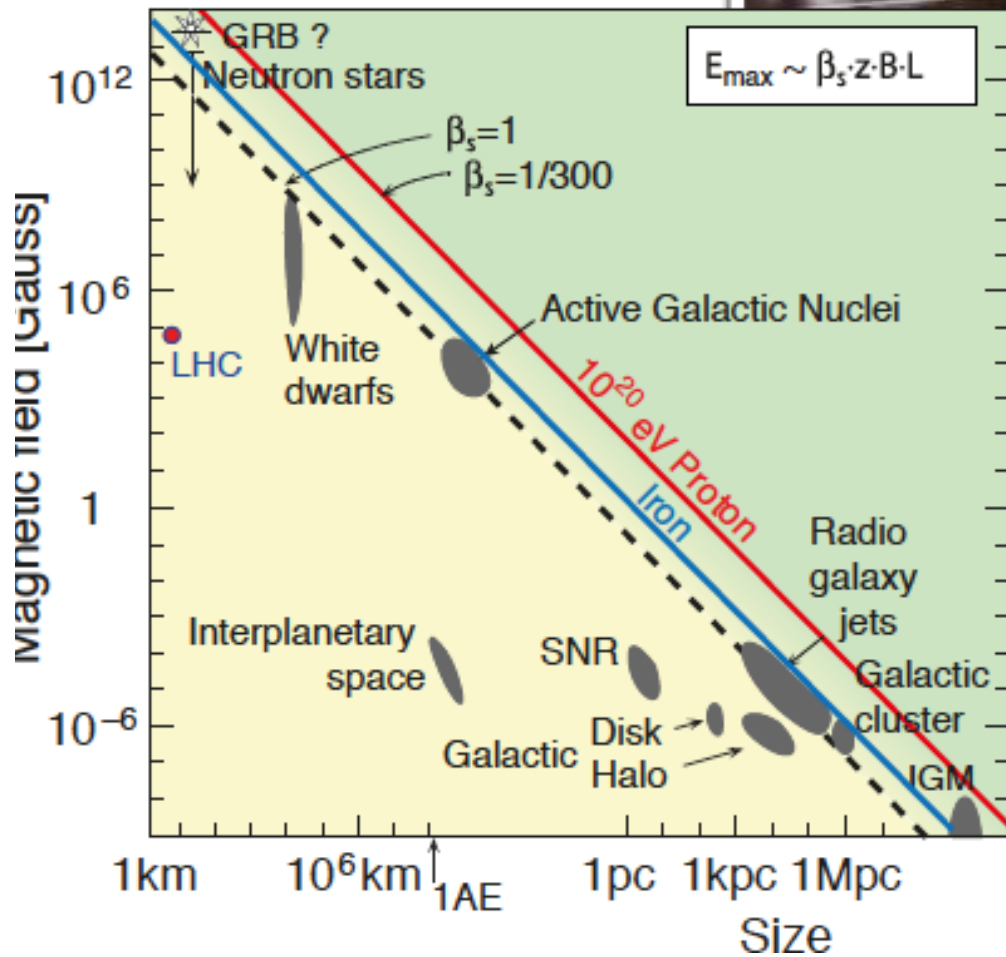
## **Astrophysical accelerators:**

- Shocks: stochastic/turbulent acceleration due to repeated collisions of particles with a shock wave due to a SN explosion, galaxy merging,...
- Magnetic reconnection (magnetic energy  $\rightarrow$  kinetic energy)
- Annihilation of DM, decay of heavy particles, leptons in B-fields (bremsstrahlung, synchrotron, Inverse Compton)

# Modernized Hillas' plot

LHC accelerator should have circumference of Mercury orbit to reach  $10^{20}$  eV!

Hillas plot (1984)



- Back of the envelope calculation (Hillas formula): **the acceleration region must be larger than the gyroradius**

$$r_L = \left(\frac{pc}{Ze}\right) \frac{1}{Bc} = \frac{E\beta_{\perp}}{ZeBc}$$

$$R_{acc} > r_L \rightarrow E \lesssim ZeBR_{acc}c$$

- If the accelerator is relativistically moving with Lorentz factor  $\Gamma$

$$E \lesssim \Gamma ZeRBc$$

(e.g. AGN jets or Gamma Ray Bursts)

# The Cosmic Ray (CR) Spectrum

- We are bombarded by stable (> 10<sup>6</sup> yrs) CR s with energy up to 10<sup>11</sup> GeV

- CRs are isotropic, sources unknown as well as the number of populations that contribute

- non-thermal spectrum:

$$\frac{dN}{dE} \propto E^{-\alpha}$$

- about 2 orders of magnitude intensity flux lost per decade

Cosmic ray are equivalent to fixed target experiment

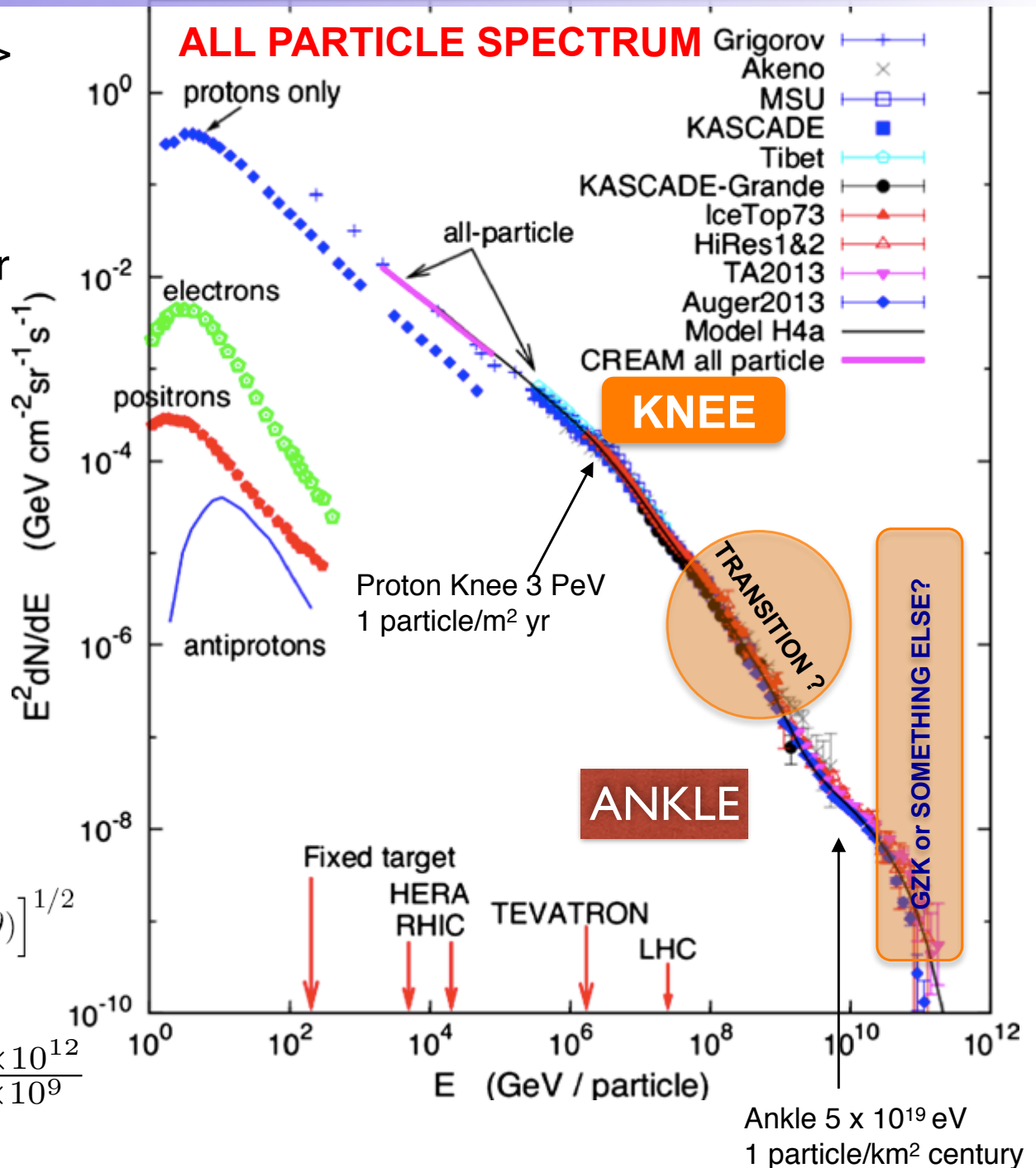
$$E_{cm} = \left[ (E_1 + E_2)^2 - (p_1 + p_2)^2 \right]^{1/2},$$

$$= \left[ m_1^2 + m_2^2 + 2E_1E_2(1 - \beta_1\beta_2 \cos \theta) \right]^{1/2}$$

$$E_{cm} \approx \text{sqrt}(2mE_{\text{projectile}})$$

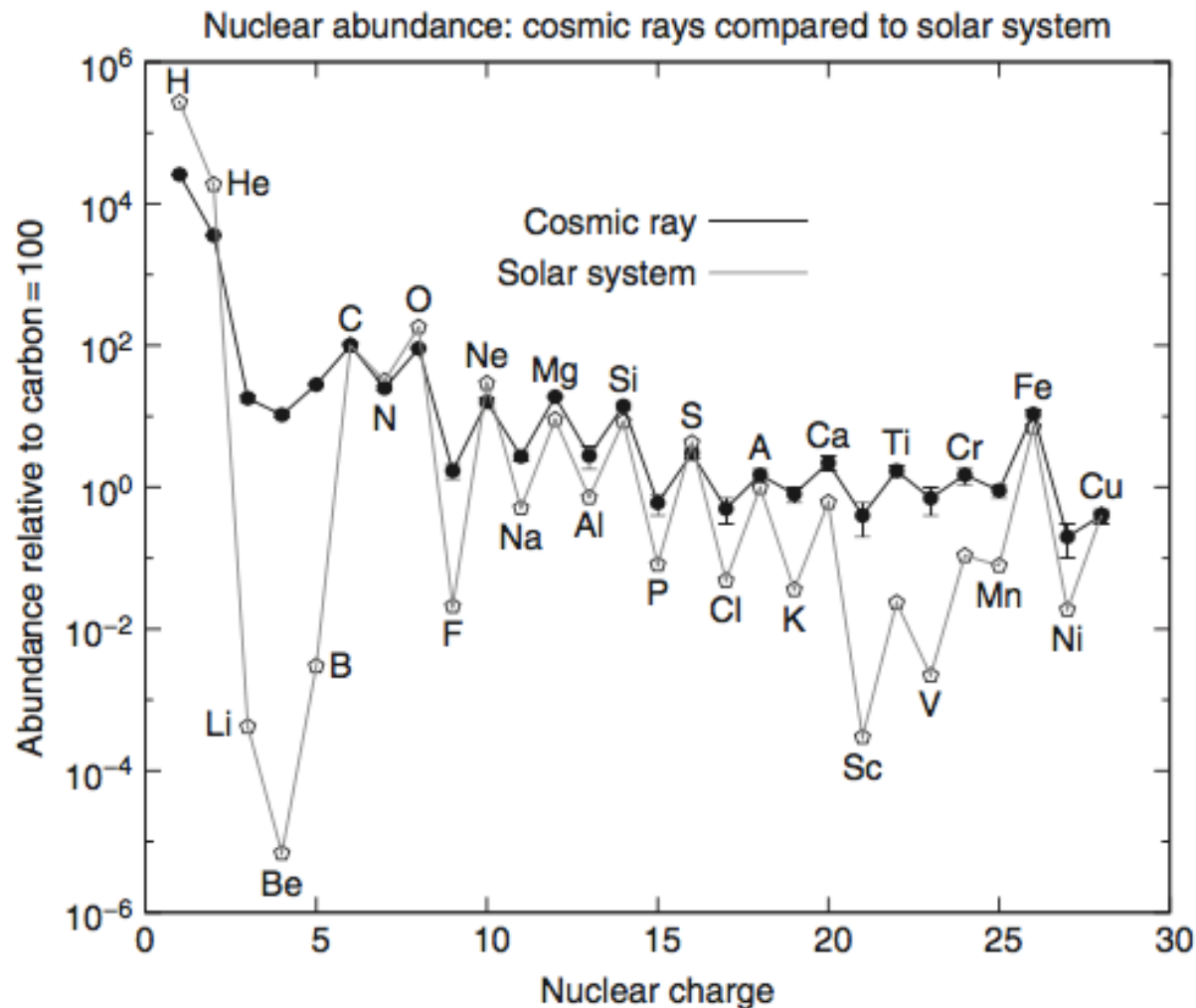
$$\begin{array}{l} \text{LHCpp} \\ 7\text{TeV}+7\text{TeV} \end{array} \quad E_{proj} = \frac{14 \times 10^{12}}{2 \times 10^9}$$

$$= 2 \times 10^{17} \text{ eV}$$





# Cosmic Ray composition below the knee

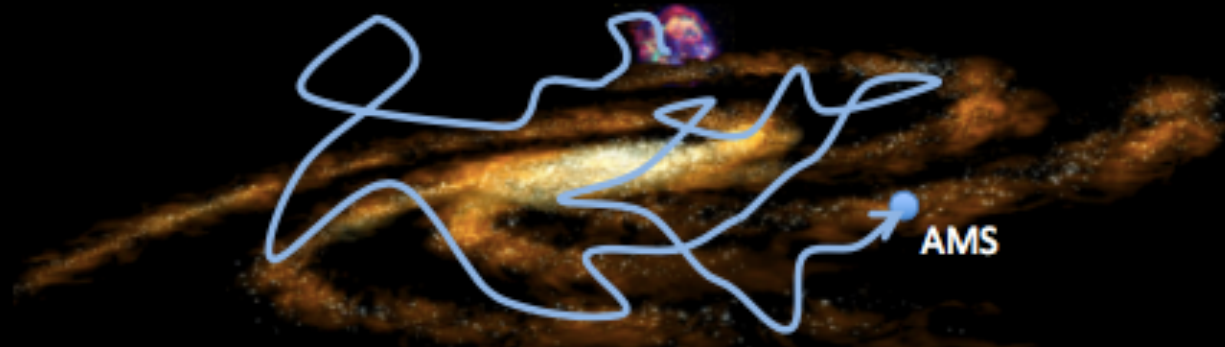


CR elemental abundances measured on Earth (filled symbols) compared to the solar system abundances (open symbols), all relative to carbon = 100.

- Elements with  $Z > 1$  are much more abundant relative to H in CRs than in the interstellar medium (ISM): H is hard to ionise;
- Li, Be, B and Sc, Ti, V, Cr, Mn are secondaries of spallation processes of the high energy primary nuclei on ISM => more abundant in CRs than ISM
- The abundances of even  $Z > odd Z$  elements in CRs (odd-even effect): nuclei with odd  $Z$  or  $A$  are more weakly bound. Magic nuclei ( $Z = 2, 8, 20, 50, 82, 126$ ) have full shells of  $n$  and  $p$ . Double magic nuclei, such as He and O) are particularly stable

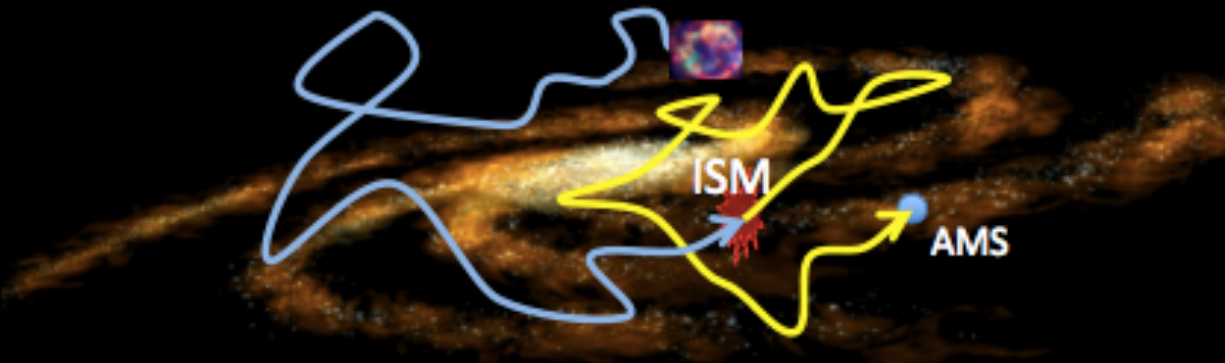
# Primary and Secondary CRs

## Primary Cosmic Rays (p, He, C, O, ...)



Primary cosmic rays carry information about their original spectra and propagation.

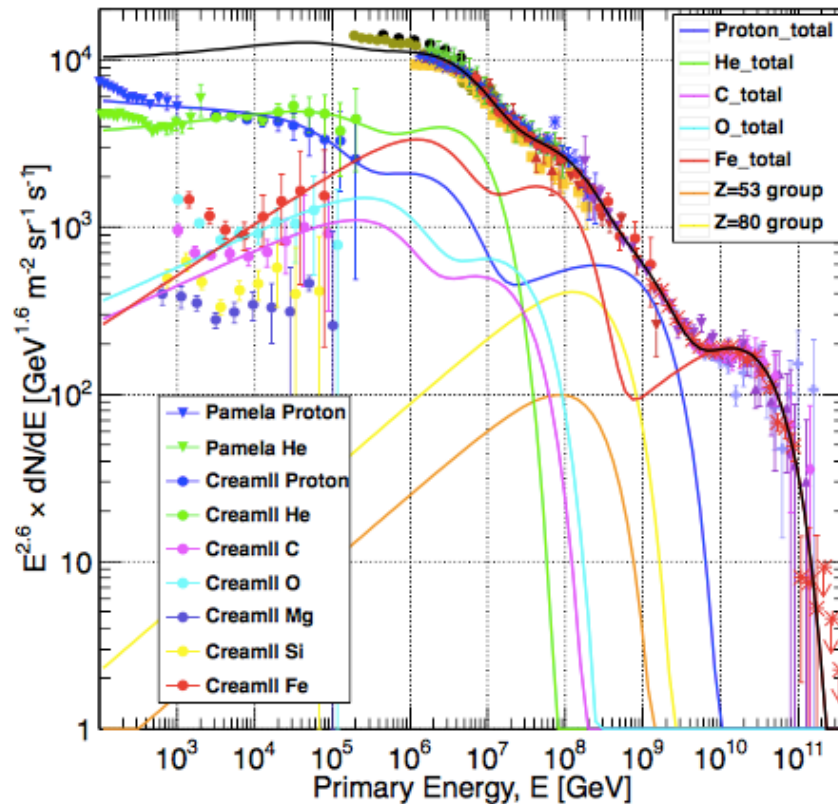
## Secondary Cosmic Rays (Li, Be, B, ...)



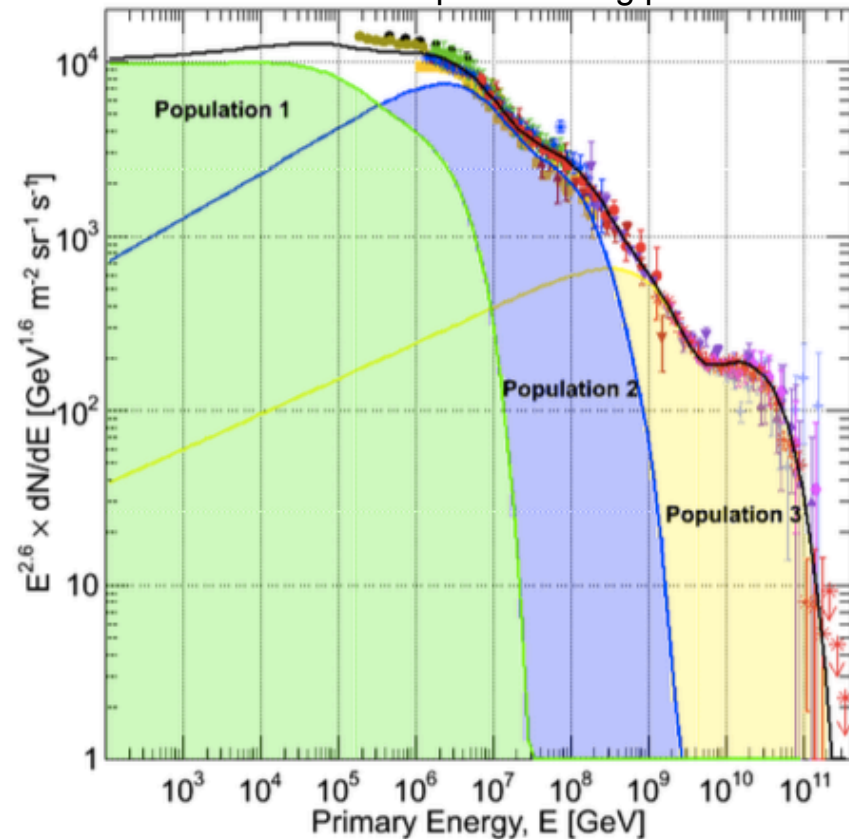
Secondary cosmic rays carry information about propagation of primaries, secondaries and the ISM.

# The All nucleon Spectrum

- The all-nucleon spectrum vs  $E/\text{nucleon}$  is the sum of free protons (about 75%), nucleons bound in He (about 17%) and heavier nuclei (about 8%) between 10-100 GeV/nucleon.
- **Peters cycle** (first measured by KASCADE): the **knee** is related to propagation and acceleration hence changes in the spectrum are rigidity-dependent. If there is a characteristic energy at which the proton spectrum steepens  $E_{\text{knee}}$ , He steepens at  $2E_{\text{knee}}$ , O at  $8E_{\text{knee}}$ , ...



<https://arxiv.org/pdf/1303.3565v1.pdf>



Below the knee (1 GeV-100 TeV): 
$$I_N(E) \approx 1.8 \times 10^4 (E/1 \text{ GeV})^{-\alpha} \frac{\text{nucleons}}{\text{m}^2 \text{ s sr GeV}}$$

# Composition

Above the proton knee of 3 PeV the composition is heavy.  
What happens at the ankle is unclear...

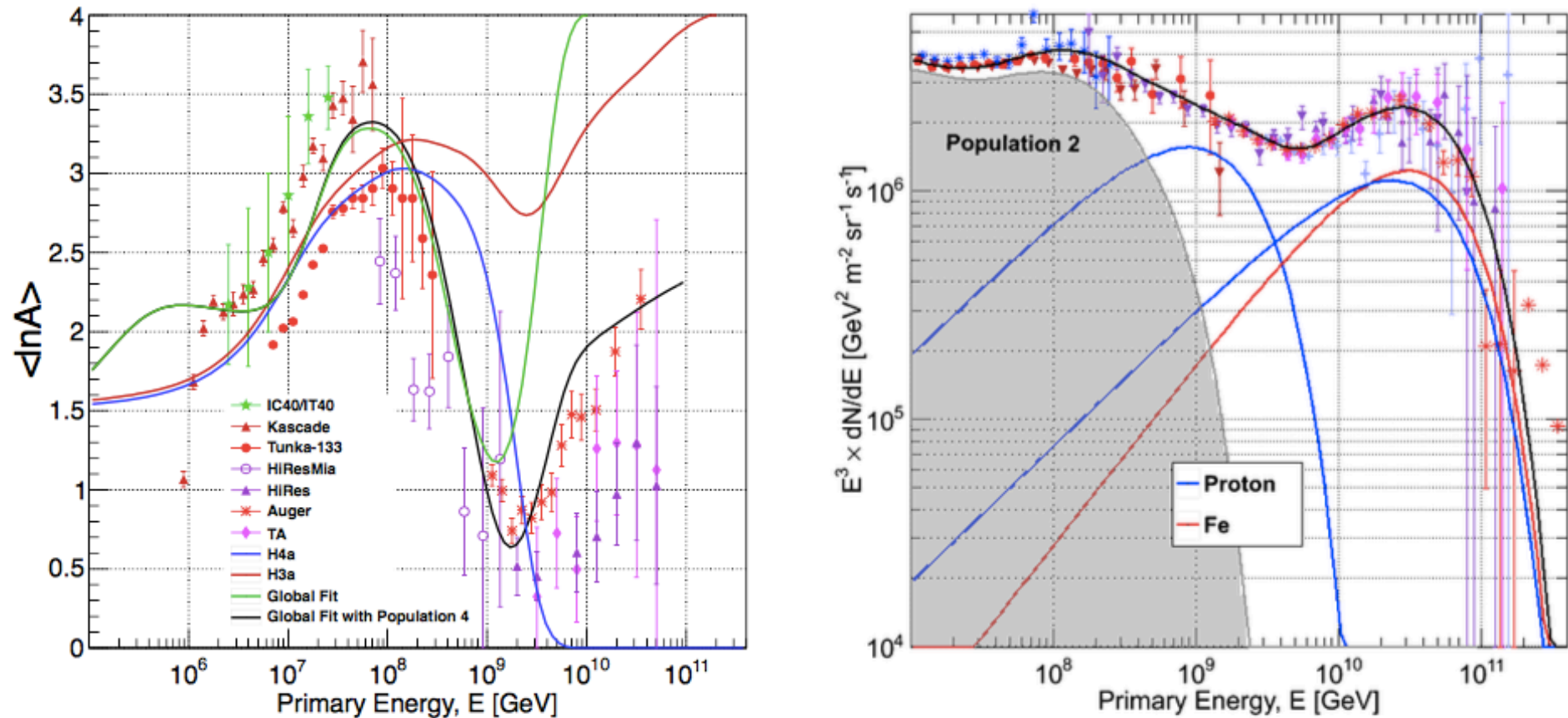


FIG. 5: Left: Mean  $\ln(A)$  for the four parameterizations of tables II and III. (For iron  $\ln(A) \approx 4$ .) Right: A modified fit with the addition of a 4th population of extra-galactic protons (see text for discussion).

# Flux and number density

Flux:  $\Phi = \frac{dN}{dAdt}$  Rate at which a flux of parallel particles cross the plane of surface  $dA$  perpendicular to the beam

The number density of particles corresponding to the beam of particles (the flux) is :

$$n(\vec{x}) = \frac{dN}{d^3x} = \frac{dN}{dl dA} = \frac{1}{\beta c} \frac{dN}{dt dA} = \frac{1}{\beta c} \Phi$$

$$d^3x = dV = dl dA \quad dl = \beta c dt$$

For astrophysical applications one considers the flux in an energy interval  $E, E+dE$  coming from an angle  $d\Omega$ :

$$\Phi(E) = \frac{dN}{dE dA dt d\Omega}$$

For an isotropic flux over the solid angle  $4\pi$  :

$$n(E, \vec{x}) = \frac{dN}{dE d^3x} = \frac{4\pi}{\beta c} \Phi(E)$$

# Galactic CR (below the knee) energy density

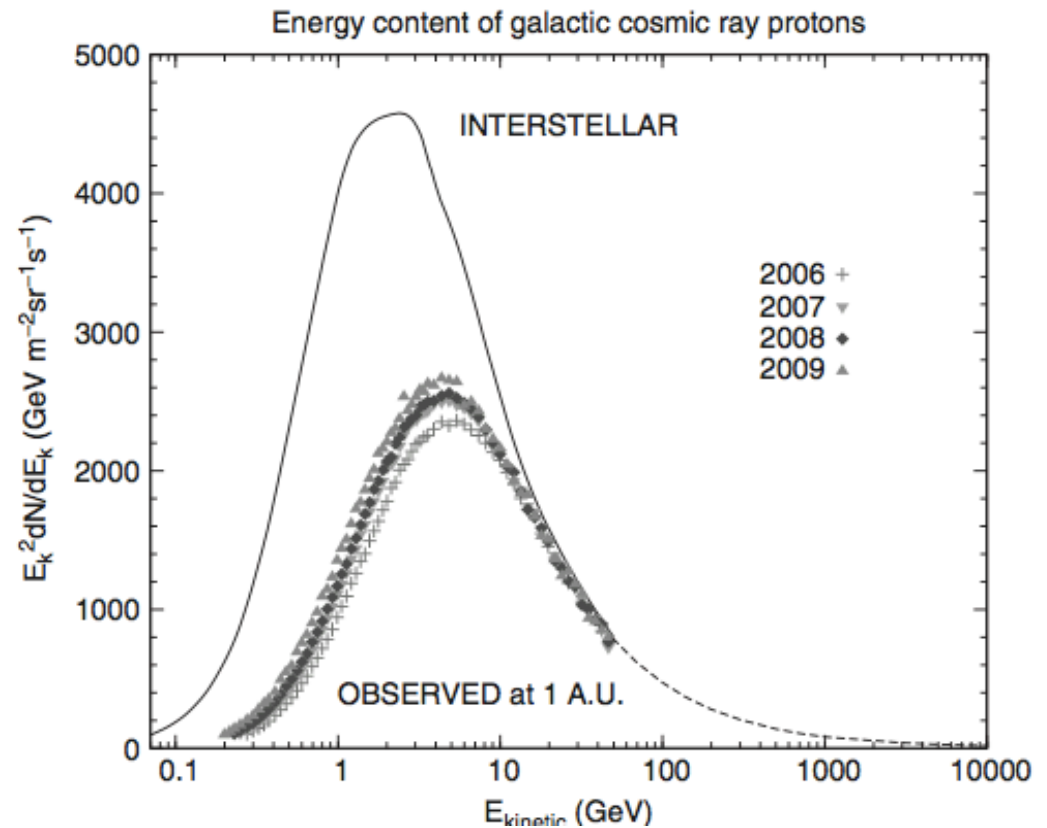
$$Flux \left( \frac{\text{particles}}{\text{cm}^2 \text{sr}} \right) = \frac{\rho_{CR} \beta c}{4\pi}$$

Hence the energy density (provided by CR sources) is:  $\rho_E = 4\pi \int \frac{E}{\beta c} \frac{dN}{dE} dE$

Below the knee:  $\frac{dN}{dE} = 1.8 \times 10^4 (E/1\text{GeV})^{-2.7} \frac{\text{nucleons}}{\text{m}^2 \text{sr s GeV}}$

$$\rho_E = \frac{4\pi}{c} \int_{1\text{GeV}}^{10^6\text{GeV}} dE 1.8 \times 10^4 (E/1\text{GeV})^{-1.7} \sim 1 \frac{\text{eV}}{\text{cm}^3}$$

for relativistic particles



# Galactic Magnetic field

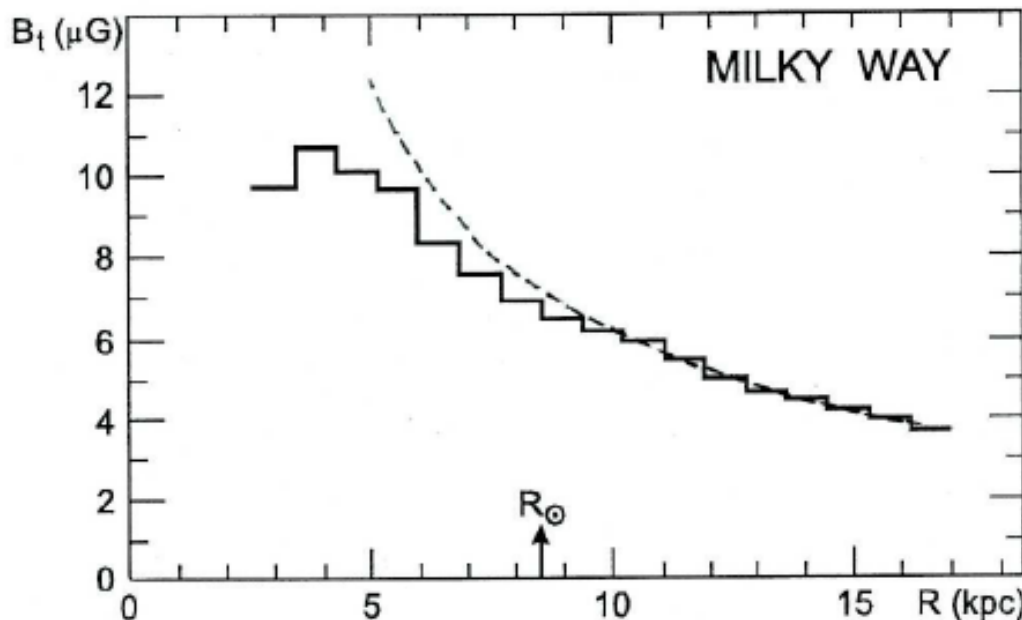
The energy density of galactic cosmic rays is comparable to the energy density of the galactic magnetic field which is on average of 3-6 uG roughly parallel to the local spiral arm:

$$\frac{B^2}{8\pi} \sim 4 \times 10^{-13} \text{ erg/cm}^3 \times 6.24 \times 10^{11} \sim 0.25 \text{ eV/cm}^3$$

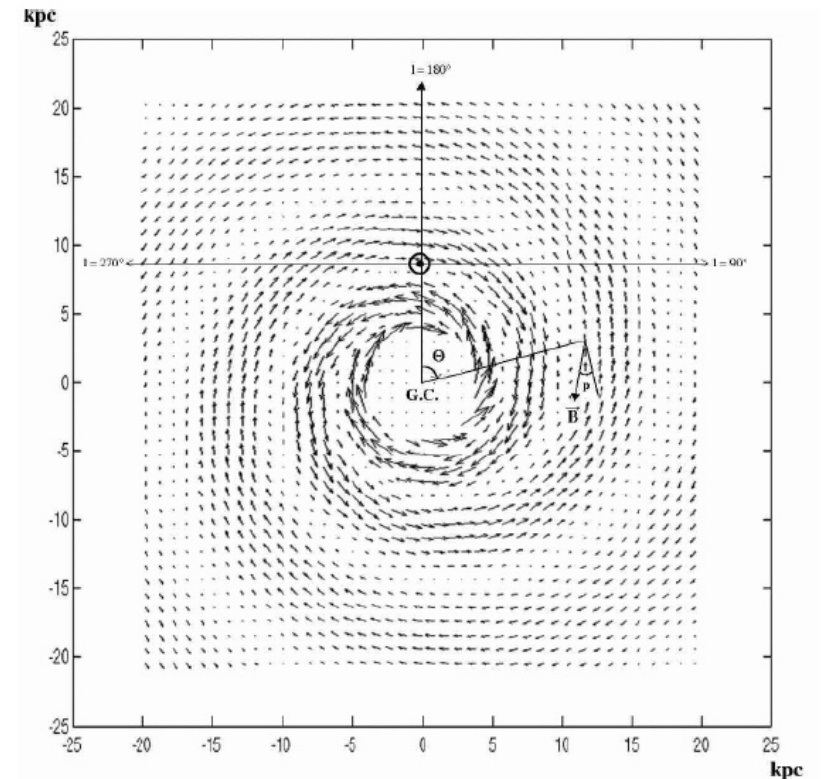
The magnetic field is frozen in to the ionised part of the gas of the Galaxy (ISM: 90% H and 10% He) which forms a magneto-hydrodynamic fluid which supports waves that travel with a characteristic speed called Alfvén velocity:

$$\frac{1}{2} \rho v_A^2 = \frac{B^2}{8\pi}$$

Particles scatter on waves. The B-field and CR are strongly coupled.



Zweibel & Heiles 1997, Nature 385,131  
Berdyugin & Teerikorpi 2001, A&A 368,635



# Origin of the transport equation

Conservation of particles:  $\frac{\partial n}{\partial t} + \nabla \cdot J = 0$        $n$  density of particles of type  $i$  at a point of space and of energy  $E$

Where we used:  $\oint J \cdot dS = \int (\nabla \cdot J) d^3r = 0$

The diffusion coefficient relates particle flow to gradient of particle density:

$$J = -D(r) \nabla n(\vec{r}, t)$$

The diffusion equation in a **stationary medium** is:

$$\frac{\partial n}{\partial t} = \nabla \cdot [D(r) \nabla n]$$

If the **fluid is in motion with a velocity field  $V(\mathbf{r})$**  the equation

becomes:  $\frac{\partial n}{\partial t} + V \cdot \nabla n - \nabla \cdot [D(r) \nabla n] = 0$

Convection

Diffusion term

yet no source term and no energy loss term



# Origin of the transport equation

If sources inject particles of type  $i$  time dependent rate  $q_i(\vec{r}, E, t)$  and we add losses of nuclei of type  $i$  by collisions with H in ISM of density  $\rho = m_p/\text{cm}^3$  and decay at a rate:

$$p_i = \frac{v\rho\sigma_i}{m_p} + \frac{1}{\gamma\tau_i} = \frac{v\rho}{\lambda_i} + \frac{1}{\gamma\tau_i}$$

rate at which nuclei  $i$  interacts with H

collision length of nuclei  $i$

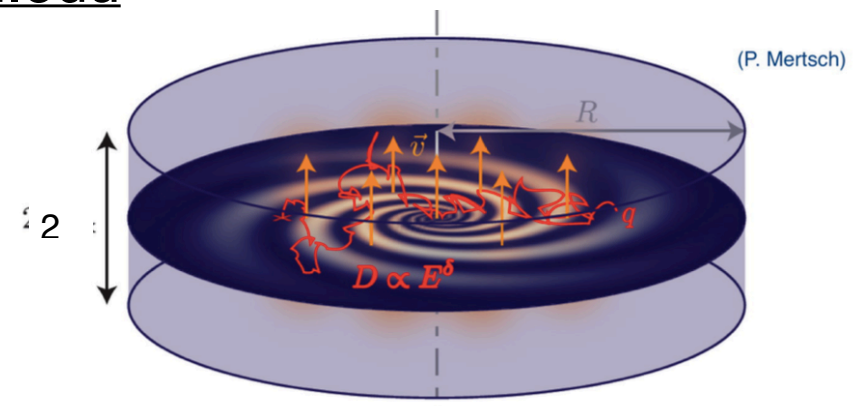
relativistic decay length of nuclei  $i$

$$\frac{\partial n_i(E, \vec{r})}{\partial t} + \underbrace{V \cdot \nabla n_i(E, \vec{r})}_{\text{convection term}} - \underbrace{\nabla \cdot [D(r)\nabla n_i(E, \vec{r})]}_{\text{Diffusion term}} = \underbrace{q_i(\vec{r}, E, t)}_{\text{Source term}} - \underbrace{p_i n_i(E, \vec{r})}_{\text{Losses term}} + \frac{v\rho(\vec{r})}{m_p} \sum_{k \geq i} \int \frac{d\sigma_{i,k}(E, E')}{dE} n_k(E', \vec{r}) dE'$$

Gain term from spallation of heavier nuclei (energy/nucleon remains constant in spallation)

To obtain the CR spectrum one would need to solve the transport equation. This is done by the GALPROP code including H and He of ISM: <http://galprop.stanford.edu>

GALPROP yields ~ the same answer for equilibrium fluxes as the 'leaky box' model and leads to exponential distributions of path lengths of CRs from sources to Earth.



# Leaky Box Model

If CR nuclei are in a stationary condition ( $n_i = \text{const}$ ) and the diffusion and convection terms are substituted by an escape probability from the Galaxy containment volume with very small characteristic time:

$$\tau_{esc} \ll \frac{c}{h}$$

Mean time in containment volume

$$\lambda_{esc} = \rho \beta c \tau_{esc}$$

Mean amount of matter traversed before escaping

$$\frac{\partial n_i(E, \vec{r})}{\partial t} + V \cdot \nabla n_i(E, \vec{r}) - \nabla \cdot [D(r) \nabla n_i(E, \vec{r})] = q_i(\vec{r}, E, t) - p_i n_i(E, \vec{r}) + \frac{v \rho(\vec{r})}{m_p} \sum_{k \geq i} \int \frac{d\sigma_{i,k}(E, E')}{dE} n_k(E', \vec{r}) dE'$$

$\downarrow$   
**0**

$\underbrace{\hspace{10em}}$   
 $\frac{n_i(E, \vec{r})}{\tau_{esc}}$

the probability of a particle remaining in the box after a time  $t$  is  $\exp(-t/\tau_{esc})$

source term

Loss term due to interactions

production term due to spallations

$$\frac{n_i(E)}{\tau_{esc}} = q_i(E) - \left[ \frac{\beta c \rho}{\lambda_i} \right] n_i(E) + \frac{\beta c \rho}{m_p} \sum_{k \geq i} \sigma_{i,k} n_k(E)$$

# The CR age

If we apply the equation to B (stable and not produced by sources  $q_B = 0$ ) and considering C and O the source nuclei with similar flux:

$$\frac{n_B(E)}{\tau_{esc}} + \left[ \frac{\beta c \rho}{\lambda_B} \right] n_B(E) = \frac{\beta c \rho}{m_p} (\sigma_{C \rightarrow B} n_C(E) + \sigma_{O \rightarrow B} n_O(E))$$

$$\frac{n_B(E)}{\tau_{esc}} \left( 1 + \frac{\lambda_{esc}}{\lambda_B} \right) = \frac{\beta c \rho}{m_p} (\sigma_{C \rightarrow B} + \sigma_{O \rightarrow B}) n_C(E)$$

$$\frac{n_B(E)}{n_C(E)} = \frac{\lambda_{esc}(E)}{1 + \frac{\lambda_{esc}(E)}{\lambda_B}} \frac{\sigma_{C \rightarrow B} + \sigma_{O \rightarrow B}}{m_p}$$

where we can plug measured values of cross sections and the interaction length of B:

$$\lambda_B \sim 7 \text{ g/cm}^2; \sigma_{C \rightarrow B} \sim 73 \text{ mb}; \sigma_{O \rightarrow B} \sim 236 \text{ mb}$$

From the measured value of B/C we find an energy dependent escape length:

$$\lambda_{esc} = \beta c \rho \tau_{esc} = 10 - 15 \frac{\text{g}}{\text{cm}^2} \beta \left( \frac{4 \text{ GV}}{R} \right)^\delta \quad \delta \sim 0.3-0.6$$

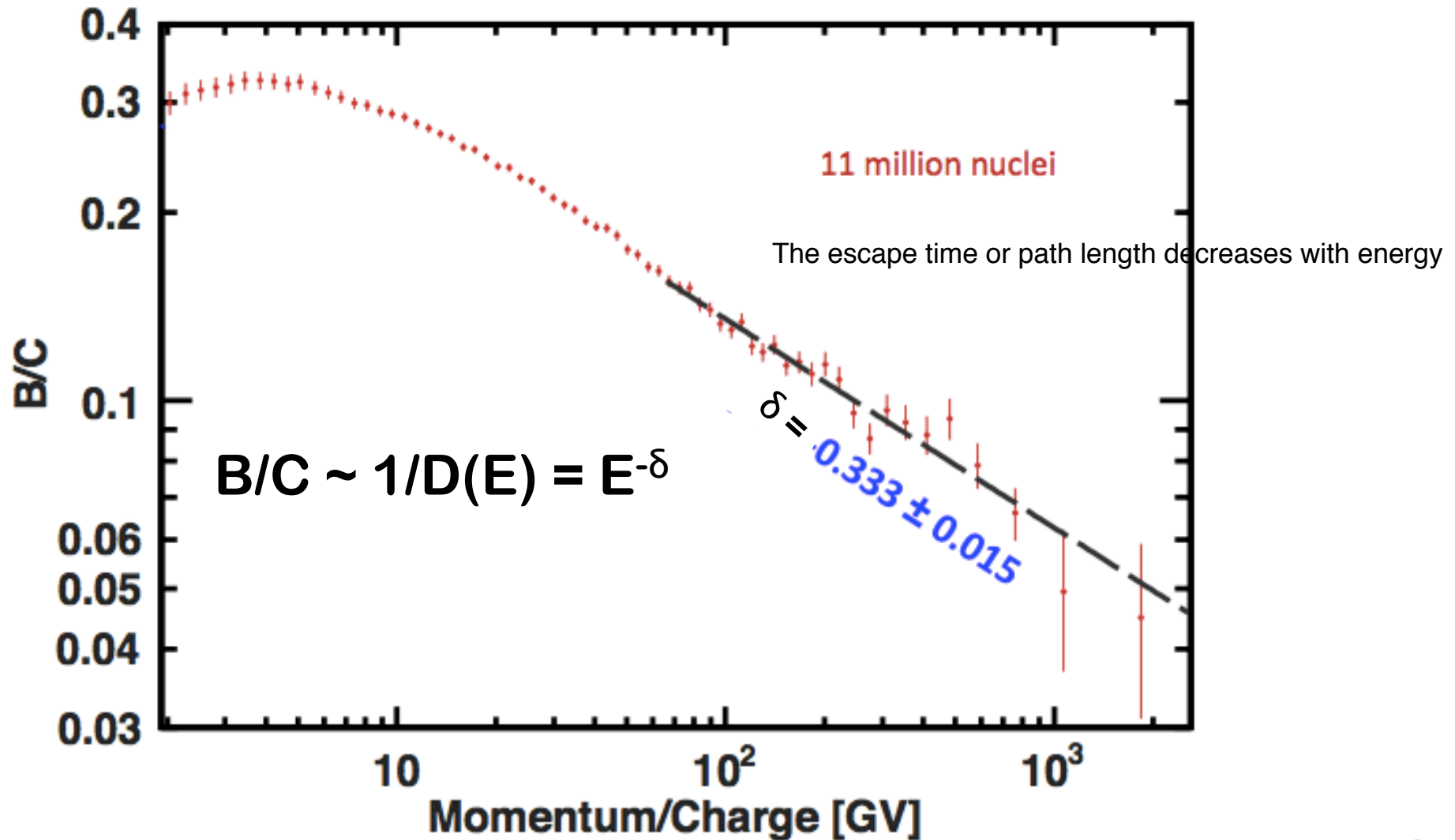
for  $R > 4 \text{ GV}$

Hence the age of the CRs in the Galaxy depends on the energy and amounts to millions of years

$$\tau_{esc} = \lambda_{esc} / \beta c \rho$$

# AMS B/C measurement

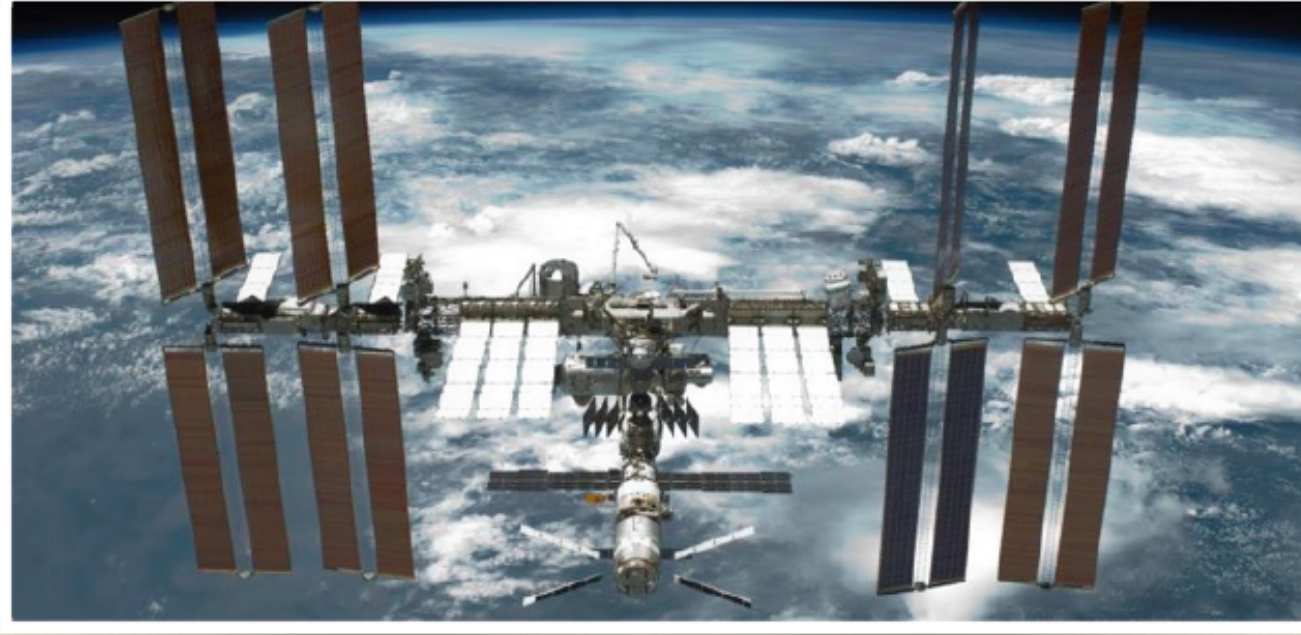
## AMS Physics Result: The Boron-to-Carbon (B/C) flux ratio



M. Aguilar *et al.*, Phys. Rev. Lett. 117, 231101 (2016)

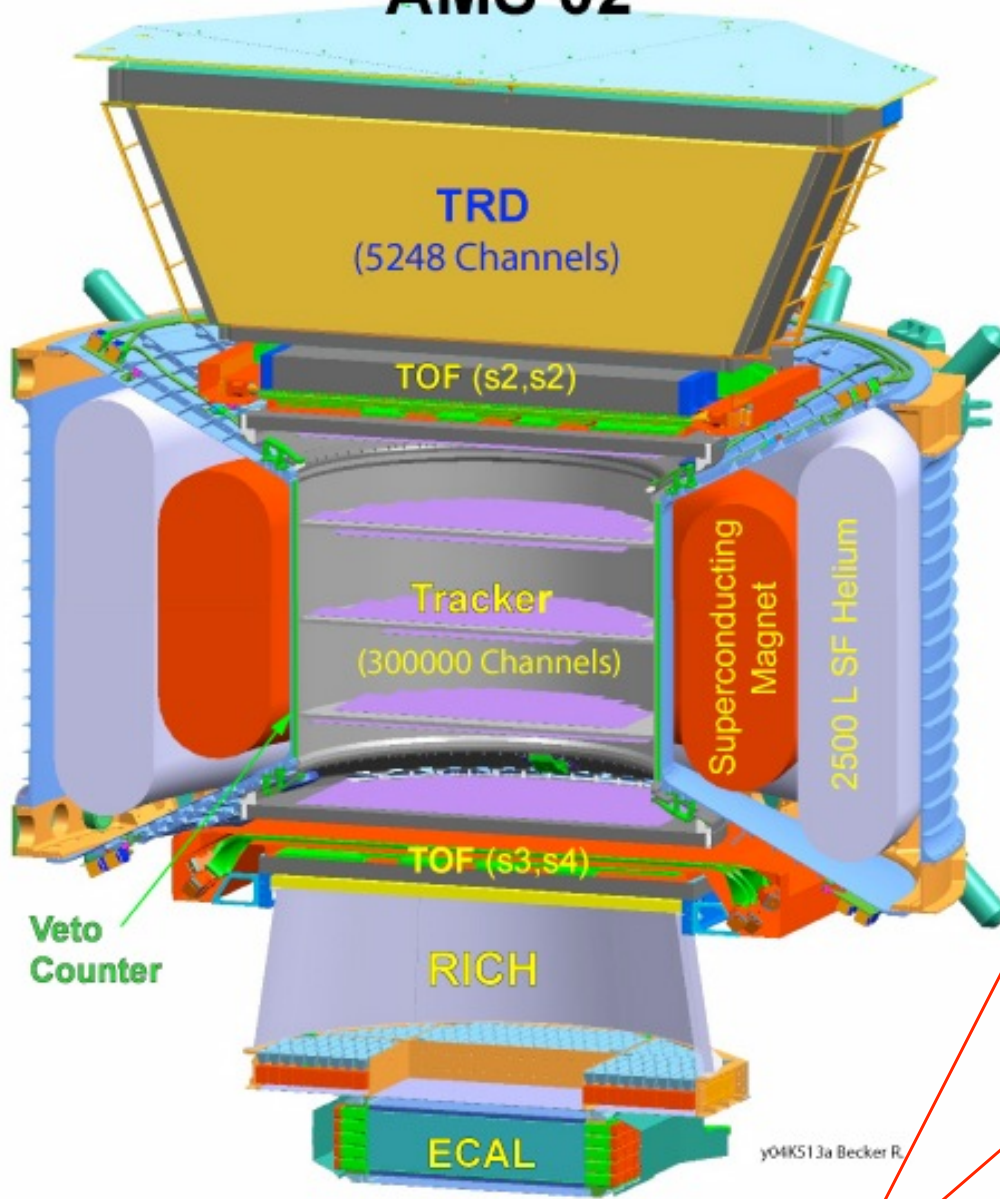
not 0.6! non-linear shock diffusion hint...

# AMS-02 on the International Space Station



- ISS : 108 m x 80m, 420 t
- orbit height 400km
- Inclination =  $51.57^\circ$
- 15.62 revolutions/day
- **AMS:** acceptance:  $0.45 \text{ m}^2 \text{ sr}$
- Long exposure: 3 years
- Redundant measurements
- Strong gradients of temperature  $-60^\circ\text{C} \div +40^\circ\text{C}$
- Weight < 7 Tons
- Power consumption < 3kW

# AMS 02



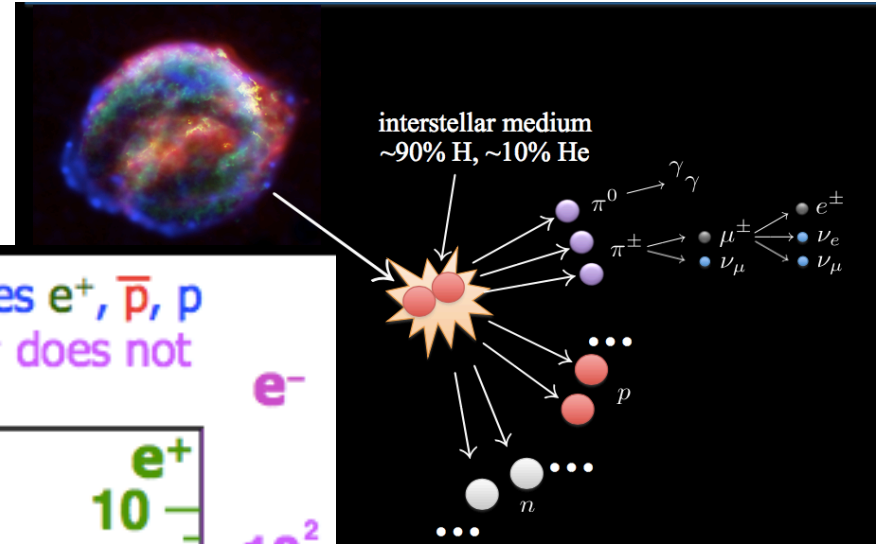
- TRD (e/p)
- Scintillator system (TOF) ( $\beta$ ,  $dE/dx$ , trigger)
- Superconducting magnet ( $BL^2= 0.85 \text{ Tm}^2$ )
- Silicon Tracker (rigidity, charge)
- RICH ( $\beta$ , charge)
- Em. Calorimeter(energy, e/p)

	$e^-$	$e^+$	P	$\bar{\text{He}}$	$\gamma$	$\gamma$
TRD						
TOF						
Tracker						
RICH						
Calorimeter						

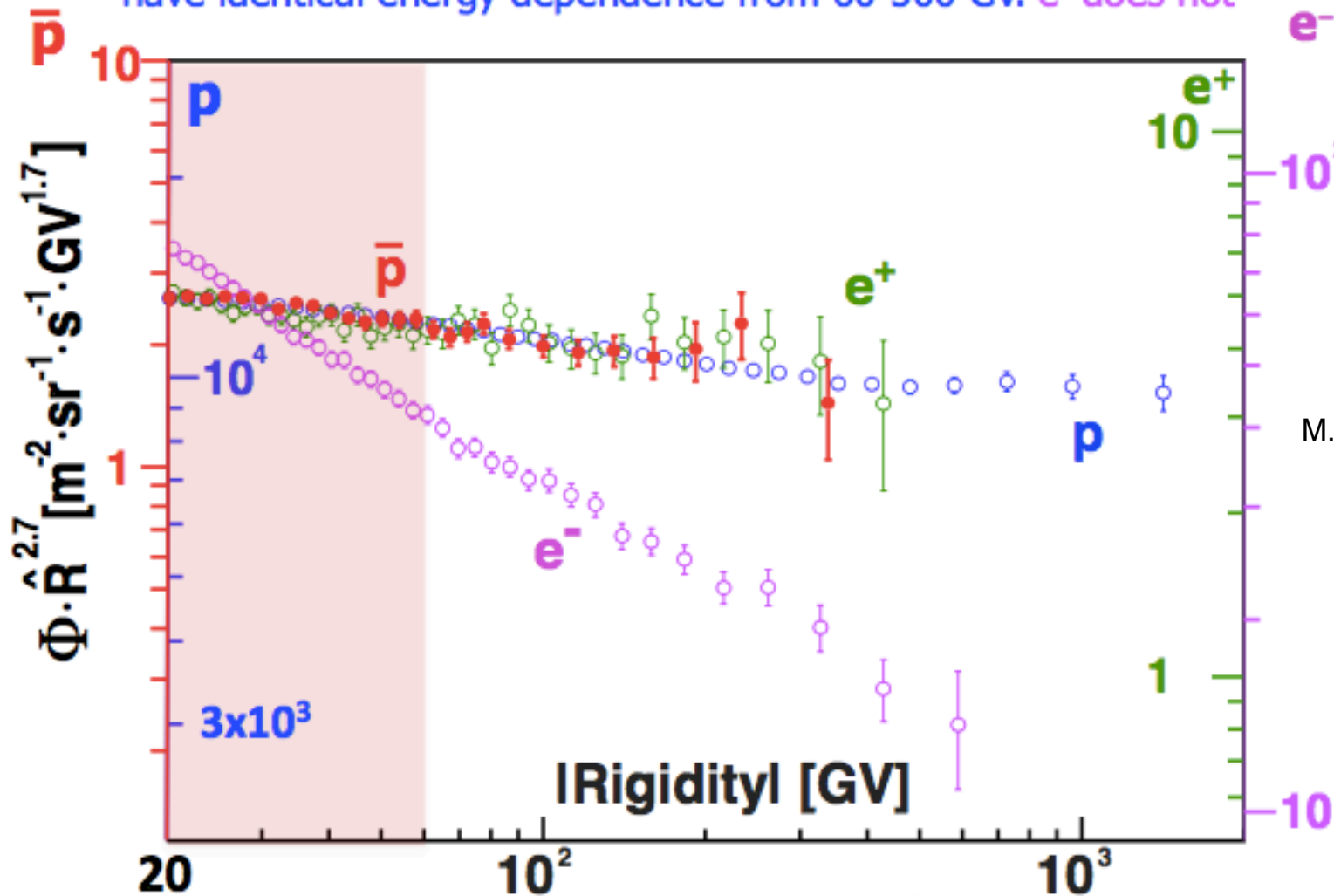
Particle ident.

Rigidity meas.

# AMS findings: local sources or DM?



Unexpected Result: The Spectra of Elementary Particles  $e^+$ ,  $\bar{p}$ ,  $p$  have identical energy dependence from 60-500 GV.  $e^-$  does not



M. Schumann's lectures on DM

# Low energy galactic spectra in the leaky box

For primary nuclei for which no secondaries are created during propagation spectra the leaky box model equation:

$$\frac{n_i(E, \vec{r})}{\tau_{esc}} = q_i(E) - \left[ \frac{\beta c \rho}{\lambda_i} \right] n_i(E) + \frac{\beta c \rho}{m_p} \sum_{k \geq i} \sigma_{i,k} n_k(E)$$

0

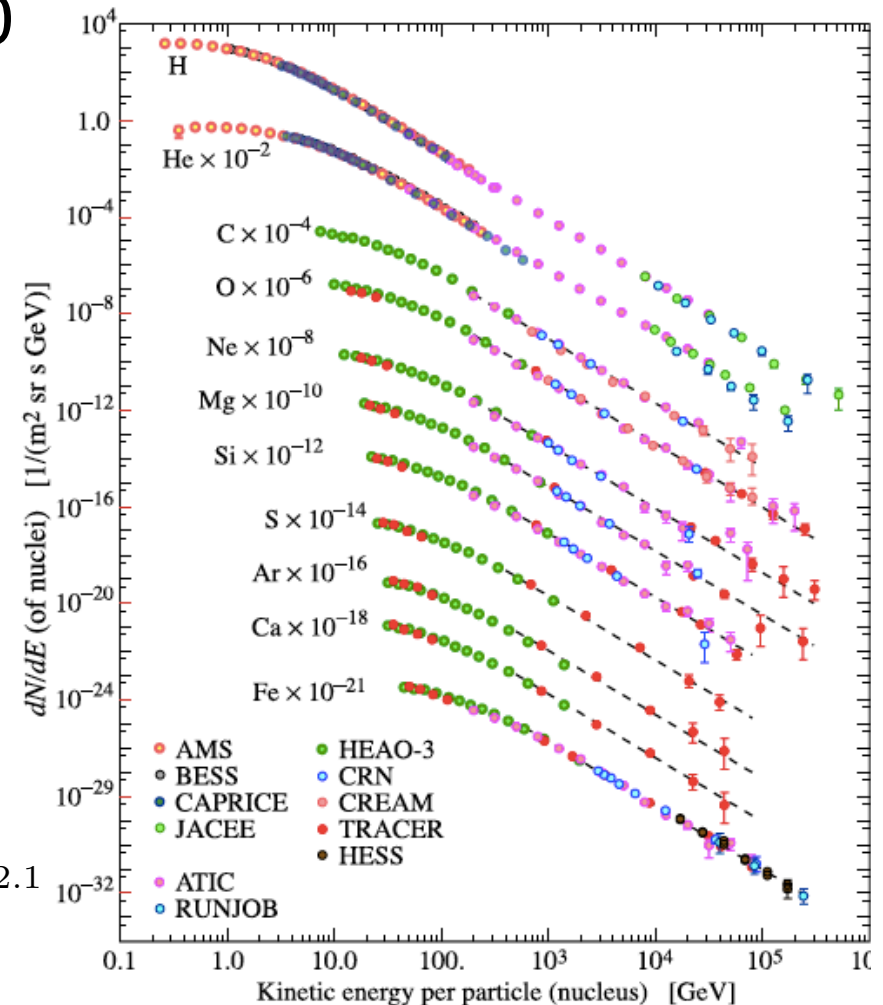
$$n_P(E) = \frac{q_P(E) \tau_{esc}(E)}{1 + \lambda_{esc}(E) / \lambda_P}$$

If the interaction term dominates on the escape one, as in the case of protons  $\lambda_{esc}$  (5-10 g/cm<sup>2</sup>) <  $\lambda_P = (\rho_{ISM} \sigma_{int})^{-1} = 1.67 \times 10^{-27} \text{ kg} / (1 \text{ cm}^{-3} \times 50 \times 10^{-27} \text{ cm}^2) = 34 \text{ g/cm}^2$  spectra resemble **the source spectrum**.

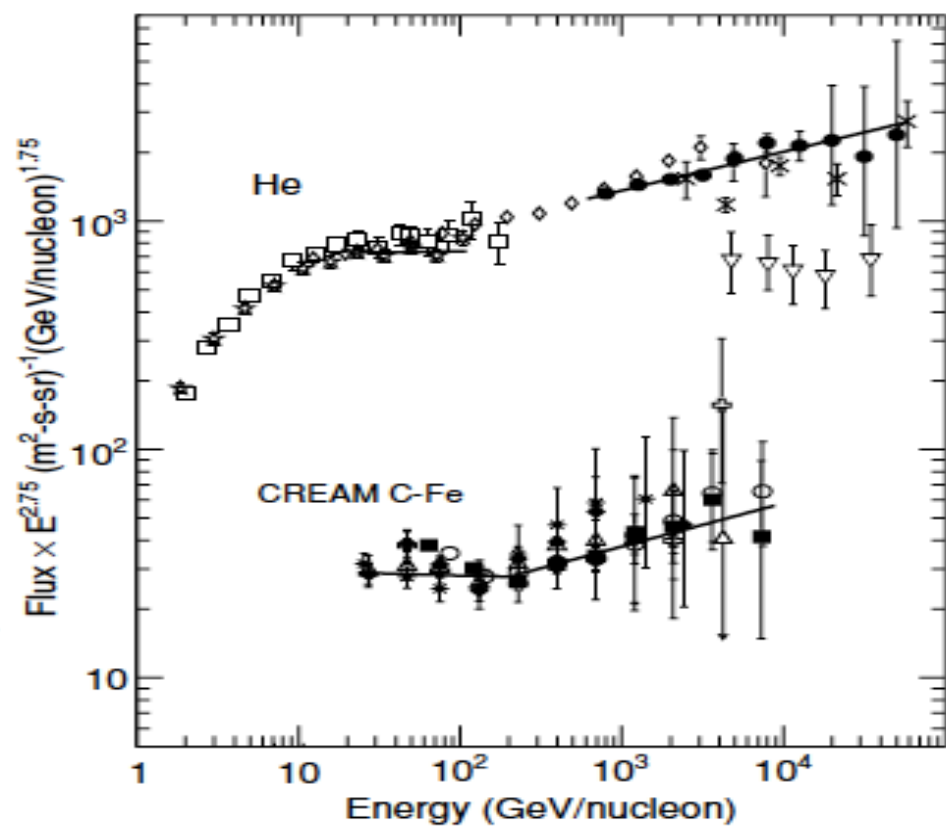
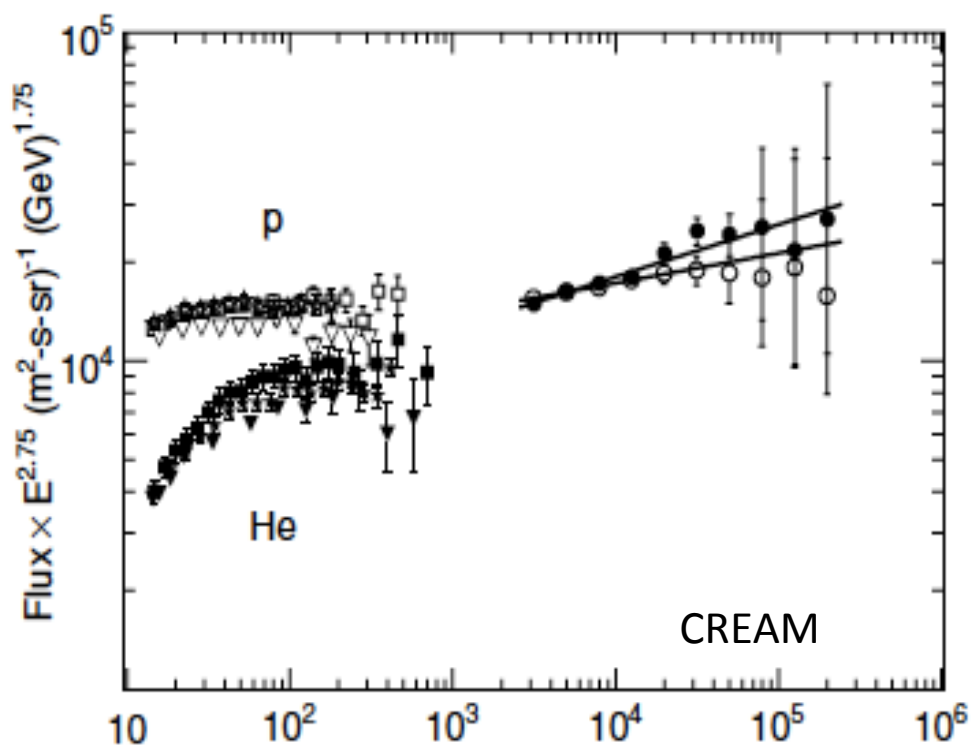
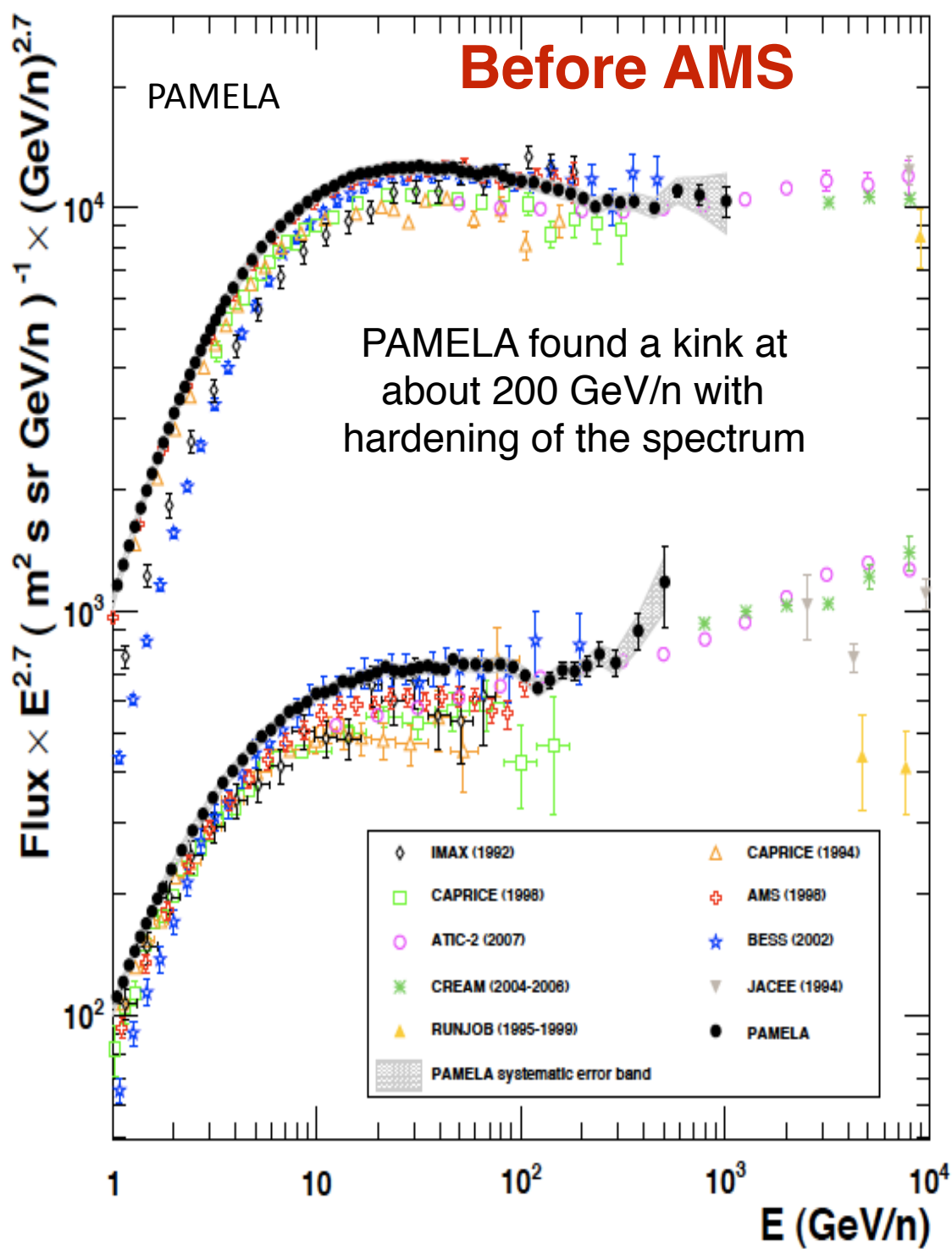
If the observed spectrum is  $n_P(E) \propto E^{-\alpha}$

The source spectrum is

$$q_P(E) \propto n_P(E) / \tau_{esc} = E^{-\alpha-\delta} \sim E^{-2.7-(0.3 \div 0.6)} \sim E^{-2.4 \div 2.1}$$







# p/He ratio

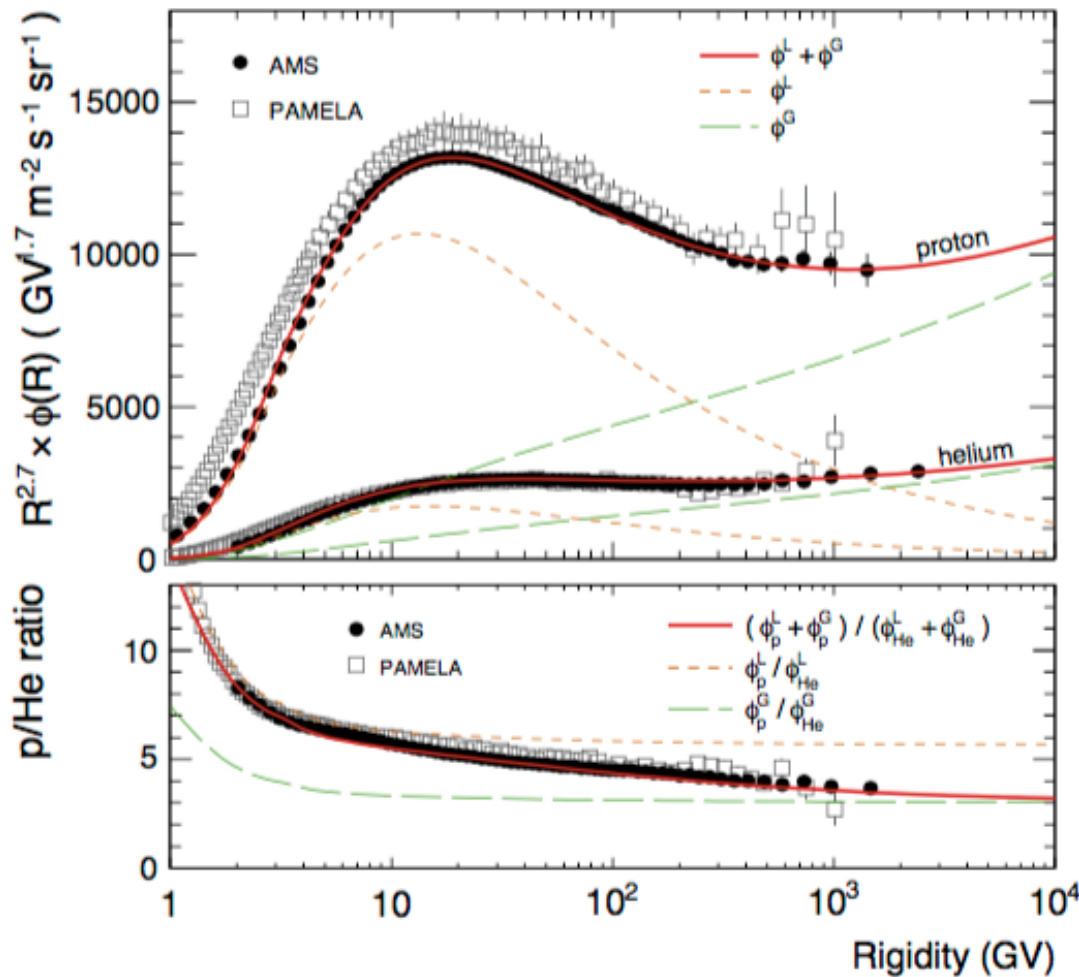


FIG. 2.— Top: rigidity spectra proton and helium multiplied by  $R^{2.7}$ . The solid lines indicate the model calculations. The flux contribution arising from the two components  $\phi^L$  and  $\phi^G$  are shown as dashed lines. The data are from and AMS (Aguilar et al. 2015a,b) and PAMELA (Adriani et al. 2011).

AMS confirmed PAMELA result and found that the He spectrum is harder than H one.

$$qvB = \frac{mv^2}{r_L} \Rightarrow r_L = \frac{p}{ZeB}$$

Gyroradius

$$r_L = 33.36 \text{ km} \left( \frac{p}{\text{GeV}/c} \right) \left( \frac{1}{Z} \right) \left( \frac{G}{B} \right)$$

Rigidity

$$R \equiv r_L Bc = \frac{pc}{Ze}$$

# Who are the accelerators and how do they accelerate?



In a SN gravitational energy released is transformed into acceleration



$E^{-2}$  spectrum

## *ON SUPER-NOVAE*

BY W. BAADE AND F. ZWICKY

MOUNT WILSON OBSERVATORY, CARNEGIE INSTITUTION OF WASHINGTON AND CALIFORNIA INSTITUTE OF TECHNOLOGY, PASADENA

Communicated March 19, 1934

# Remember: energy density - flux

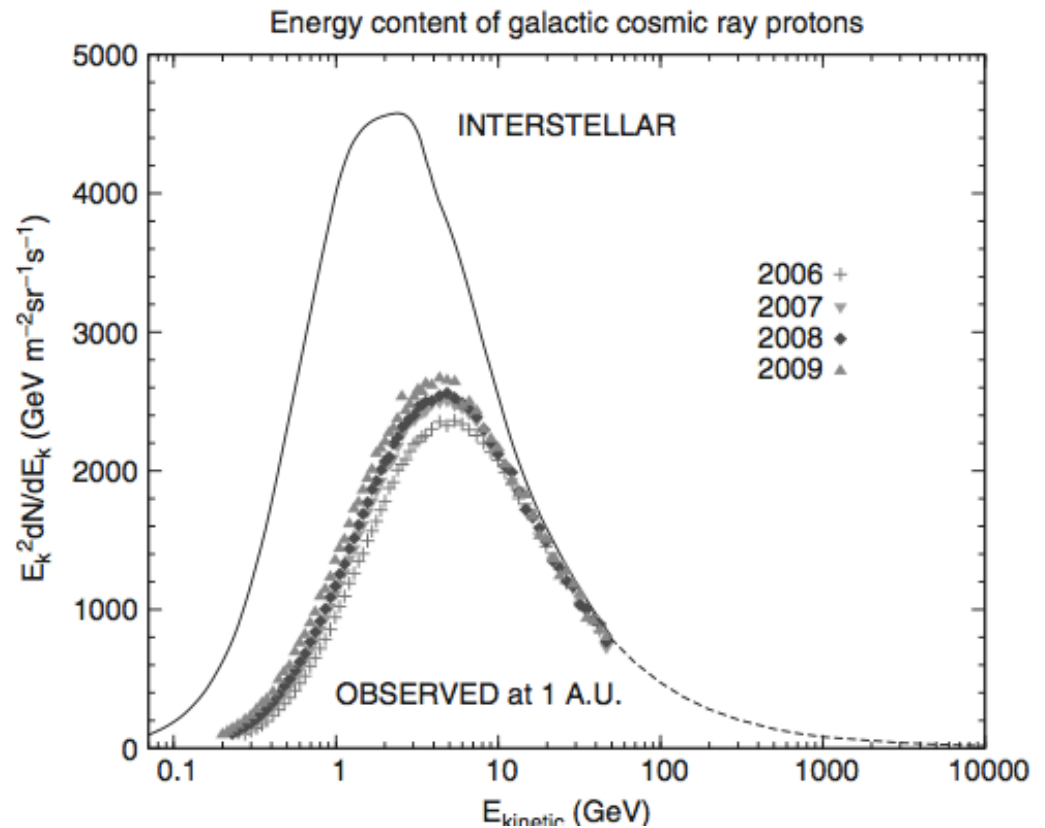
$$Flux \left( \frac{\text{particles}}{\text{cm}^2 \text{sr}} \right) = \frac{\rho_{CR} \beta c}{4\pi}$$

Hence the energy density (provided by CR sources) is:  $\rho_E = 4\pi \int \frac{E}{\beta c} \frac{dN}{dE} dE$

Below the knee:  $\frac{dN}{dE} = 1.8 \times 10^4 (E/1\text{GeV})^{-2.7} \frac{\text{nucleons}}{\text{m}^2 \text{sr s GeV}}$

$$\rho_E = \frac{4\pi}{c} \int_{1\text{GeV}}^{10^6\text{GeV}} dE 1.8 \times 10^4 (E/1\text{GeV})^{-1.7} \sim 1 \frac{\text{eV}}{\text{cm}^3}$$

for relativistic particles

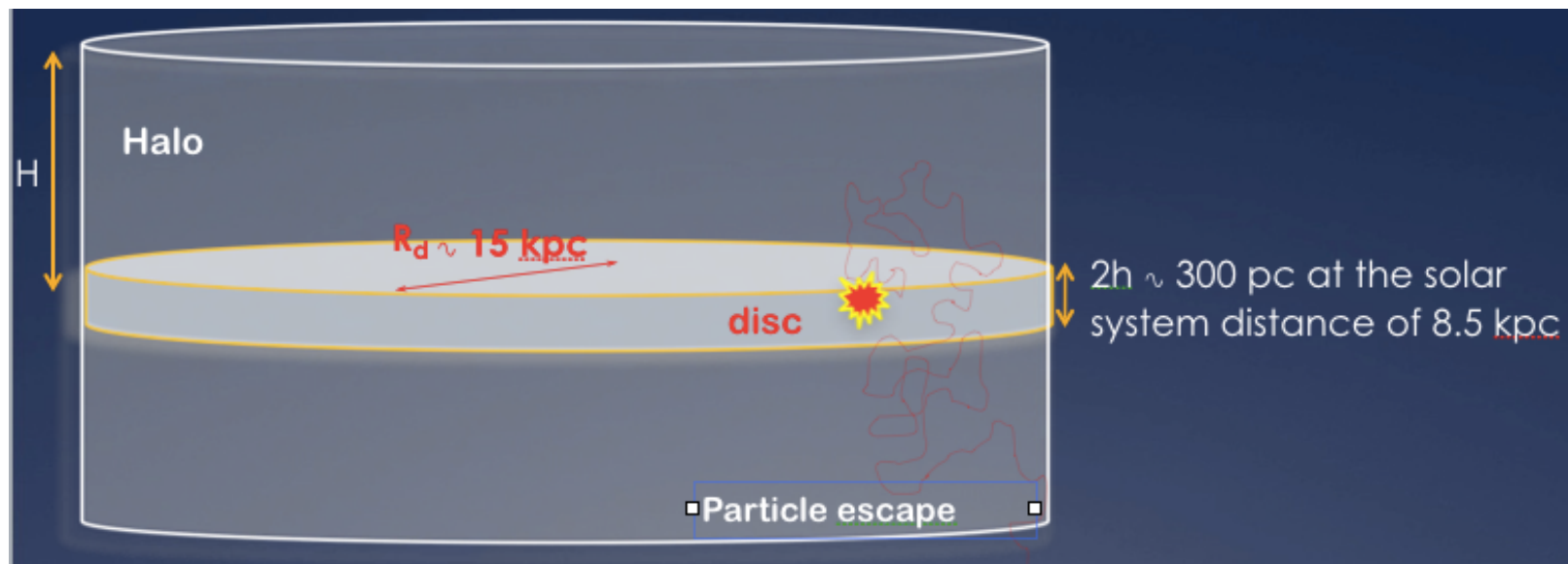


# The volume of the Galaxy

The volume of the Milky Way can be approximated by a disk with a thickness of 300 pc and a radius of 0.3 kpc. Compute the volume of the Milky Way in cubic centimetres.

$$\begin{aligned}V_{disk} &\sim \pi R_{disk}^2 h_{disk} \\ &\sim \pi [15 \text{ kpc}]^2 [0.3 \text{ kpc}] \\ &\sim 6 \times 10^{66} \text{ cm}^3\end{aligned}$$

$$1 \text{ kpc} = 3.0857 \times 10^{21} \text{ cm}$$



# Energy balance

The luminosity in galactic CRs is:

$$L_{CR} = \rho_E \frac{V}{\tau_{esc}} \sim \frac{1 \text{ eV/cm}^3}{6.24 \times 10^{11} \text{ erg/eV}} \times \frac{6 \times 10^{66} \text{ cm}^3}{3 \times 10^6 \text{ yr} \times 3.15 \times 10^7 \text{ s/yr}} \sim 10^{41} \text{ erg/s}$$

The energy emitted from the Sun is approximately  $3.6 \times 10^{33}$  erg/s

1 eV =  $6.24 \times 10^{11}$  erg

For a typical SN:

FREE EXPANSION VELOCITY

$$M = 10M_{\text{sun}} (=10 \times 2 \times 10^{33} \text{ g})$$

$$K = 10^{51} \text{ erg}$$



$$V \cong \sqrt{\frac{2K}{M}} = \sqrt{\frac{2 \cdot 10^{51} \text{ erg}}{10 \cdot (2 \cdot 10^{33} \text{ g})}} \cong 3 \cdot 10^8 \text{ cm/s}$$

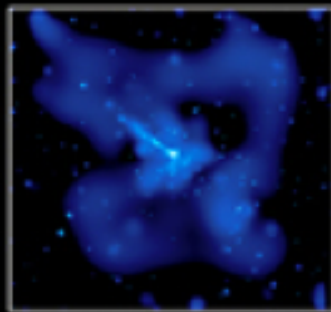
$$\frac{V}{c} \cong 10^{-2}$$

Rate of SN  $\sim 3$  / century =

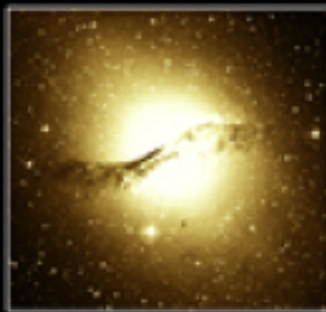
Power =  $K \times \text{rate} = 10^{51} \text{ erg} \times 3 / 3.15 \times 10^9 \sim 10^{42} \text{ erg/s}$

5-10% of the energy in the ejecta suffices to produce the measured galactic CR flux

# EXTRAGALACTIC SOURCES: AGN jets, GRB fireballs



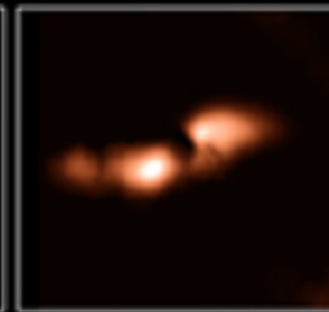
CHANDRA X-RAY



DSS OPTICAL



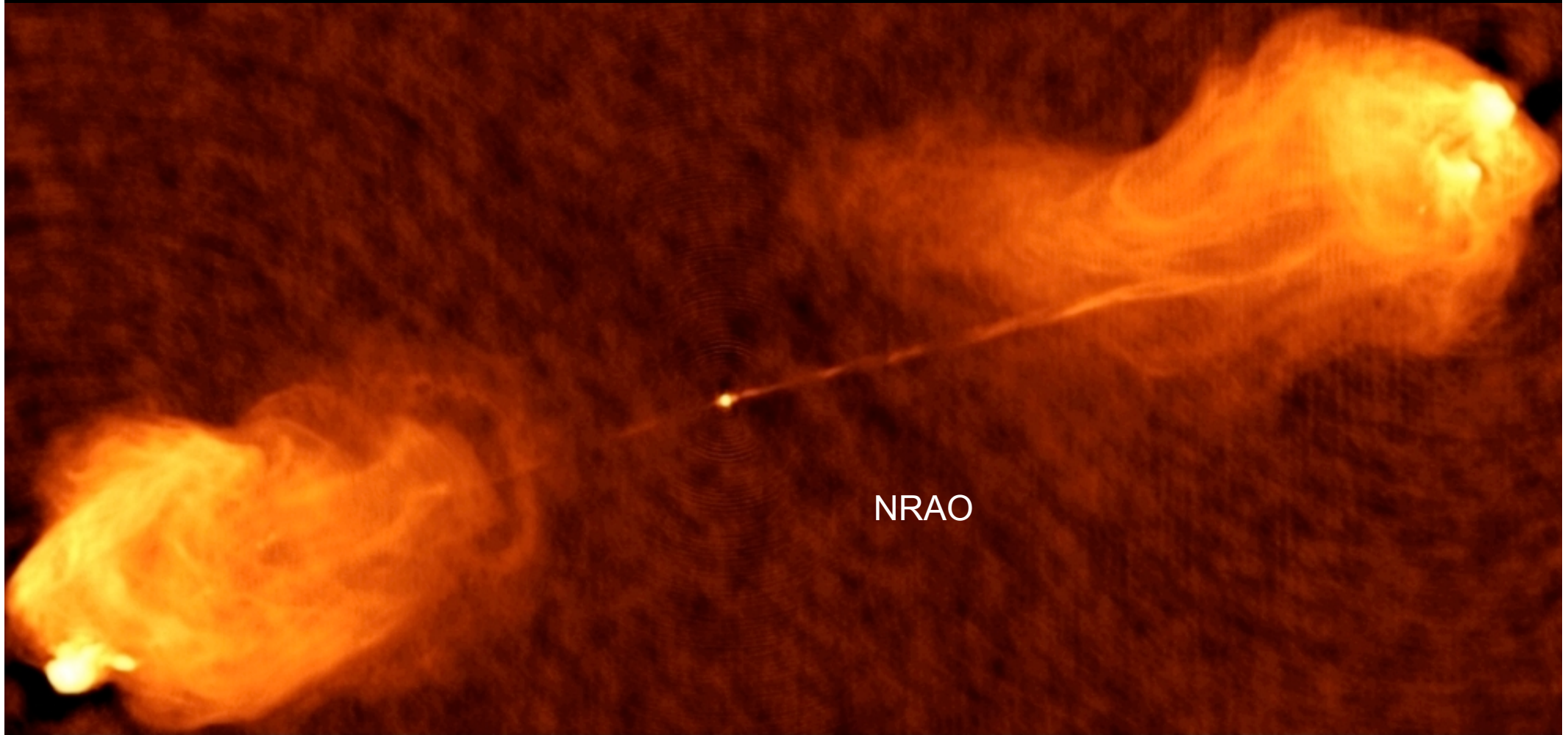
NRAO RADIO  
CONTINUUM



NRAO RADIO  
(21-CM)

Centaurus A

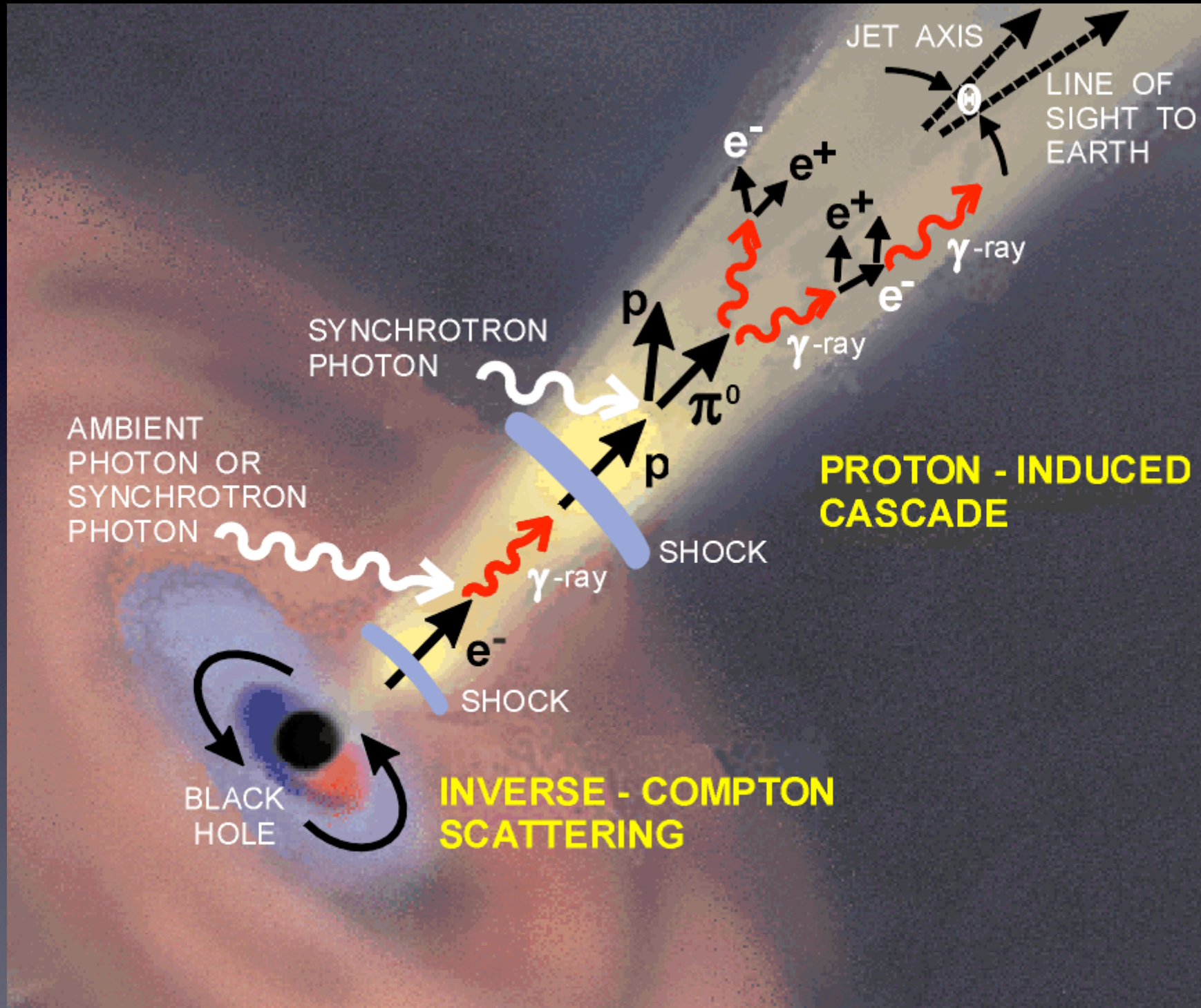
# The most powerful sky accelerators: AGN jets, GRB fireballs



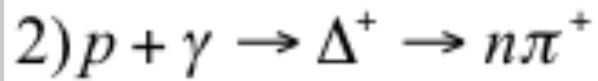
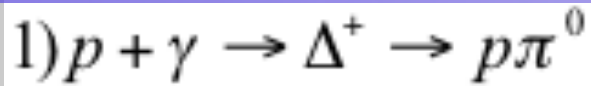
The radio source Cygnus A is produced in a galaxy some 600 million light-years away. The radio waves are coming from electrons propelled at nearly the speed of light from the bright center of the galaxy -- the location of a black hole. Electrons are trapped by the magnetic field around the galaxy.



# The most powerful sky accelerators: AGN jets, GRB fireballs



# Energy balance for extra-galactic sources



Waxman & Bahcall, PRD59, 1999 and PRD64, 2001)

The cosmic ray flux above the ankle is given by “one  $3 \times 10^{10}$  GeV particle per kilometer square per year per steradian.” This can be translated into an energy flux

$$E^2 \frac{dN_{CR}}{dE} = \frac{3 \times 10^{10} \text{ GeV}}{(10^{10} \text{ cm}^2)(3 \times 10^7 \text{ s})\text{sr}} = 10^{-7} \text{ GeV cm}^{-2} \text{ s}^{-1} \text{ sr}^{-1}$$

Energy density in extra-galactic CRs:  $\rho_E = \frac{4\pi}{c} \int_{E_{min}}^{E_{max}} \frac{10^{-7}}{E} dE \frac{\text{GeV}}{\text{cm}^3} \sim 3 \times 10^{-19} \frac{\text{erg}}{\text{cm}^3}$

$E_{min} \approx 10^{10} \text{ GeV}$  and  $E_{max} = 10^{12} \text{ GeV}$        $E_{max}/E_{min} \sim 10^3$

Power needed by a population of sources of protons with  $E^{-2}$  to generate  $\rho_E$  over the Hubble time =  $10^{10}$  yrs  $\approx 10^{44}$  erg Mpc<sup>-3</sup> yr<sup>-1</sup>  $\approx 3 \times 10^{37}$  erg Mpc<sup>-3</sup> s<sup>-1</sup>

Which work out to a luminosity of :

$$3 \times 10^{39} \text{ erg/s per galaxy}$$

$$3 \times 10^{42} \text{ erg/s per cluster of galaxies}$$

$$2 \times 10^{44} \text{ erg/s per AGN}$$

$$2 \times 10^{51} \text{ erg per cosmological GRB.}$$

From BATSE: 300 GRB / Gigaparsec<sup>3</sup> yr       $1 \text{ Gpc}^3 = 2.9 \times 10^{82} \text{ cm}^3$       Hubble time =  $10^{10}$  years

$$2 \times 10^{51} \text{ erg} \times \frac{300}{\text{Gpc}^3 \text{ yr}} \times 10^{10} \text{ yr} \times \frac{\text{Gpc}^3}{2.9 \times 10^{82} \text{ cm}^3} \sim 2 \times 10^{19} \text{ erg/cm}^3$$

equal to the observed energy density of extragalactic CRs

# The Fermi acceleration mechanism

Reprinted from Physical Review 75, 8, April 15, 1949, by Permission

## On the Origin of the Cosmic Radiation

ENRICO FERMI  
Institute for Nuclear Studies, University of Chicago, Chicago, Illinois  
(Received January 3, 1949)

A theory of the origin of cosmic radiation is proposed according to which cosmic rays are originated and accelerated primarily in the interstellar space of the galaxy by collisions against moving magnetic fields. One of the features of the theory is that it yields naturally an inverse power law for the spectral distribution of the cosmic rays. The chief difficulty is that it fails to explain in a straightforward way the heavy nuclei observed in the primary radiation.

### I. INTRODUCTION

IN recent discussions on the origin of the cosmic radiation E. Teller<sup>1</sup> has advocated the view that cosmic rays are of solar origin and are kept relatively near the sun by the action of magnetic fields. These views are amplified by Alfvén, Richtmyer, and Teller.<sup>2</sup> The argument against the conventional view that cosmic radiation may extend at least to all the galactic space is the very large amount of energy that should be present in form of cosmic radiation if it were to extend to such a huge space. Indeed, if this were the case, the mechanism of acceleration of the cosmic radiation should be extremely efficient.

I propose in the present note to discuss a hypothesis on the origin of cosmic rays which attempts to meet in part this objection, and according to which cosmic rays originate and are accelerated primarily in the interstellar space, although they are assumed to be prevented by magnetic fields from leaving the boundaries of the galaxy. The main process of acceleration is due to the interaction of cosmic particles with wandering magnetic fields which, according to Alfvén, occupy the interstellar spaces.

Such fields have a remarkably great stability because of their large dimensions (of the order of magnitude of light years), and of the relatively high electrical conductivity of the interstellar space. Indeed, the conductivity is so high that one might describe the magnetic lines of force as attached to the matter and partaking in its streaming motions. On the other hand, the magnetic field itself reacts on the hydrodynamics<sup>3</sup> of the interstellar matter giving it properties which, according to Alfvén, can pictorially be described by saying that to each line of force one should attach a material density due to the mass of the matter to which the line of force is linked. Developing this point of view, Alfvén is able to calculate a simple formula for the velocity  $V$  of propagation of magneto-elastic waves:

$$V = H / (4\pi\rho)^{1/2} \quad (1)$$

<sup>1</sup> Nuclear Physics Conference, Birmingham, 1948.

<sup>2</sup> Alfvén, Richtmyer, and Teller, Phys. Rev., to be published.

<sup>3</sup> H. Alfvén, Arkiv Mat. f. Astr., o. Fys. 29B, 2 (1943).

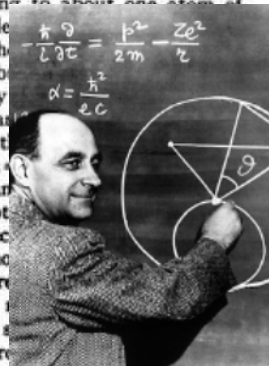
where  $H$  is the intensity of the magnetic field and  $\rho$  is the density of the interstellar matter.

One finds according to the present theory that a particle that is projected into the interstellar medium with energy above a certain injection threshold gains energy by collisions against the moving irregularities of the interstellar magnetic field. The rate of gain is very slow but appears capable of building up the energy to the maximum values observed. Indeed one finds quite naturally an inverse power law for the energy spectrum of the protons. The experimentally observed exponent of this law appears to be well within the range of the possibilities.

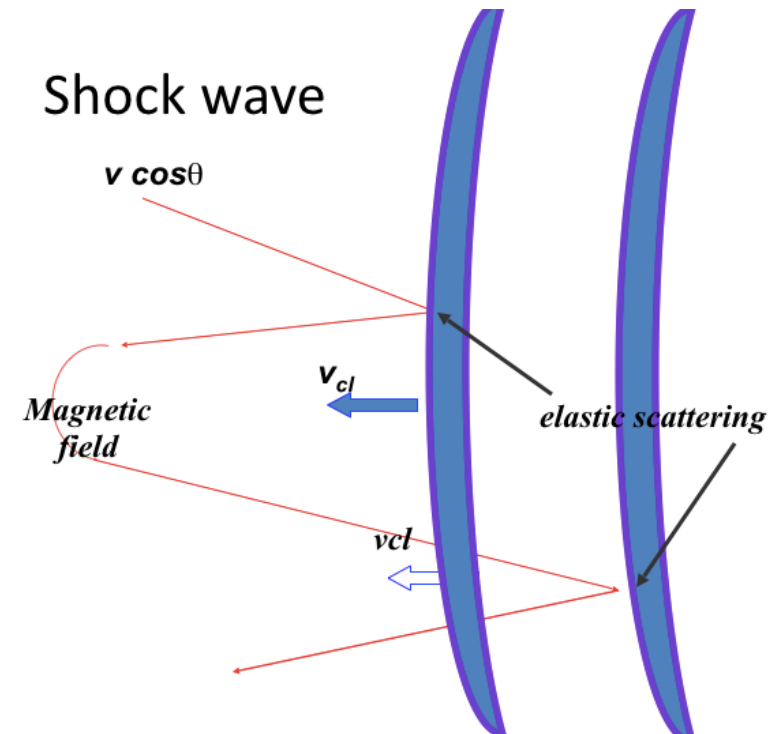
The present theory is incomplete because no satisfactory injection mechanism is proposed except for protons which apparently can be regenerated at least in part in the collision processes of the cosmic radiation itself with the diffuse interstellar matter. The most serious difficulty is in the injection process for the heavy nuclear component of the radiation. For these particles the injection energy is very high and the injection mechanism must be correspondingly efficient.

### II. THE MOTIONS OF THE INTERSTELLAR MEDIUM

It is currently assumed that the interstellar space of the galaxy is occupied by matter at extremely low density, corresponding to about one atom of hydrogen per cc, or to a density of  $10^{-24}$  gm/cc. The evidence indicates, however, that the density is not uniformly spread, but that there are concentrations where the density is a hundred times as large as the average dimensions of the clouds (1 parsec. =  $3.1 \times 10^{18}$  cm). The measurements of Adams<sup>4</sup> of the interstellar absorption of the radial velocity with respect to such clouds located at various distances from us. The root mean square velocity is corrected for the proper motion of the clouds. We may assume that the



A "collision" with a magnetic cloud or the crossing across high magnetic fields close to a shock can cause an increase in energy of a particle. The energy increase is  $\Delta E/E = \xi$



<sup>4</sup> W. S. Adams, A.p.J. 97, 105 (1943).

# The Fermi acceleration mechanism

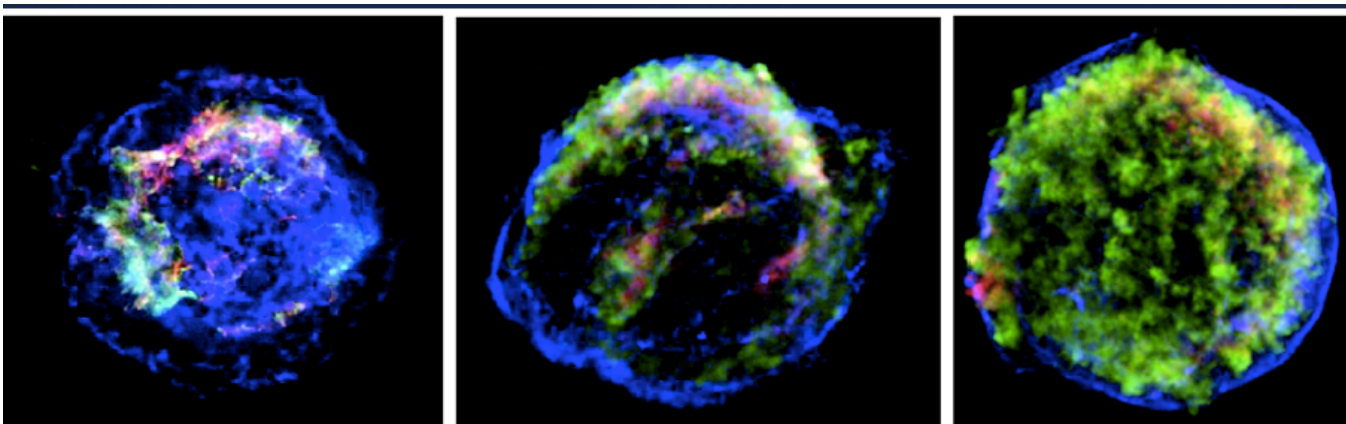
- CR acceleration is a stochastic process. At each accelerating event particle gains:  $\Delta E = \xi E$
- Probability that the particle is not followed up:  $P_{esc}$
- Probability that the particle is iterated in acceleration:  $1 - P_{esc}$
- For a particle with injection energy  $E_0$ , after  $k$  iterations:
- The probability of having received  $k$  accelerations and then escape is:

$$\bar{E}_k = E_0(1 + \xi)^k \quad \longrightarrow \quad k = \frac{\ln(E_k/E_0)}{\ln(1 + \xi)}$$

- The number of particles after  $k$  encounters that remain (if  $N_0$  where there initially) is

$$P_k = (1 - P_{esc})^k P_{esc}$$

$$N_k = N_0 P_k = N_0 (1 - P_{esc})^k P_{esc}$$



# The spectrum of the Fermi acceleration mechanism

$$N_k = N_0 P_{esc} (1 - P_{esc})^{\frac{\ln(E_k/E_0)}{\ln(1+\xi)}} = N_0 P_{esc} \exp \left[ \ln(1 - P_{esc}) \frac{\ln(E_k/E_0)}{\ln(1+\xi)} \right] =$$

$$N_0 P_{esc} \exp \left[ \frac{\ln(E_k/E_0) \ln(1 - P_{esc})}{\ln(1 + \xi)} \right] \Rightarrow N_k = N_0 P_{esc} \left( \frac{E_k}{E_0} \right)^{\frac{\ln(1 - P_{esc})}{\ln(1 + \xi)}}$$

Differentiating we get:  $\frac{dN}{dE} \propto E^{\frac{\ln(1 - P_{esc})}{\ln(1 + \xi)} - 1} = E^{-\gamma - 1}$

$$\ln(1 + x) \sim x + \frac{x^2}{2} - \frac{x^3}{3} + \dots \sim x \text{ for } x \ll 1$$

$$\ln(1 - P_{esc}) \sim -P_{esc} + \dots$$

$$\ln(1 + \xi) \sim \xi + \dots$$

Integral spectrum slope

$$\gamma = -\frac{\ln(1 - P_{esc})}{\ln(1 + \xi)} \sim \frac{P_{esc}}{\xi}$$

for  $P_{esc} \ll 1$  and  $\xi \ll 1$

$$P_{esc} = \frac{T_{cycle}}{T_{esc}}$$

characteristic time for the acceleration cycle  
characteristic time for escape from the acceleration region

# The spectrum of the Fermi acceleration mechanism

- The number of iterations after the acceleration has been working for a time  $t$ :

$$k_{max} = t/T_{cycle}$$

- And

$$E \leq E_0(1 + \xi)^{t/T_{cycle}}$$

- 1) Higher-energy particles take longer to accelerate than low-energy particles.

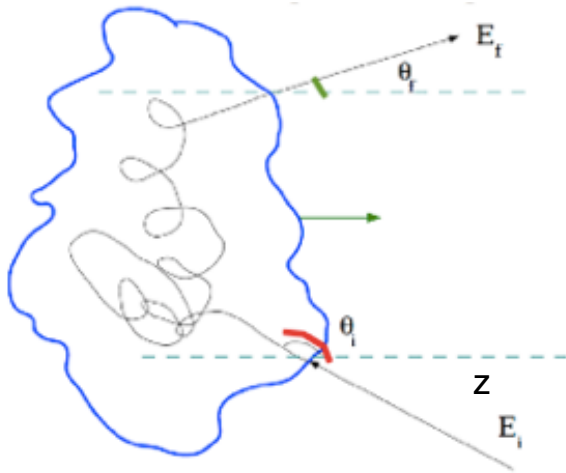
$$\xi = \frac{E - E_0}{E_0} = \frac{E}{E_0} - 1$$

- 2) If a Fermi accelerator has a limited lifetime,  $T_A$ , then it will also be characterised by a maximum energy per particle that it can produce:

$$E \leq E_0(1 + \xi)^{T_A/T_{cycle}}$$

This would be true if  $T_{cycle}$  is independent on energy which maybe not true for SNR

# Fermi acceleration



Collision-less plasma: The interaction with the turbulent magnetic field is practically elastic.

Particles are relativistic particles:  $E = pc$  and  $c = 1$   
 Cloud speed  $\beta = V/c$  (not relativistic)

elastic scattering

$$E_i^* = E_f^*$$

cloud frame

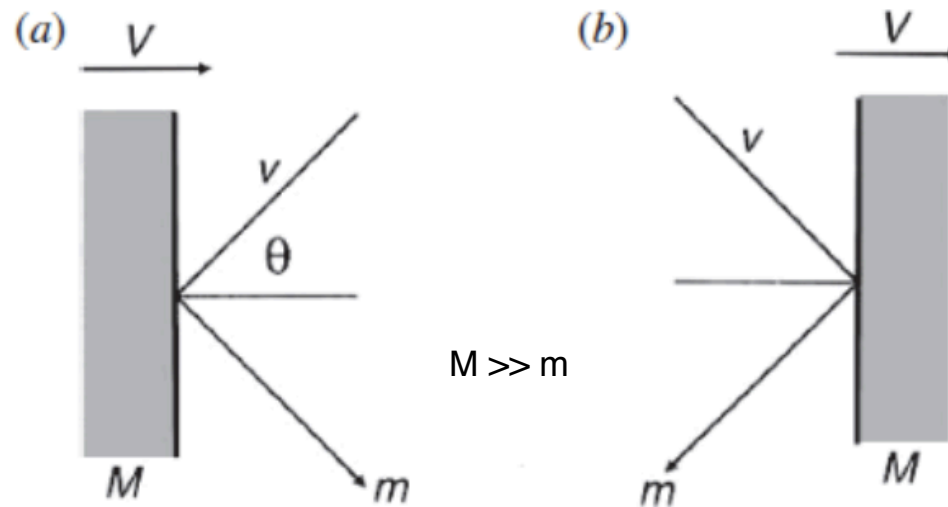
Lorentz transformation to the cloud frame from the lab frame:

$$E_i^* = \gamma(1 - \beta p_{z,i}) = \gamma E_i(1 - \beta \cos \theta_i)$$

$$E_f = \gamma(1 + \beta \cos \theta_f^*) E_f^* = \gamma^2 (1 - \beta \cos \theta_i)(1 + \beta \cos \theta_f^*) E_i$$

$$\frac{\Delta E}{E_i} = \frac{E_f}{E_i} - 1 = \gamma^2 (1 - \beta \cos \theta_i)(1 + \beta \cos \theta_f^*) - 1$$

# Geometry for the cloud (2nd order)



- ▶ Energy is gained during a head-on collision (a) and lost during a trailing collision (b)

- ▶ The probability of a head-on collision is proportional to

$$v + V \cos \theta$$

- ▶ The probability of a trailing collision is proportional to

$$v - V \cos \theta$$

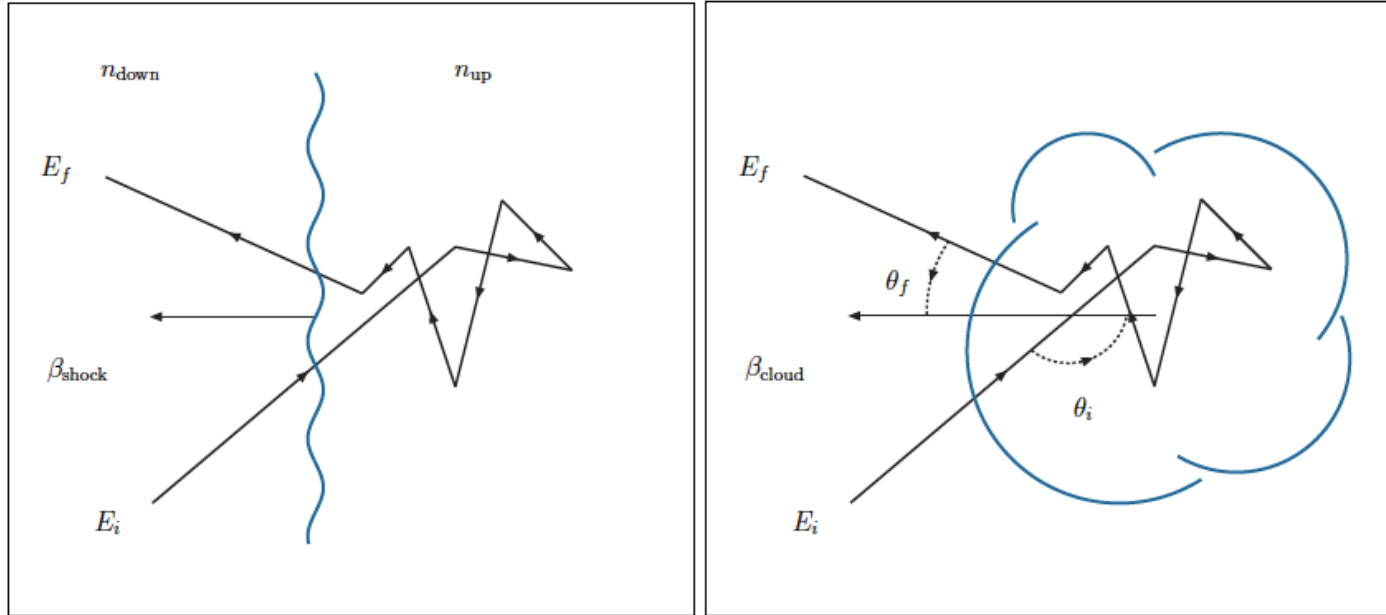
The prob. of particle head-on or rear-end collisions on the cloud is **prop. to the relative velocity between the particle and the cloud.**

- ▶ Same principle as driving on a highway: there will be more cars passing you by from oncoming traffic than traffic going in the same direction



# 1<sup>st</sup> and 2<sup>nd</sup> order Fermi acceleration

$$\left\langle \frac{\Delta E}{E_i} \right\rangle = \gamma^2 (1 - \beta \langle \cos \theta_i \rangle) (1 + \beta \langle \cos \theta_f^* \rangle) - 1$$



$$\frac{dN}{d \cos \theta_f^*} = \text{const} \quad -1 \leq \cos \theta_f^* \leq 1$$

$\langle \cos \theta_f^* \rangle = 0$  directions of escape velocity are isotropic in the cloud frame

$$\frac{dN}{d \cos \theta_i} \propto v_{rel} \propto (1 - \beta \cos \theta_i) \quad -1 \leq \cos \theta_i \leq 1$$

Prob of particle head-on or rear-end collisions on the cloud prop. to the relative velocity between the particle and the cloud.

$$\langle \cos \theta_i \rangle = -\beta/3$$

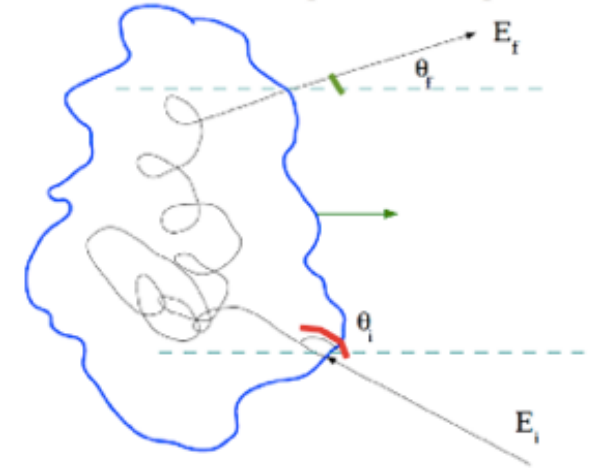
# Average incident angle in 2<sup>nd</sup> order

The probability of a head-on or rear-end collision of particles on the cloud is proportional to the relative velocity between the particle and the cloud:

$$\frac{dN}{d \cos \theta_i} \propto v_{rel} \propto (1 - \beta \cos \theta_i)$$

As a matter of fact:

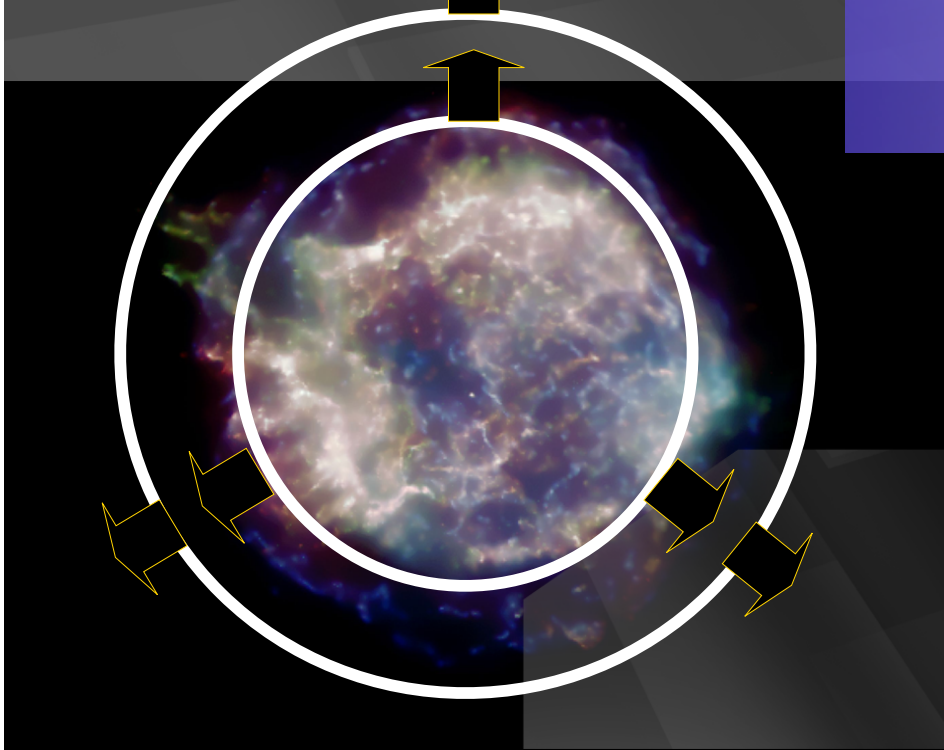
$$\begin{aligned} v_{rel} &= |\vec{v}_{particle} - \vec{V}_{cloud}| \\ &= \sqrt{(c - V \cos \theta_i)^2 + V^2 \sin^2 \theta_i} = \\ &= c \sqrt{(1 - \beta \cos \theta_i)^2 + \beta^2 \sin^2 \theta_i} = \\ &= c \sqrt{1 + \beta^2 - 2\beta \cos \theta_i} \\ &\sim c \sqrt{1 - 2\beta \cos \theta_i} \sim c(1 - \beta \cos \theta_i) \text{ for } \beta \ll 1 \end{aligned}$$



The average incident angle is:

$$\begin{aligned} \langle \cos \theta_i \rangle &= \frac{\int_{-1}^1 \cos \theta_i (1 - \beta \cos \theta_i) d \cos \theta_i}{\int_{-1}^1 (1 - \beta \cos \theta_i) d \cos \theta_i} = \\ &= \frac{[\cos^2 \theta_i / 2 - \beta \cos^3 \theta_i / 3]_{-1}^1}{[\cos \theta_i - \beta \cos^2 \theta_i / 2]_{-1}^1} = \frac{\frac{1}{2} - \frac{\beta}{3} - \frac{1}{2} + \frac{\beta}{3}}{1 - \frac{\beta}{2} + 1 + \frac{\beta}{2}} = -\frac{\beta}{3} \end{aligned}$$

# Collision-less shock



Shock = discontinuity surface in thermodynamic properties (density, temperature, velocity and pressure)

Collision-less shock: the transition from pre- to post-shock states  $\ll$  particle mean free path between collisions (observed by astronomers)

For a strong shock (the Mach number is very large) and for a monoatomic gas:

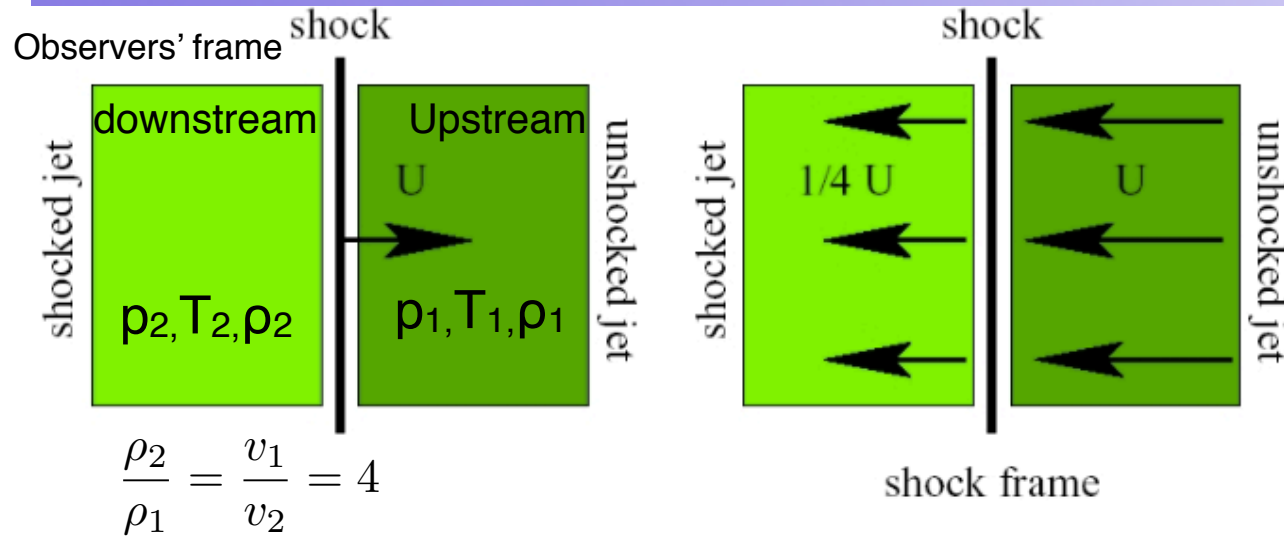
$$\frac{\rho_2}{\rho_1} = \frac{v_1}{v_2} = 4$$

$$\rho_1 v_1 = \rho_2 v_2 \quad \text{mass conservation across the shock}$$

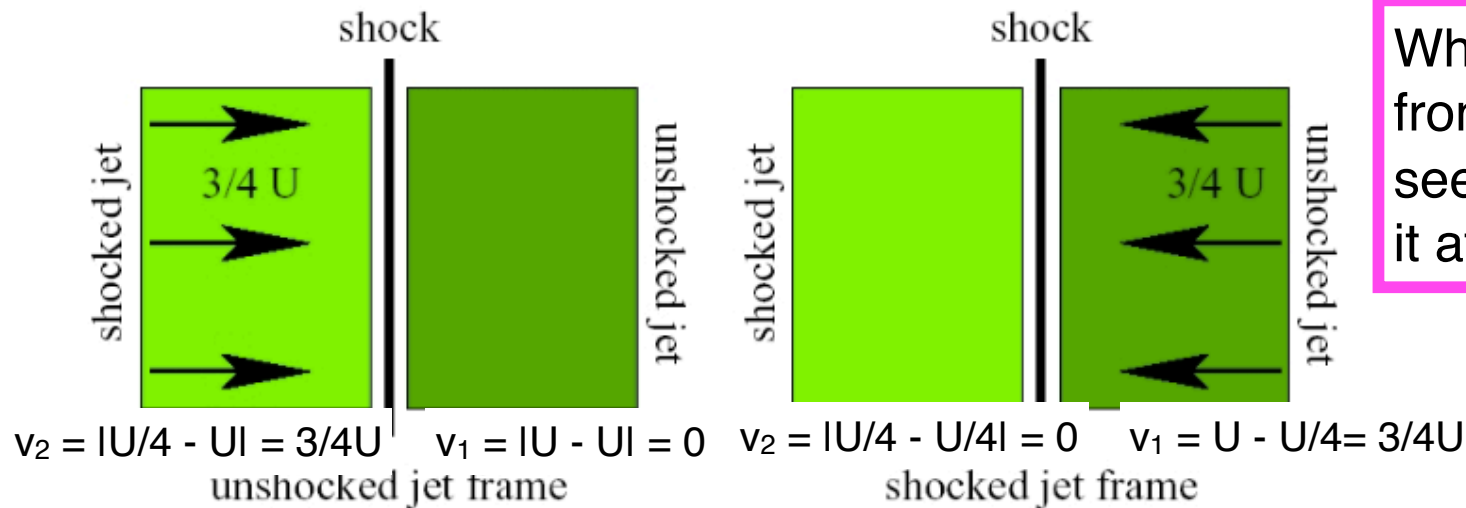
$$\rho_1 + \rho_1 v_1^2 = \rho_2 + \rho_2 v_2^2 \quad \text{pressure equation}$$

$$\rho_1 v_1 \left( \frac{v_1^2}{2} + \frac{P_1}{\rho_1} + u_1 \right) = \rho_2 v_2 \left( \frac{v_2^2}{2} + \frac{P_2}{\rho_2} + u_2 \right) \quad \text{Energy conservation, where } u \text{ is internal energy}$$

# Why 1<sup>st</sup> order is efficient?



In Shock frame: the unshocked gas flows into the shock with velocity  $v_1 = |U|$   
 And shocked gas flows away behind us with velocity  $v_2 = v_1/4 = U/4$



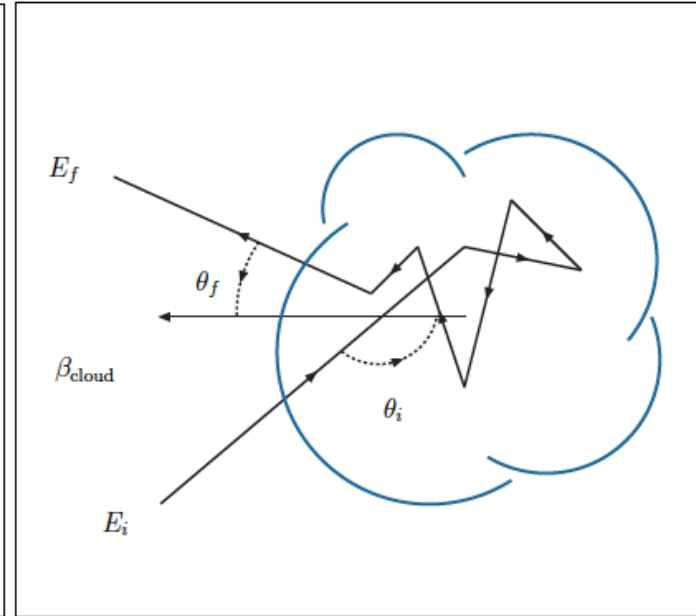
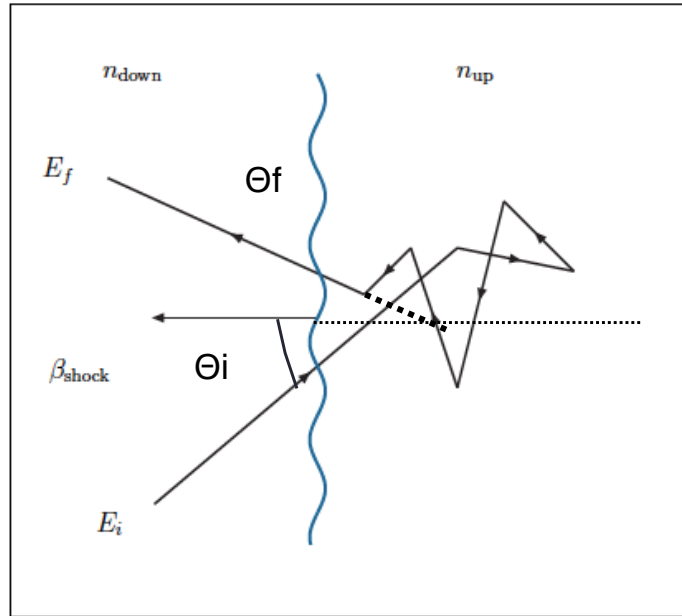
When crossing the shock from either side, the particle sees plasma moving toward it at a velocity of  $3/4U$

A particle at rest in the unshocked gas frame (upstream) sees the shock approaching at velocity  $U$  and the shocked gas approaching at  $3/4U$ . As it crosses the shock, the particle is accelerated at mean speed  $3/4U$ .

A particle at rest in the shocked gas frame (downstream) sees the shock approaching at velocity  $U/4$  and the shocked gas approaching at  $3/4U$ .

# 1<sup>st</sup> and 2<sup>nd</sup> order Fermi acceleration

$$\left\langle \frac{\Delta E}{E_i} \right\rangle = \gamma^2 (1 - \beta \langle \cos \theta_i \rangle) (1 + \beta \langle \cos \theta_f^* \rangle) - 1$$



$$\frac{dN}{d \cos \theta_i} \propto \cos \theta_i$$

$$\frac{dN}{d \cos \theta_f^*} \propto \cos \theta_f^*$$

$\langle \cos \theta_f^* \rangle = 2/3$  normalised projection of an isotropic flux on a plane with  $0 \leq \cos \theta_f^* \leq 1$

$\langle \cos \theta_i \rangle = -2/3$  normalised projection of an isotropic flux on a plane with  $-1 \leq \cos \theta_i \leq 0$

$$\frac{dN}{d \cos \theta_f^*} = \text{const} \quad -1 \leq \cos \theta_f^* \leq 1$$

$\langle \cos \theta_f^* \rangle = 0$  directions of escape velocity are made isotropic in the cloud frame

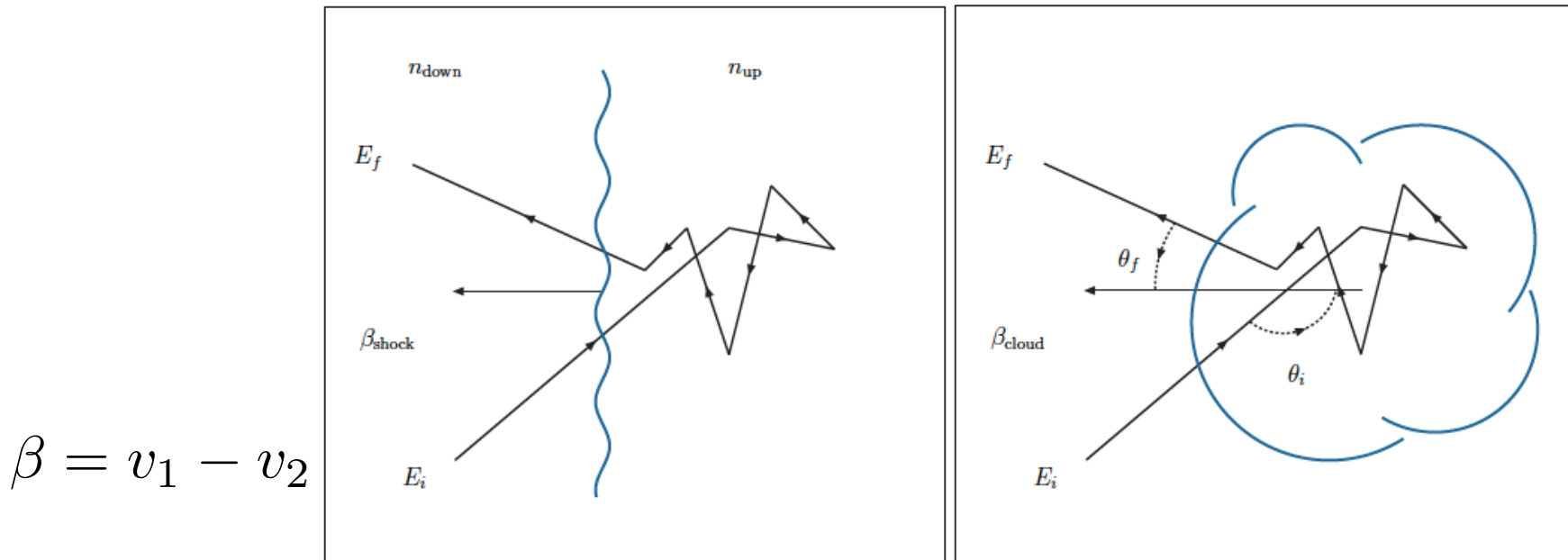
$$\frac{dN}{d \cos \theta_i} \propto v_{rel} \propto (1 - \beta \cos \theta_i) \quad -1 \leq \cos \theta_i \leq 1$$

Prob of particle head-on or rear-end collisions on the cloud prop. to the relative velocity between the particle and the cloud.

$$\langle \cos \theta_i \rangle = -\beta/3$$

# 1<sup>st</sup> and 2<sup>nd</sup> order Fermi acceleration

$$\left\langle \frac{\Delta E}{E_i} \right\rangle = \gamma^2 (1 - \beta \langle \cos \theta_i \rangle) (1 + \beta \langle \cos \theta_f^* \rangle) - 1$$



$$\beta = v_1 - v_2$$

$\beta \ll 1$  The shock is not relativistic!

$$\left\langle \frac{\Delta E}{E_i} \right\rangle = \gamma^2 (1 + 2\beta/3)(1 + 2\beta/3) - 1 =$$

$$= \sim 4\beta/3$$

$$\left\langle \frac{\Delta E}{E_i} \right\rangle = \gamma^2 (1 + \beta^2/3) - 1 =$$

$$= \frac{1 + \beta^2/3}{1 - \beta^2} - 1 \sim 4\beta^2/3$$

Speed of the cloud

# 1<sup>st</sup> order Fermi shock acceleration

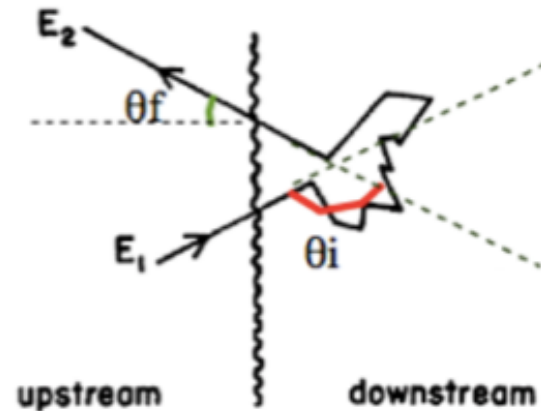
For a plane shock:  $-1 \leq \cos\theta_i \leq 0$   
and  $0 \leq \cos\theta_f^* \leq 1$  and the  
distribution of particles

$$\frac{dN}{d \cos \theta_i} \propto \cos \theta_i$$

$$\frac{dN}{d \cos \theta_f^*} \propto \cos \theta_f^*$$

$$\left\langle \frac{\Delta E}{E_i} \right\rangle = \frac{(1 - \beta \langle \cos \theta_i \rangle)(1 + \beta \langle \cos \theta_f^* \rangle)}{1 - \beta^2} - 1$$

Acceleration



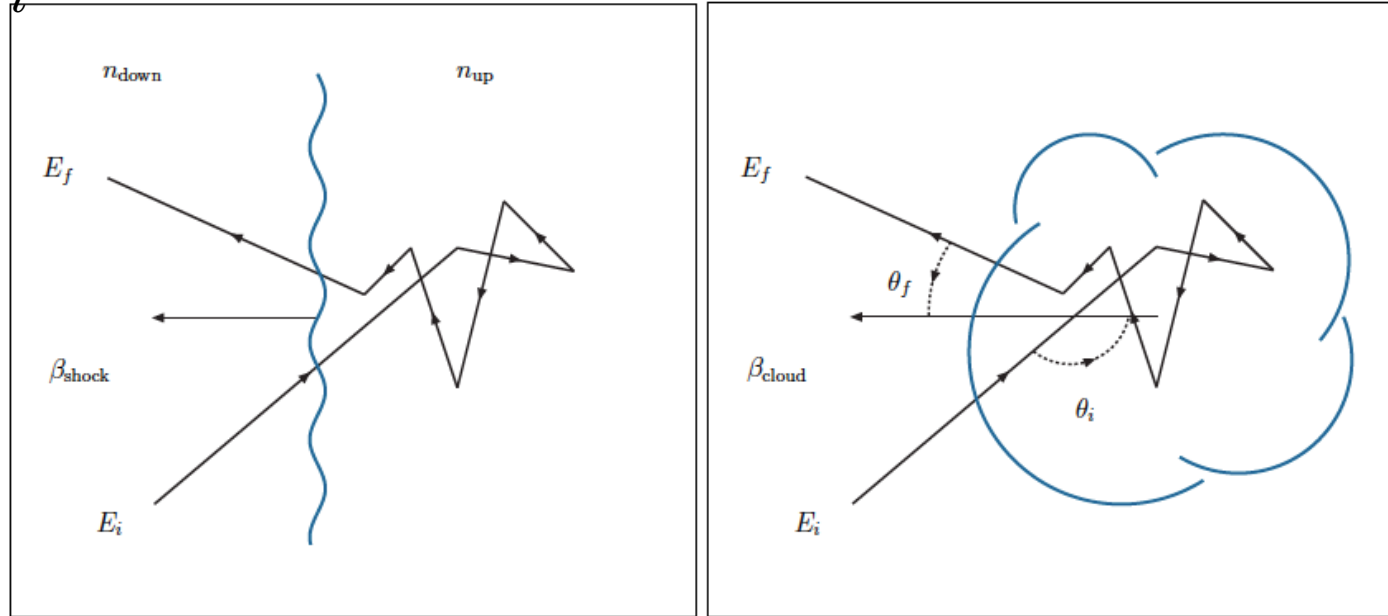
$$\langle \cos \theta_i \rangle = \frac{\int_{-1}^0 \cos \theta_i \cos \theta_i d \cos \theta_i}{\int_{-1}^0 \cos \theta_i d \cos \theta_i} = \frac{[\cos \theta_i^3]_{-1}^0 / 3}{[\cos \theta_i^2]_{-1}^0 / 2} = \frac{1/3}{-1/2} = -2/3$$

$$\langle \cos \theta_f^* \rangle = \frac{\int_0^1 \cos \theta_f^* \cos \theta_f^* d \cos \theta_f^*}{\int_0^1 \cos \theta_f^* d \cos \theta_f^*} = \frac{[\cos \theta_f^*]_0^1 / 3}{[\cos \theta_f^*^2]_0^1 / 2} = \frac{1/3}{1/2} = 2/3$$

$$\left\langle \frac{\Delta E}{E} \right\rangle = \frac{(1 + \frac{2}{3}\beta)(1 + \frac{2}{3}\beta)}{1 - \beta^2} - 1 \sim \frac{4}{3}\beta \quad \text{linear in the speed}$$

# 1<sup>st</sup> and 2<sup>nd</sup> order Fermi acceleration

$$\left\langle \frac{\Delta E}{E_i} \right\rangle = \gamma^2 (1 - \beta \langle \cos \theta_i \rangle) (1 + \beta \langle \cos \theta_f^* \rangle) - 1$$



A shock wave moves with speed  $-\mathbf{v}_1$  relative to  $\mathbf{v}_2$  is the relative speed with respect to the shock front of the gas flowing away from the shock in the downstream region ( $v_2 < v_1$ )

In the lab frame the gas behind the shock moves with  $\mathbf{U} = -\mathbf{v}_1 + \mathbf{v}_2 =$  speed of the shocked gas (downstream) relative to the unshocked gas (upstream)

$$\xi = \frac{1 + \frac{4}{3}\beta + \frac{4}{9}\beta^2}{1 - \beta^2} - 1 \sim \frac{4}{3}\beta = \frac{4}{3} \frac{v_1 - v_2}{c}$$

1<sup>st</sup> order

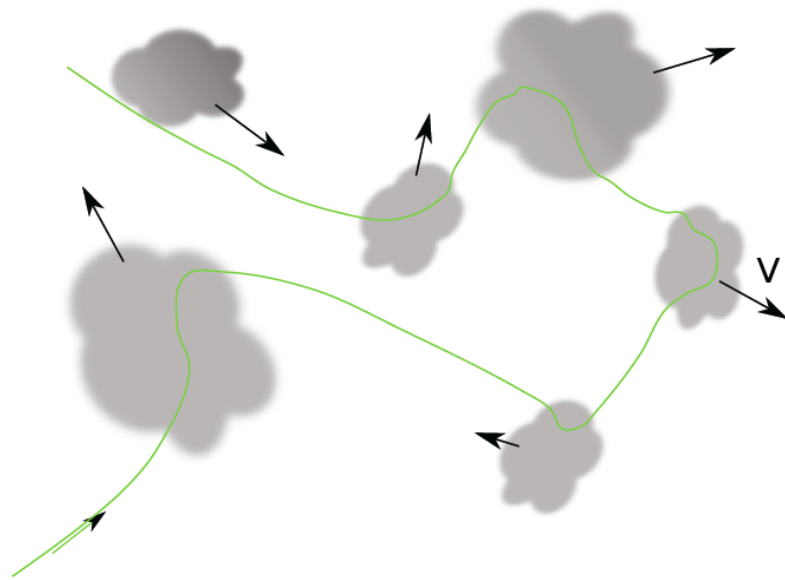
$$\xi = \frac{1 + \frac{1}{3}\beta^2}{1 - \beta^2} - 1 \sim \frac{4}{3}\beta^2$$

2<sup>nd</sup> order



# 2<sup>nd</sup> order Fermi acceleration spectrum

2<sup>nd</sup> order Fermi acceleration: elastic scattering on irregularities of the B-field into magnetized clouds



$$\xi = \frac{\Delta E}{E_i} \sim \frac{4}{3}\beta^2$$

prob to exit the Galaxy between one encounter and the next with the clouds

$$\gamma = \frac{P_{esc}}{\xi} \sim \frac{(\Delta t)_{encounters}/\tau_{esc}}{\frac{4}{3}\beta^2} \sim \frac{n_{clouds}(\pi r_{cloud}^2)c}{\frac{4}{3} \times (10^{-3})^2} \sim 10$$

$$\tau_{esc} \sim 10^6 \text{ yrs}$$

- the random velocity of clouds is small  $\beta < 10^{-4} - 10^{-2}$
- For particles scattering among the magnetic clouds in the galaxy before escaping, the mean free path would be of the order of 0.1 - 1 pc with only few collisions per year leading to rather slow energy gain.
- Not all collisions result in an energy gain! **positive energy gain but inefficient!**

# 1<sup>st</sup> order Fermi acceleration spectrum

For a large plane shock the rate of encounters is given by the projection of an isotropic cosmic ray flux onto the plane of the shock front:

$$\int_0^1 d\cos\theta \int_0^{2\pi} d\phi \frac{c\rho_{CR}}{4\pi} \cos\theta = \frac{c\rho_{CR}}{4}$$


$\rho_{CR}$  = number density of relativistic particles being accelerated.

The rate of convection downstream away from the shock is:  $\rho_{CR} \times v_2$

$$P_{esc} = \frac{\rho_{CR}v_2}{c\rho_{CR}/4} = \frac{4v_2}{c}$$

$$\gamma = \frac{P_{esc}}{\xi} = \frac{4v_2}{\frac{4}{3}(v_1 - v_2)} = \frac{3}{v_1/v_2 - 1} = \frac{3}{4 - 1} = 1$$

depends only on the ratio of velocities of gas upstream and downstream


$$\frac{dN}{dE} \propto E^{-(\gamma+1)} = E^{-2}$$

# Characteristic duration of the shock wave

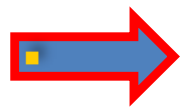
Since the characteristic length for diffusion of particles  $\ll$  radius of curvature of the shock we can use the plane approximation to SNR which are candidates for 1st order Fermi mechanism acceleration.

During the free expansion phase the relation  $R_{shock} = \text{speed of expansion} \times t$  applies

A shock wave loses its accelerating efficiency when the ejected mass = mass of the swept up in ISM

or  $\rho_{SN} = \rho_{ISM} \sim 1 \text{p/cm}^3$

$$\rho_{SN} = \frac{10M_{\odot}}{\frac{4}{3}\pi R_{shock}^3} = \rho_{ISM} = 1.6 \times 10^{-24} \text{g/cm}^3$$



$$R_{shock} = \left( \frac{3 \cdot 10M_{\odot}}{4\pi\rho_{ISM}} \right)^{1/3} = \left( \frac{30 \times 2 \times 10^{33} \text{g}}{4\pi \times 1.6 \times 10^{-24} \text{g/cm}^3} \right)^{1/3}$$

$$= 1.4 \times 10^{19} \text{cm} \sim 5 \text{pc} \quad \text{Radius of shock wave}$$

$$T_{shock} = \frac{R_{shock}}{v_1} \sim \frac{1.4 \times 10^{19}}{5 \times 10^8 \text{cm/s}} \sim 5 \times 10^{10} \text{s} \sim 1000 \text{yr}$$

After this phase the Sedov-Taylor phase starts when the shock speed decreases due to the reverse shock when ISM begins to exercise significant pressure on ejecta. For  $t \gg T_{shock}$  the initial energy has been transferred almost entirely to swept up material:

$$v_{shell} = \sqrt{\frac{3E}{2\pi R_{shock}^3 \rho}} \Rightarrow v_{shell} \propto R_{shock}^{-3/2} \propto t^{-3/5} \quad \text{from} \quad R_{shock}^{3/2} \frac{dR_{shock}}{dt} = \text{const} \quad \text{and} \quad R_{shock} \propto t^{\alpha}$$

# Maximum energy problem

Maximum number of possible scattering cycles:  $N_{cycle} = \frac{T_{shock}}{T_{cycle}}$

$$E_{max} = N_{cycle} \Delta E = \frac{\xi E_0 T_{shock}}{T_{cycle}}$$

$T_{shock}$  = duration of acceleration process

$T_{cycle}$  = time of back and forth encounter of the shock

$$T_{cycle} = \frac{4}{c} \left( \frac{D_1}{v_1} + \frac{D_2}{v_2} \right) \quad \cdot \quad \begin{array}{l} \text{when } B_1 = B_2 \text{ one can assume that } D_1 = D_2 \\ v_2 = 1/4 v_1 \end{array}$$

Because the diffusion length of energetic particles cannot be smaller than the Larmor radius of the particle in the galactic B-field for acceleration to occur in the irregularities of the B-field:

$$D_{min} = \frac{r_L c}{3} \sim \frac{1}{3} \frac{Ec}{ZeB} \quad \rightarrow \quad T_{cycle} = \frac{20Ec}{3ZeBv_1}$$

$$E_{max} = \frac{v_1}{c} \frac{ET_{shock} 3ZeBv_1 c}{20Ec} \sim \frac{3 \times 10^3 \text{ yr} \times Ze \times 3 \times 10^{-6} \text{ G} \times (5 \times 10^8 \text{ cm/s})^2}{20} \text{ erg}$$

$$E_{max} \sim Z \times 300 \text{ TeV}$$

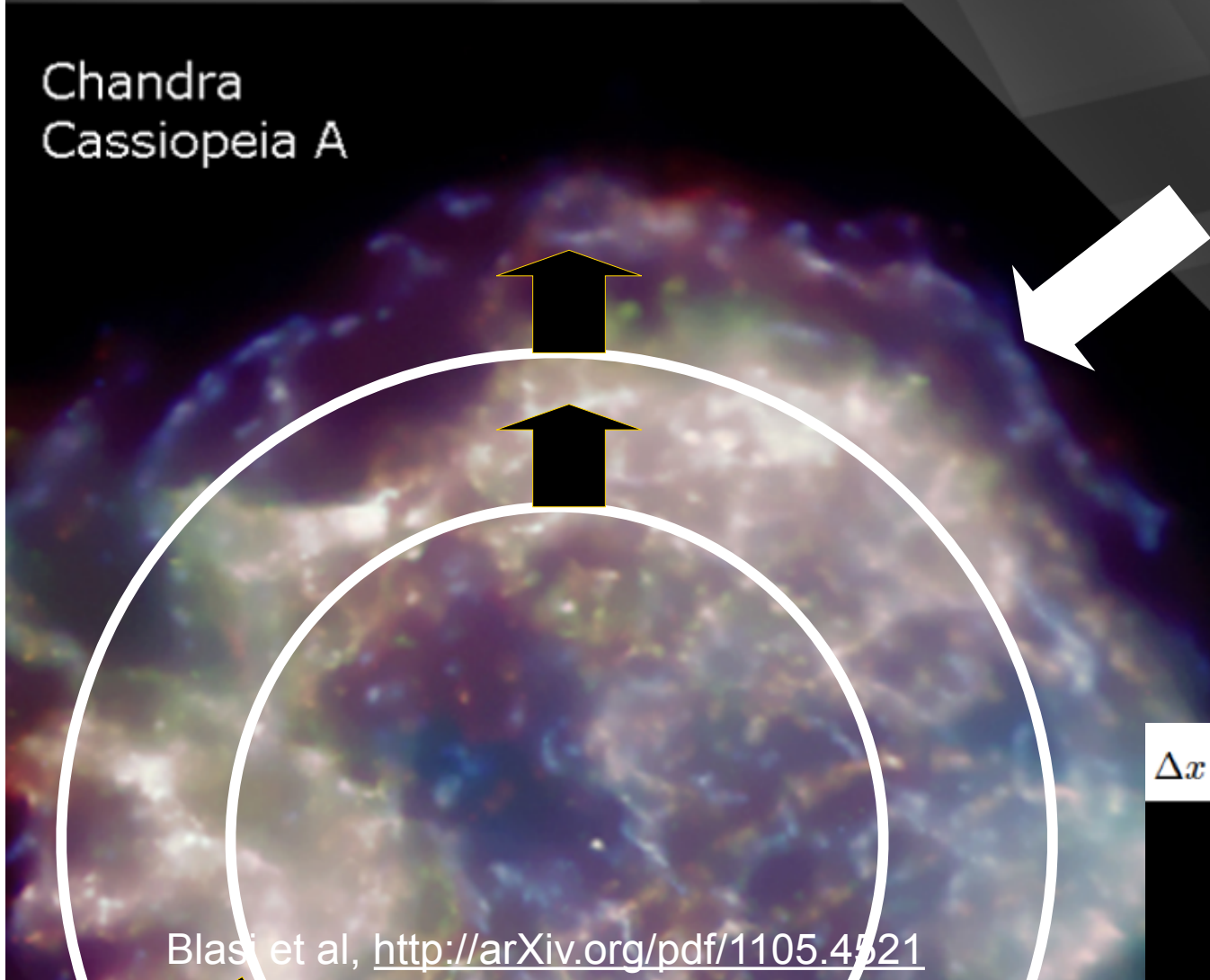
**Diffusive Shock Acceleration cannot explain the knee of CRs.**

# The B-field in SNRs

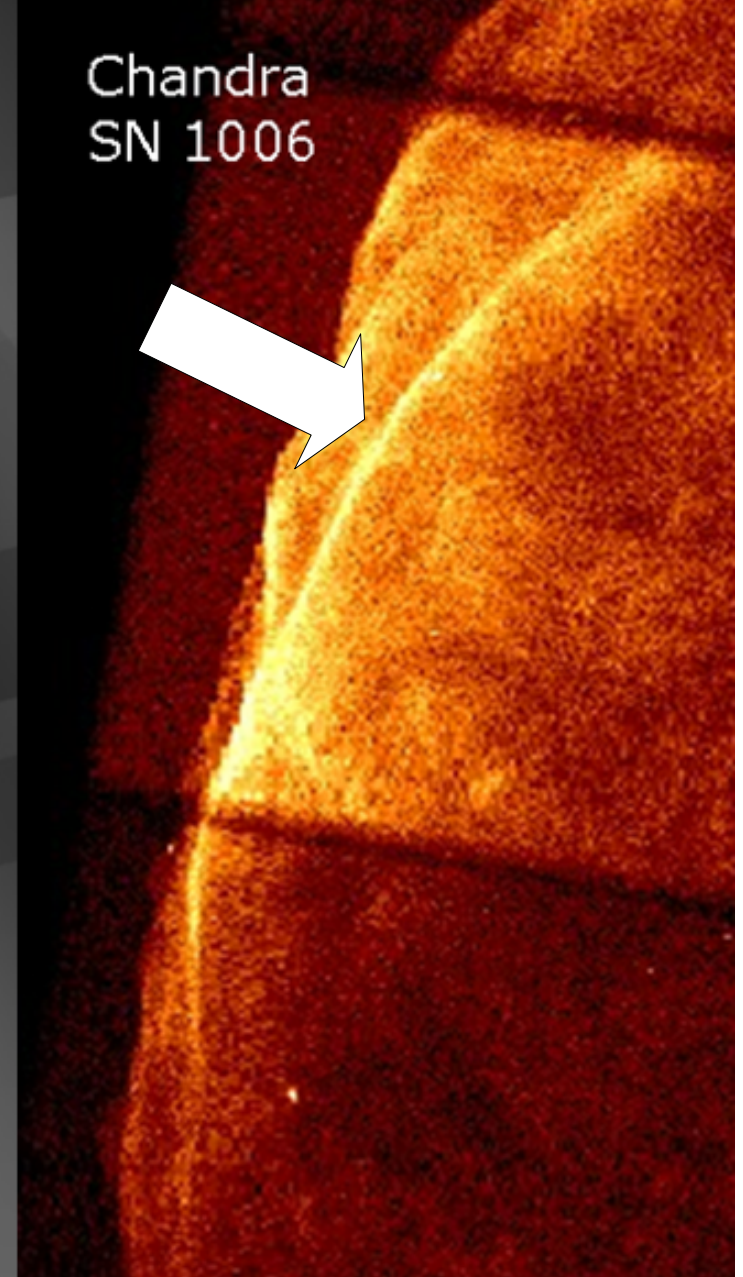
Diffusive Shock Acceleration:  $E_{\max} \sim 100 \text{ TeV} \times Z$

Need non-linear processes of magnetic field amplification consistent with observed filaments of dimension  $10^{-2} \text{ pc}$  that imply synch. emission in large magnetic fields

Chandra  
Cassiopeia A



Chandra  
SN 1006



$$\Delta x \approx \sqrt{D(E_{\max})\tau_{\text{loss}}(E_{\max})} \approx 0.04 B_{100}^{-3/2} \text{ pc}$$

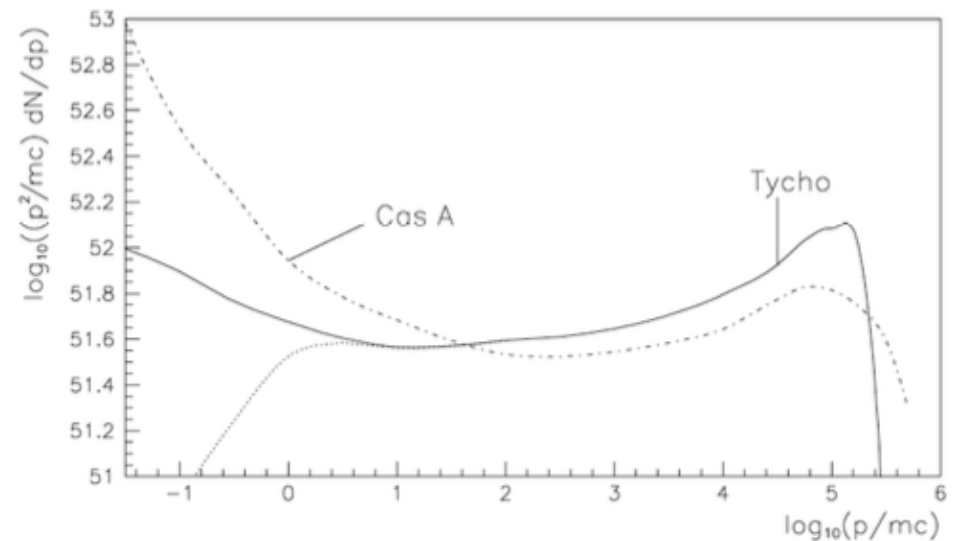
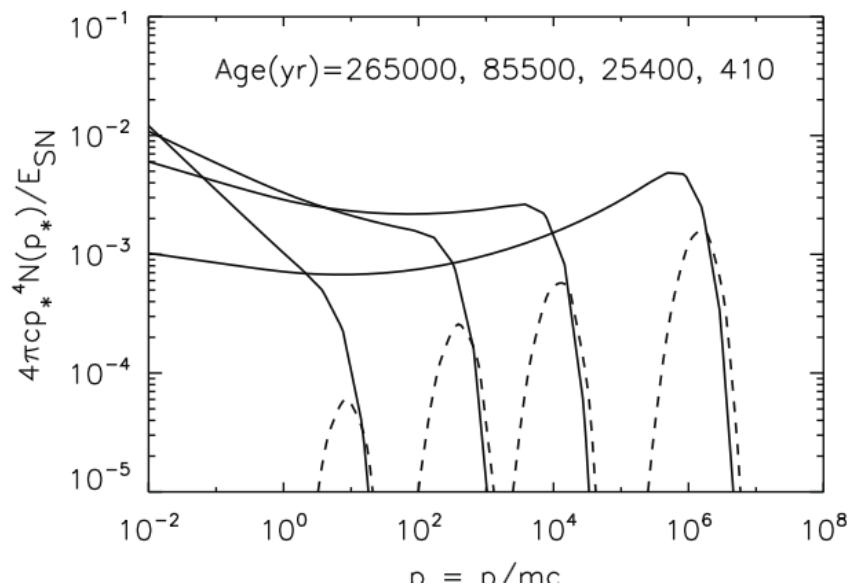
$B \approx 100 \mu\text{Gauss}$

Blasi et al, <http://arXiv.org/pdf/1105.4521>

# Non linear DSA and spectra

The cosmic rays being accelerated can cause streaming instabilities and generate hydromagnetic waves. These waves themselves can be the source of diffusion in the upstream, un-shocked region. With this coupling, the acceleration process is nonlinear, and spectra do not follow  $E^{-2}$  power law.

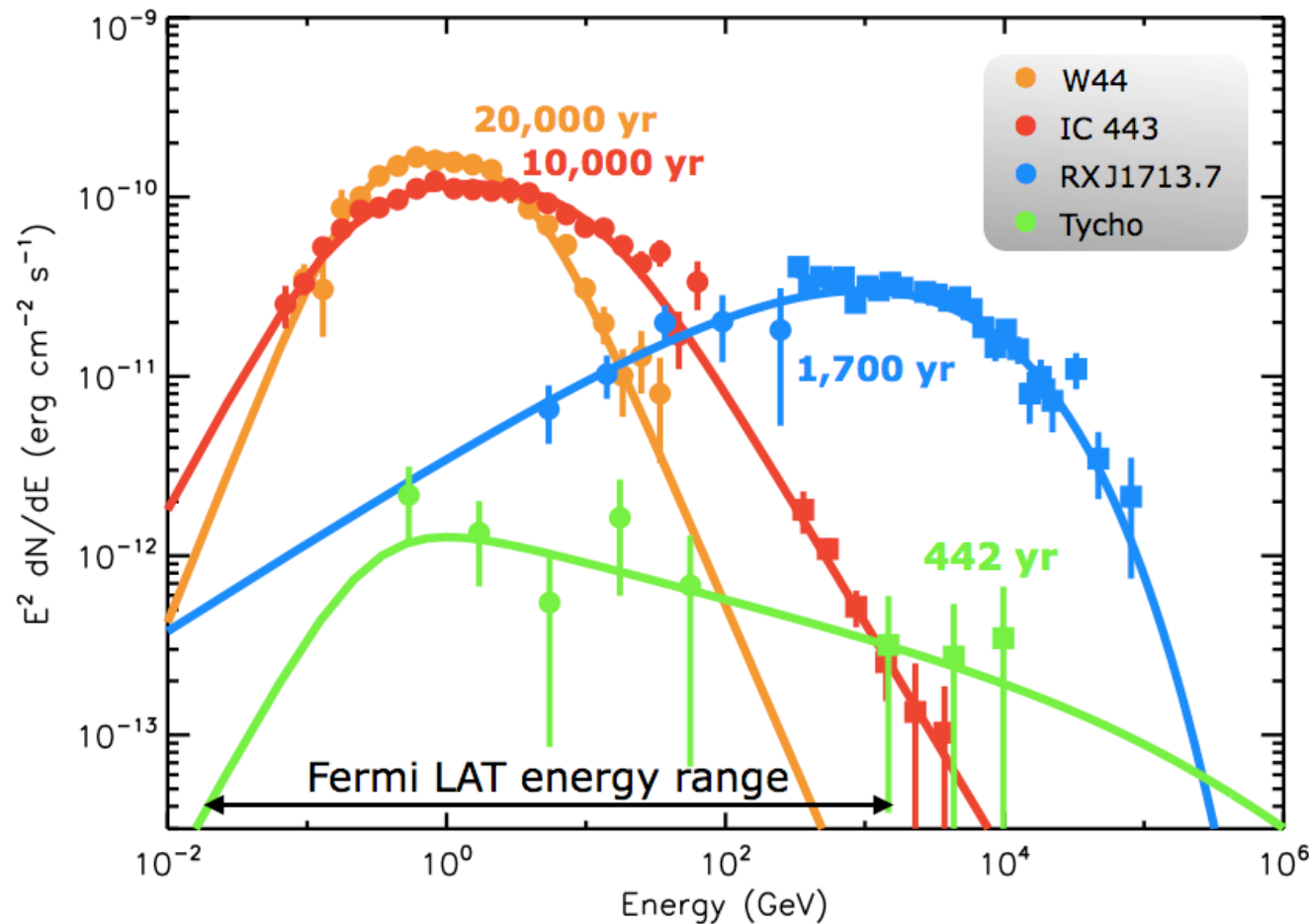
Non linear DSA can reach  $Z \times \text{PeV}$  thanks to the dynamical connection between particles being accelerated and the background plasma but predicts harder spectra than what observed with a concave shape.



(Voelk *et al*, A&A396:649,2002)

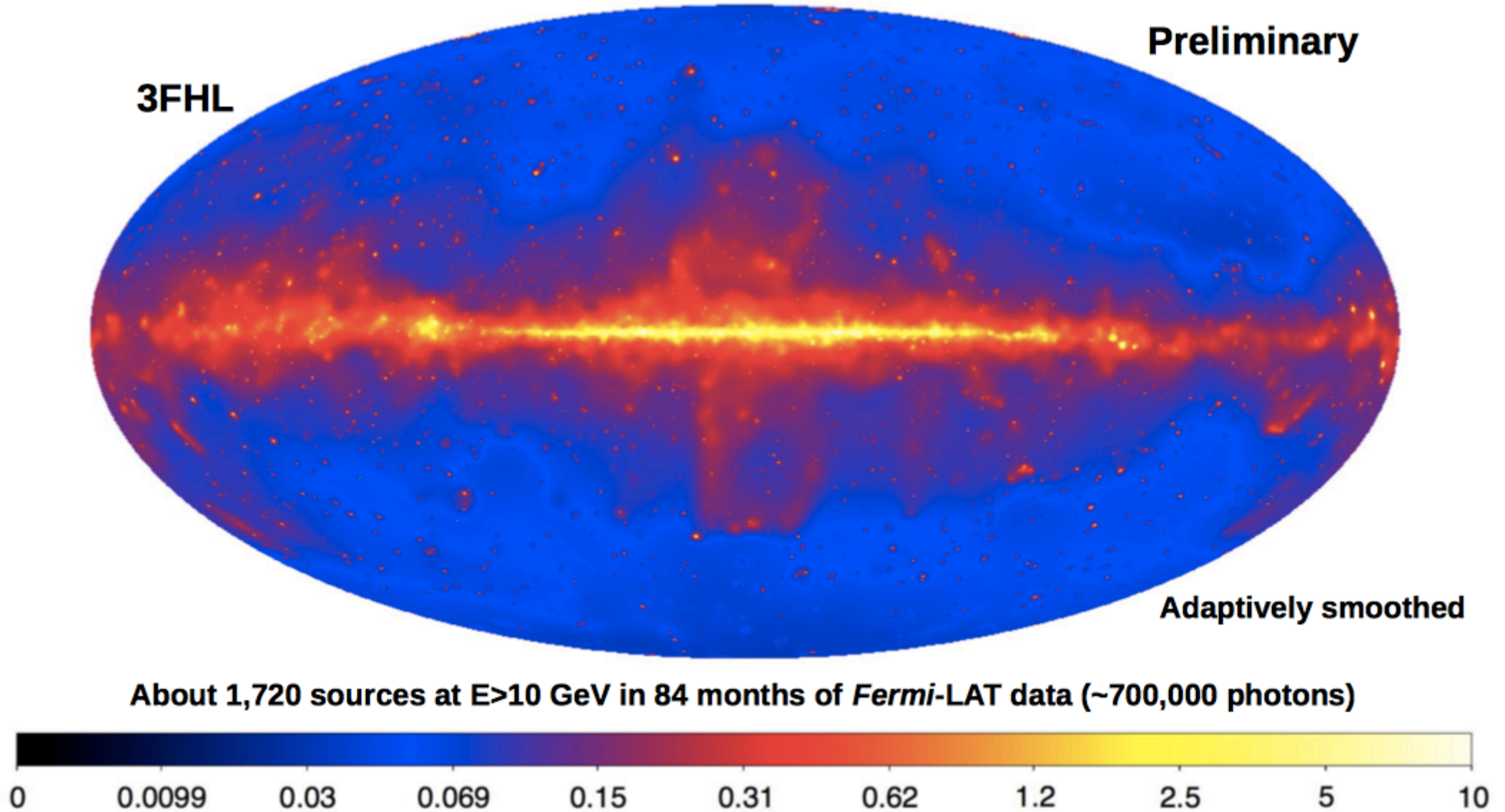
# What is gamma astronomy telling on SN?

Can 1<sup>st</sup>-order Fermi acceleration at SNR shocks explain the spectrum (injection, magnetic field amplification, diffusion losses)? Observed spectra are convex. It is possible that the 2<sup>nd</sup> order is still a valid explanation but also that there unobserved SN... Age dependent efficient of accelerators. We need CTA for a clear classification!



# Fermi 7 yr sky survey

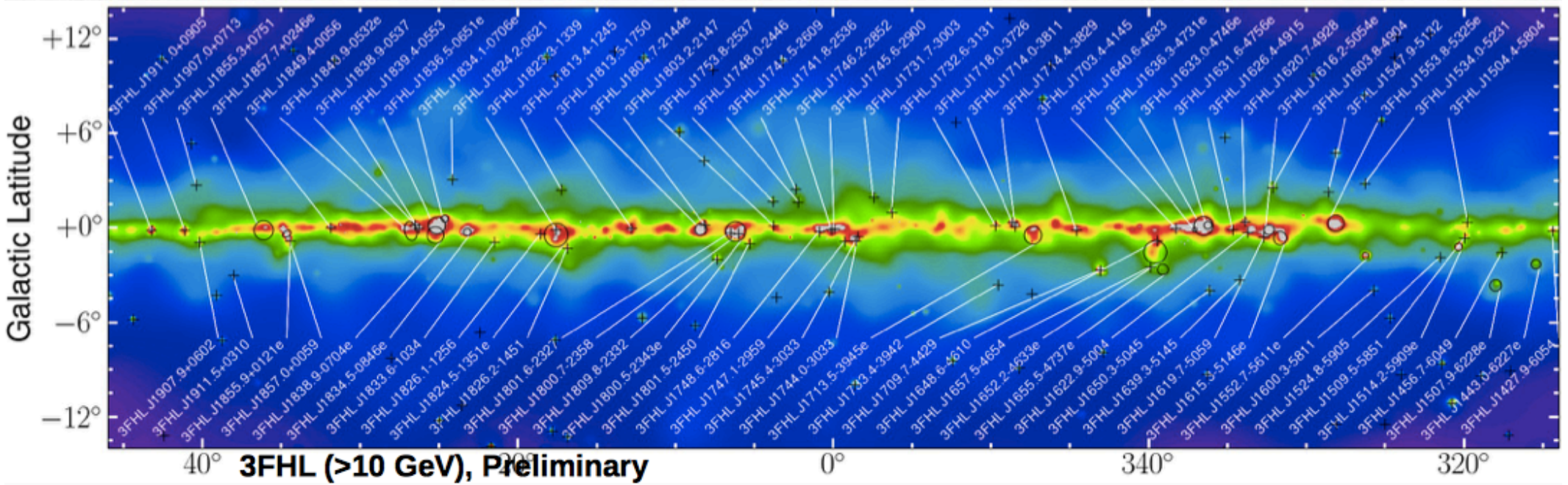
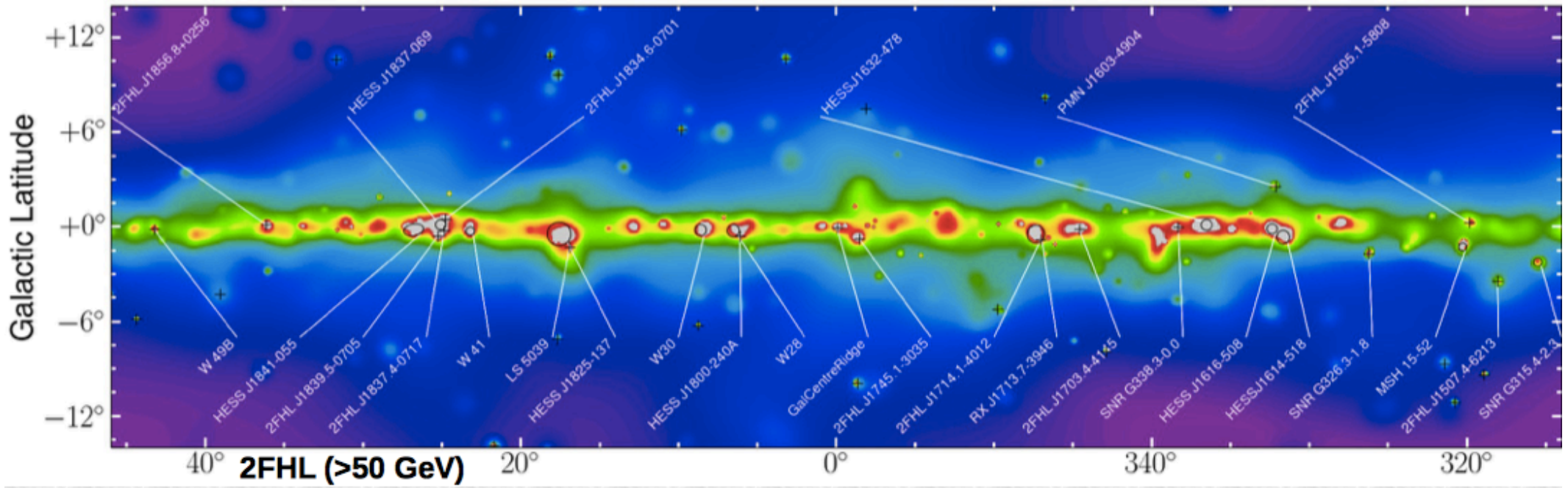
Julie McEnery, TeVPA2016  
<https://cds.cern.ch/record/2216217>





# Fermi 7 yr Galactic plane survey

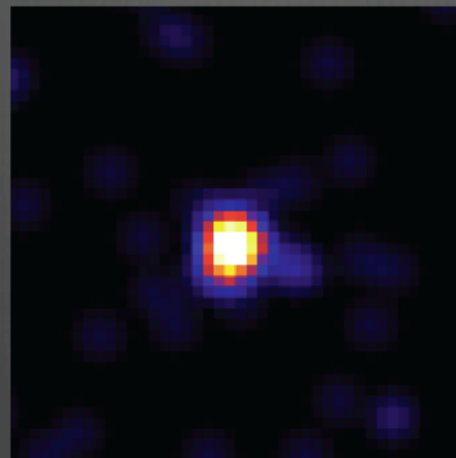
1720 sources (54 extended)



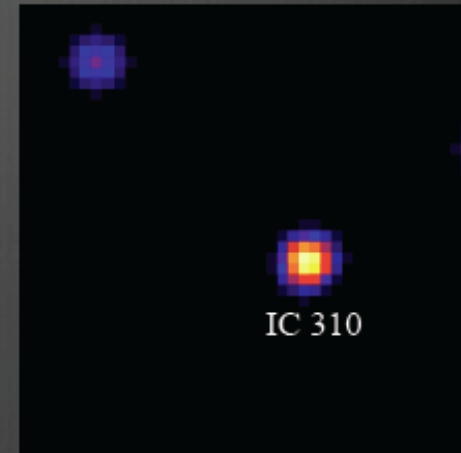
# New sources with increasing energy...



1-10 GeV



10-100 GeV



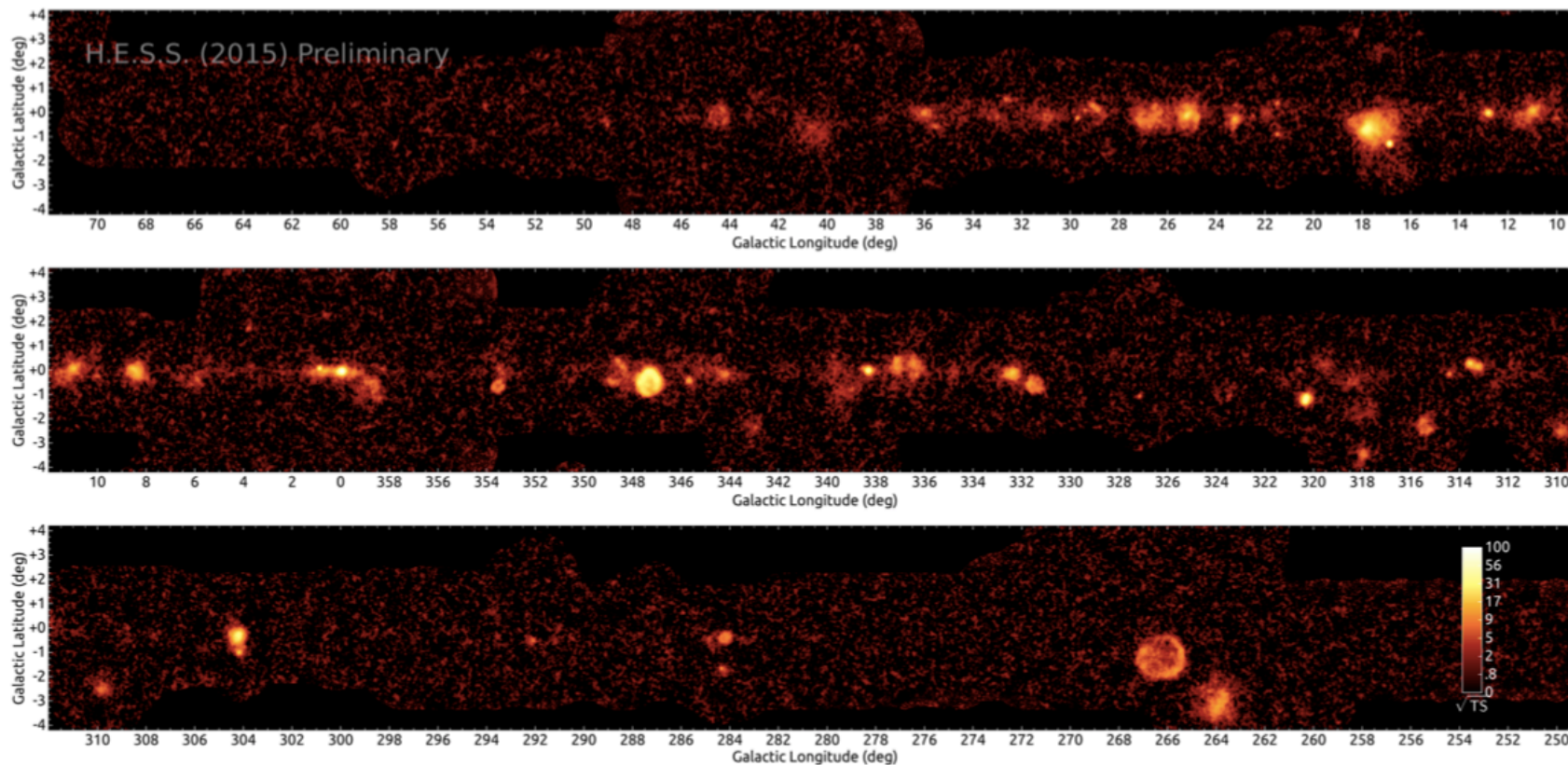
>100 GeV

At energies below 10 GeV, only the radio galaxy NGC 1275 (Perseus A) is visible, but above 10 GeV a second source (to the lower right) emerges. Above 100 GeV, only this source, the head-tail galaxy IC 310, remains. From Neronov et al (2010)

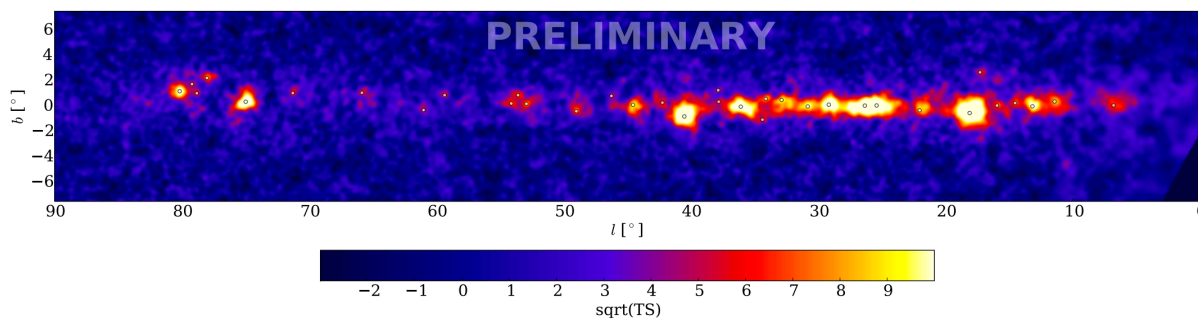
New sources and features emerge in the gamma-ray sky with increasing energy

# Galactic plane survey

Diffuse emission suppressed by background modelling technique



Sensitivity 0.5-2% of Crab Nebula Flux

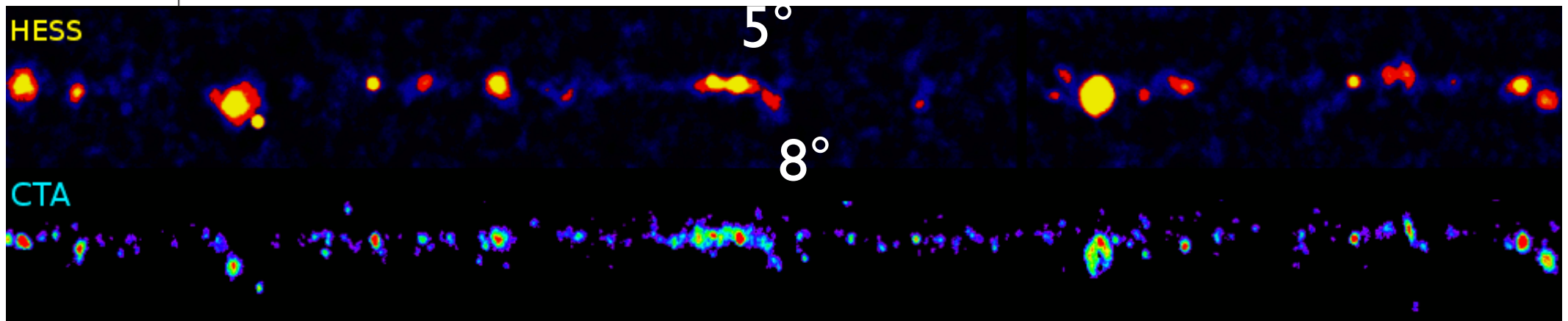


Unidentified gamma-ray TeV sources (pulsar wind nebula, magnetars, galactic black hole,...other acceleration mechanisms), Extended PeVatrons?

# The Galactic disk beyond 200 GeV

First survey of the Galactic disk with H.E.S.S. (2005)

CTA

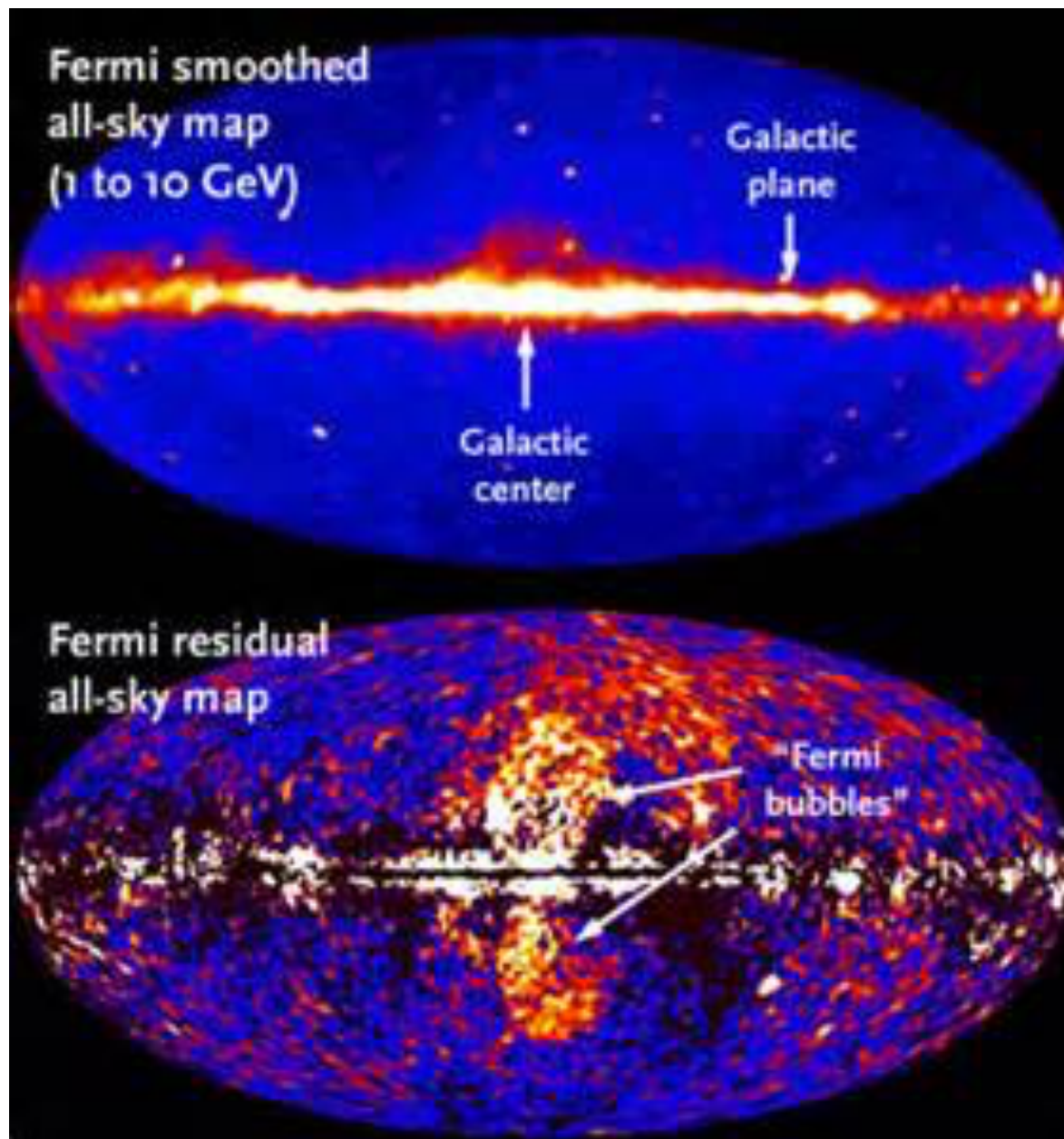


$$e^- \gamma \rightarrow e^- \gamma$$

$$p p \rightarrow p p \pi^0$$

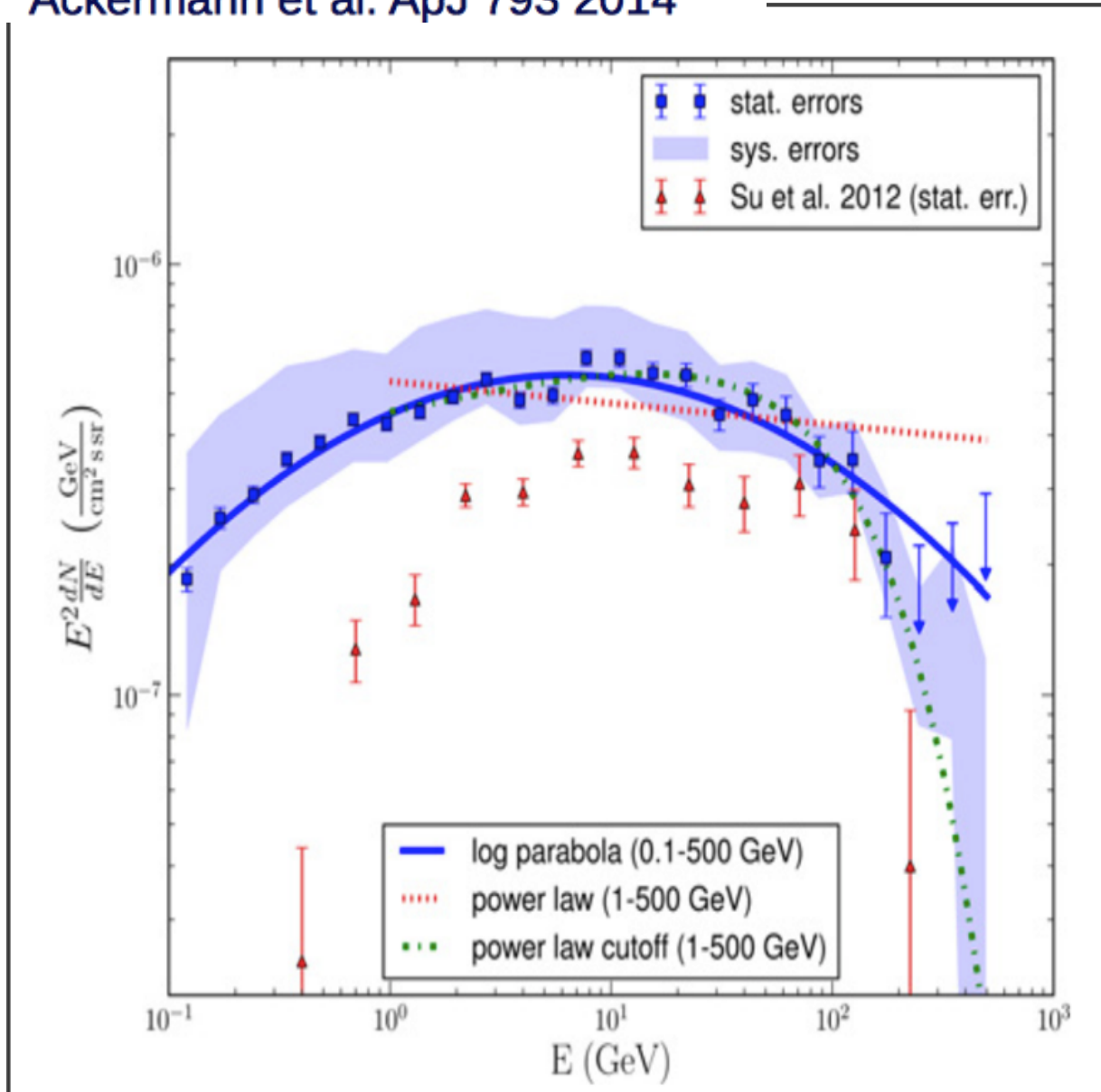
$$\pi^0 \rightarrow \gamma \gamma$$

# New features in the gamma band: the Fermi bubbles

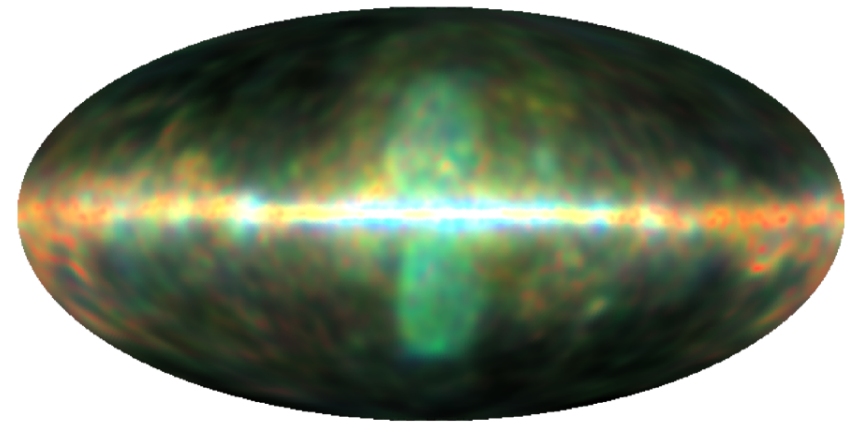


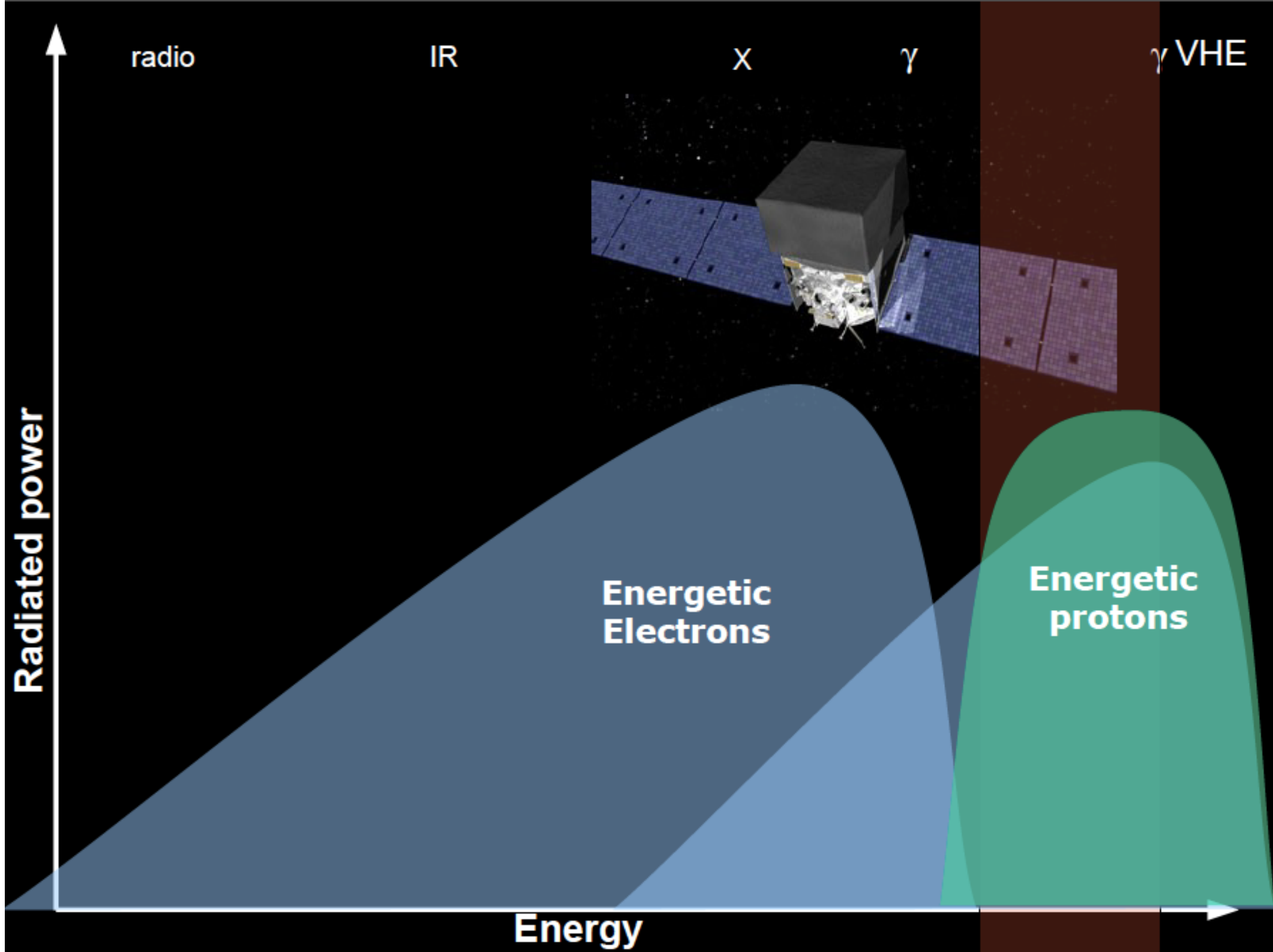
# The bubble spectrum

Ackermann et al. ApJ 793 2014



$\gamma$ -ray emission leptonic or hadronic?  
CTA can contribute adding statistics  
above 500 GeV and scanning different  
latitude regions





radio

IR

X

$\gamma$

$\gamma$  VHE

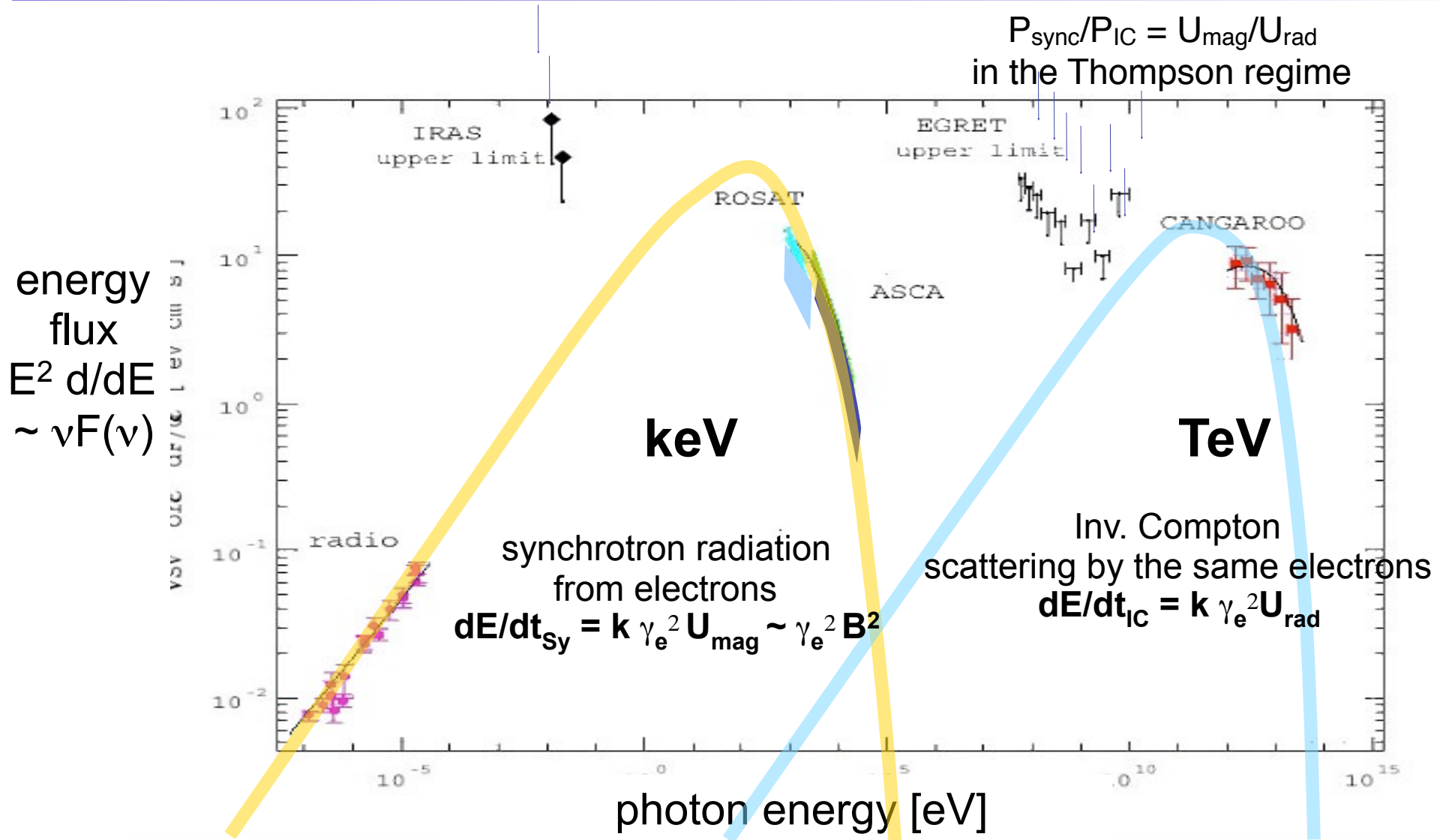
Radiated power

Energetic  
Electrons

Energetic  
protons

Energy

# Spectral energy distribution of RXJ 1713.7-3946

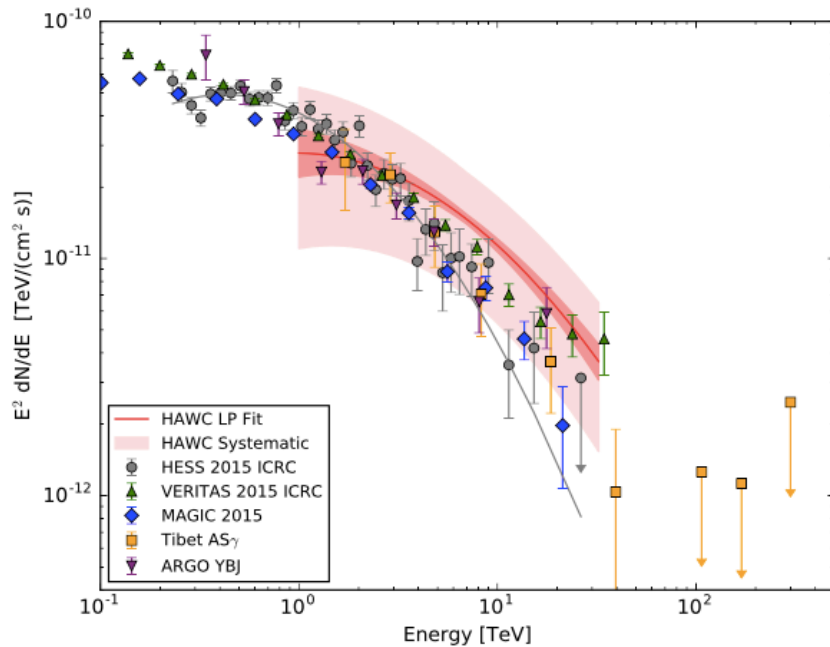
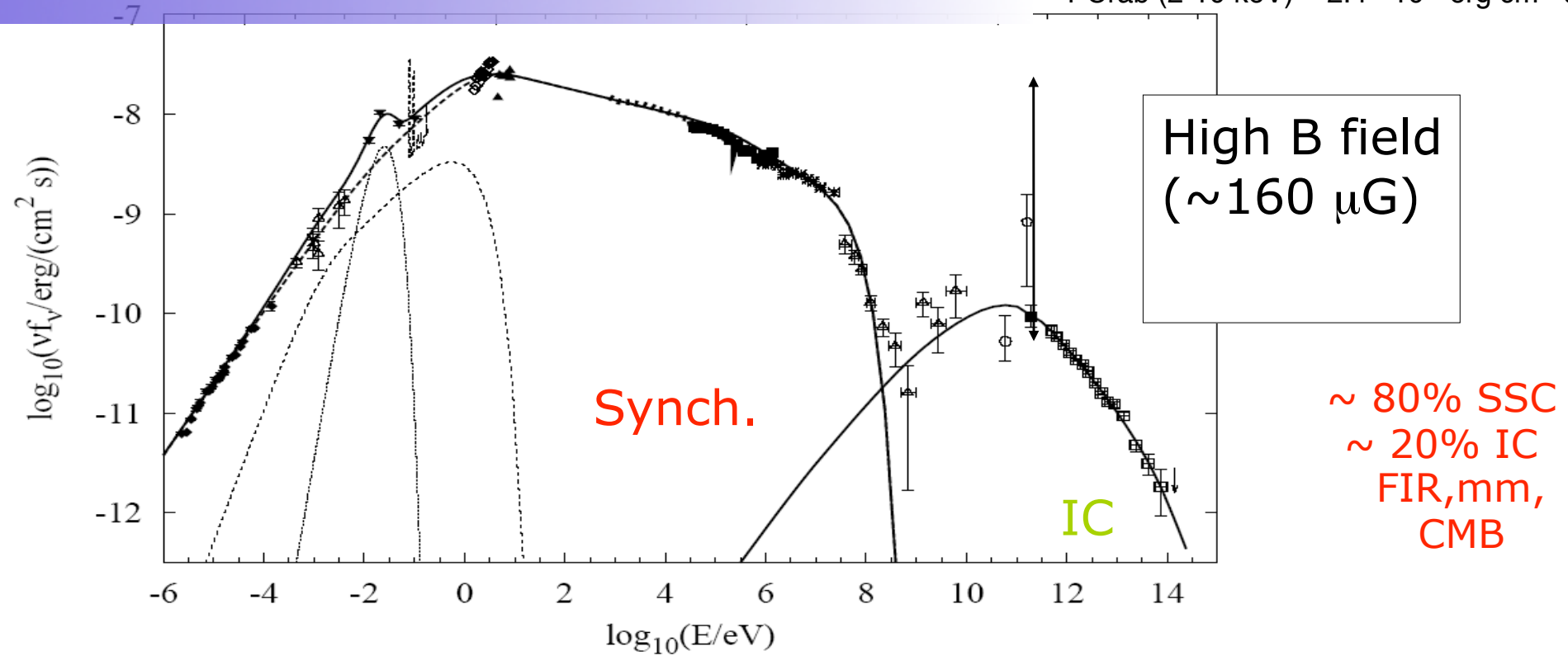


In leptonic processes: the **synchrotron luminosity** is proportional to the **B-field strength** and **Lorentz factor of electrons** radiating. **Inverse Compton**: in the rest frame of an electron the photon energy is boosted by  $\gamma_e$  and after scattering, transforming in the lab again, the photon energy is boosted by  $\gamma_e^2$ . The IC luminosity is also proportional to the energy density of seed photons which can be the synchrotron photons. Synchrotron cooling is faster than IC if  $B > 3 \mu\text{G}$ . In hadronic processes, photons are produced via  $\pi^0 \rightarrow \gamma\gamma$ .



# Crab Nebula SED

1 Crab (2-10 keV) =  $2.4 \cdot 10^{-8}$  erg cm<sup>-2</sup> s<sup>-1</sup>



Spectra extend to about 40 TeV  
New HAWC measurement:  
<https://arxiv.org/pdf/1701.01778.pdf>

# Hadronic/Leptonic SEDs

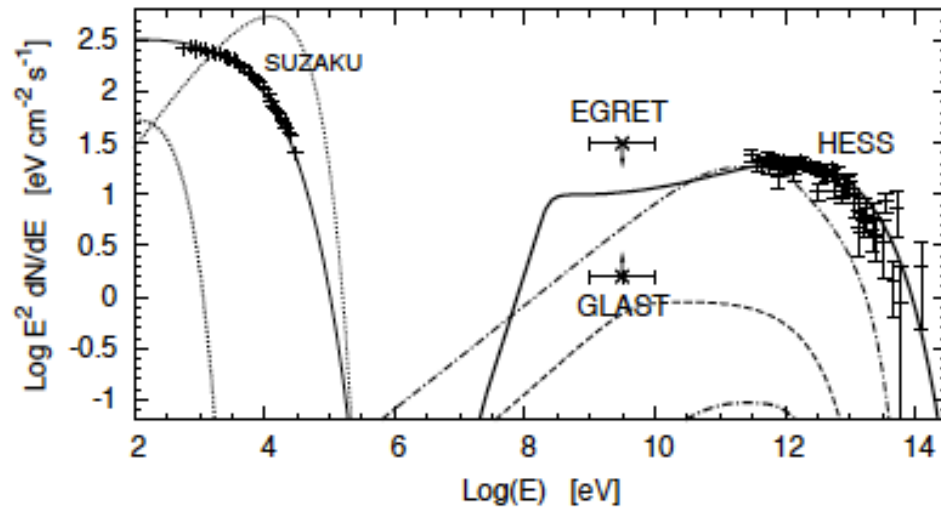


**Figure 3.** Spatially integrated spectral energy distribution of RX J1713.7-3946 in the hadronic scenario, for  $n_0 = 0.12 \text{ cm}^{-3}$ ,  $u_0 = 4300 \text{ km/s}$ ,  $B_0 = 2.6 \mu\text{G}$ ,  $\xi = 3.8$ . The following components are plotted: synchrotron (dotted line) thermal emission (dotted line), Compton scattering with CMB (dashed line) and with Opt+IR background (dot-dashed line). The contribution from pion decay is shown as a thick solid line and corresponds to  $p_{p,\text{max}} = 1.26 \times 10^5$ . HESS data taken from 2003 to 2005 are plotted together with Suzaku data in the X-ray band. Also EGRET upper limit and GLAST sensitivity are shown.

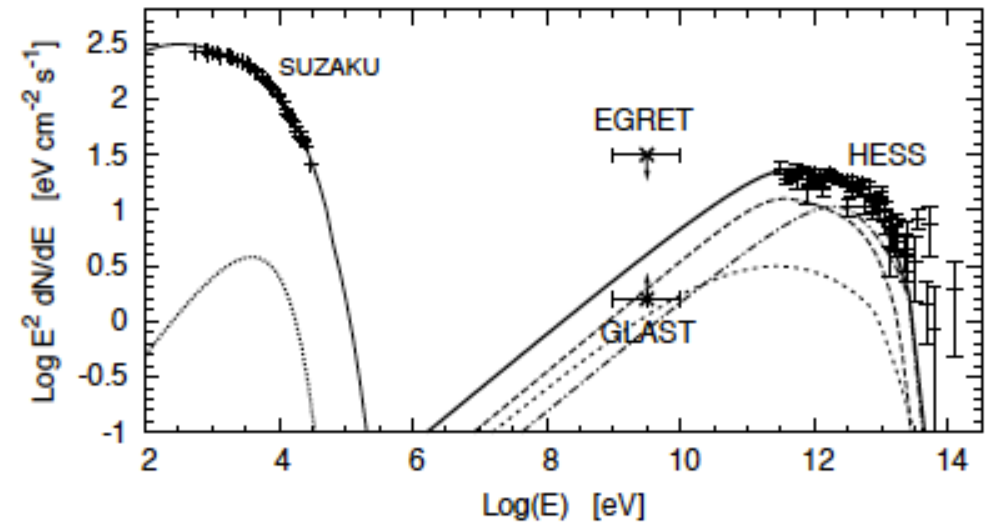
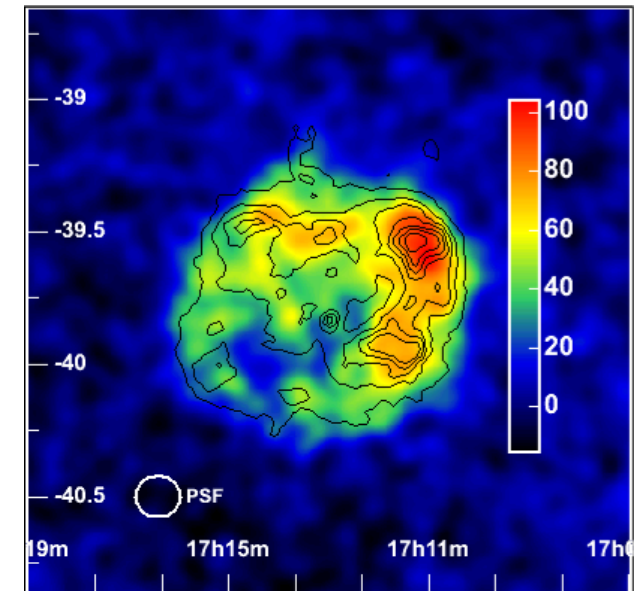
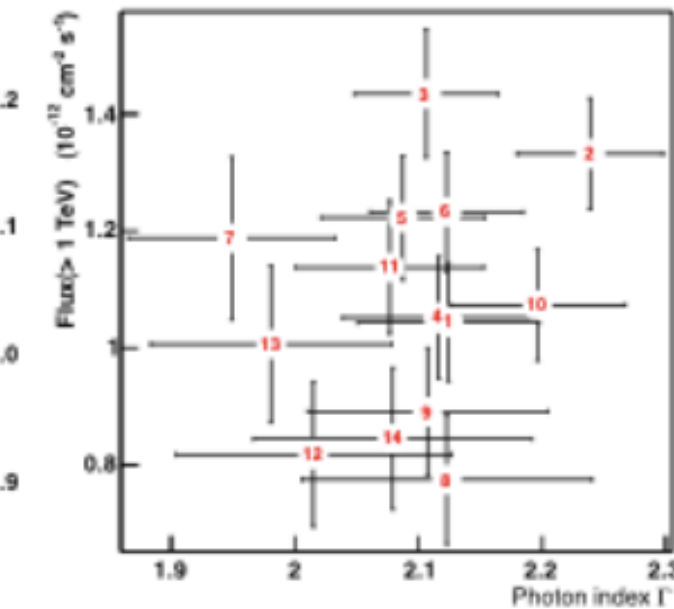
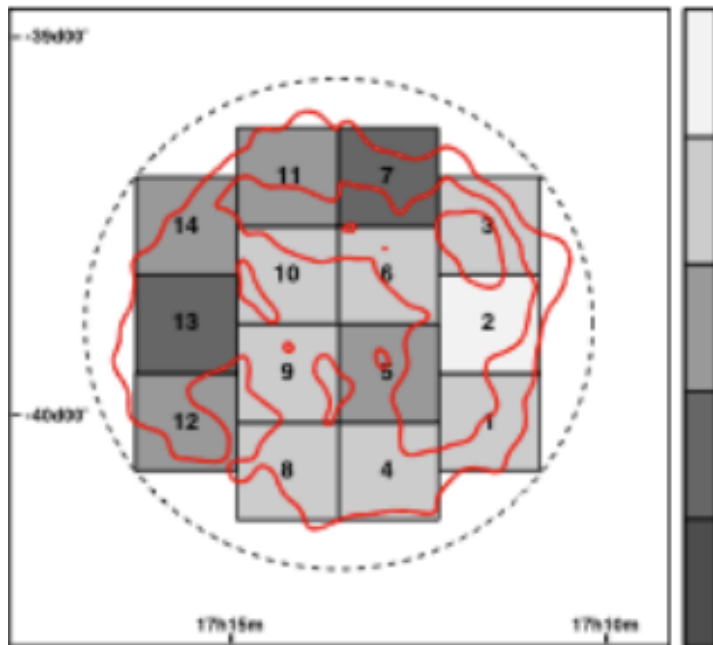


**Figure 4.** Spatially integrated spectral energy distribution of RX J1713.7-3946 in the leptonic scenario. The following components are plotted: synchrotron (thin solid line) and thermal (thick dotted line) electron emission, ICS component for CMB (dashed line), optical (dotted line) and IR (dot-dashed line) photons, and the sum of the three (thick solid line). The Opt+IR components are assumed to have energy density 24 times the mean ISM value. The other parameters are:  $n_0 = 0.01 \text{ cm}^{-3}$ ,  $u_0 = 4300 \text{ km/s}$ ,  $B_0 = 1.5 \mu\text{G}$  and  $\xi = 4.1$ . The experimental data are the same as in Fig. 3

# Hadrons in SNRs? RXJ 1713.7-3946

Do we see  $\gamma$ -rays from hadronic interactions ( $\pi^0$  decays), or are they from inverse-Compton scattering by (radio synchrotron emitting) electrons?

- First claim from CANGAROO (Nature 2002) not confirmed by Fermi
- TeV emission is often following the CO matter contours.

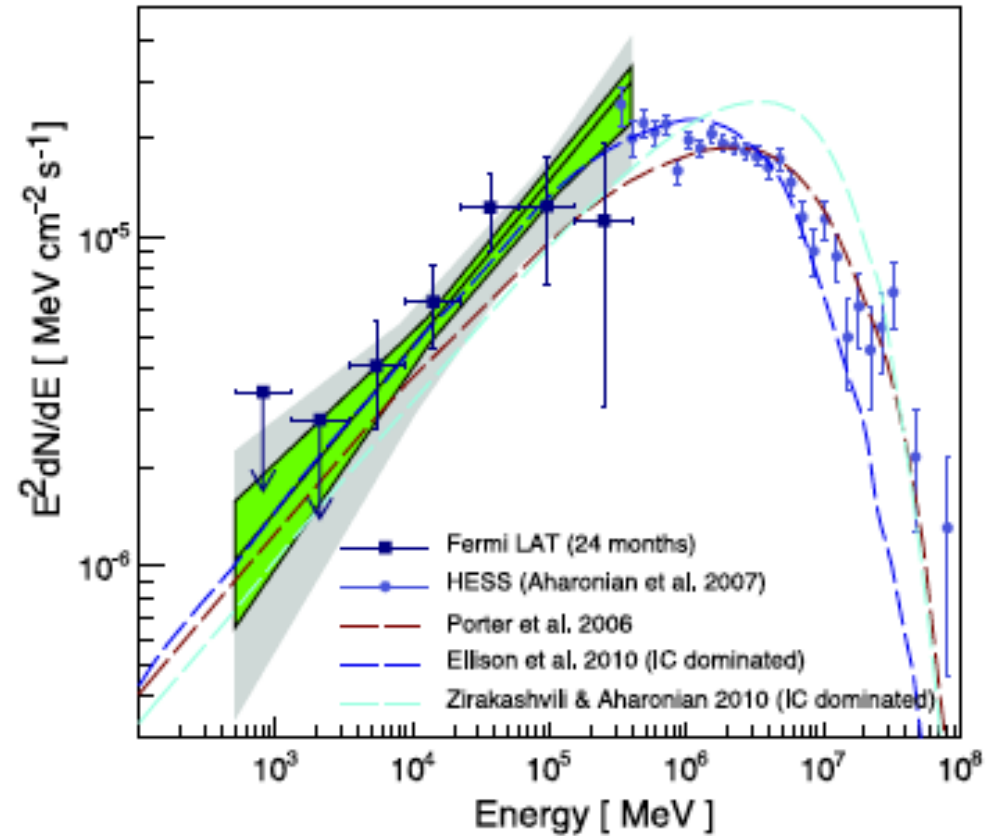
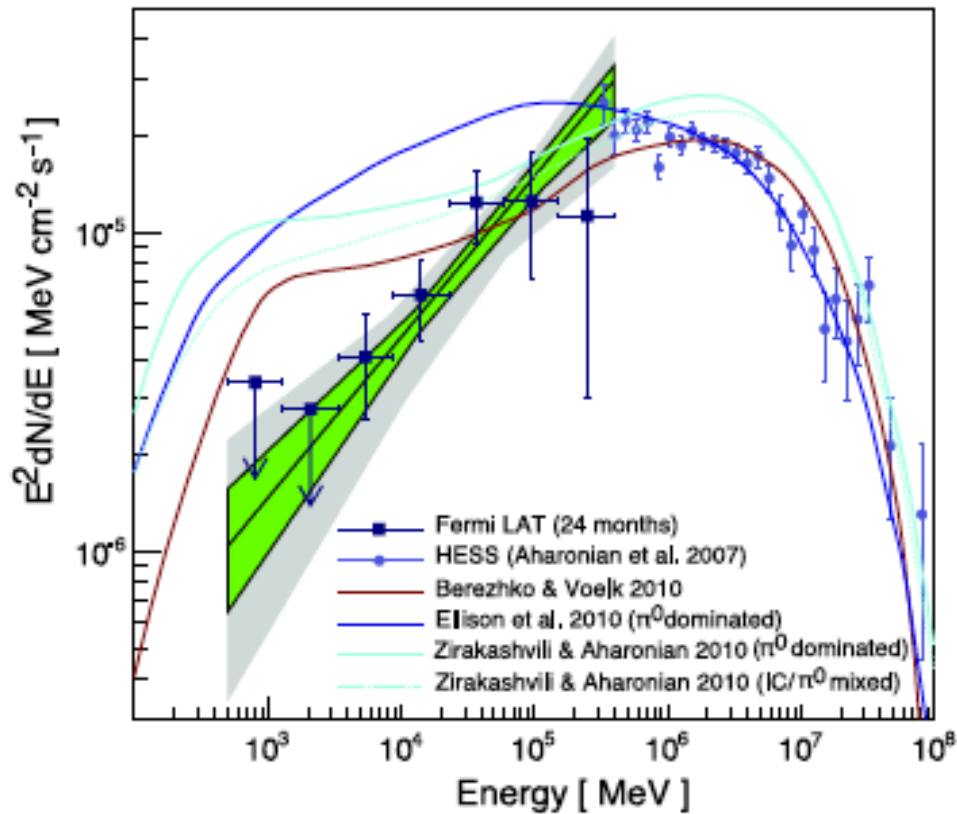


**HESS morphology study**

**Aharonian et al., Nature, 432, 75 (2004) ;  
Aharonian et al., A&A, 464, 235 (2007)**

# Fermi observations of RXJ 1713.7-3946

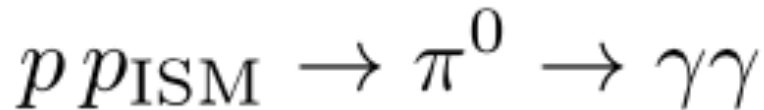
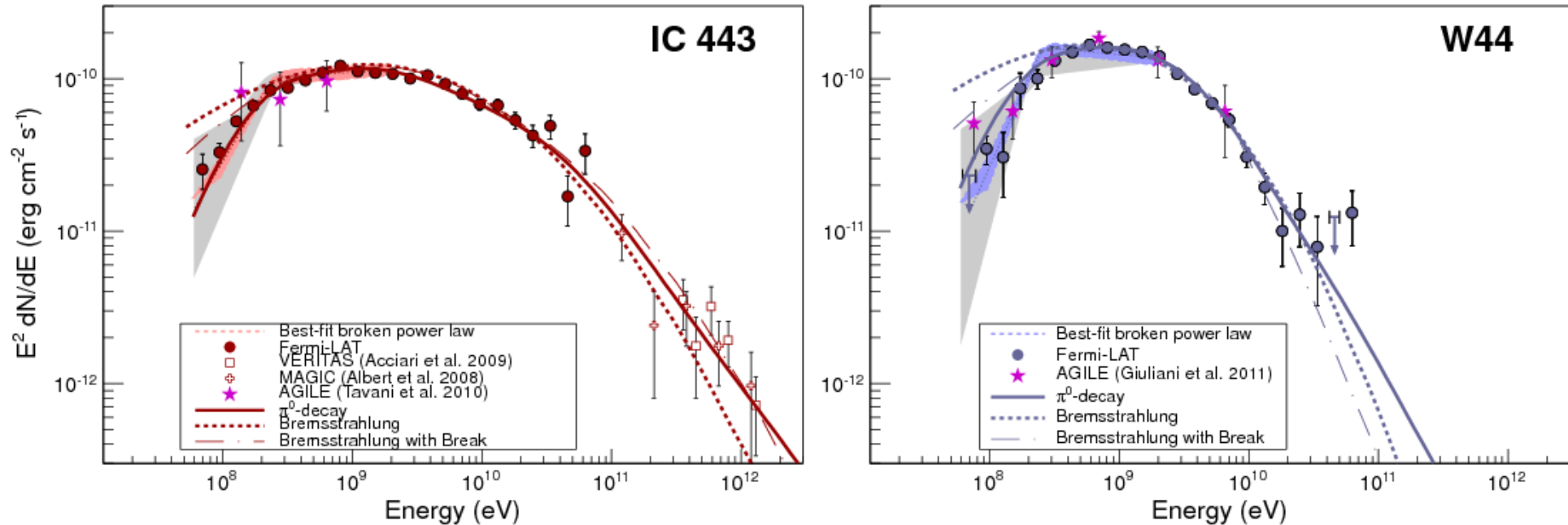
Aharonian et al., *Nature*, 432, 75 (2004) ; Aharonian et al., *A&A*, 464, 235 (2007)



'The dominance of leptonic processes in explaining the gamma-ray emission does not mean that no protons are accelerated in this SNR, but that the ambient density is too low to produce a significant hadronic gamma-ray signal.' (arXiv:1103.5727).

# Evidence for pion decay?

Fermi identified various candidates for pionic gammas but yet did not verify that what we yet do not have a convincing model on CR acceleration



Ackermann et al. (Fermi Collaboration), *Science*, 339, 807 (2013)

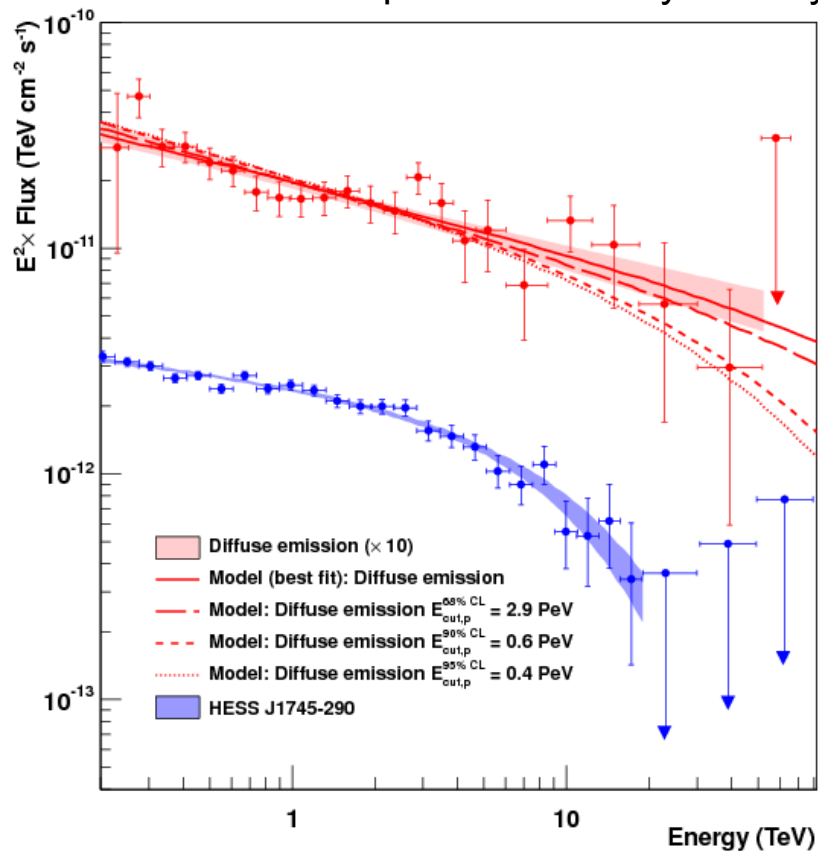
# THE FIRST PEVATRON!

Nature 531 (2016) 476 (<https://inspirehep.net/record/1434943>)

The Galactic Centre PeVatron appears to be located in the same region as the central  $\gamma$ -ray source HESS J1745-290.

Interpretation: Sgr A\*, the pulsar wind nebula G 359.95-0.0416,17, and a spike of annihilating dark matter. Sgr A\*, black hole of 3.6 million solar masses: the current rate of particle acceleration is not sufficient to provide a substantial contribution to Galactic cosmic rays, Sgr A\* could have plausibly been more active over the last  $\geq 10^{6-7}$  yr, and therefore should be considered as a viable alternative to SNRs as a source of PeV Galactic cosmic rays.

H.E.S.S. : Central 10 pc of the Galaxy for 10 yrs



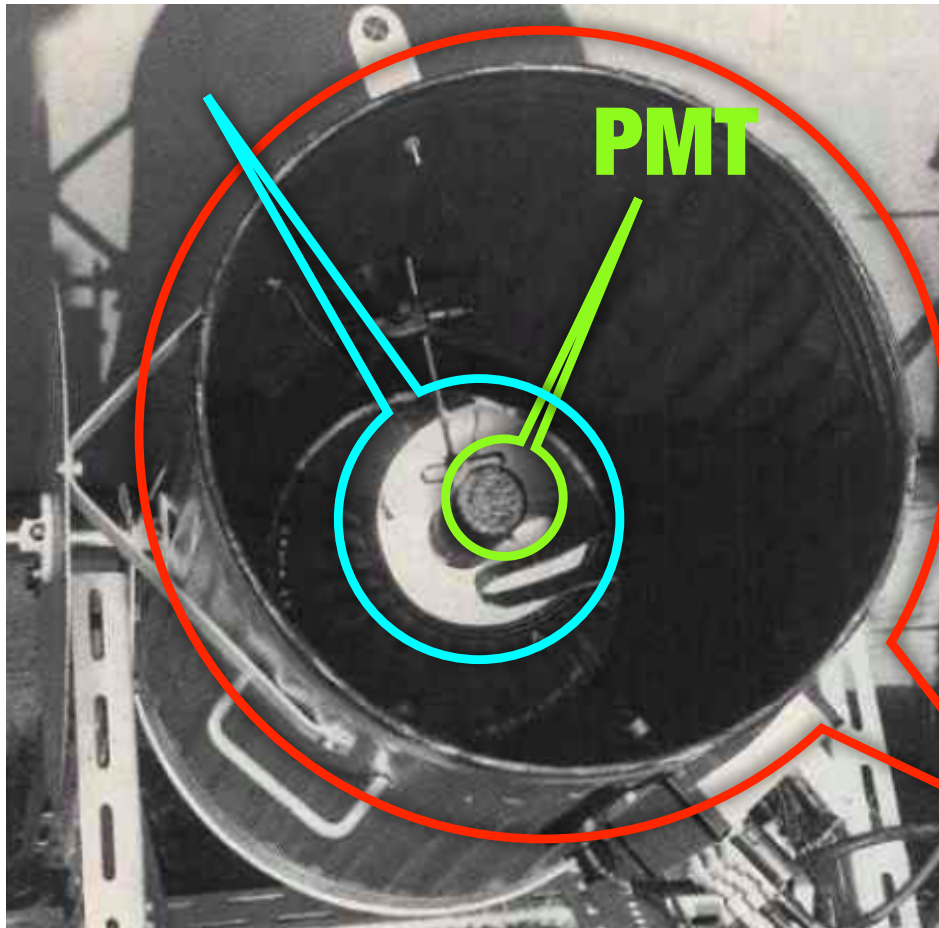
VHE  $\gamma$ -ray spectra of the diffuse emission and HESS J1745-290. The vertical and horizontal error bars show the  $1\sigma$  statistical error and bin size, respectively. Arrows represent  $2\sigma$  flux upper limits. The  $1\sigma$  confidence bands of the best-fit spectra of the diffuse and HESS J1745-290 are shown in red and blue shaded areas, respectively. The red lines show the numerical computations assuming that  $\gamma$ -rays result from the decay of **neutral pions** produced by proton-proton interactions. The fluxes of the diffuse emission spectrum and models are multiplied by 10.



# Imaging Cherenkov Telescopes history

C. Galbreith and J. Jelley when visiting the Harwell Air Shower Array in UK in 1951, had the idea to try to detect a short light pulse from a CR air shower which involves millions of charged particles. They tested the hypothesis with a **5 cm PMT mounted on a focal plane of a 25 cm parabolic mirror in a garbage can.**

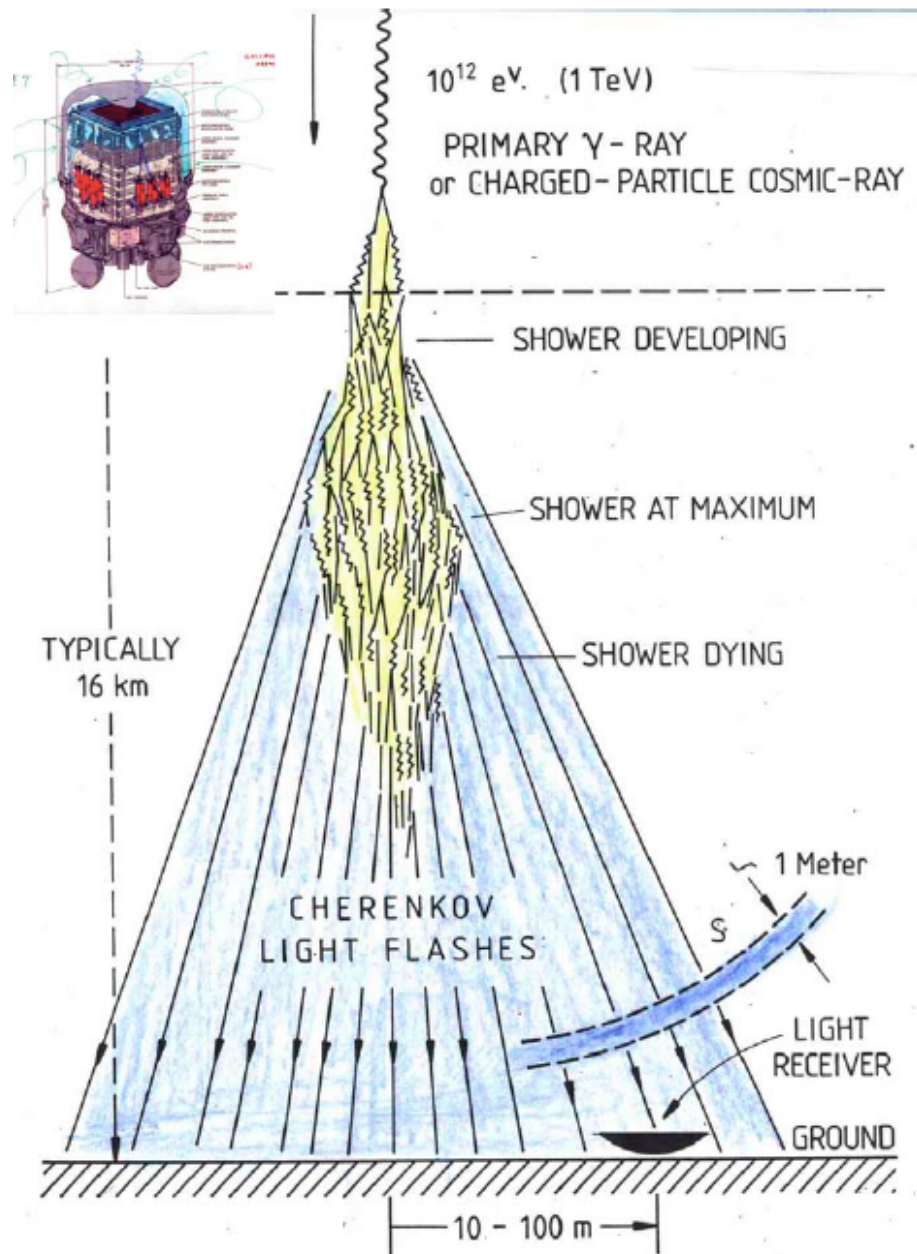
## Mirror



- They observed oscilloscope triggers from light pulses that exceeded the average night-sky background every 2 min.
- Gamma signals from sources (Crab) were detected only in 1989 by Whipple...

**Trash Bin !!**

# Early History of Atmospheric Cherenkov Technique



1948 PMS Blackett (Nobel) in the Royal Society Report on the study of the night-sky light and aurora pointed out that  **$\approx 0.01\%$  of the night light sky comes from Cherenkov light emitted by CRs and their secondaries** as they traverse the atmosphere.



# Imaging Air Cherenkov Technique

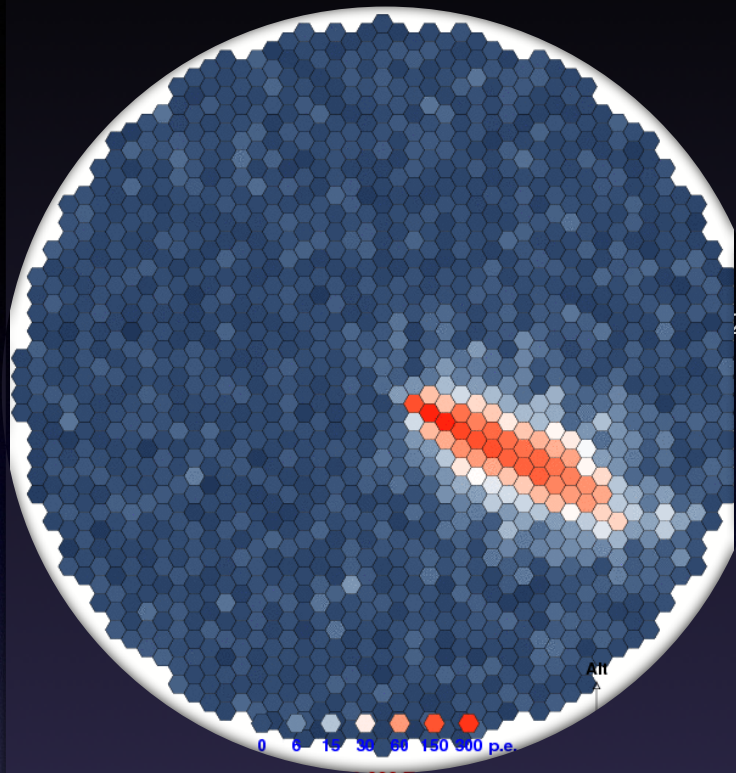
$\gamma$

“Shower”

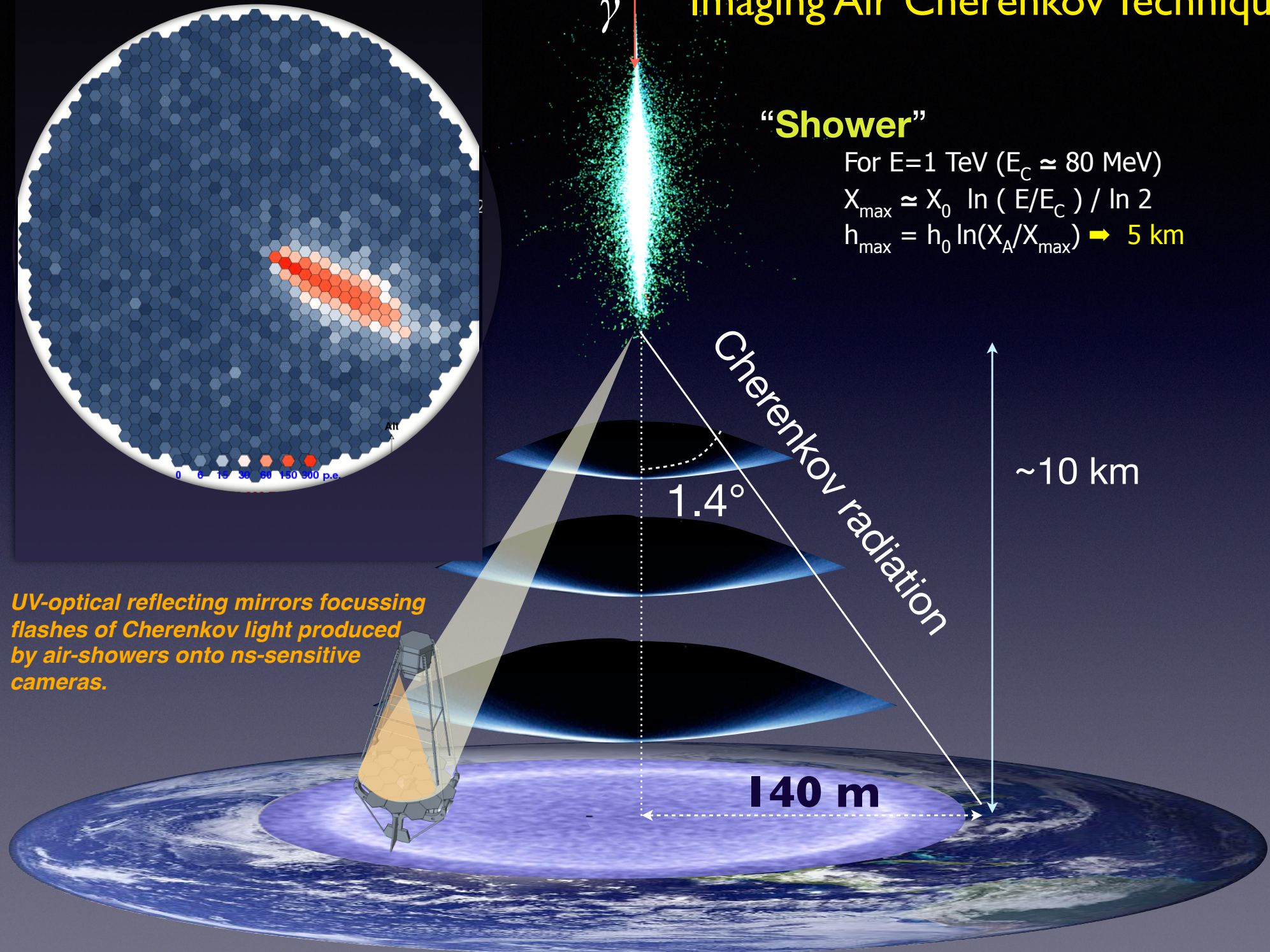
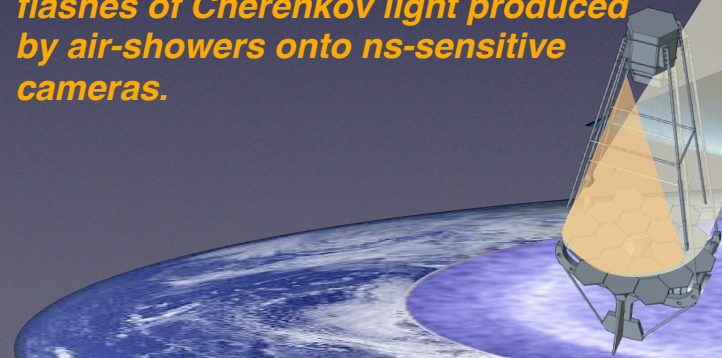
For  $E=1$  TeV ( $E_C \approx 80$  MeV)

$$X_{\max} \approx X_0 \ln ( E/E_C ) / \ln 2$$

$$h_{\max} = h_0 \ln ( X_A / X_{\max} ) \rightarrow 5 \text{ km}$$



*UV-optical reflecting mirrors focussing flashes of Cherenkov light produced by air-showers onto ns-sensitive cameras.*



Cherenkov radiation

1.4°

~10 km

140 m

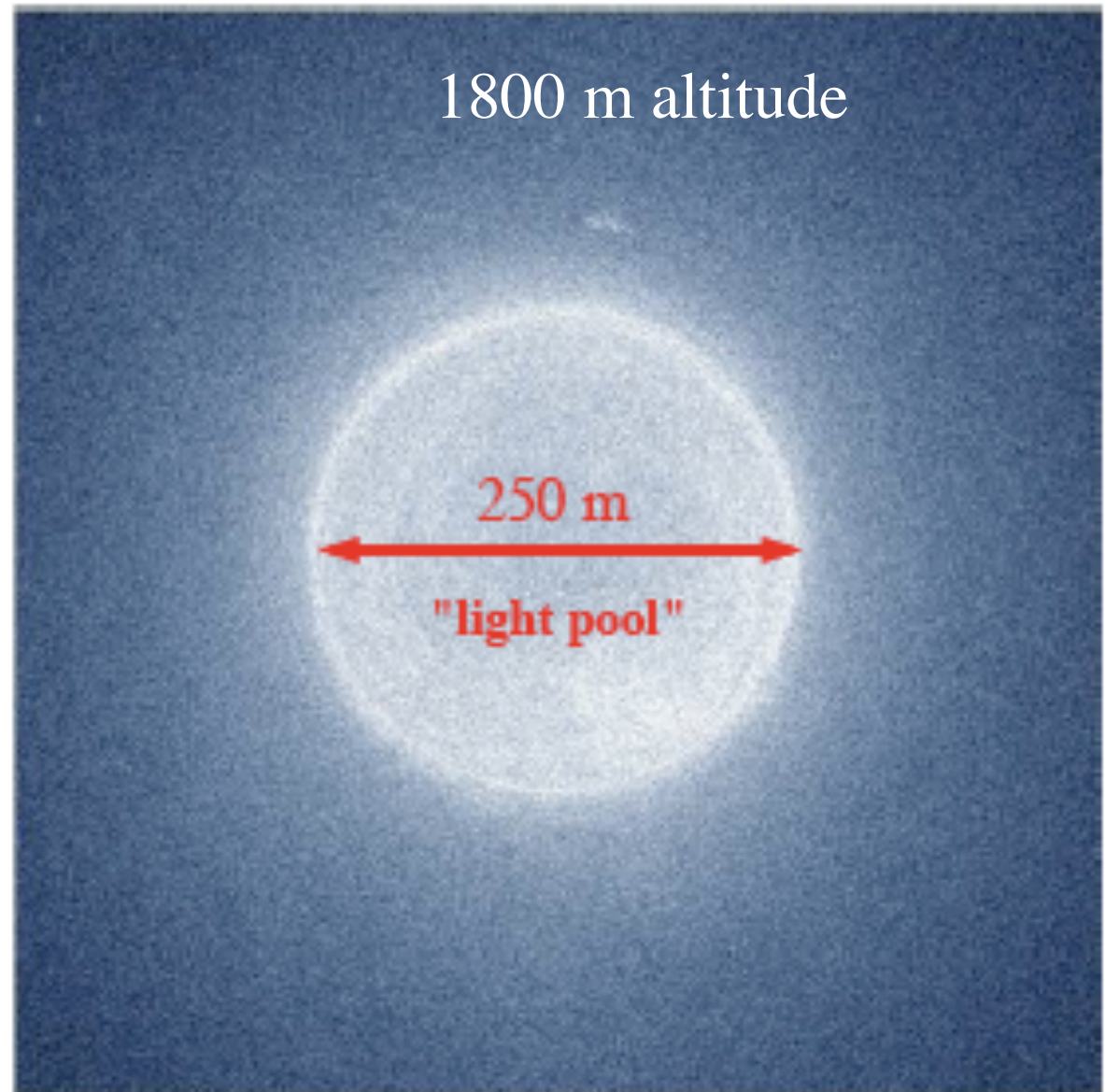
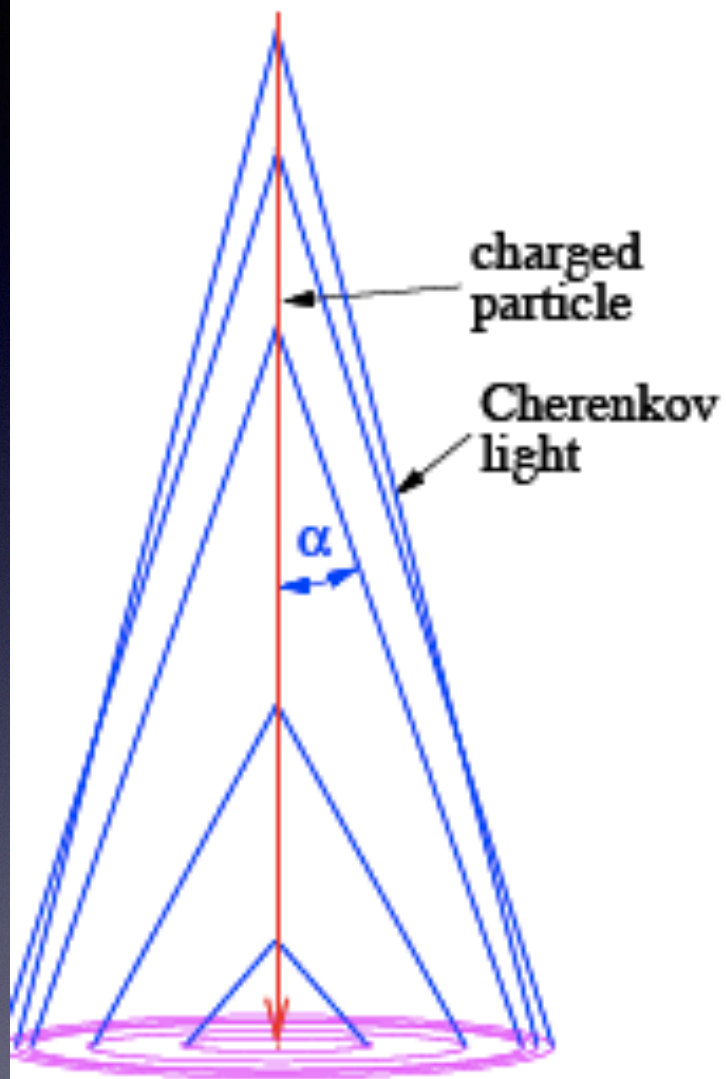
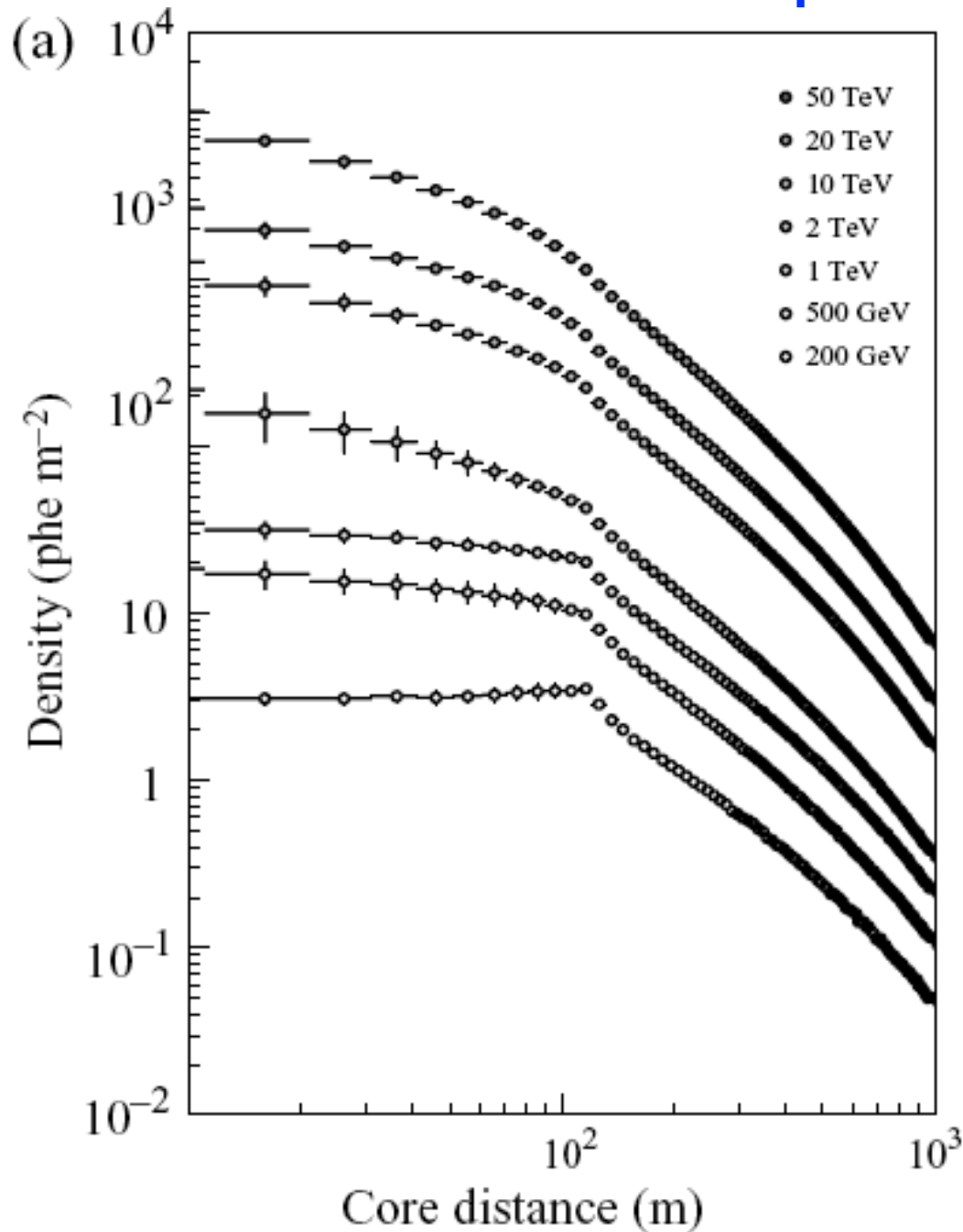


Fig. 3 Left: Atmospheric Cherenkov emission from a downward-moving single particle. Right: The "light pool" at an observation level at 1800 m above sea level from a  $\gamma$ -ray shower with a primary energy of 1 TeV (from K. Bernlöhner).

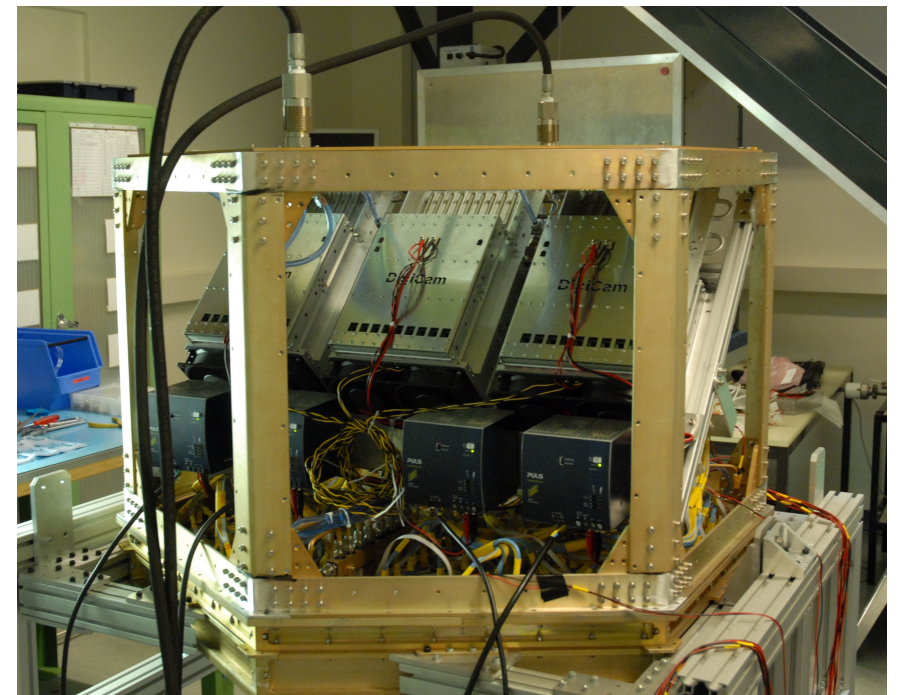
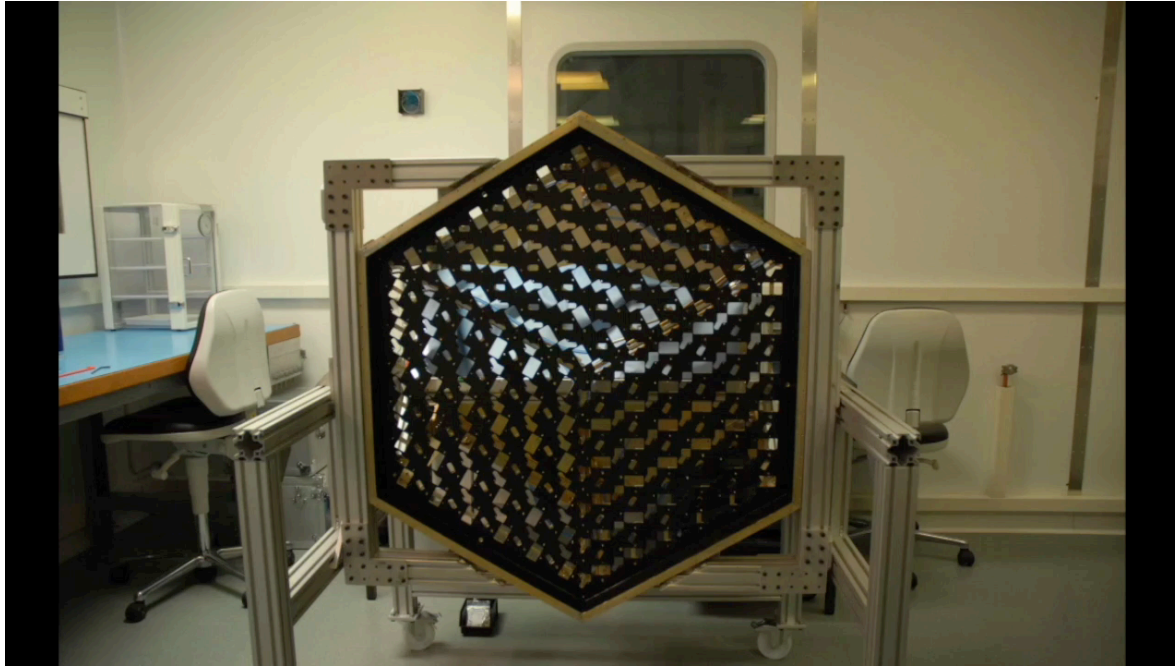
# Dependency of the lateral distribution on the primary energy



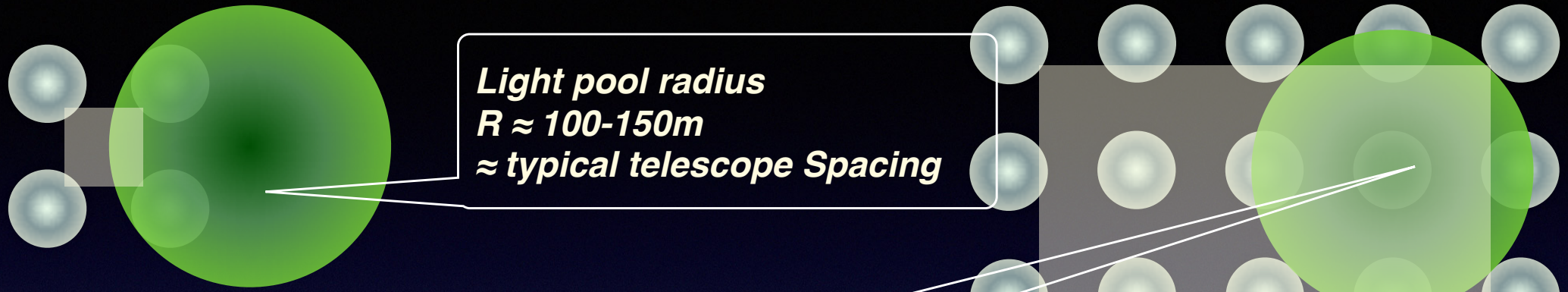
The density is about **100 photons/m<sup>2</sup>/TeV between 300-600 nm.**

For a typical instrumental efficiency of 10% (reflectivity of mirror surfaces and QE of photosensors) **primary reflectors of 100 m<sup>2</sup>** are needed to produce images containing **100 ph** for a primary gamma of **100 GeV**.

# New photosensors

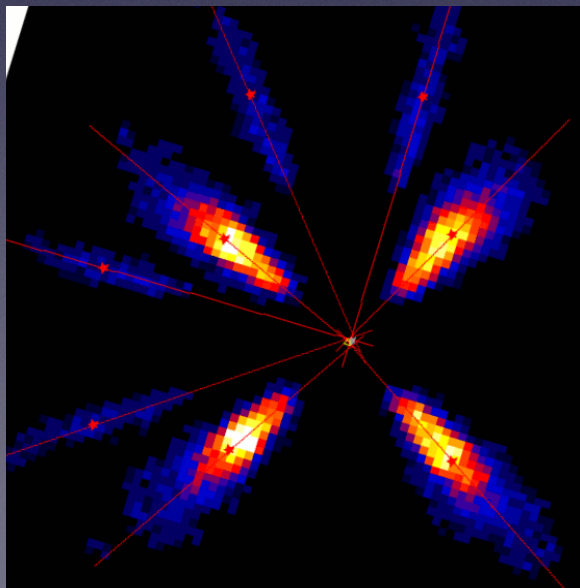


# From current arrays to CTA



*Light pool radius*  
 $R \approx 100-150\text{m}$   
 $\approx$  typical telescope Spacing

- ✓ Large detection Area
- ✓ More Images per shower
- ✓ Lower trigger threshold



✓ Improved angular resolution

✓ Improved background rejection power

➔ More telescopes!

# Cherenkov - basic formulas

- Cherenkov condition:  
 $\beta_{th} > 1/n \implies \theta > 0$

- The **energy threshold** (Lorentz factor) is determined by the refractive index.

- The **number of photons scales with  $\lambda^{-2}$** :  
 Cherenkov light is dominantly **blue** in typical media such as water and air.

- The number of photons scales with  $\sin^2\theta$

$$\cos \theta = \frac{1}{n\beta}$$

- For  $\beta \sim 1$
- Water  $\approx 41^\circ$
- Air  $\approx 1.0$  to  $1.3^\circ$

$$\gamma > \frac{1}{\sqrt{1 - n^{-2}}} = E/m$$

For electrons:

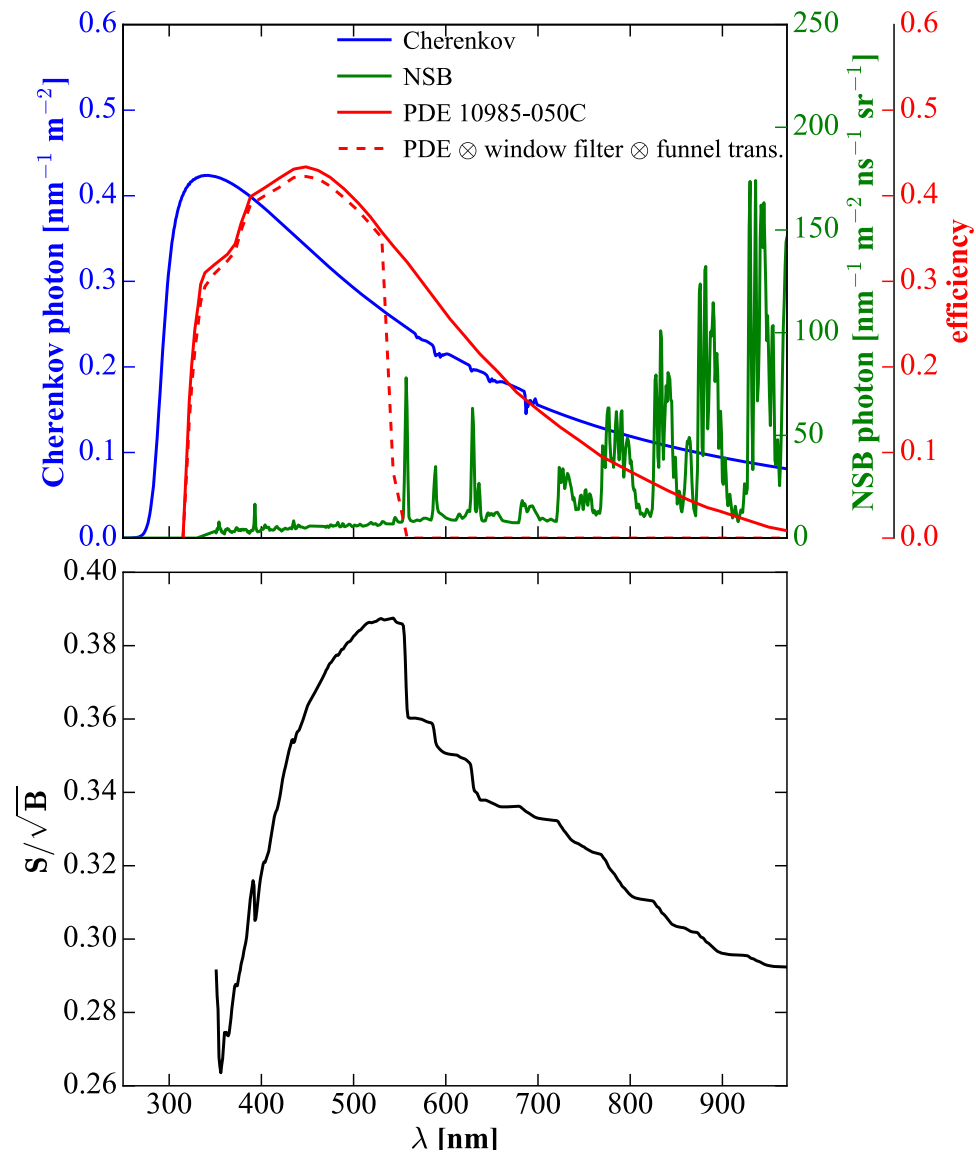
$$E_{th} = m_e c^2 / \sqrt{1 - 1/n^2}$$

- Air: 20 MeV
- Water/ice: 0.7 MeV

$$\frac{dN}{dx} = 2\pi\alpha z^2 \int \sin^2\theta \frac{d\lambda}{\lambda^2}$$

$$\frac{dN}{dx} = 2\pi\alpha z^2 \int \left(1 - \frac{1}{n^2\beta^2}\right) \frac{d\lambda}{\lambda^2}$$

# Signal and background spectra and photosensor efficiency



# Signal to noise example for photon of 100 GeV

- Night sky background:  $\phi_{NSB} \approx 10^{12}$  photons/(m<sup>2</sup> s sr)
- Cherenkov pulse:  $\phi_{Ch} \approx 7$  photons/m<sup>2</sup> in 2ns at 100 GeV
- Transmittance of atmosphere  $T = 1$  for simplicity
- $\tau = 2$  ns integration time of pulse counting system
- $qE = 0.25$  quantum efficiency PMT, lightguide detection eff., mirror transmittance
- Number of signal photoelectrons:  $\phi_{Ch} \cdot A \cdot T \cdot qE$
- Number of background photoelectrons:  $\phi_{NSB} \cdot A \cdot T \cdot qE \cdot \tau \cdot \Omega$
- Solid angle  $\Omega$  greater than shower ( $> 1^\circ$ )
- We neglect that  $T$ ,  $qE$ ,  $\phi_{NSB}$  and  $\phi_{Ch}$  depend on the wavelength

$$\frac{Signal}{Noise} = N_\sigma = \frac{\Phi_{ch} \cdot A \cdot T \cdot qE}{\sqrt{\Phi_{NSB} \cdot A \cdot \Omega \cdot T \cdot qE \cdot \tau}} \quad \stackrel{=5 \text{ sigma}}{N_\sigma} = \Phi_{ch} \sqrt{\frac{T \cdot A \cdot qE}{\Phi_{NSB} \cdot \Omega \cdot \tau}}$$

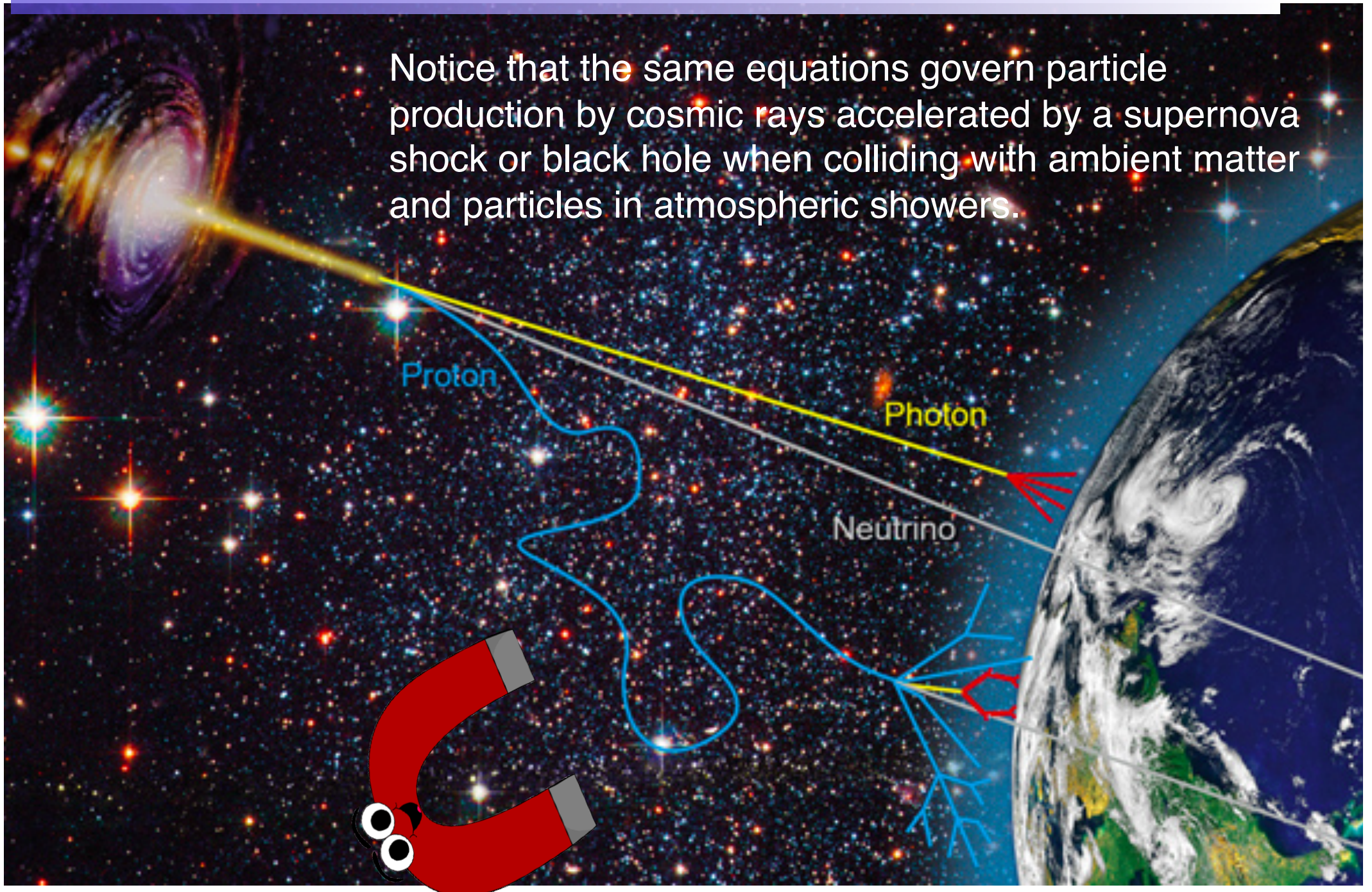
$$A = \left( \frac{N_\sigma}{\Phi_{ch}} \right)^2 \frac{\Phi_{NSB} \cdot \Omega \cdot \tau}{T \cdot qE} \quad A = 2 \times 10^5 \Phi_{Ch}^{-2} \frac{\Omega}{T} m^2$$

$$\text{Since } \Phi_{Ch} \propto N_{e^\pm} \propto E_{\gamma, primary} \quad E_{th} \propto \frac{1}{\sqrt{A_{mirror}}}$$



# A new multi-messenger Astrophysics

Notice that the same equations govern particle production by cosmic rays accelerated by a supernova shock or black hole when colliding with ambient matter and particles in atmospheric showers.



# Reminder: Mean free path

$$w = \text{interaction prob.} = w = N\sigma dx$$

$\sigma$  = cross section

$N$  = n. of target particles / volume

$P(x)$  = prob. that a particle does not interact after traveling a distance  $x$

$P(x + dx)$  = prob that a particle has no interaction between  $x$  and  $x+dx$  =  $P(x+dx) = P(x) (1-wdx)$

$$P(x + dx) = P(x) + \frac{dP}{dx}dx = P(x) - P(x)wdx$$

$$\frac{dP}{P} = -wdx \Rightarrow P(x) = P(0)e^{-wx}$$

$P(0) = 1$  it is sure that initially the particle did not interact

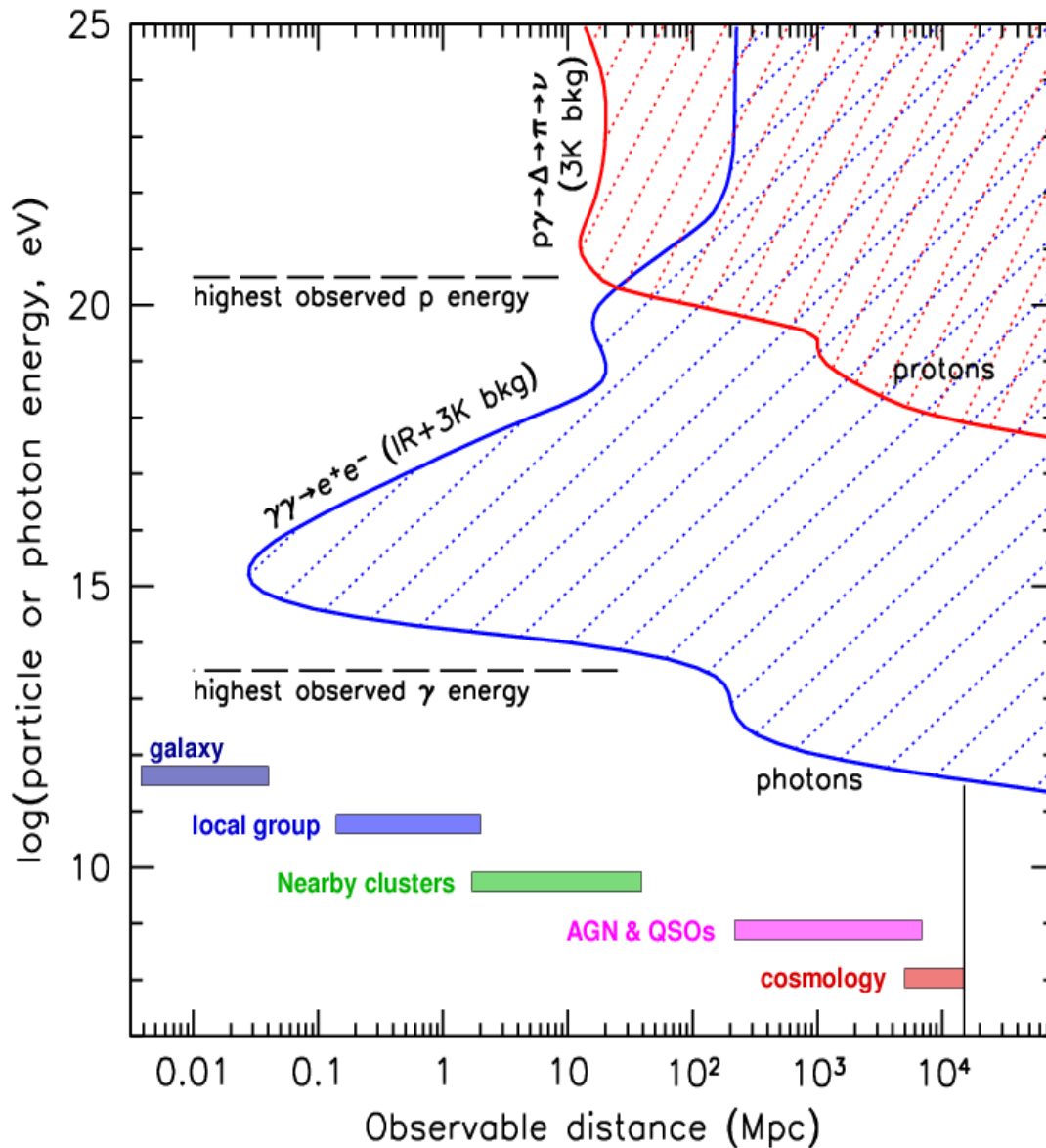
$$\lambda = \frac{\int xP(x)dx}{\int P(x)dx} = \frac{1}{w} = \frac{1}{N\sigma}$$

$$\lambda_I = \lambda\rho = \frac{\rho}{N_c\sigma} = \frac{Am_p}{\sigma} \quad \text{in g/cm}^2$$

Medium density

Atomic number

# The multi-messenger's horizons

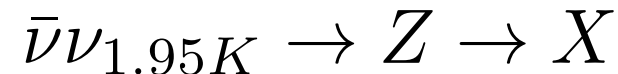


**Proton horizon (GZK cut-off):**



$$L_\gamma = \frac{1}{\sigma_{p-\gamma_{CMB}} n_\gamma} \sim \frac{1}{10^{-28} \text{cm}^2 \times 400 \text{cm}^{-3}} \sim 10 \text{ Mpc}$$

**The neutrino horizon is comparable to observable universe!**



$$E_{res} = \frac{M_Z^2}{2m_\nu} \cong 4 \times 10^{21} \left( \frac{1\text{eV}}{m_\nu} \right) \text{eV}$$

$$L_\nu = \frac{1}{\sigma_{res} \times n} = \frac{1}{5 \times 10^{31} \text{cm}^2 \times 112 \text{cm}^{-3}} \approx 6 \text{Gpc}$$

[arxiv.org/pdf/0811.1160v2.pdf](https://arxiv.org/pdf/0811.1160v2.pdf)

# The proton horizon

$$r_{\phi\pi}(E_{20}) \cong \frac{13.7 \exp[4/E_{20}]}{[1 + 4/E_{20}]} \text{ Mpc}$$

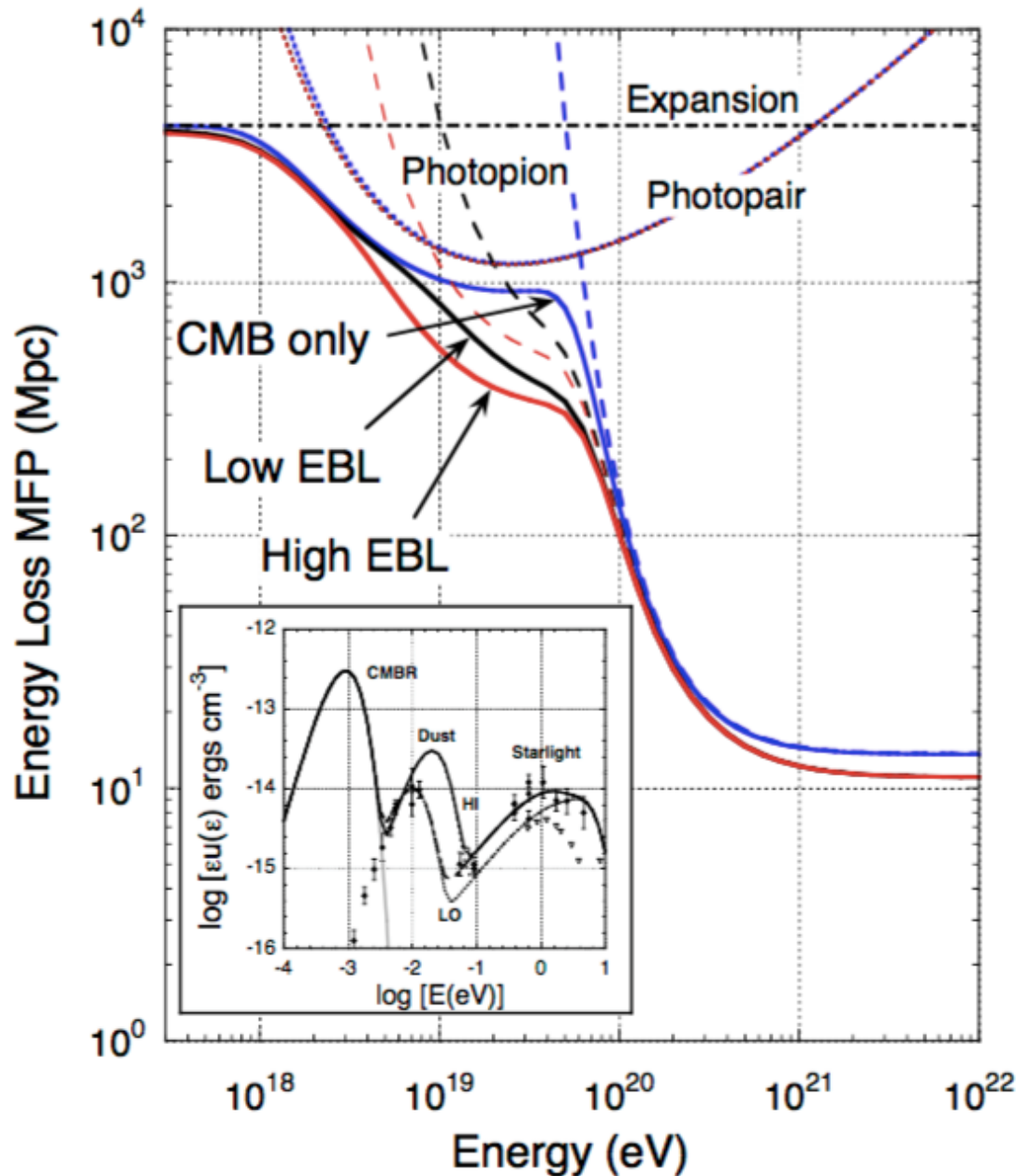
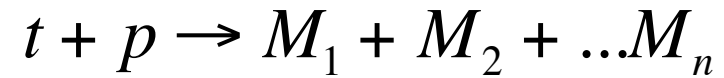


**Figure 1.** Mean-free paths for energy loss of UHECR protons in different model EBLs are shown by the solid curves, with photopair (dotted) and photopion (dashed) components shown separately. “CMB only” refers to total energy losses with CMB photons only, using eq. (4) for the energy-loss rate of protons due to photopion production. Inset: Measurements of the EBL at optical and infrared frequencies, including phenomenological fits to low-redshift EBL in terms of a superposition of modified blackbodies. A Hubble constant of  $72 \text{ km s}^{-1} \text{ Mpc}^{-1}$  is used throughout.

What about neutrons? for a neutron of  $E = 10^9 \text{ GeV}$ ,  
 $l_{\text{decay}} = \gamma c \tau = E/mc^2 \times c \times 886 \text{ s} = 10^9 \text{ GeV}/1 \text{ GeV} \times 3 \times 10^8 \text{ m/s} \times 886 \text{ s} = 2.66 \times 10^{20} \text{ m} \times 3.24 \times 10^{-20} \text{ kpc/m} = 8.6 \text{ kpc}$

# Reminder: Reaction thresholds



$$\sqrt{s}_{th} = \sum_f M_f = \sqrt{E_{tot}^2 - |\mathbf{p}_{tot}|^2}$$

The threshold of a reaction corresponds to the energy to produce all final states at rest.

Remember also that from the invariance of total 4-momentum squared in the CM and Lab frame:

$$\sqrt{s} = \sqrt{\overbrace{(E_p + E_t)^2 - (\vec{p}_p + \vec{p}_t)^2}^{\text{total energies in the lab}}} = \sqrt{m_p^2 + m_t^2 + 2E_p E_t (1 - \beta_p \beta_t \cos \theta)}$$

At threshold:

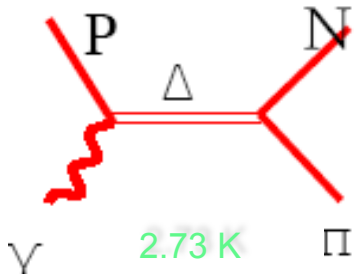
$$\sqrt{s_{th}} = \sqrt{m_p^2 + m_t^2 + 2E_p m_t} = \sum_f M_f \quad m_p^2 + m_t^2 + 2(E_{k,p} + m_p)m_t = \left(\sum_f M_f\right)^2$$

The projectile kinetic energy in the target rest frame (lab frame):

$$E_{k,p} = \frac{(\sum_f M_f)^2 - (m_p + m_t)^2}{2m_p}$$

# The GZK cut-off

[Greisen 66;  
Zatsepin & Kuzmin66]



$$\epsilon = \frac{m_{\Delta}^2 - m_p^2}{2m_p} \sim 340 \text{ MeV}$$

effective energy for Planck spectrum of CMB

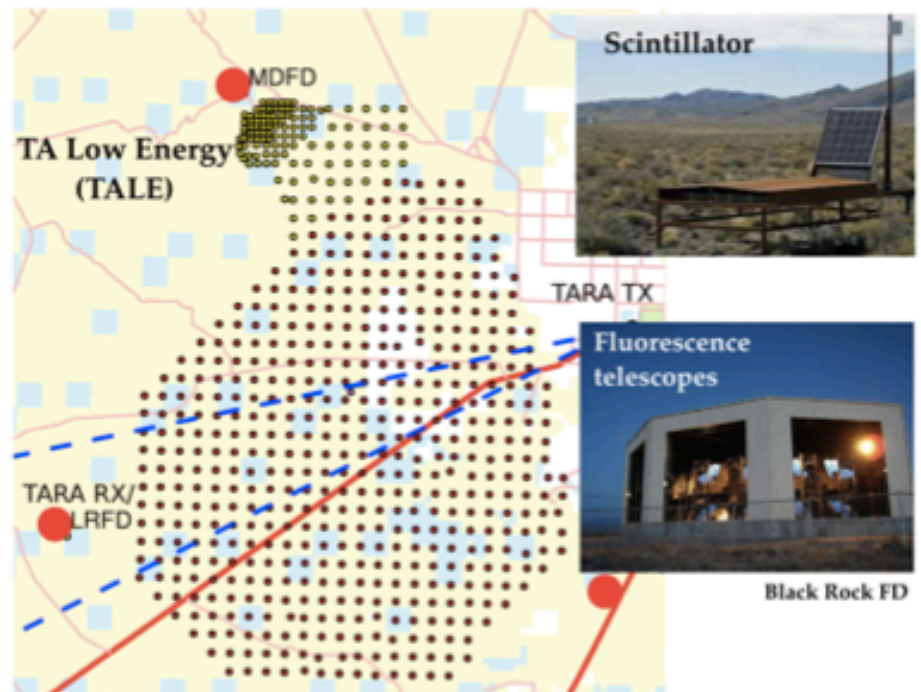
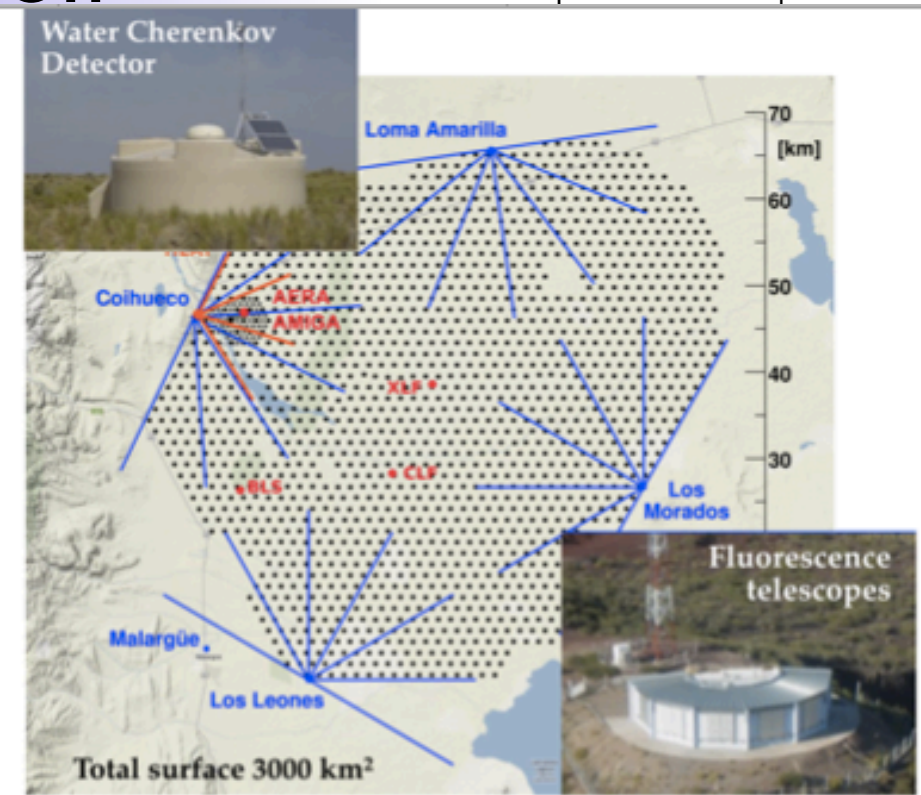
$$\epsilon' = 3k_B T = 4 \times 2.73 \times 8.62 \times 10^{-5} \text{ eV}$$

$$\gamma_p = \frac{\epsilon'}{\epsilon} = 2 \cdot 10^{11}$$

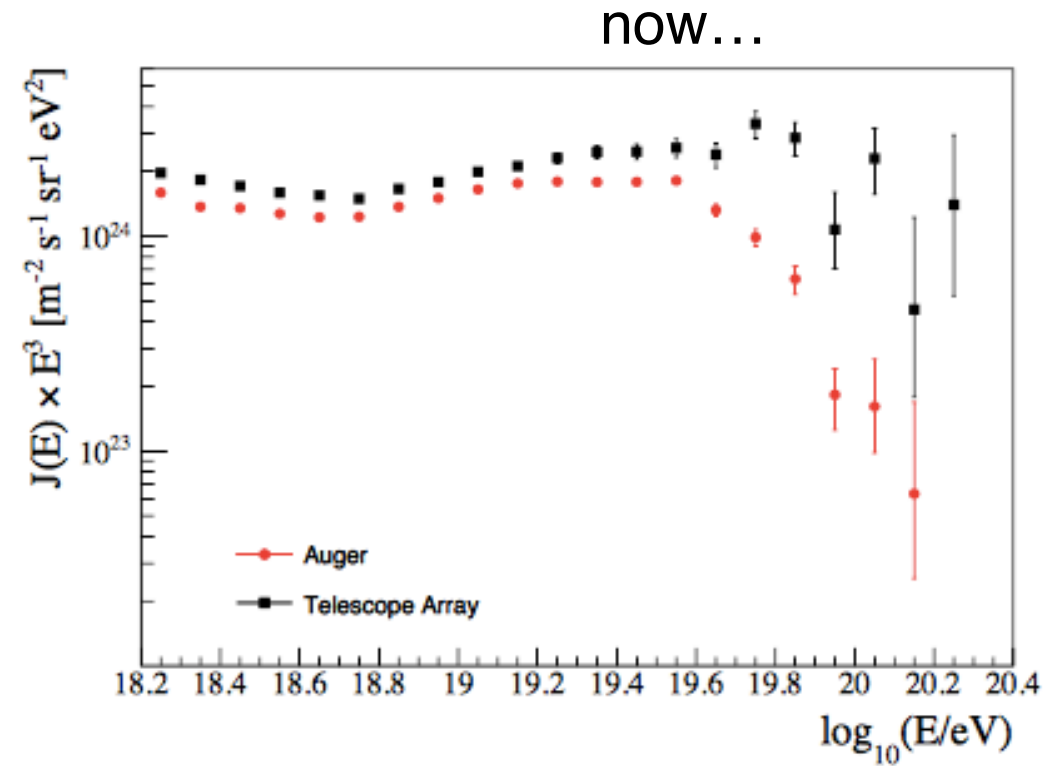
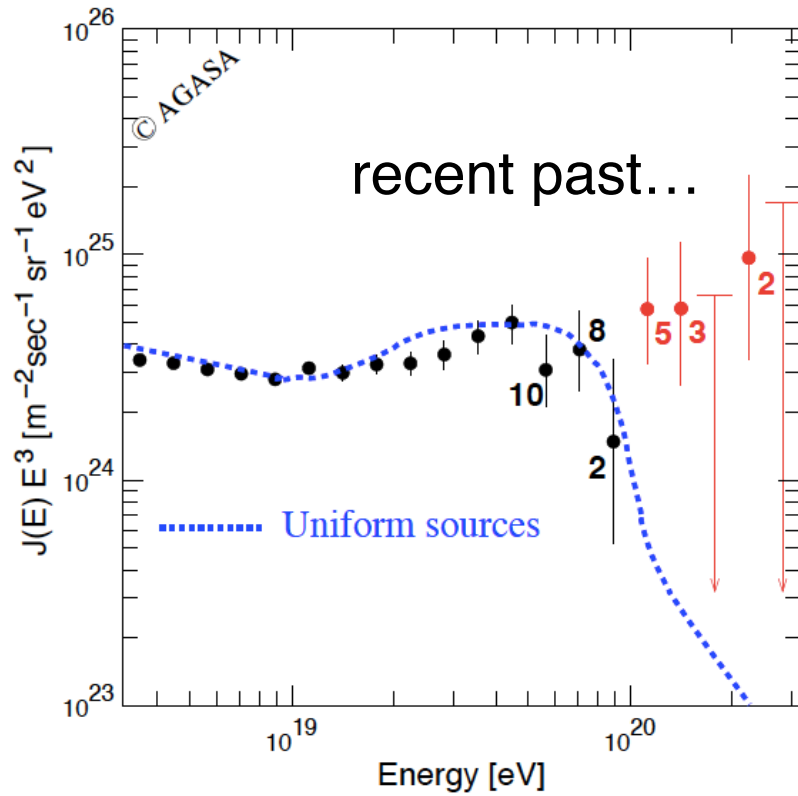
⇒ Hence the threshold energy of the proton in the CM is

$$\Rightarrow E'_p \sim \gamma_p m_p = 2 \cdot 10^{20} \text{ eV}$$

Integrating over Planck spectrum  
 $E_{p,\text{th}} \sim 5 \cdot 10^{19} \text{ eV}$



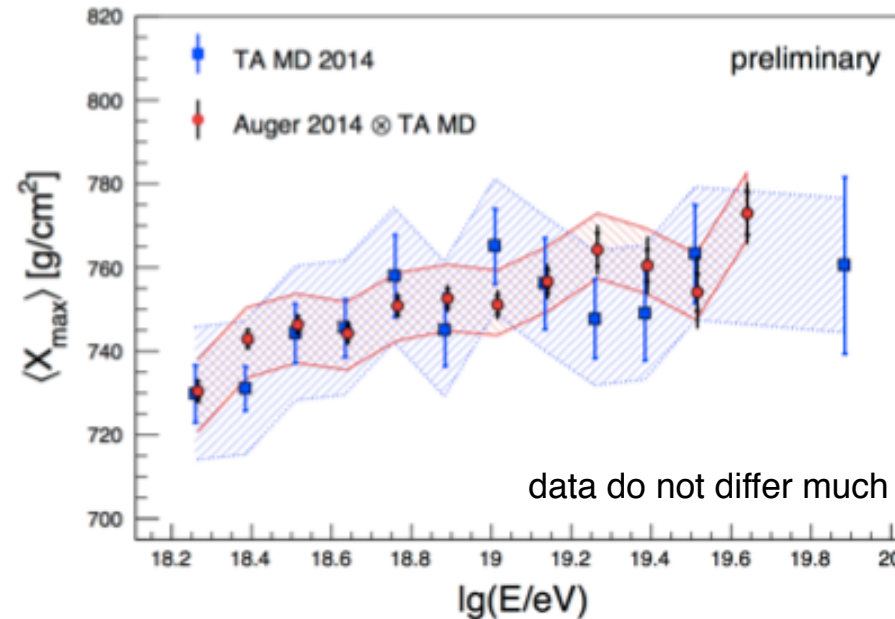
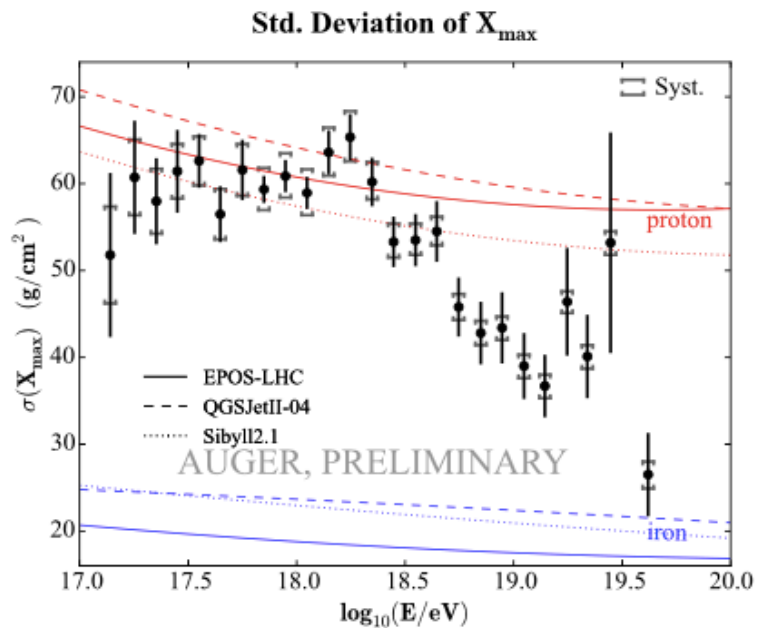
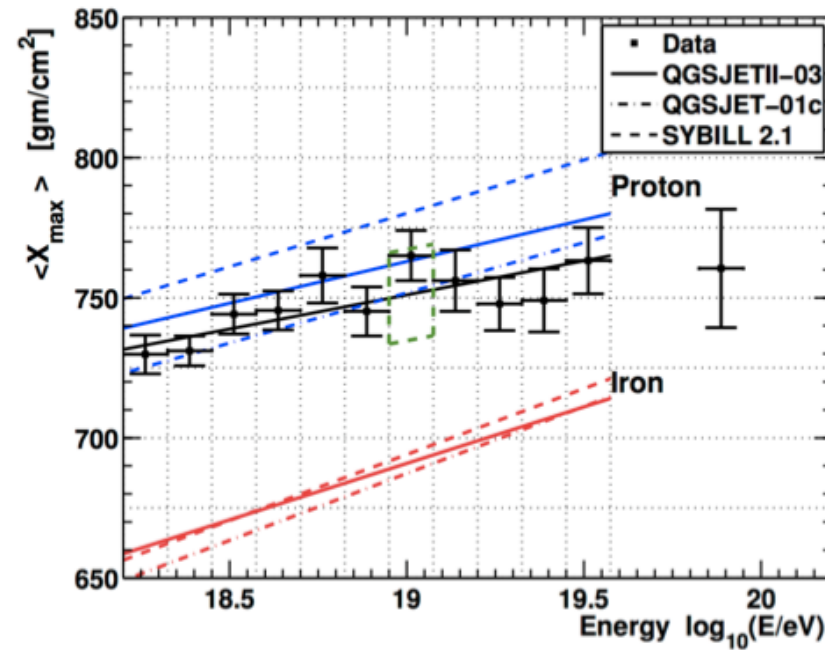
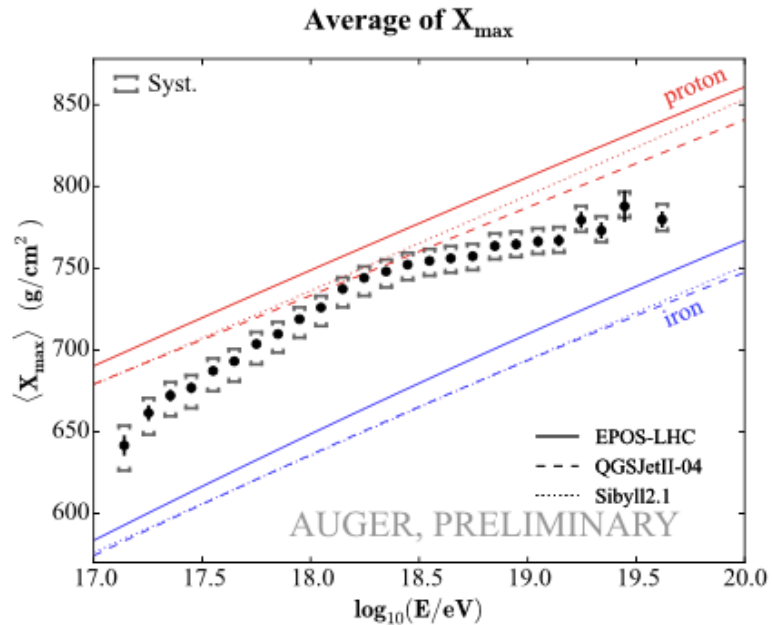
# UHECR spectra



	Auger	Telescope Array
$E_{\text{ankle}}$ [EeV]	$4.82 \pm 0.07 \pm 0.8$	$5.2 \pm 0.2$
$E_{1/2}$ [EeV]	$42.1 \pm 1.7 \pm 7.6$	$60 \pm 7$
$\gamma_1$ ( $E < E_{\text{ankle}}$ )	$3.29 \pm 0.02 \pm 0.05$	$3.226 \pm 0.007$
$\gamma_2$ ( $E > E_{\text{ankle}}$ )	$2.60 \pm 0.02 \pm 0.1$	$2.66 \pm 0.02$

based on ICRC 2015

# The ankle region: composition



Is the extra-galactic component Fe or p dominated??

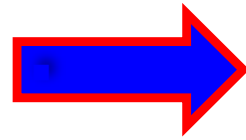


# CR deflections in magnetic fields

$$mv^2 / r = pv / r = ZevB / c$$

$$r = pc / ZeB$$

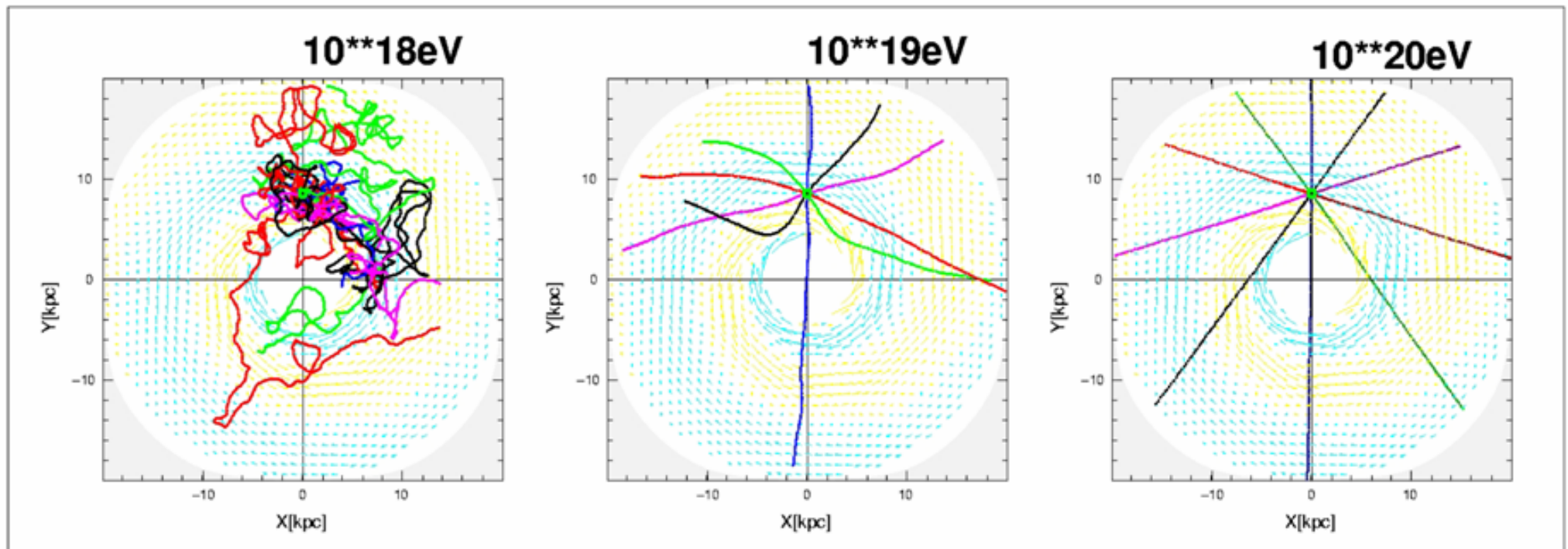
$$r(\text{cm}) = \frac{1}{300} \frac{E(\text{eV})}{ZB(\text{G})}$$



$$(10^{12} \text{ eV}) = 10^{15} \text{ cm} = 3 \times 10^{-4} \text{ pc}$$

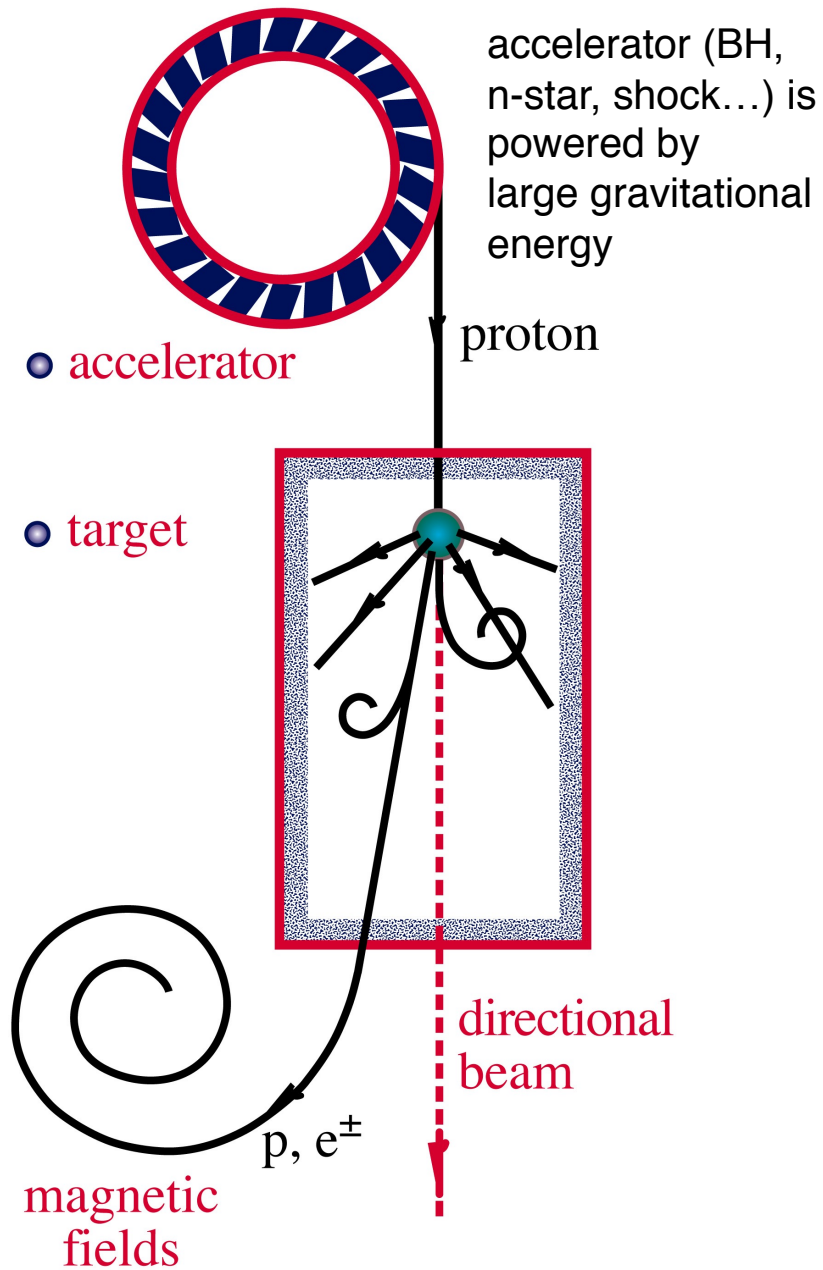
$$r = (10^{15} \text{ eV}) = 10^{18} \text{ cm} = 3 \times 10^{-1} \text{ pc}$$

$$(10^{18} \text{ eV}) = 10^{21} \text{ cm} = 300 \text{ pc}$$

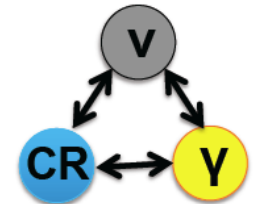
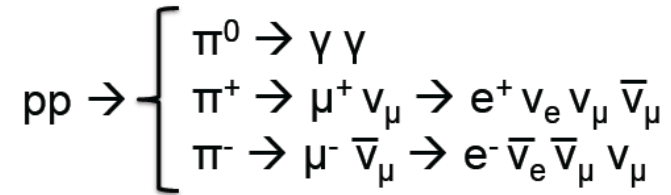


# The generic cosmic source: beam dump model

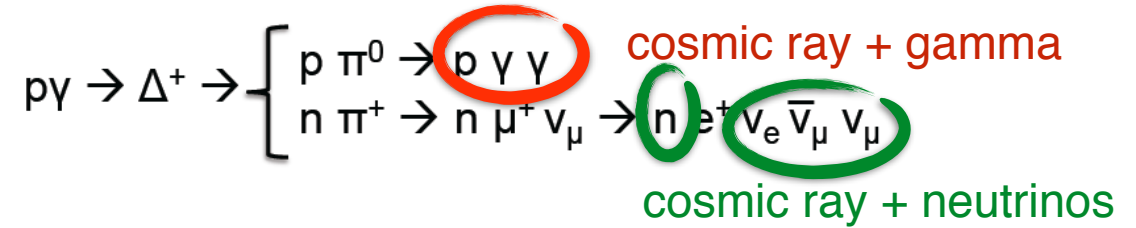
## $\nu$ and $\gamma$ beam dumps



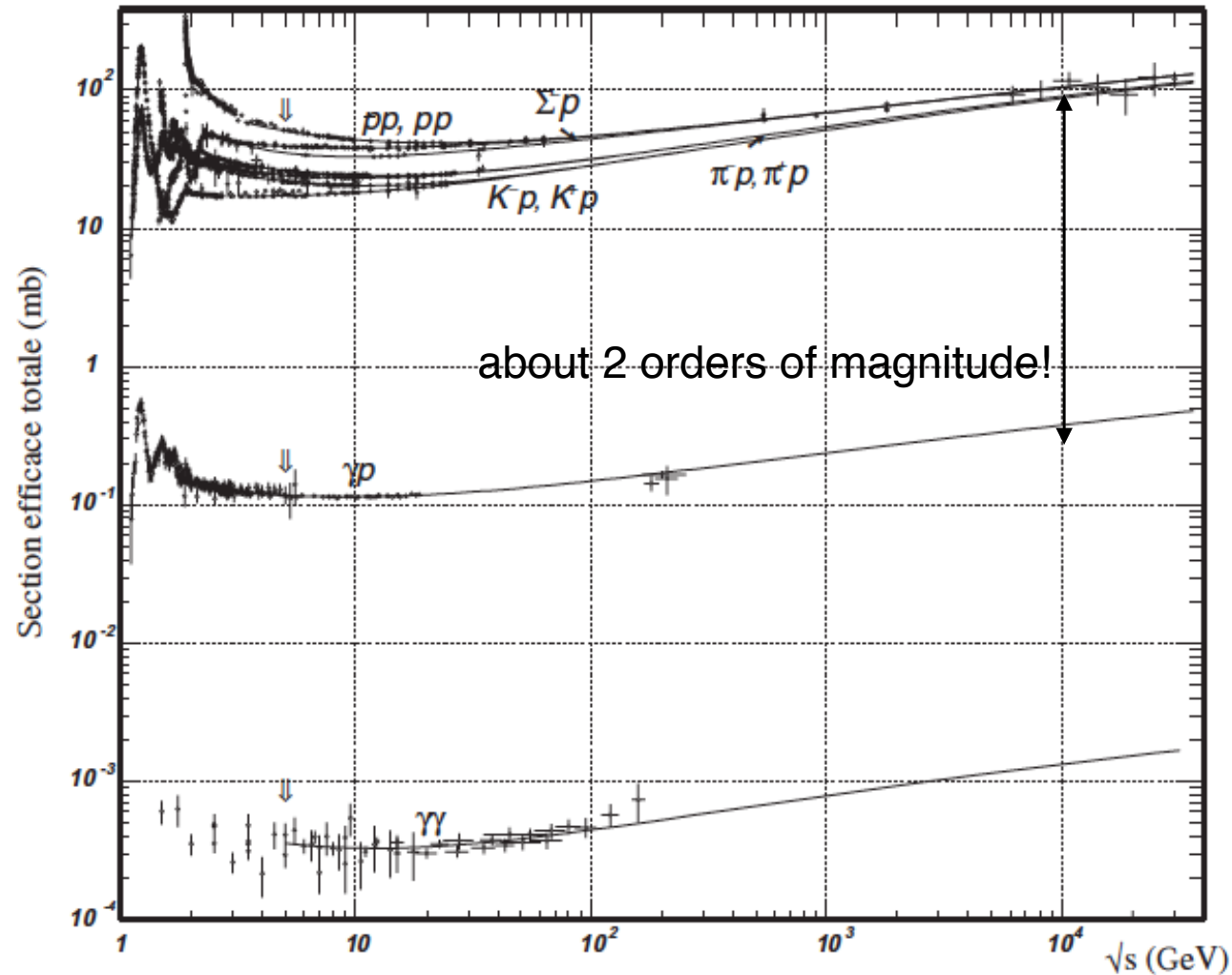
Hadronuclear (e.g. star burst galaxies and galaxy clusters)



Photohadronic (e.g. gamma-ray bursts, active galactic nuclei)

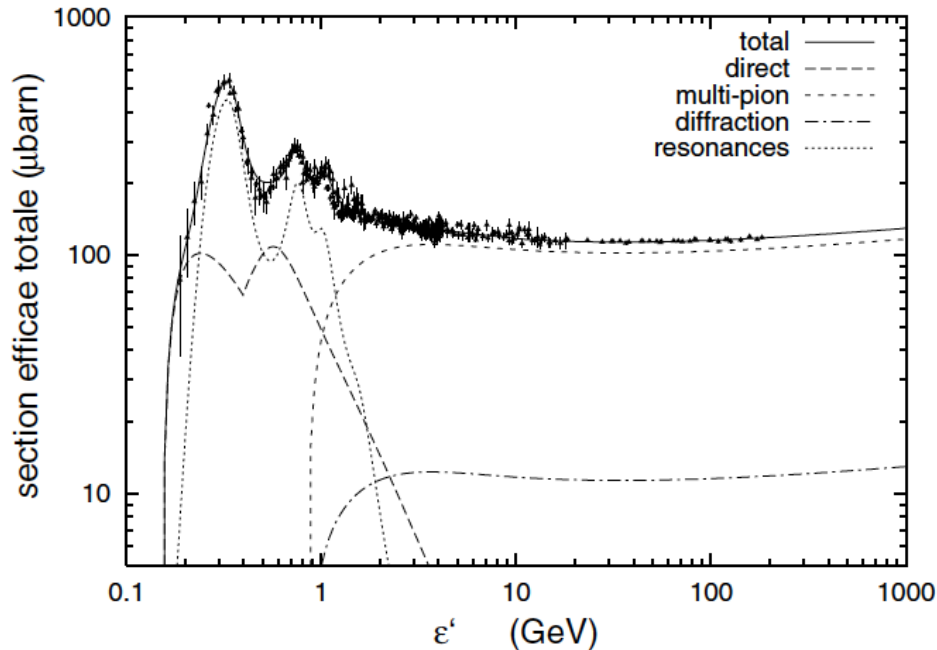


# Pp and p-gamma processes

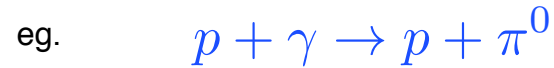


*In astrophysical environments, the density of photons is typically much larger than that of protons, unless there are residual masses from explosions (SNRs) or an accelerator with a molecular clouds and large rate of star formation (starbursts). Hence, even if the cross section for pp interaction is about 2 orders of magnitude larger than that of  $p\gamma$ , this last may dominate.*

# p-gamma



Direct photo-production of pions:



$$\sqrt{s_{th}} = m_p + m_\pi = 1.08 \text{ GeV}$$

Energy of the photon in the lab:

$$\epsilon = \frac{m_\pi(m_\pi + 2m_p)}{2m_p} \sim 150 \text{ MeV}$$

For delta-resonance  $\Delta(1232)$  it is larger:

$$\epsilon = \frac{m_\Delta^2 - m_p^2}{2m_p} \sim 340 \text{ MeV}$$

If the proton is at rest ( $E_p = m_p$ ),  $\epsilon = 340 \text{ MeV}$  in the lab

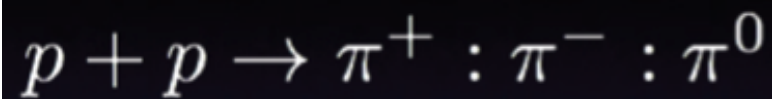
Hence in the CM:  $E'_p = \gamma_p m_p$  and the photon energy is :

$$\epsilon' = \gamma_p \frac{m_\Delta^2 - m_p^2}{2m_p} = \gamma_p^2 \frac{m_\Delta^2 - m_p^2}{2E'_p}$$

Hence the accelerated proton must have a threshold energy in the CM frame of:

$$E'_p = \gamma_p^2 \frac{m_\Delta^2 - m_p^2}{2\epsilon'} \sim \gamma_p^2 \times 300 \text{ GeV} \times \left( \frac{1 \text{ MeV}}{\epsilon'} \right)$$

# p-p



In the lab

$$E_{p,th} = \frac{(2m_p + m_\pi)^2 - 2m_p^2}{2m_p} \sim 1.23 \text{ GeV}$$

□ In the CM:  $E_{p,th} = \gamma \times 1.23 \text{ GeV}$  □

# Assuming average energy fractions...

$$x_\nu = \frac{E_\nu}{E_p} = \frac{1}{4} \langle x_F \rangle = \frac{1}{20}$$

$$x_\gamma = \frac{E_\gamma}{E_p} = \frac{1}{2} \langle x_F \rangle = \frac{1}{10}$$

$$dE_{\nu,\gamma} = x_{\nu,\gamma} dE_p$$

Kelner & Aharonian  
<http://arxiv.org/pdf/astro-ph/0606058.pdf>

<https://inspirehep.net/record/718405>

$x^2 F_\gamma(x, E_p)$

Gamma

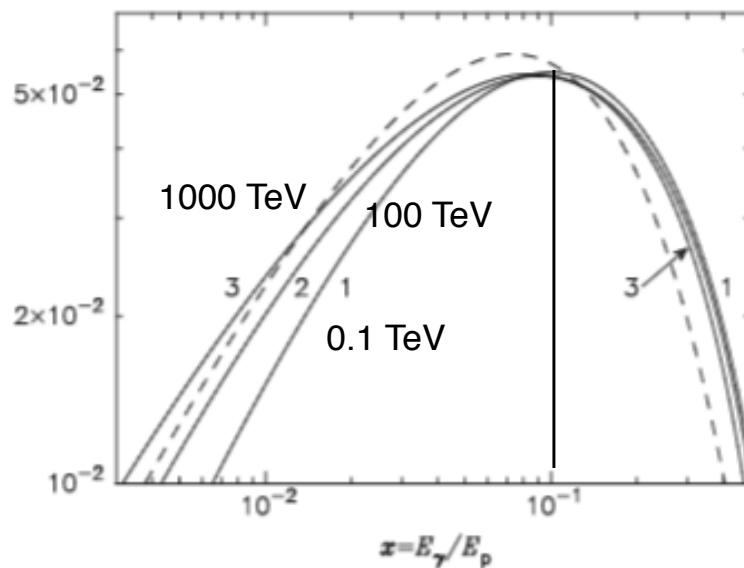


Figure 7: Energy spectra of gamma-rays described by Eq.(58) for three energies of incident protons: 0.1 TeV (curve 1), 100 TeV (curve 2) and 1000 TeV (curve 3). The dashed curve corresponds to the Hillas parameterization of the spectra obtained for proton energies of several tens of TeV.

$x^2 F_{\nu_\mu}(x, E_p)$

Neutrino

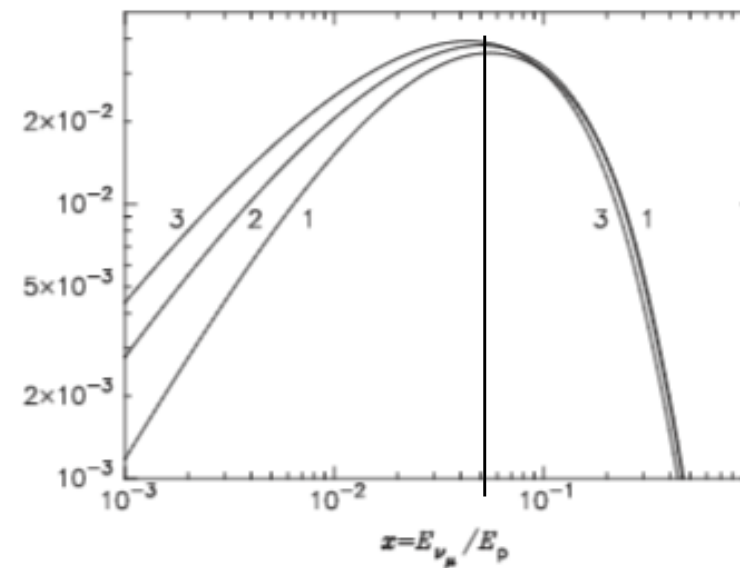


Figure 9: Energy spectra of all muonic neutrinos described by Eq.(62) and (66) for three energies of incident protons: 0.1 TeV (curve 1), 100 TeV (curve 2) and 1000 TeV (curve 3).

# Two Body Decay Kinematics

Each neutrino takes about 1/4 of the pion energy (on average)

In the Lab (pion at rest)

“Neutrino massless” means  $E_\nu = p_\nu$ . Therefore the energy and momentum conservation yield

$$m_\pi = \sqrt{p_\mu^2 + m_\mu^2} + E_\nu, \quad (23)$$

$$0 = \mathbf{p}_\mu + \mathbf{p}_\nu. \quad (24)$$

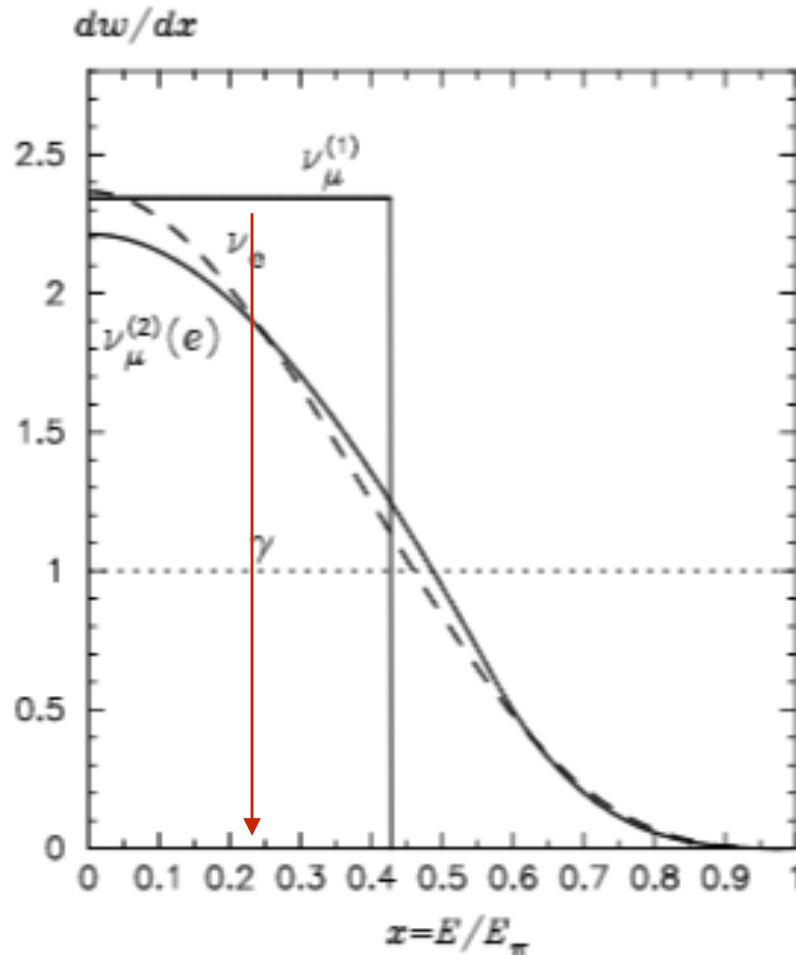
Through Equation (24),  $p_\mu^2 = E_\nu^2$ . Isolating the root square in Equation (23) and squaring gives

$$\begin{aligned} (m_\pi - E_\nu)^2 &= E_\nu^2 + m_\mu^2 \\ \Rightarrow m_\pi^2 + \cancel{E_\nu^2} - 2m_\pi E_\nu &= \cancel{E_\nu^2} + m_\mu^2, \end{aligned}$$

therefore, with  $m_\pi = 139.6$  MeV and  $m_\mu = 105.7$  MeV,

$$\Rightarrow E_\nu = p_\nu = p_\mu = \frac{m_\pi^2 - m_\mu^2}{2m_\pi} = 29.7839183 \simeq 29.8 \text{ MeV (in natural units)}. \quad (25)$$

# Three Body Decay Kinematics



In the LAB and for  $E_\pi \gg m_\pi$   
(mass of electrons/neutrinos neglected)

$$E_{\nu, \max} = \frac{1}{m_\pi} (E_\pi E_\nu^0 + p_\pi p_\nu^0) \approx \lambda E_\pi ,$$

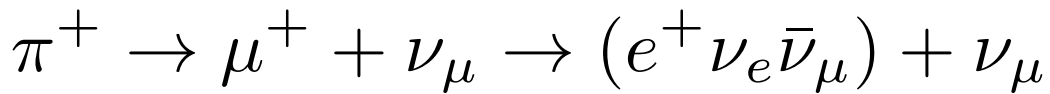
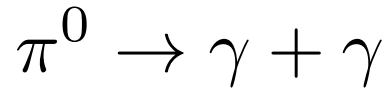
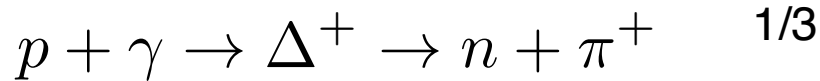
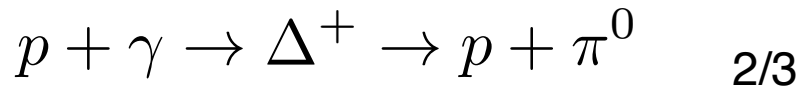
where

$$\lambda = 1 - m_\mu^2/m_\pi^2 = 0.427 .$$

Figure 4: Energy distributions of the secondary products (photons, electrons, muonic and electronic neutrinos) of decays of monoenergetic ultrarelativistic neutral and charged pions. All distributions are normalized,  $\int_0^1 dw = 1$ .

# p-gamma

On average 1/3 of the p energy goes into pions



branching ratios

	$p\pi^+$	$p\pi^0$	$p\pi^-$	$n\pi^+$	$n\pi^0$	$n\pi^-$
$\Delta^{++}$	1					
$\Delta^+$		2/3		1/3		
$\Delta^0$			1/3		2/3	
$\Delta^-$						1

Assuming :  $\frac{dN_p}{dE_p} \propto E_p^{-2} \Rightarrow \frac{dN_p}{dE_p} \propto E_p^{-2} = E_\nu^{-2} x_\nu^2$  and

Since :  $\frac{E_\nu}{E_p} = x_\nu \sim \frac{1}{20} \Rightarrow dE_p = x_\nu^{-1} dE_\nu$

multiplicity and BR

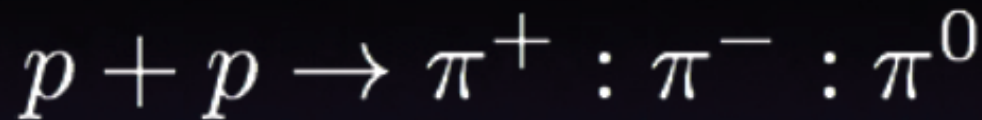
$$\frac{dN_\gamma}{dE_\gamma} \propto \underset{\downarrow}{2} \times \frac{\underset{\downarrow}{2}}{3} \frac{dN_p}{x_\gamma dE_p} = 2 \times \frac{2}{3} E_\gamma^{-2} x_\gamma = 2 \times \frac{2}{3} \frac{1}{10} E_\gamma^{-2}$$

$$\frac{dN_\nu}{dE_\nu} \propto 2 \times \frac{1}{3} \frac{dN_p}{x_\nu dE_p} = 2 \times \frac{1}{3} E_\nu^{-2} x_\nu = 2 \times \frac{1}{3} \frac{1}{20} E_\nu^{-2} \Rightarrow \frac{dN_\nu}{dE} = \frac{1}{4} \frac{dN_\gamma}{dE} \text{ for } p - \gamma$$



# Proton-proton

In Galactic SN shocks CRs interact with the H in the Galactic disk (pp interactions, lower threshold than p-gamma)



$$E_{p,th} = \frac{(2m_p + m_\pi)^2 - 2m_p^2}{2m_p} \sim 1.23 \text{ GeV}$$

if all muons decay and for  $E^{-2}$  p spectrum:

2 pions  $\times$  1/3 of energy to each pion

$$\frac{dN_\nu}{dE} \sim 2 \times \frac{2}{3} \times \frac{1}{20} E_\nu^{-2}$$

$$\frac{dN_\gamma}{dE} \sim 2 \times \frac{1}{3} \times \frac{1}{10} E_\nu^{-2}$$

Assume always:

$$x_\nu = \frac{E_\nu}{E_p} = \frac{1}{4} \langle x_F \rangle = \frac{1}{20}$$

$$x_\gamma = \frac{E_\gamma}{E_p} = \frac{1}{2} \langle x_F \rangle = \frac{1}{10}$$

Ignoring oscillations there is a factor of about 1 between the gamma and neutrino flux.

For a full calculation see: <http://arxiv.org/pdf/astro-ph/0606058> for pp

# Gamma-neutrino connection at source

$$\frac{dN_\nu}{dE} = \frac{dN_\gamma}{dE} \text{ for } p - p$$

$$\frac{dN_\nu}{dE} = \frac{1}{4} \frac{dN_\gamma}{dE} \text{ for } p - \gamma$$

What happens during propagation  
of messengers to us?

# Oscillation probability (3 families)

oscillation probability in 3 families (A. Blondel's lectures)

$$P(\nu_\alpha \rightarrow \nu_\beta) = \sum |U_{\alpha,i}|^2 |U_{\beta,i}|^2 + 2 \sum_{i < j} U_{\alpha,i} U_{\beta,i} U_{\alpha,j} U_{\beta,j} \cos \left( \frac{\Delta m_{ij}^2 L}{2E} \right).$$

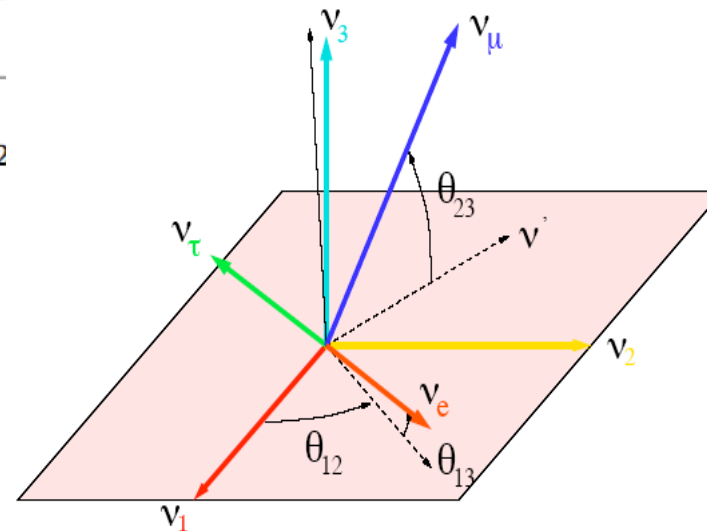
solar  $U_{e1}, U_{e2} \leftrightarrow \theta_{12}$  CHOOZ  $U_{e3} \leftrightarrow \theta_{13}$

$$U = \begin{pmatrix} U_{e1} & U_{e2} & U_{e3} \\ U_{\mu 1} & U_{\mu 2} & U_{\mu 3} \\ U_{\tau 1} & U_{\tau 2} & U_{\tau 3} \end{pmatrix} = \begin{pmatrix} c_{12}c_{13} & s_{12}c_{13} & s_{13}e^{-i\delta} \\ -s_{12}c_{23} - c_{12}s_{13}s_{23}e^{i\delta} & c_{12}c_{23} - s_{12}s_{13}s_{23}e^{i\delta} & c_{13}s_{23} \\ s_{12}s_{23} - c_{12}s_{13}c_{23}e^{i\delta} & -c_{12}s_{23} - s_{12}s_{13}c_{23}e^{i\delta} & c_{13}c_{23} \end{pmatrix}$$

atmospheric  $U_{e3} \leftrightarrow \theta_{13}$   $U_{\mu 3}, U_{\tau 3} \leftrightarrow \theta_{23}$

MNSP matrix

Parameter	best-fit ( $\pm 1\sigma$ )	$3\sigma$
$\Delta m_{21}^2$ [ $10^{-5}$ eV <sup>2</sup> ]	$7.54^{+0.26}_{-0.22}$	6.99 – 8.18
$ \Delta m^2 $ [ $10^{-3}$ eV <sup>2</sup> ]	$2.43 \pm 0.06$ ( $2.38 \pm 0.06$ )	2.23 – 2.61 (2.19 – 2)
$\sin^2 \theta_{12}$	$0.308 \pm 0.017$	0.259 – 0.359
$\sin^2 \theta_{23}, \Delta m^2 > 0$	$0.437^{+0.033}_{-0.023}$	0.374 – 0.628
$\sin^2 \theta_{23}, \Delta m^2 < 0$	$0.455^{+0.039}_{-0.031}$	0.380 – 0.641
$\sin^2 \theta_{13}, \Delta m^2 > 0$	$0.0234^{+0.0020}_{-0.0019}$	0.0176 – 0.0295
$\sin^2 \theta_{13}, \Delta m^2 < 0$	$0.0240^{+0.0019}_{-0.0022}$	0.0178 – 0.0298



$$\tan^2 \theta_{23} \equiv \frac{|U_{\mu 3}|^2}{|U_{\tau 3}|^2},$$

$$\tan^2 \theta_{12} \equiv \frac{|U_{e2}|^2}{|U_{e1}|^2},$$

$$\sin^2 \theta_{13} \equiv |U_{e3}|^2,$$

# Astrophysical neutrino oscillations

$$P(\nu_\alpha \rightarrow \nu_\beta) = \sum_i |U_{\alpha,i}|^2 |U_{\beta,i}|^2 + 2 \sum_{i < j} U_{\alpha,i} U_{\beta,i} U_{\alpha,j} U_{\beta,j} \cos \left( \frac{\Delta m_{ij}^2 L}{2E} \right)$$

We can express the phase in astro units:

$$\varphi \sim 3 \cdot 10^8 \left( \frac{\Delta m^2}{8 \cdot 10^{-5} \text{ eV}^2} \right) \left( \frac{D}{1 \text{ kpc}} \right) \left( \frac{10 \text{ TeV}}{E_\nu} \right)$$

For astrophysical source at kpc-distances emitting  $\nu$ s of 10 TeV:  $\cos \varphi$  averages to zero since the extension of sources is about 1 pc and their distance is of the order of 1 kpc so the baseline is known with precision 1/1000 not 1/10<sup>8</sup> hence oscillations average out

$$P(\nu_\alpha \rightarrow \nu_\beta) = \sum_i |U_{\alpha,i}|^2 |U_{\beta,i}|^2$$

$$P(\nu_e \rightarrow \nu_e) = \sum_i |U_{ei}|^2 |U_{ei}|^2 = |U_{e1}|^4 + |U_{e2}|^4 + |U_{e3}|^4 = 0.82^4 + 0.57^4 + 0 = 0.56$$

$$P(\nu_e \rightarrow \nu_\mu) = \sum_i |U_{ei}|^2 |U_{\mu i}|^2 = |U_{e1}|^2 |U_{\mu 1}|^2 + |U_{e2}|^2 |U_{\mu 2}|^2 + |U_{e3}|^2 |U_{\mu 1}|^2 = 0.82^2 \cdot 0.4^2 + 0.57^2 \cdot 0.58^2 + 0 = 0.22$$

$$P(\nu_e \rightarrow \nu_\tau) = \sum_i |U_{ei}|^2 |U_{\tau i}|^2 = |U_{e1}|^2 |U_{\tau 1}|^2 + |U_{e2}|^2 |U_{\tau 2}|^2 + |U_{e3}|^2 |U_{\tau 1}|^2 = 0.82^2 \cdot 0.4^2 + 0.57^2 \cdot 0.58^2 + 0 = 0.22$$

$\nu_\alpha \backslash \nu_\beta$	$\nu_e$	$\nu_\mu$	$\nu_\tau$
$\nu_e$	60%	20%	20%
$\nu_\mu$	20%	40%	40%
$\nu_\tau$	20%	40%	40%

# Flavor ratio at Earth

At source:

$$\nu_e : \nu_\mu : \nu_\tau \sim 1 : 2 : 0$$

pion-muon decay

$\nu_\alpha / \nu_\beta$	$\nu_e$	$\nu_\mu$	$\nu_\tau$
$\nu_e$	60%	20%	20%
$\nu_\mu$	20%	40%	40%
$\nu_\tau$	20%	40%	40%

Maybe not true if charmed meson threshold is overcome: 0:1:0 (Sarcevic et al., arXiv:0808.2807)

At Earth:

$$\nu_e : \nu_\mu : \nu_\tau \sim 1 : 1 : 1$$

Maybe not true if muons cannot decay  
(Kashti & Waxman, PRL 95 (2005) 181101)

60% of  $\nu_e$  survive and  $2 \times 20\%$  come from  $2 \times \nu_\mu = 100\%$   
 $2 \times 40\% = 80\%$  of  $2 \times \nu_\mu$  survive and 20% come from  $\nu_e = 100\%$   
20% of  $\nu_\tau$  come from  $\nu_e$  and  $2 \times 40\%$  from  $\nu_\mu = 100\%$

# Gamma-neutrino connection at Earth

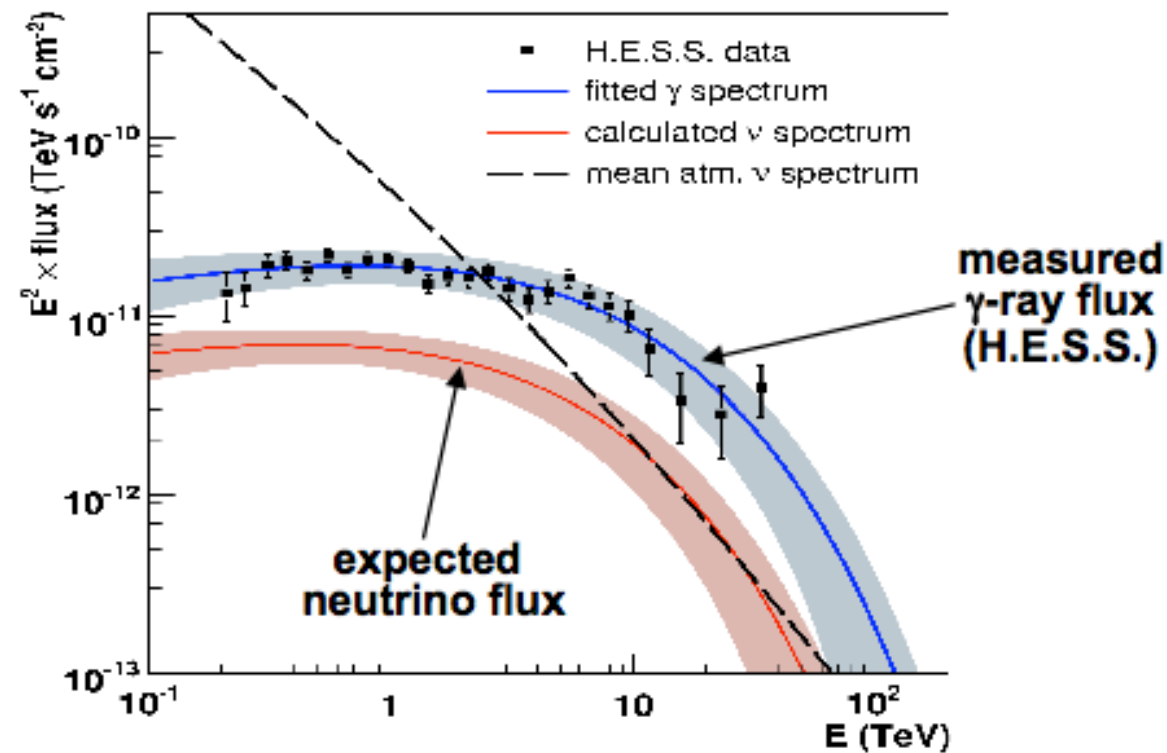
$$\frac{dN_\nu}{dE} = \frac{1}{2} \frac{dN_\gamma}{dE} \text{ for } p - p$$

$$\frac{dN_\nu}{dE} = \frac{1}{8} \frac{dN_\gamma}{dE} \text{ for } p - \gamma$$

Warning: we neglected absorption  
of photons

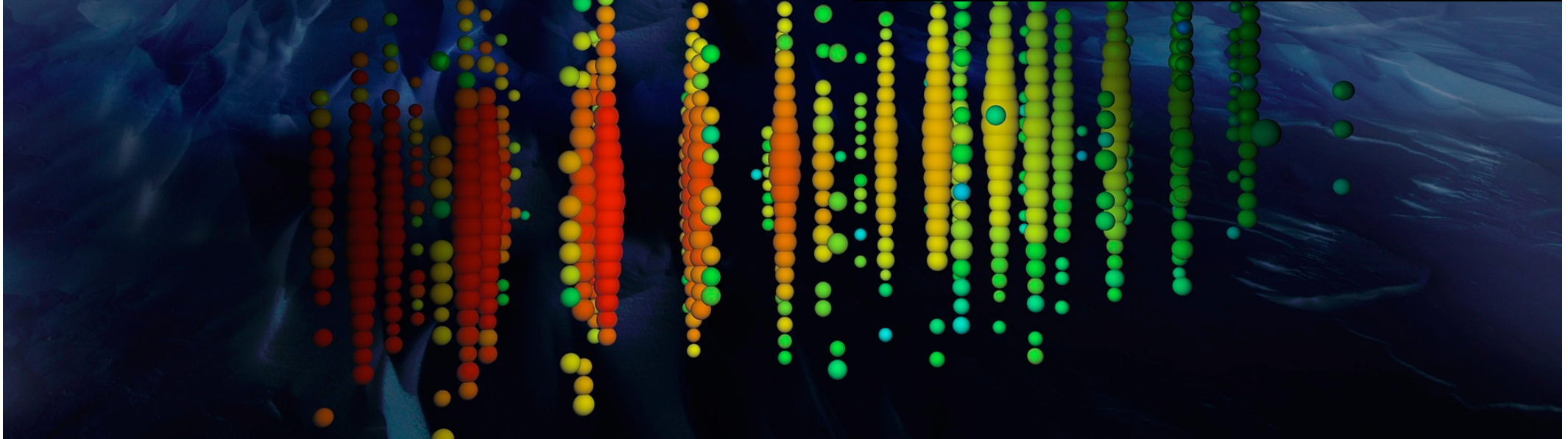
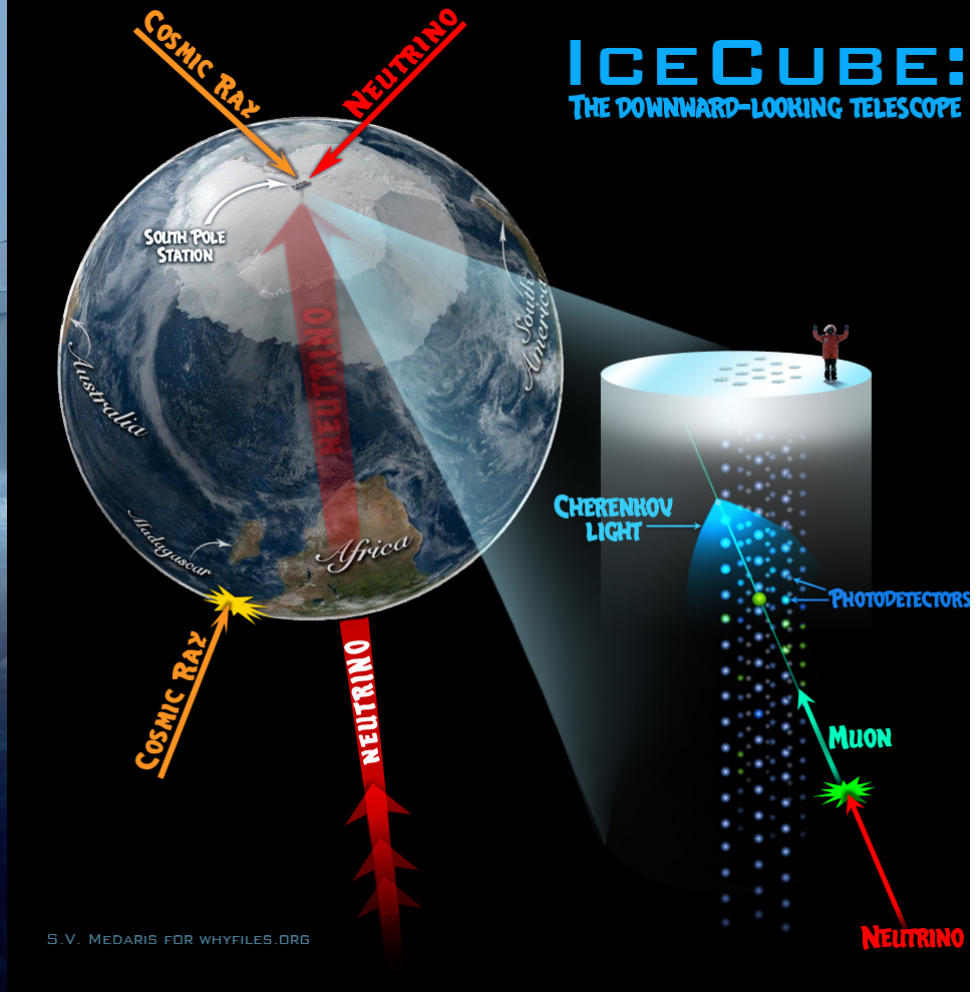
# Neutrino - gamma fluxes

## Neutrino and $\gamma$ -Ray Spectra for RX J1713.7-3946 (SNR)

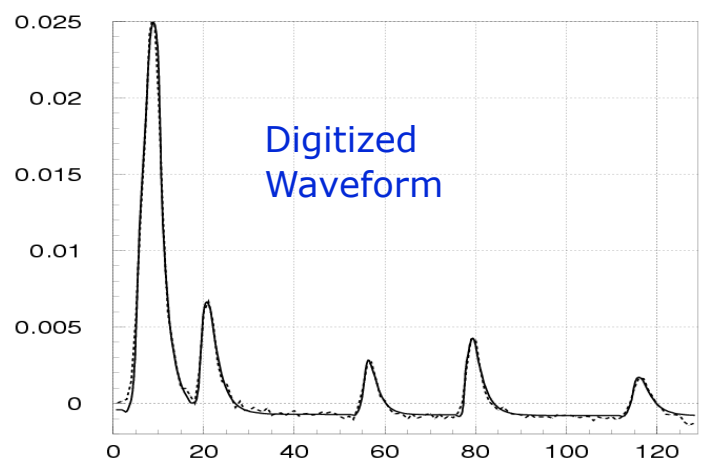


$$N = T \times \int_{E_{\min}}^{E_{\max}} A_{\text{eff}}(E) \times \frac{dN}{dE} dE$$

$$N = T \times \sum_{\text{bins}} A_{\text{eff}} \left( \frac{dN}{dE} (\text{bin center}) \times \Delta E_{\text{bin}} \right)$$





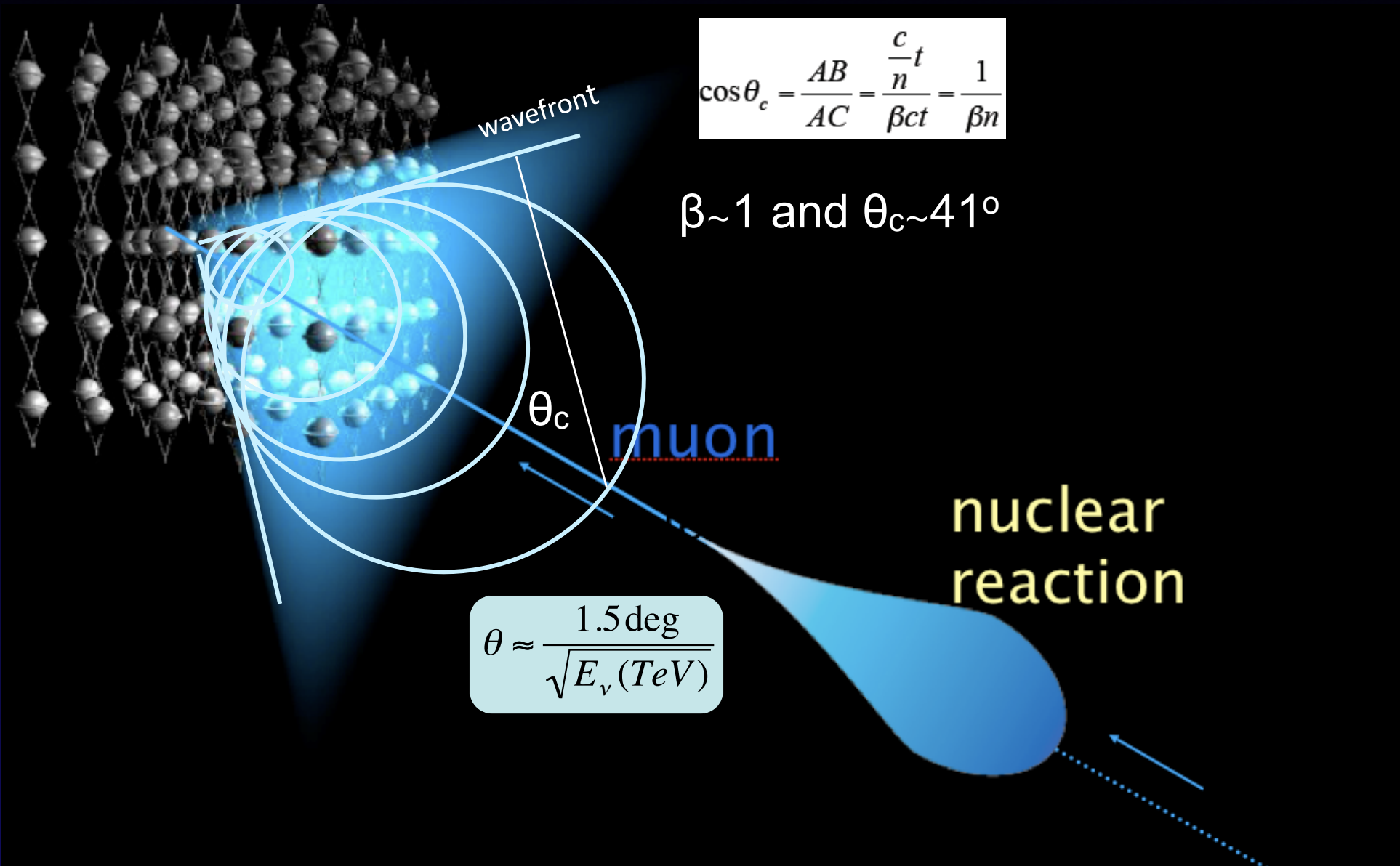


10" PMT

13" Glass  
(hemi)sphere

**> 98.5% of DOMs in stable operation**

# Concept of Neutrino Detector



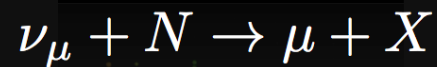
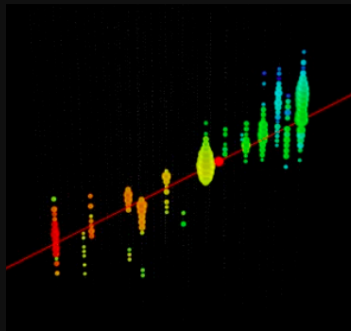
Between 300-600 nm about  $3.5 \times 10^4$  Cherenkov photons/m of a muon track



# Neutrino events in a neutrino telescope



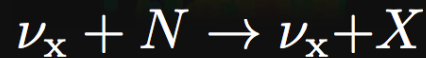
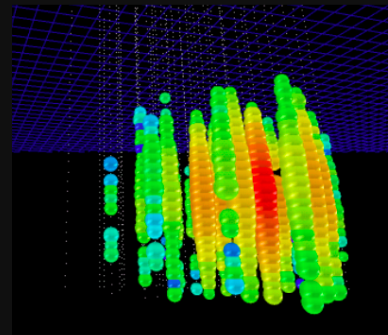
## CC Muon Neutrino



track (data)

factor of  $\approx 2$  energy resolution  
<  $1^{\circ}$  angular resolution

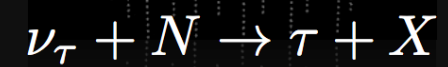
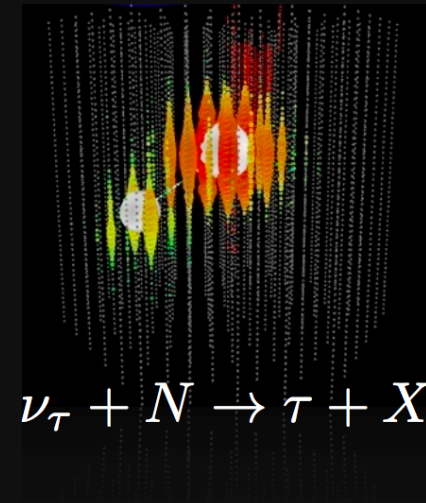
## Neutral Current /Electron Neutrino



cascade (data)

$\approx \pm 15\%$  deposited energy resolution  
 $\approx 10^{\circ}$  angular resolution  
(at energies  $\gtrsim 100$  TeV)

## CC Tau Neutrino



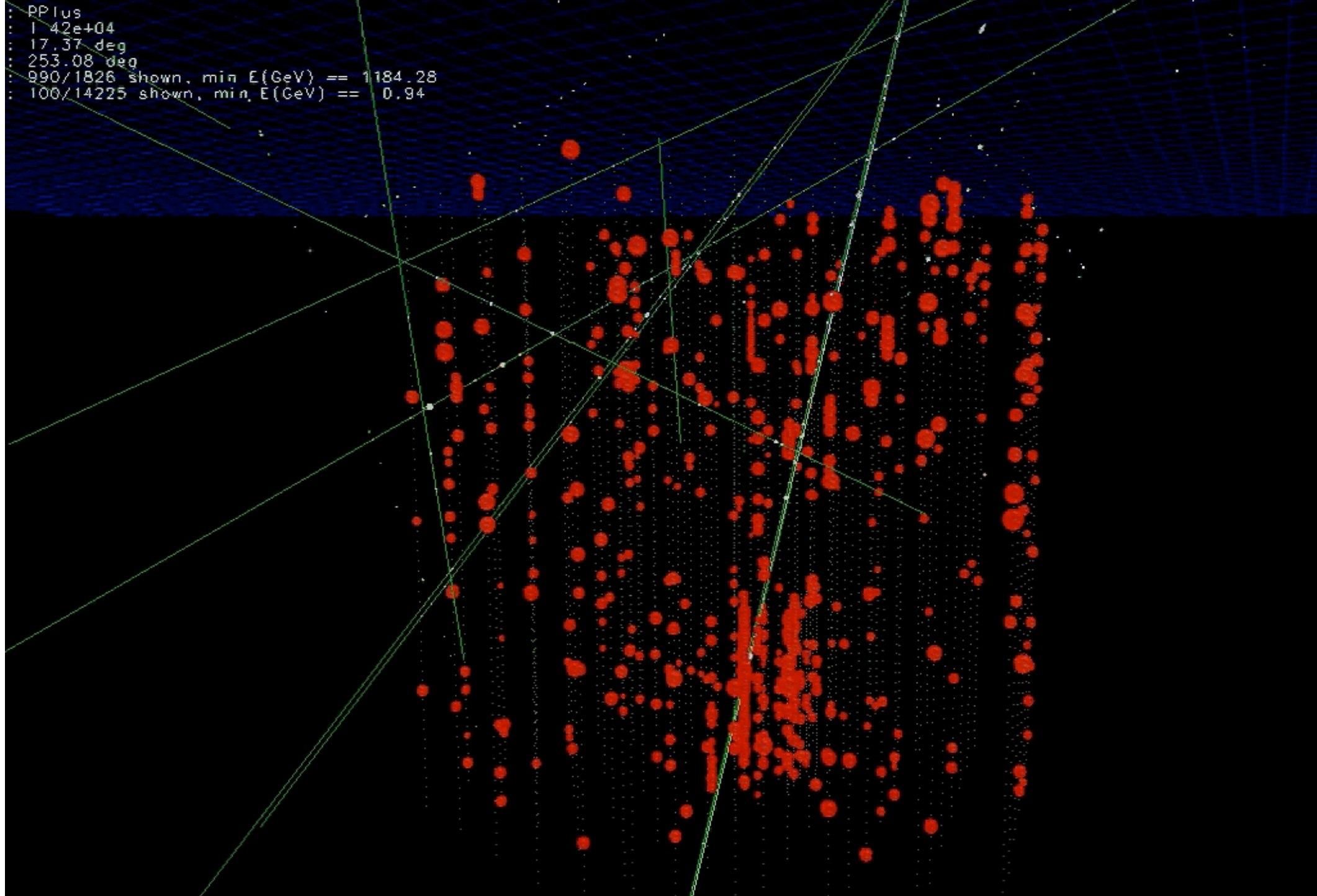
“double-bang” and other signatures  
(simulation)

(not observed yet)



muon track: time is color; number of photons is energy

```
: PPlus  
: 1.42e+04  
: 17.37 deg  
: 253.08 deg  
: 990/1826 shown, min E(GeV) == 1184.28  
: 100/14225 shown, min E(GeV) == 0.94
```



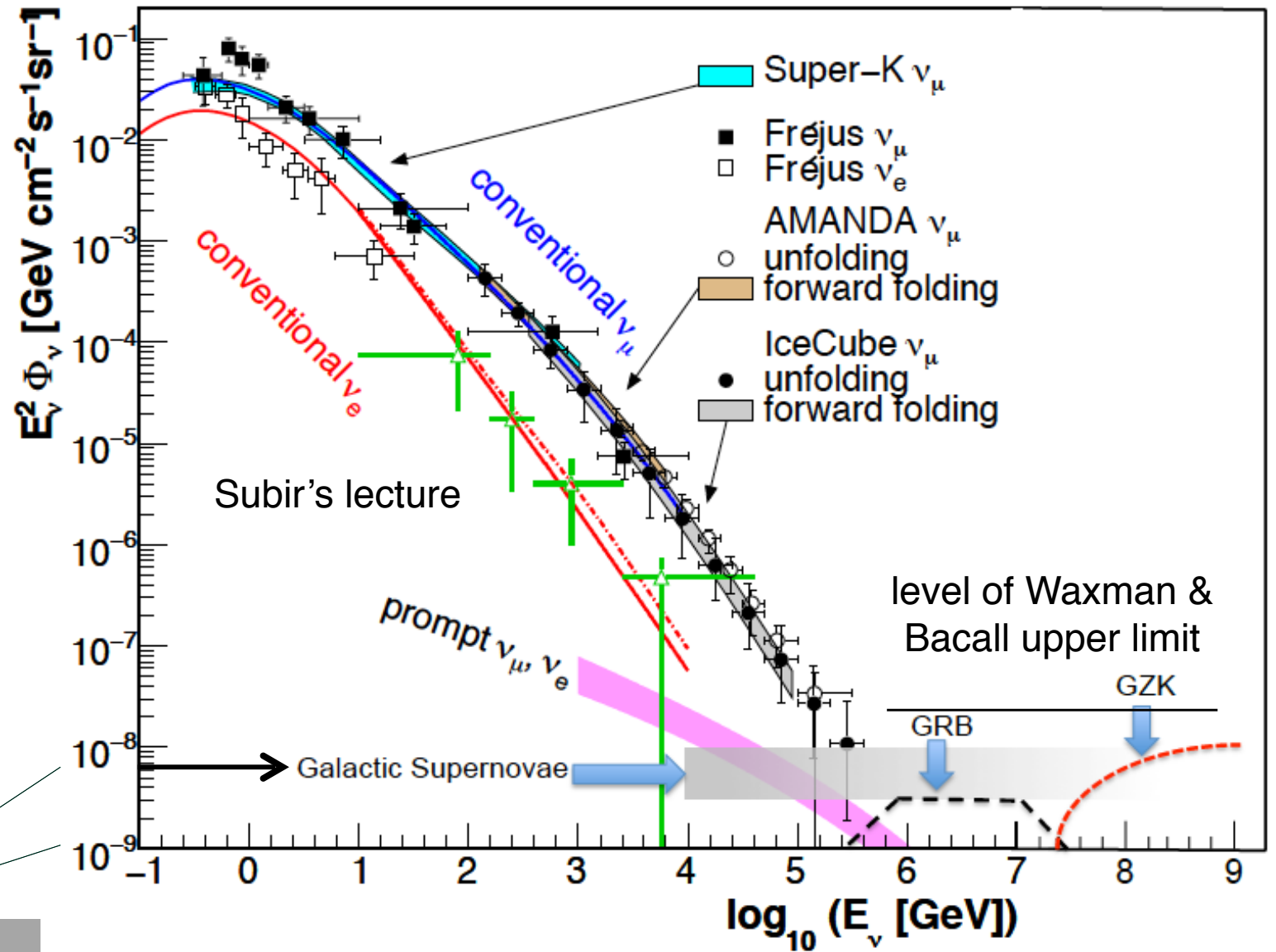
You have seen only 10 nms of data taking

above 100 TeV

- cosmic neutrinos:
- atmospheric background disappears

$$dN/dE \sim E^{-2}$$

1-10 events per year for fully efficient 1 km<sup>3</sup> detector



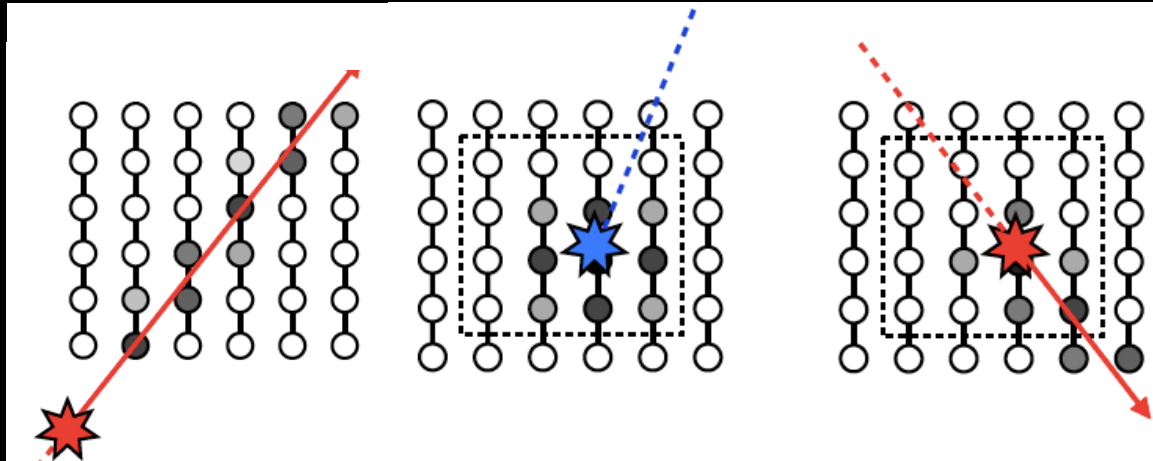
atmospheric

cosmic

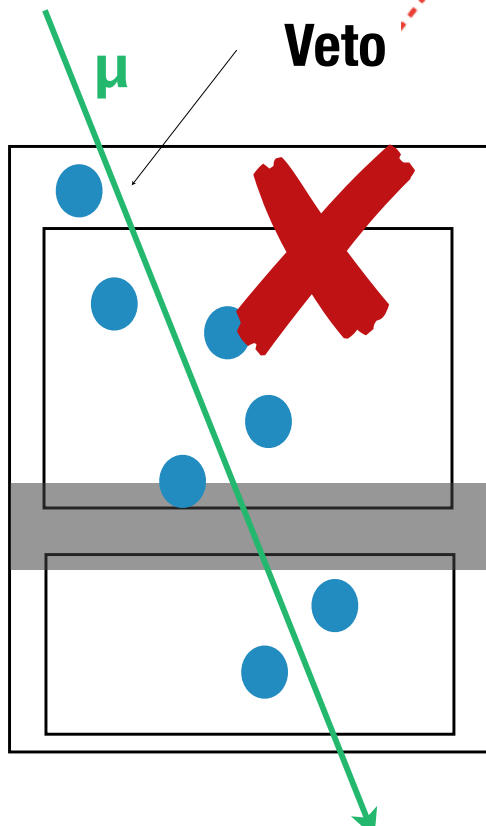
100 TeV

# Neutrino selection & background rejection

Upgoing thoroughgoing neutrino induced muons - Earth is a filter - or vertex identification of 'starting events' (tracks and cascades)

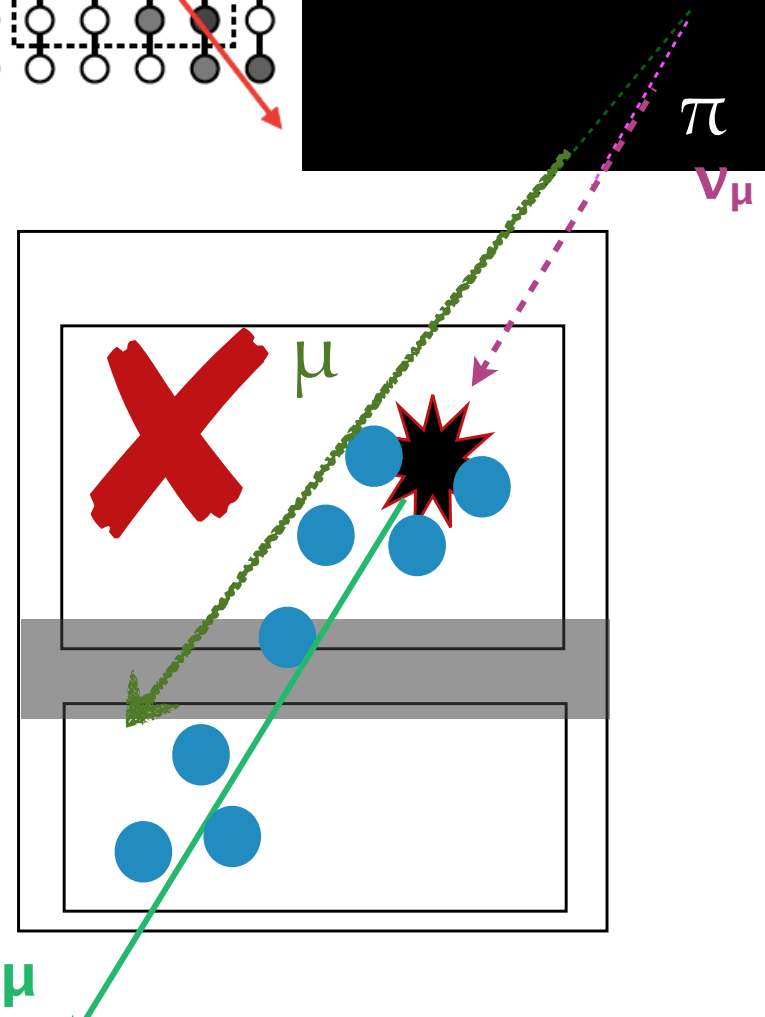


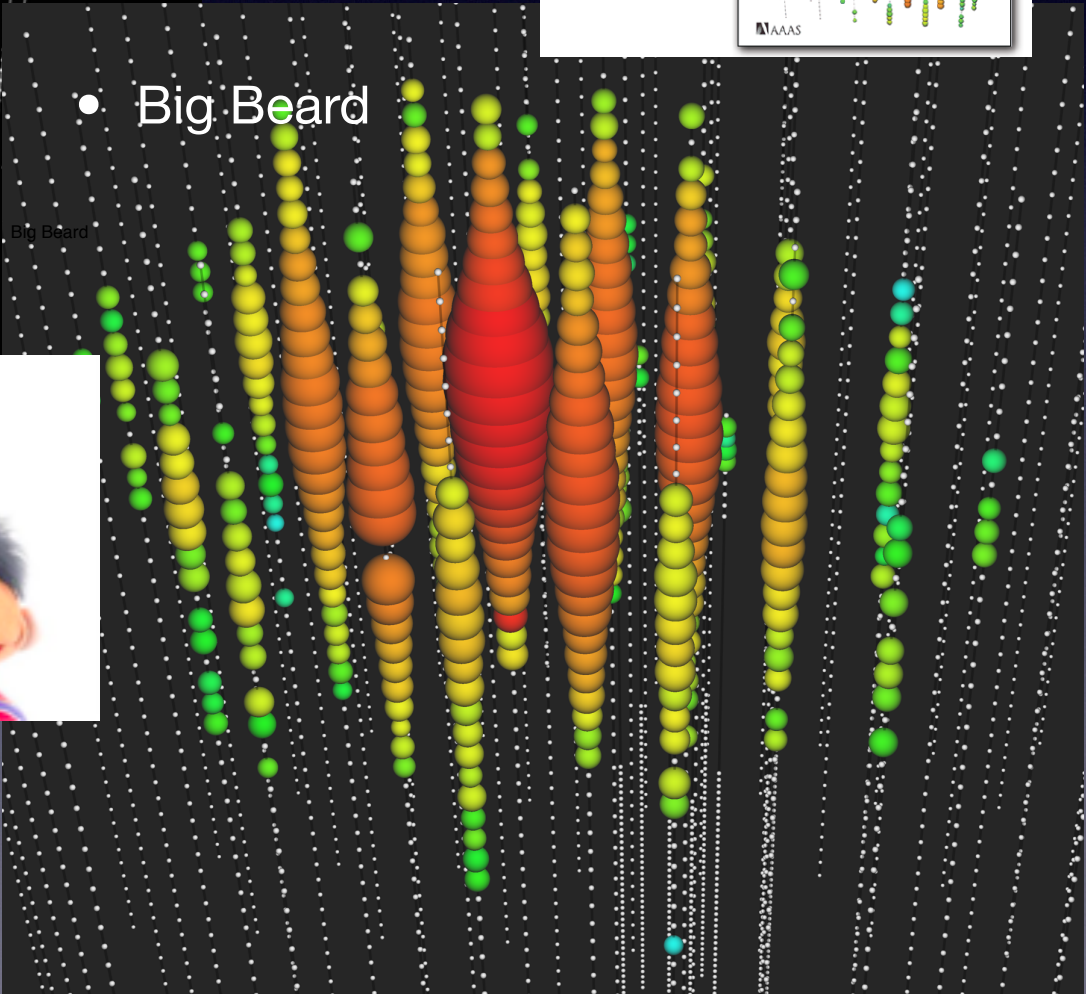
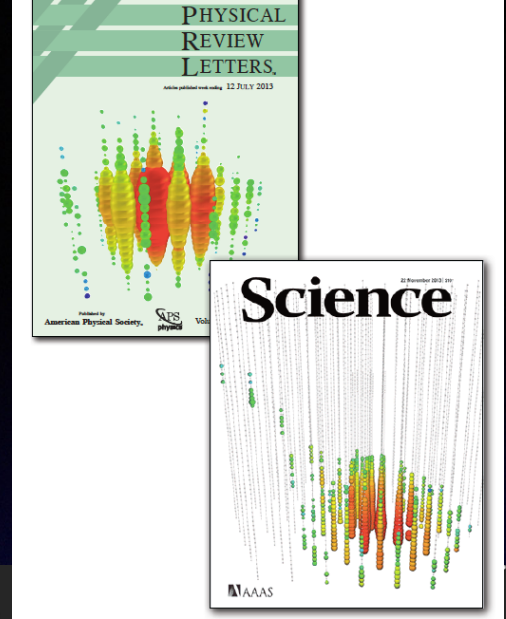
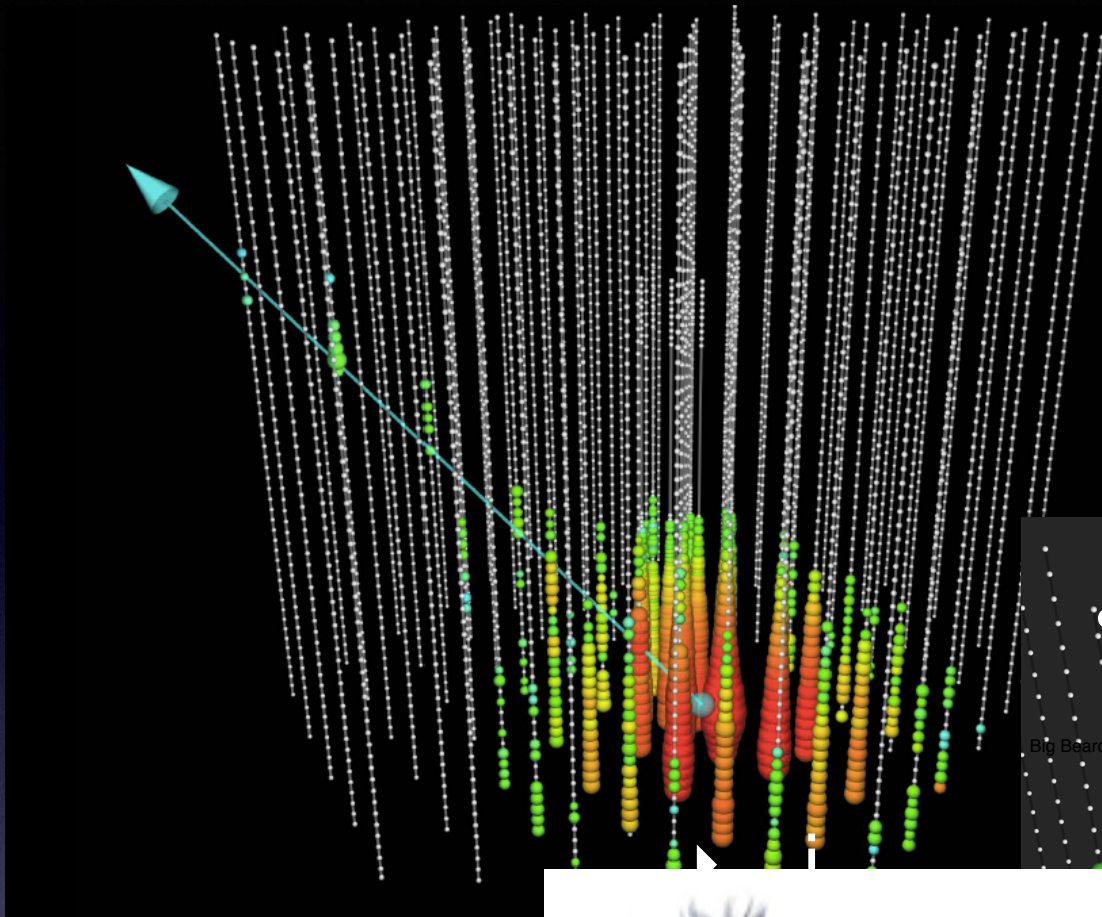
Schönert, Resconi, Schulz, Phys. Rev. D, 79:043009 (2009)  
Gaisser, Jero, Karle, van Santen, Phys. Rev. D, 90:023009 (2014)



atmospheric muon tag

atmospheric neutrino tag





• Big Beard

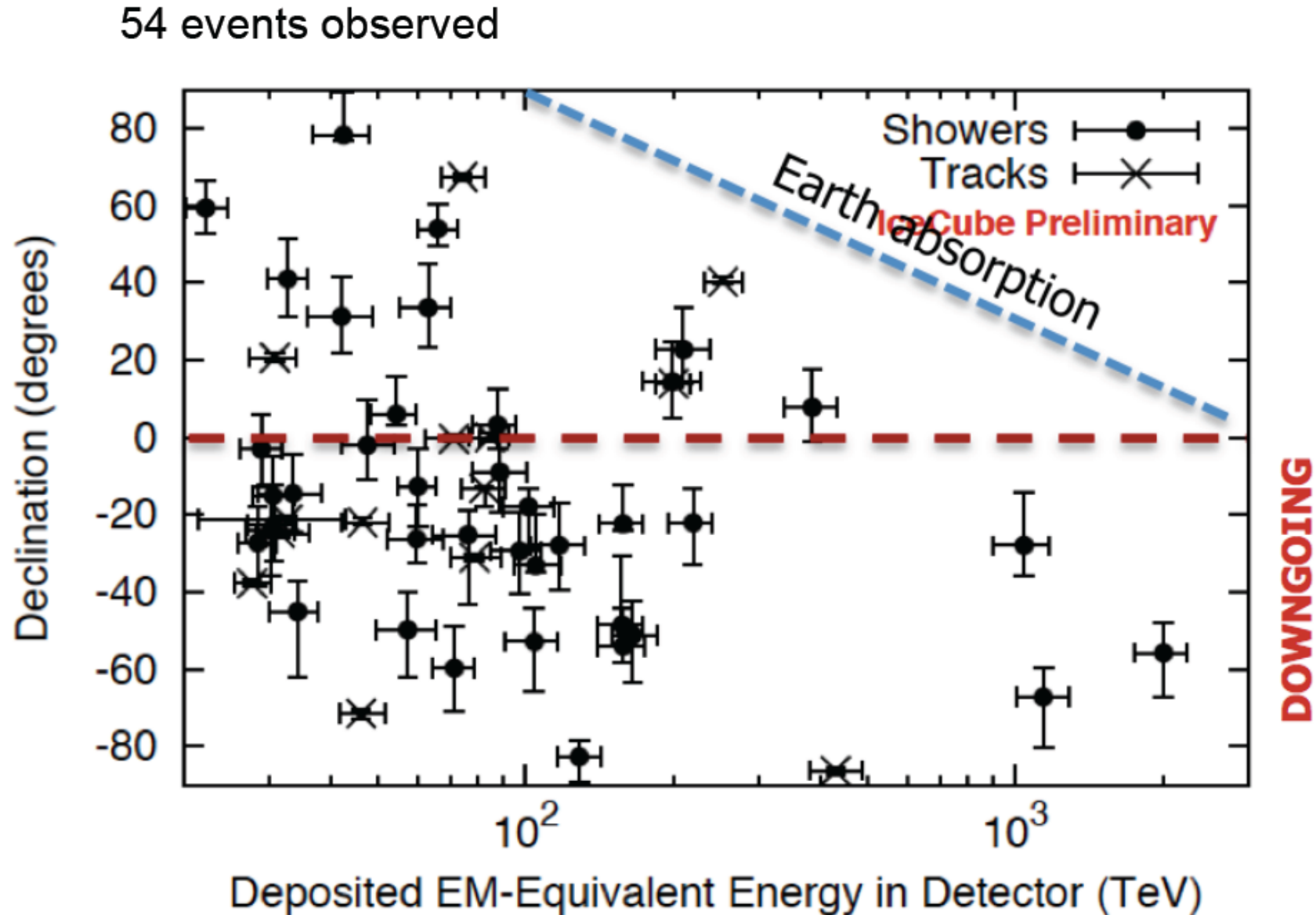


After 3 yrs 37 events  
 with background:  
 $6.6^{+5.9}_{-1.6}$  atm. neutrinos  
 ▶  $8.4 \pm 4.2$  atm. muons

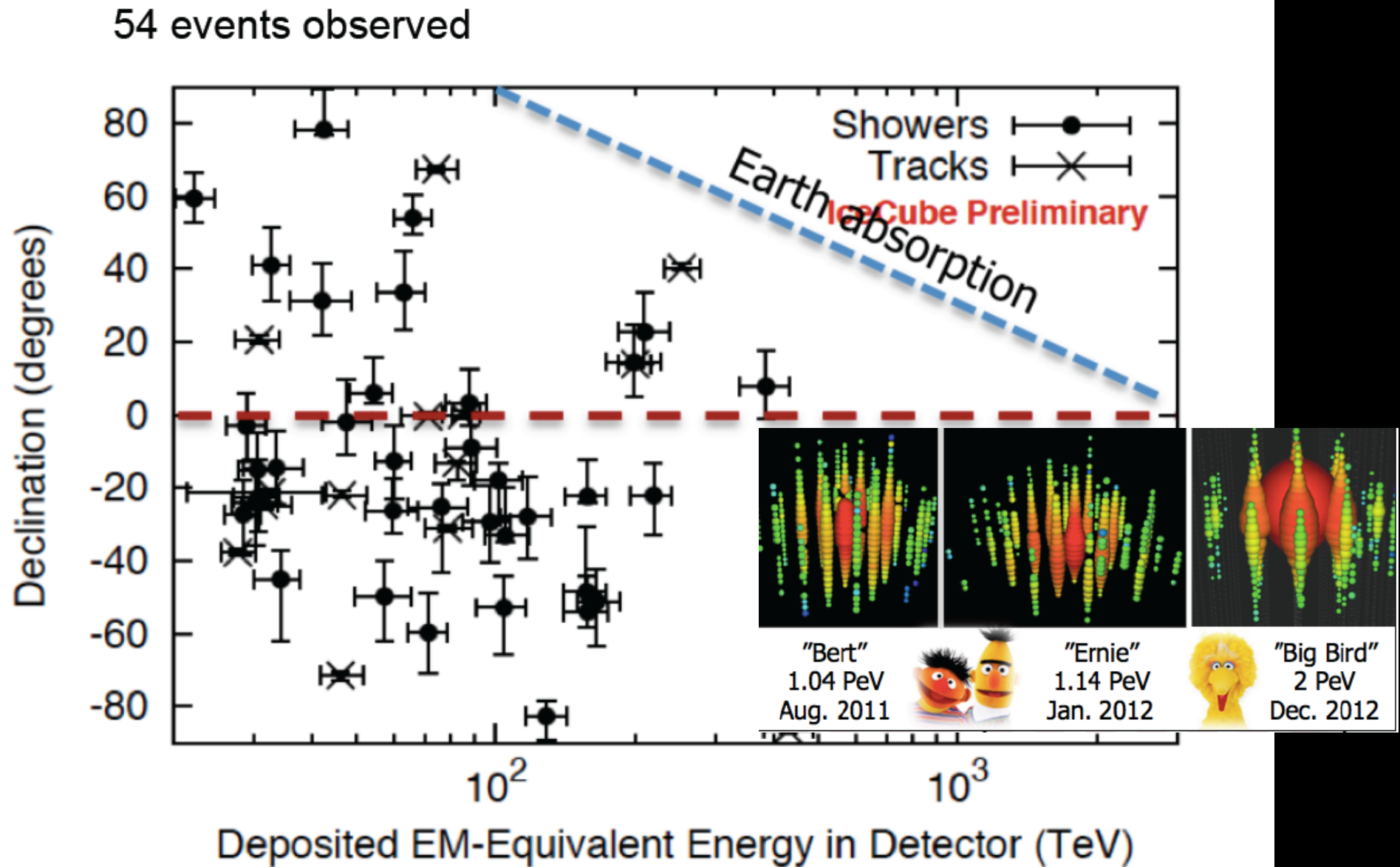


# High Energy Starting Events (4 yr)

Kopper, Giang, Kurahashi, ICRC 2015, POS 1081,  
PRL 113 (2014) 101101, Science 2013



# High Energy Starting Events (4 yr)



# 4 yr (2010-14) of HESE

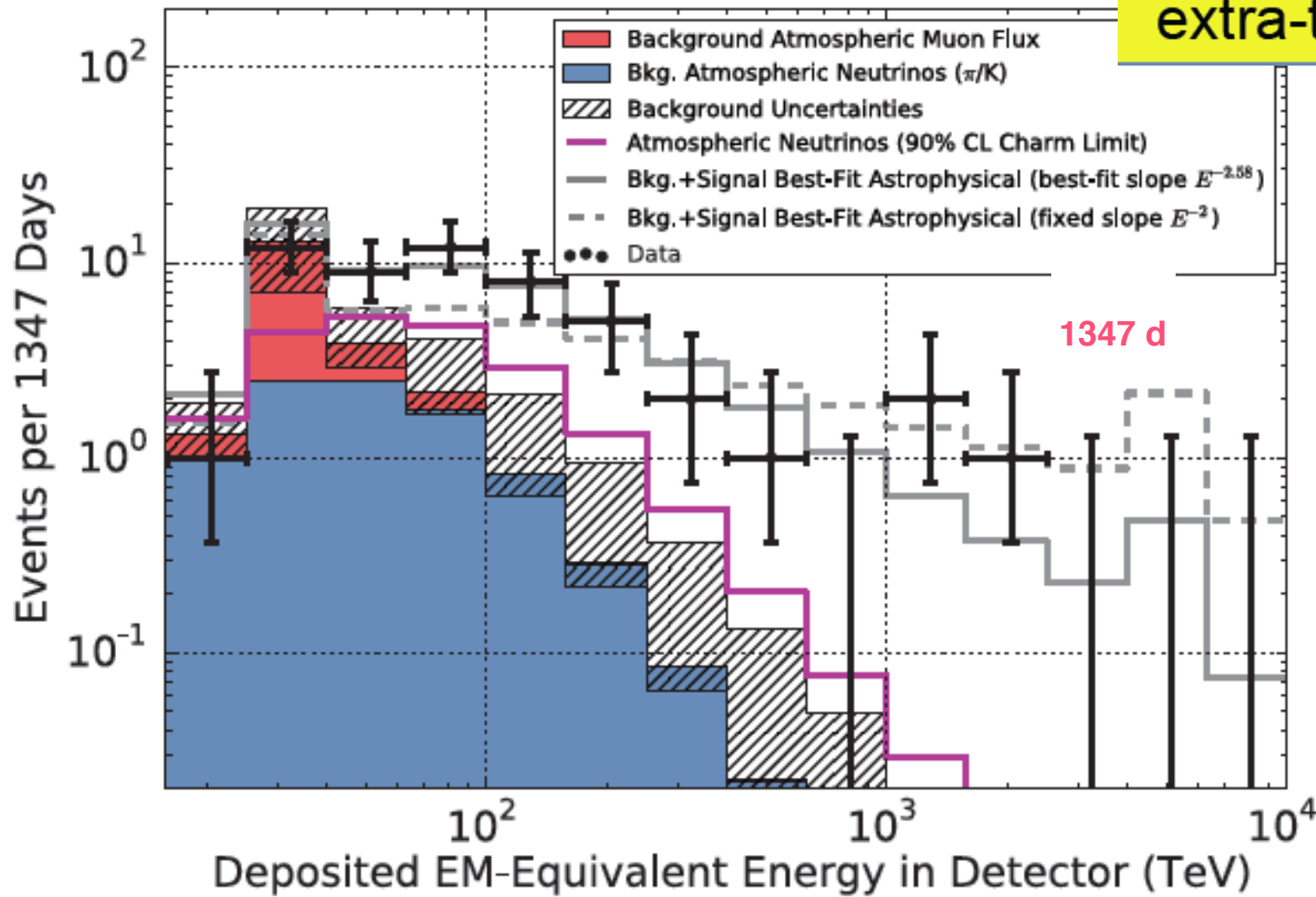
Anti-coincidence veto + >6000 p.e. (>30 TeV)

54 events (17+events in PRL 113 (2014) 101101) of which 2 are evident background events.

Background: Measured:  $12.6 \pm 5.1$  atmospheric muon events

Atmospheric prompt component estimated using a previously set limit on atmospheric neutrinos with 59 strings:  $9.0_{-2.2}^{+8.0}$

$\sim 7 \sigma$  evidence for  
extra-terrestrial  $\nu$



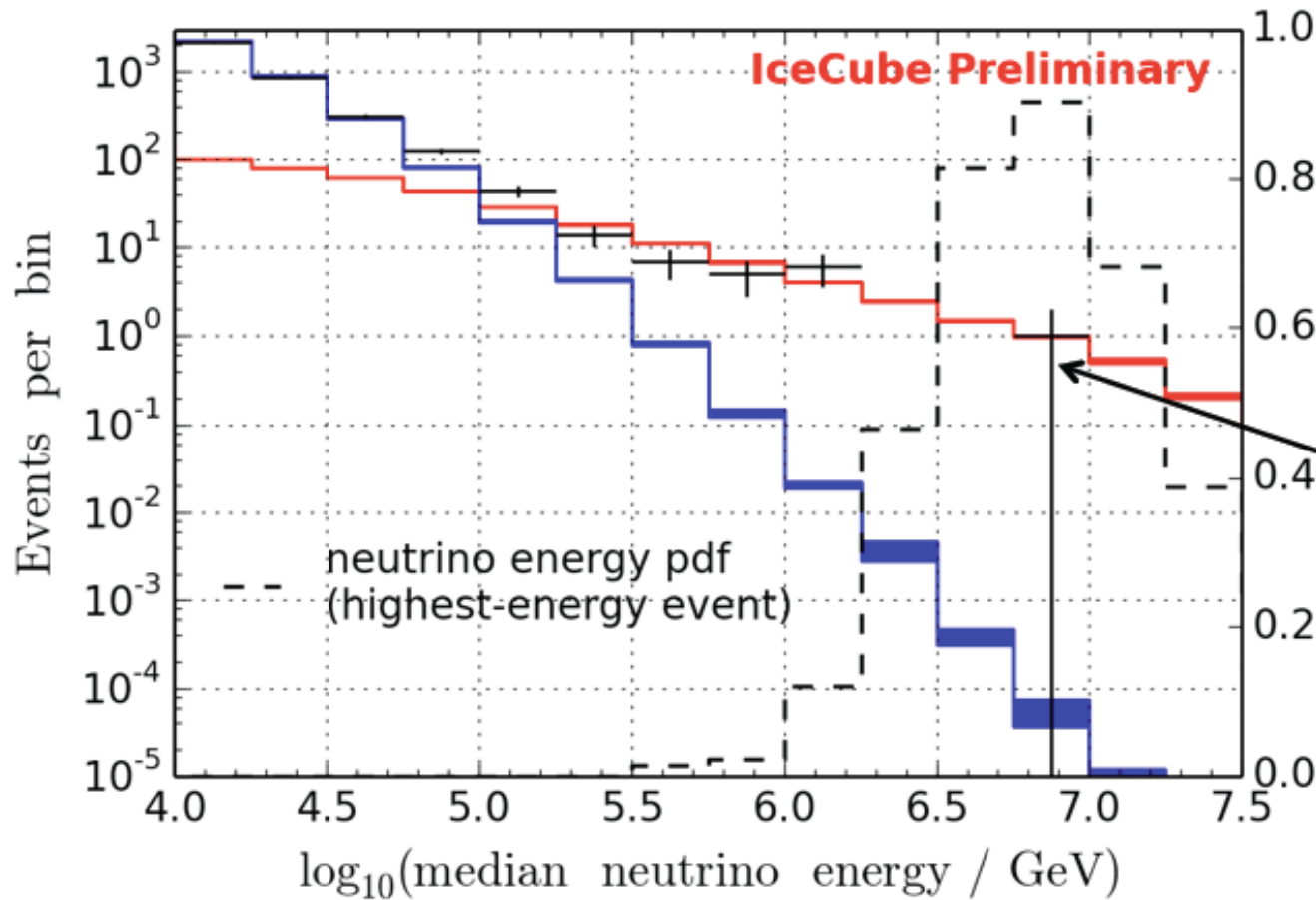
# Through going muon tracks



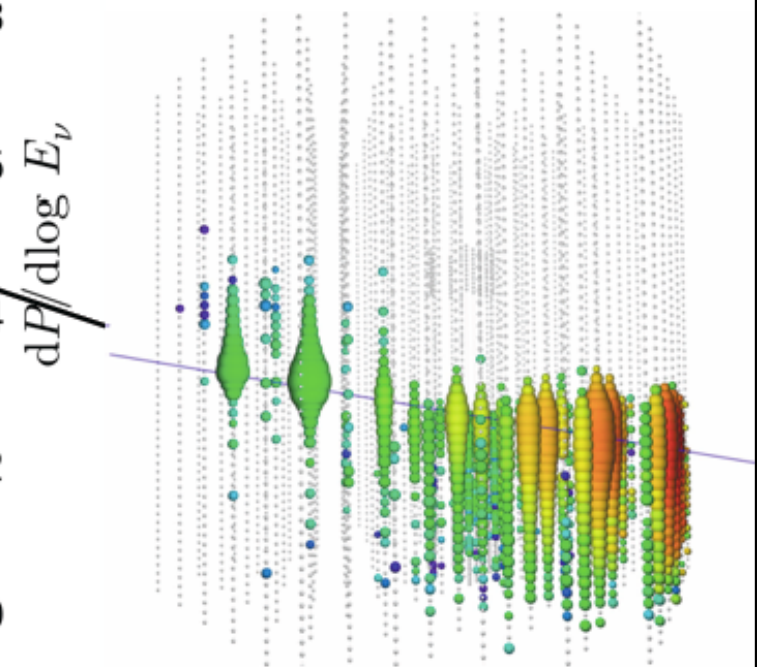
Best fit astrophysical spectral index of  $\gamma = 2.13 \pm 0.13$

Assuming best-fit power law:

- +++ Unfolding
- Conv. atmospheric  $\nu_\mu + \bar{\nu}_\mu$
- Astrophysical  $\nu_\mu + \bar{\nu}_\mu$



5.6 sigma detection of astrophysical neutrinos with through-going muons analysis

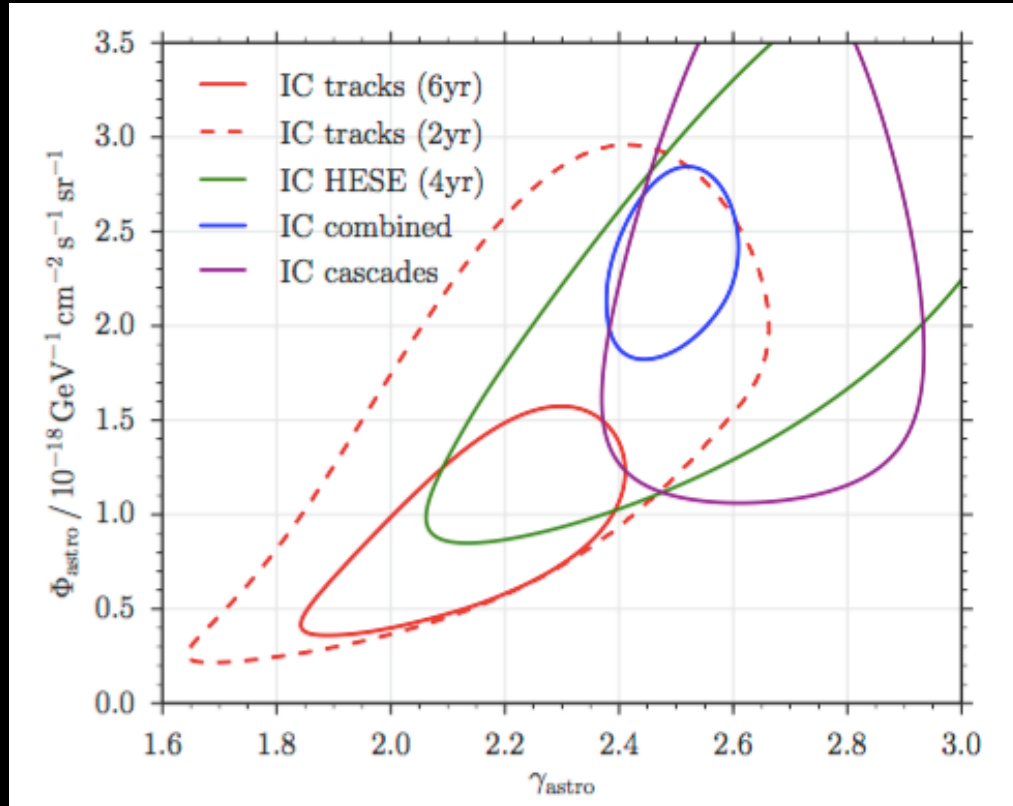


Deposited energy:  
 $2.6 \pm 0.3$  PeV

subm. to ApJ

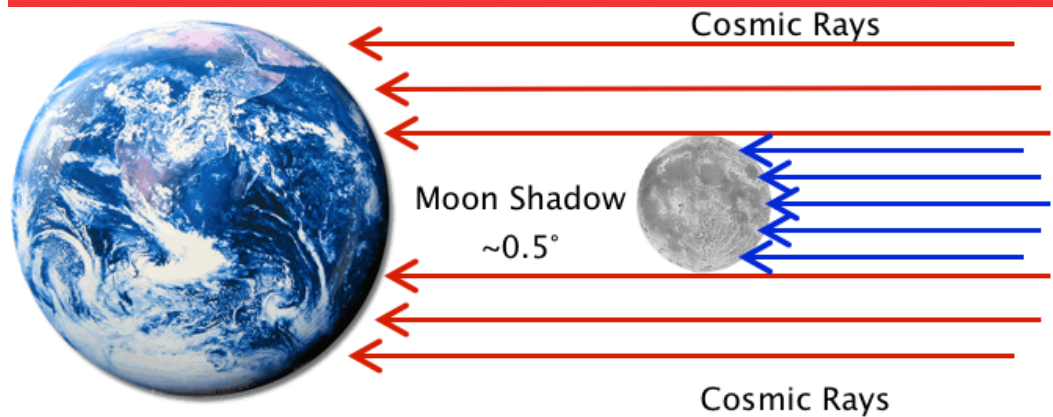
# Combined fit

<http://arxiv.org/pdf/1607.08006v1.pdf>



The p-value for obtaining the combined fit result and the result reported here from an unbroken powerlaw flux is  $3.3\sigma$ , and is therefore in significant tension.

# Use the Moon to verify pointing



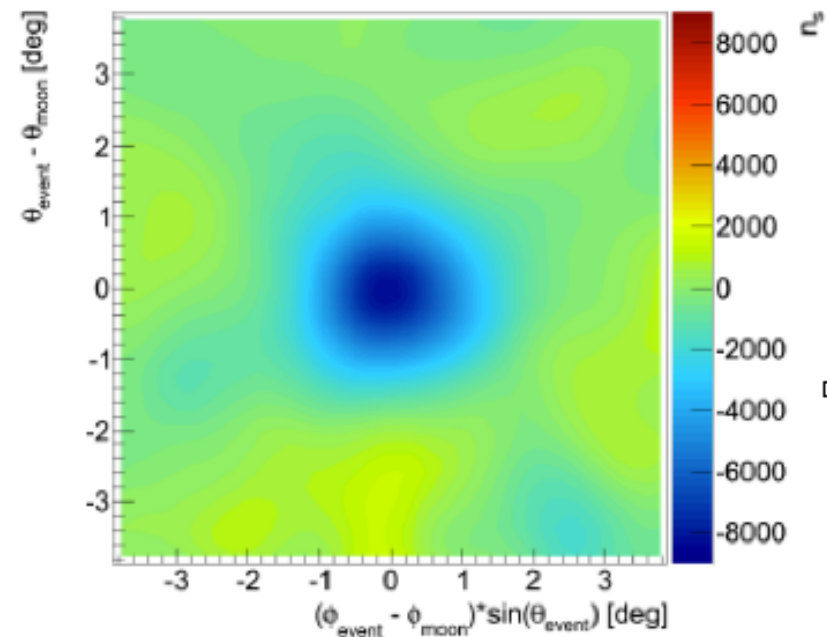
Moon shadow LH analysis :

$> 6\sigma$

$0.2^\circ$  shift from expected position

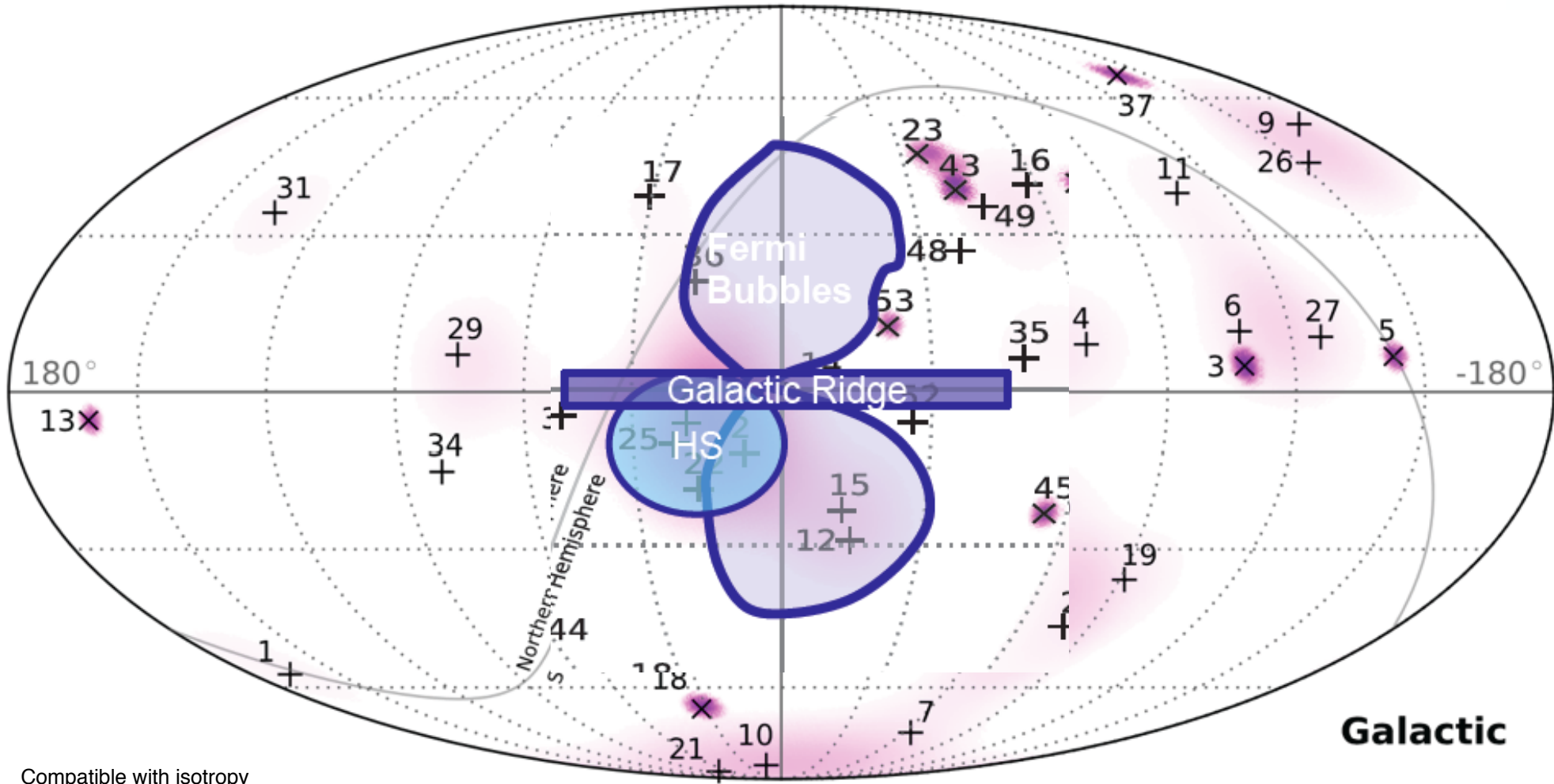
[http://journals.aps.org/prd/abstract/  
10.1103/PhysRevD.89.102004](http://journals.aps.org/prd/abstract/10.1103/PhysRevD.89.102004)

59 strings (2009-2010)

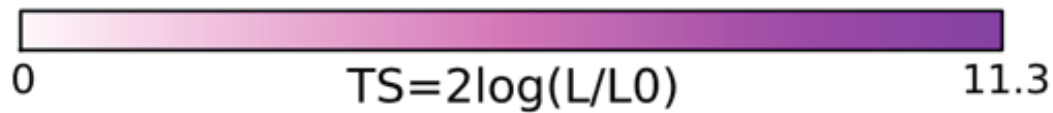


- $n_s^{\text{obs}} = -8660 \pm 565 \pm 681$
- $n_s^{\text{exp}} = -8192 \pm 91$
- $\vec{\chi}_s^{\text{obs}} = (-0.1^\circ \pm 0.1^\circ, 0.0^\circ \pm 0.1^\circ)$

# Sky map of 54 High Energy Starting Events

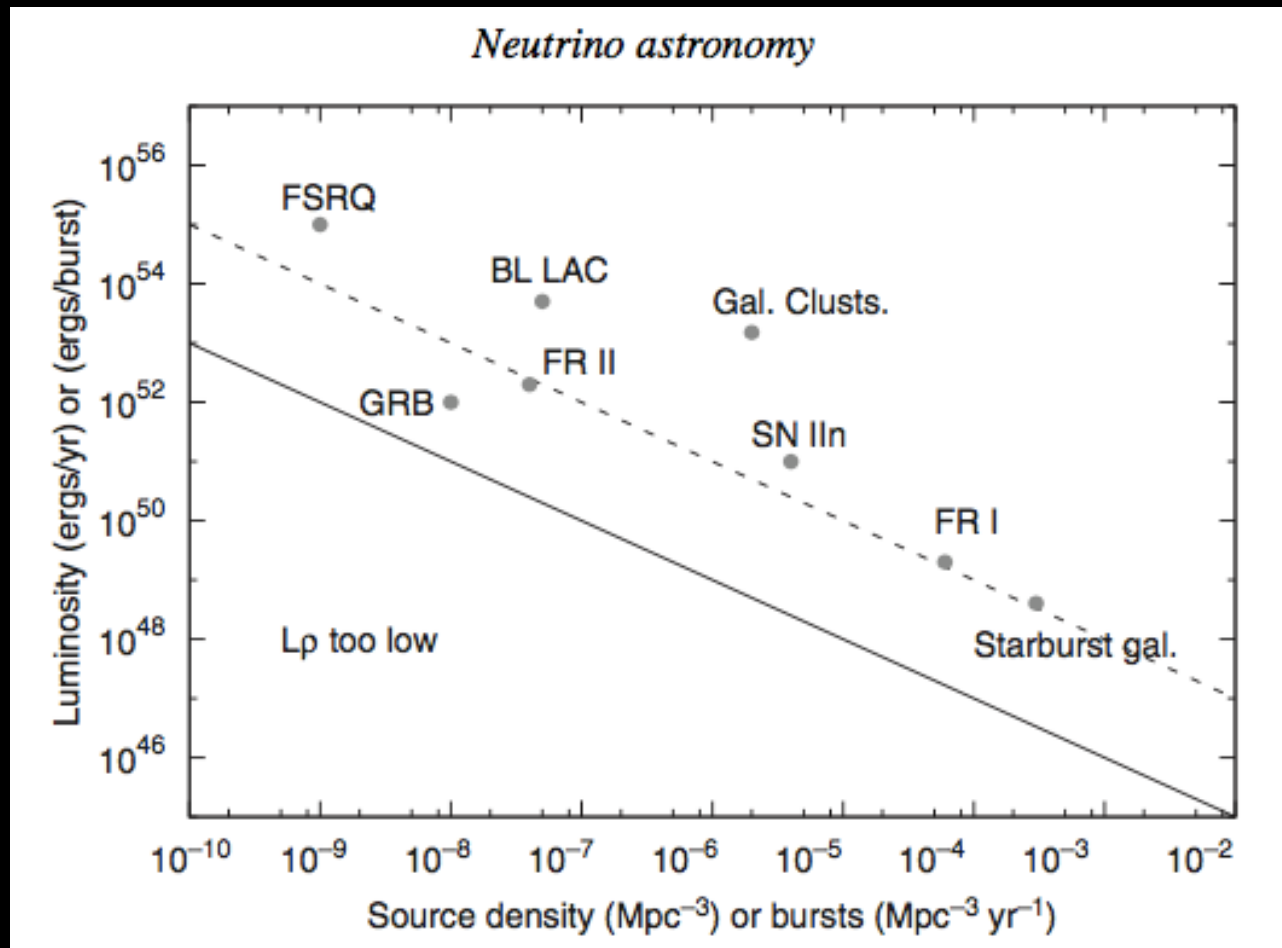


Compatible with isotropy  
Moderate excess from Southern Hemisphere



Clustering of events test and did not yield significant evidence.  
A galactic plane clustering test using a fixed width of 2.5° around the plane (post trial p-value 7%)  
and using a variable-width scan (post trial p-value 2.5%).

# The Kowalski's plot



Luminosity vs density for potential sources of high-energy astro- physical neutrinos.  
minimum power-density needed to produce the observed neutrino flux as